Genetic instability upon the loss of the tumour suppressor folliculin (FLCN)

Rachel-Ann Russell

June 2019

Thesis submitted to Cardiff University in fulfilment of the requirements for the degree of Doctor of Philosophy

Declaration

This work has not previously been accepted in substance for any degree and is not concurrently submitted in candidature for any degree.

Signed…………………………………. (Candidate) Date………………………………….

STATEMENT 1 This thesis is being submitted in partial of the requirements for the degree of …………………………………. (Insert MCh, MD, MPhil, PhD etc., as appropriate)
Signed…………………………………. (Candidate) Date ………………………………….

STATEMENT 2 This thesis is the result of my own independent work/investigation, except where otherwise stated. Other sources are acknowledged by explicit references.
Signed…………………………………. (Candidate) Date ………………………………….

STATEMENT 3 I hereby give consent for my thesis, if accepted, to be available for photocopying and for inter-library loan, and for the title and summary to be made available to outside organisations. Signed…………………………………. (Candidate) Date ………………………………….

STATEMENT 4: PREVIOUSLY APPROVED BAR ON ACCESS I hereby give consent for my thesis, if accepted, to be available for photocopying and for inter-library loans after expiry of a bar on access previously approved by the Graduate Development Committee.
Signed…………………………………. (Candidate) Date ………………………………….

Acknowledgments

Firstly, I would like to express my sincere gratitude to my supervisors Dr Andrew Tee and Dr Elaine Dunlop, for their continuous support and guidance throughout my PhD. For their patience, motivation, and immense knowledge. I could not have imagined better advisors and mentors for my studies.

A special thanks goes out to all down at Tenovus Cancer Care for not just providing the funding for the work, but also their friendship and infinite opportunities to engage the public with science. To Mr Jesse Champion and Mr Matthew Lines for whom I partly supervised during their research placements, and whose work I have used to strengthen ideas laid out in this thesis.

I am endlessly grateful to my parents, Nigel and Christine Russell, who have provided me with an abundance of moral and emotional support in my life, and whom taught me the value of hard work through their actions.

And finally, to the greatest friend I'll ever have, my husband. Daniel Jones, you are myF everything. Thank you for believing in me when I couldn't believe in myself.

Summary

Folliculin (FLCN) is a tumour suppressor protein with unclear cellular function. Inactivating germline mutations in FLCN lead to Birt-Hogg-Dubé (BHD) syndrome. BHD patients have an increased risk of developing renal cell carcinoma (RCC). Unlike other genetic disorders with a predisposition to RCC, BHD patients are prone to all tumour subtypes (Khoo et al. 2003; Hudon et al. 2010). FLCN acts as a classical tumour suppressor in that a 'second-hit', deactivating mutation in the second allele, is required for cellular transformation. FLCN has been implicated in numerous signalling pathways and cellular processes. Most notably it is involved in mTOR, AMPK and HIF signalling, mitochondrial biogenesis, autophagy and membrane trafficking (Klomp et al. 2010; Tee and Pause 2013; Dunlop et al. 2014; Yan et al. 2016a). Despite this breadth of function, its currently unclear how FLCN loss contributes to the development of RCC. Therefore, to better define the tumour suppressor role of FLCN a protein-protein interaction assay, using FLCN as bait, was carried out. This revealed that FLCN interacts with numerous proteins involved in DNA-damage response and/or cell cycle regulation. To explore this further, RNAi was used to generate *FLCN* knockdown in human proximal tubule kidney cells. In this study, FLCN was demonstrated to interact with DNA-dependent protein kinase catalytic subunit (DNA-PKcs); the apical protein in non-homologous end joining repair (NHEJ) of double strand DNA breaks (DSB). The association of FLCN with DNA-PKcs was shown to weaken when cells are subjected to DNA damage (via ionising radiation). As a direct consequence of FLCN knockdown evidence suggest kidney cells accumulate double-strand DNA damage. Furthermore, FLCN-deficient cells display perturbed G1/S checkpoint and it is thought these cells prematurely commit to cellular division. Ultimately, this thesis highlights a novel role of FLCN within renal cell tumorigenesis and suggests it could function to maintain genomic stability. Our basic understanding of RCC within the general population is limited. Nevertheless, genetic conditions (such as BHD) that predispose individuals to cancer, provide valuable insights into somatic tumour development. By using BHD syndrome as a model of genetic instability, further work should focus on mechanistically establishing FLCN's role in genomic integrity and will provide valuable insight into sporadic renal cancer within the general population.

Abbreviations

ABC lymphoma	Activated B-cell
ACC	Acetyl-CoA carboxylase
AEC	Alveolar epithelial cells
AICAR	5-Aminoimidazole-4-carboxamide ribonucleotide
AMPK	5' AMP-activated protein kinase
APBB1	Amyloid beta A4 precursor protein-binding family B member 1
ATM	Ataxia telangiectasia mutated
ATP	Adenosine triphosphate
ATR	Ataxia telangiectasia and Rad3 related
BC	Betweenness centrality
BER	Base excision repair
BHD	Birt-Hogg-Dube
BRCA1	Breast Cancer Type 1 Susceptibility Protein
BRCA2	Breast Cancer Type 2 Susceptibility Protein
BrdU	5-bromo-2'-deoxyuridine
BSA	Bovine serum albumin
C.elegans	Caenorhabditis elegans
CC	Closeness centrality
CDK	Cyclin-dependent kinases
cDNA	Copy deoxyribonucleic acid
Chk1	Checkpoint kinase 1
Chk2	Checkpoint kinase 2
CT	computerized tomography
CYP1A1	cytochrome P4501A1
dBHD	Drosophila melanogaster homolgue of folliculin
ddH2O	Double distilled water
DDR	DNA damage response
DEGs	Differentailly expressed genes
DENN	differentially expressed in neoplastic versus normal cells protien domain
DNA-PKcs	DNA-dependent protein kinase catalytic subunit
DSB	Double-strand DNA breaks
dsDNA	Double-strand DNA
DTT	Dithiothreitol
EdU	5-ethynyl-2´-deoxyuridine
EGFR	Epidermal growth factor receptor
eIF4E	Eukaryotic translation initiation factor 4E
FDR	False discovery rate
FLCN	Folliculin
Flcn-1 (OK975)	flcn deficient Caenorhabditis elegans model
FNIP1	Folliculin interacting protien 1
FNIP2	Folliculin interacting protien 2
GABARAP	Gamma-aminobutyric acid receptor-associated protein
GAP	GTPase-activating proteins

GCB lymphoma	Germinal center B-cell
GEF	Guanine nucleotide exchange factors
GG-NER	Global genomic -nucleotide excision repair
GO-BP	Gene ontology cellular component
GO-CC	Gene ontology biological processes
GPNMB	Transmembrane glycoprotein NMB
GSEA	Gene set enrichment analysis
GST	Glutathione S-transferases
HBE	Human bronchial epithelial
HCC1937	Breast epithelial cell line
HEK293	Human embryoic kideny cells 293
HeLa cells	Cervical carcinoma cell line
HIF	Hypoxia-inducible factor
His3	Histone 3
HK2	Human proximal tubule 2 cells
HOCT	hybrid oncocytic/chromophobe tumor
HOX	homeobox genes
HP	High passage
HR	Homologous recombination
HRP	Horseraddish peroxidase
HSP90α	Heat-shock protein 90 alpha
IMCD-3	Murine inner medullary collecting duct cells
Indel	Insertion deletion
IPA	Ingenuity Pathway Analysis
IR	Ionising radiation
k	Degree
KD	Knockdown
KIF3A	Kinesin-like protein
LC-MS/MS	Liquid chromatography–mass spectrometry / mass spectrometry
LDHA	Lactose dehydrogenase
Lig IV	DNA ligase IV
LKB1	Liver kinase B1
LP	Low passage
MDM2	Mouse double minute 2 homolog
MEFs	Mouse embryonic fibroblasts
MMR	Mis-match repair
MRI	Magnetic resonance imaging
mTOR	Mechanistic target of rapamycin
mTORC1	Mechanistic target of rapamycin complex 1
mTORC2	Mechanistic target of rapamycin complex 2
NaCl	Sosium chloride
NER	Nucleotide excision repair
NHEJ	Non-homologue end joining
NRF1	Nuclear Respiratory Factor 1
NRF2	Nuclear Respiratory Factor 2
PALB2	Partner and localizer of BRCA2

PARP1	Poly [ADP-ribose] polymerase 1
PBS	Phosphate buffered saline
PCC	Pearson's correlation coefficient
PCNA	Proliferating cell nuclear antigen
PCR	Polymerase chain reaction
PGC1α	Peroxisome proliferator activated receptor gamma coactivator 1 alpha
PLCB1	Phospholipase C Beta 1
PP2A	Protein phosphatase 2
PPI	Protein-protein interaction
PVDF	Polyvinylidene fluoride
qPCR	quantitative polymerase chain reaction
Rb	Retinoblastoma protein
RIF1	Telomere-associated protein RIF1
RNA-Seq	RNA sequencing
ROS	Reactive oxygen speices
RPA1	Replication Protein A1
RPA2	Replication Protein A2
Rpt4	26S proteasome subunit RPT4
S.pombe	Schizosaccaromyces pombe
SDS-PAGE	sodium dodecyl sulfate–polyacrylamide gel electrophoresis
shRNA	short hairpin RNA
siRNA	small interfering RNA
SNP	Single-nucleotide polymorphism
SP1	Transcription Factor Sp1
SQSTM1/p62	Sequestosome-1
SSBs	Single-strand breaks
TAMs	Tumour associated macrophage
TBST	Tris-buffered saline tween
TC-NER	Transcription-coupled nucleotide excision repair
TFAM	transcription factor A, mitochondrial
TGFA	Transforming Growth Factor Alpha
TSC1	Tuberous Sclerosis 2 Protein
TSC2	Tuberous Sclerosis 1 Protein
ULK1	Unc-51 Like Autophagy Activating Kinase 1
UV	Ultraviolet index
VHL	Von Hippel-Lindau
WT	Wild type
XLF	XRCC4-like factor
XPO1	Exportin 1
XRCC4	X-ray repair cross-complementing protein 4

Table of Content

List of figures and tables

Chapter 1: Introduction

1.1 A putative tumour suppressor protein; folliculin

Birt–Hogg–Dubé syndrome (BHD) is an autosomal dominant disorder predisposing individuals to lung cysts, spontaneous pneumothorax, fibrofolliculomas, and renal cell carcinoma (Nickerson et al. 2002; Zbar et al. 2002). BHD was first described in 1977 (Birt et al. 1977), however, it wasn't until 2002 that the gene encoding folliculin (FLCN) was identified, and its mutations associated with the disease (Nickerson et al. 2002). FLCN is a putative tumour suppressor, of which the cellular function is currently undefined.

1.1.1 The folliculin gene

FLCN was first mapped by genome wide linkage analysis, using polymorphic microsatellite markers, linking the gene to chromosome 17p12-q11.2 (Khoo et al. 2001; Schmidt et al. 2001). The *FLCN* gene was identified shortly after when the critical region was narrowed to a 700 kb segment on 17p11.2 (Nickerson et al. 2002). This genomic region is rich in unstable, low-copy number repeat elements. These are often subject to aberrant recombination events, resulting in deletions and duplications of the region (Stankiewicz and Lupski 2002). Deletions within this region cause Smith-Magenis Syndrome (Lucas et al. 2001), while duplications cause Charcot-Marie-Tooth Syndrome (Patel et al. 1992). Curiously, while the *FLCN* gene is often heterozygously deleted in Smith-Magenis Syndrome, patients do not seem to develop any BHD associated symptoms (Truong et al. 2010).

The *FLCN* gene contains 14 exons spanning approximately 30 kb of genomic DNA (Figure 1.1) (Nickerson et al. 2002). To date 194 different *FLCN* mutations have been identified; 149 of which are thought to be pathogenic (Fokkema et al. 2011). Most of the mutations are predicated to introduce a premature stop codon and result in a C-terminal truncated FLCN protein (Nickerson et al. 2002; Schmidt et al. 2005). Exon 11 is a mutation hotspot and contains a mononucleotide tract of eight cytosines (C8). Over half the mutations identified in exon 11 involve either a cytosine insertion or deletion; probably

caused by a slippage-mediated mechanism during DNA replication (Khoo et al. 2001; Nickerson et al. 2002; Schmidt et al. 2005). More recently, a second mutational hotspot was described within the non-coding region of exon 1. This region contains the *FLCN* promoter and the identified mutations were predicted to dramatically reduce FLCN expression (Benhammou et al. 2011).
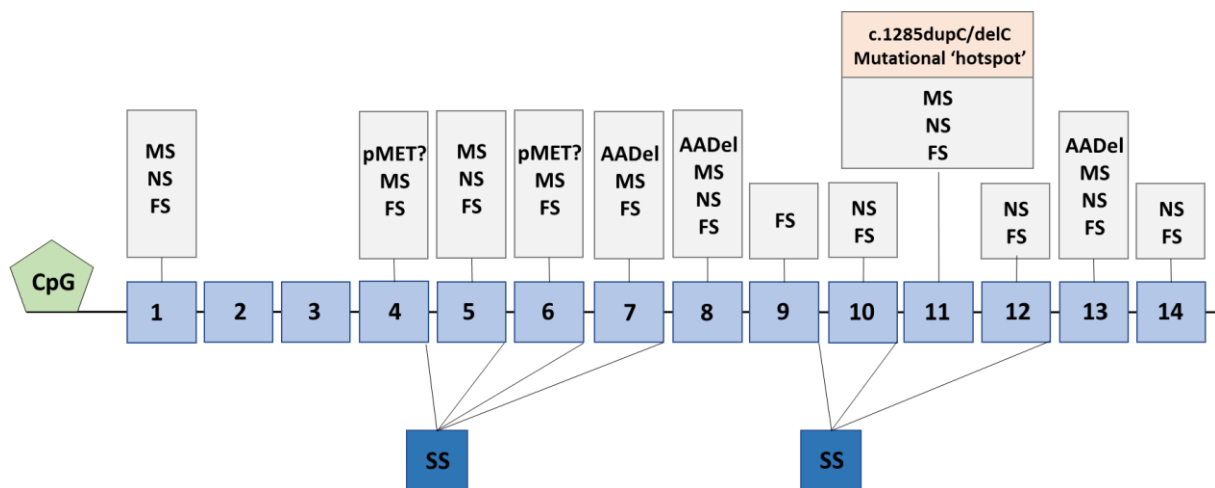
Figure 1.1 The mutation spectrum of the folliculin (FLCN) gene. Abbreviations: pMET = proposed deletion of initiator codon; MS = missense; FS = frameshift; NS = nonsense; AADel = amino acid deletion in-frame; SS = splice site. Image adapted from (Schmidt and Linehan 2015; Zhang et al. 2016).

1.1.2 The folliculin protein

The human FLCN protein is 579 amino acids long (64 kDa), comprising of a short hydrophobic N-terminal sequence, a single N-glycosylation site, three myristoylation sites and a glutamic acid-rich coiled coil domain located centrally in the protein (Nickerson et al. 2002). While FLCN is a highly evolutionarily conserved protein, the sequence has no significant homology to any known protein (Nickerson et al. 2002). It does, however, share domain similarities with proteins involved in cell trafficking. X-ray crystallography of FLCN's C-terminal domain (PDB ID: 3V42, figure 1.2A) shows a β-sheet with helices on one side, followed by an all helical region (Nookala et al. 2012). This formation is akin to differentially expressed in normal and neoplastic cells (DENN) domain proteins (figure 1.2B). The DENN domain is a poorly characterised protein component. Proteins that contain a DENN domain

typically function as Rab guanine nucleotide exchange factors (GEFs) (Marat et al. 2011) and facilitate the recruitment of effectors that control multiple aspects of membrane trafficking. To date, the N-terminal domain of FLCN remains uncharacterised. Work is currently ongoing to establish the crystal structure of this region; it has been computationally predicted to form the longin domain. Longin domains seem to be important for regulating membrane trafficking and are typically present in other DENN-domain containing proteins. The N- and C-terminal domains of FLCN are connected by a 40 amino acid flexible linker region, containing a bipartite tryptophan (WD-WQ) motif, sharing similarity with a binding motif present in the intracellular trafficking protein, kinesin light chain 1 (Dodding et al. 2011). Collectively, early studies into its structure suggest FLCN may play a role in membrane trafficking.
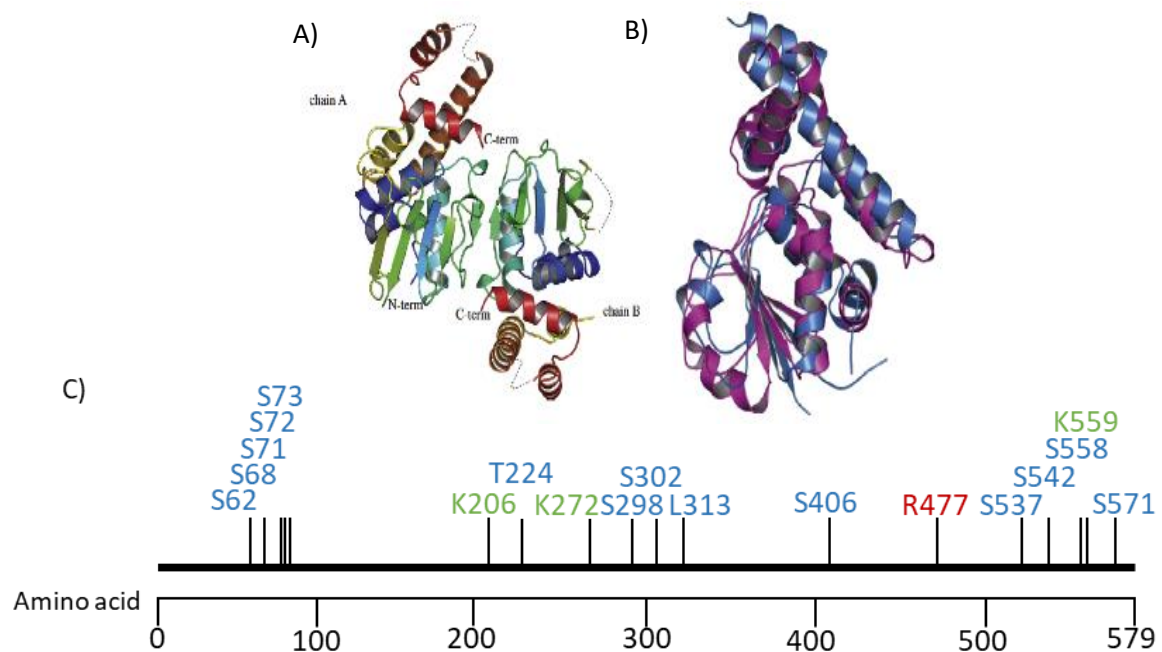
Figure 1.2 The folliculin (FLCN) protein. A) Crystal structure of C-terminal domain of FLCN at 2Å resolution. Two FLCN molecules are present in the asymmetric unit. The N-terminus of the FLCN molecule is blue and the C-terminus is red. B) C-terminal domain of FLCN is structurally similar to the DENN domain of DENN1B protein. C-terminal domain of FLCN is shown in blue and DENN domain of DENN1B is shown in magenta. Images A and B taken from (Schmidt and Linehan 2018). C) Post-translational modification sites of FLCN. Single letter amino acid code used to denote amino acid that is modified, S = serine; T = threonine; K = lysine; R = arginine. Posttranslational modification sites were identified using PhosphositePlus® online resource, blue text = phosphorylation, green text = ubiquitination, red text = methylation.

1.1.2.1 Post-translational modifications

Several post-transcriptional modification sites have been identified on FLCN; the majority of which are phosphorylation events (figure 1.2C). Of note, serine 62 (Ser62) phosphorylation is indirectly up-regulated by 5'-AMP activated protein kinase (AMPK) (Wang et al. 2010) and phosphorylation at Ser302 by an unknown kinase(s) downstream of mTORC1 (Piao et al. 2009). Given that mTORC1 is known to be down regulated by AMPK, this process could be a feedback mechanism that regulates mTOR signalling. Furthermore, mTORC1 has been shown to phosphorylate Ser62 and Ser73 of FLCN (Yu et al. 2011). Interestingly, phosphorylation of these sites appears to be cell-cycle related, where Ser62 and Ser73 of FLCN become phosphorylated as the cell cycle progresses, with the maximum number of phosphorylated protein seen during the mitotic phase (Dephoure et al. 2008; Laviolette et al. 2013). These modifications correlated with a reduction in FLCN stability (Laviolette et al. 2013). Additionally, the Ser302 site is maximally phosphorylated during G1 phase (Dephoure et al. 2008), but it is unclear why.

ULK1 inhibits FLCN's interaction with GABARAP by phosphorylating three sites in the C-terminus of FLCN; Ser406, Ser537 and Ser542. However, ULK1 was still able to block the interaction of GABARAP and a triple serine-to-alanine FLCN mutant *in vitro*, meaning other phosphorylation sites in FLCN, GABARAP and/or the FNIP proteins (see section 2) are important for this interaction (Dunlop et al. 2014). Two other ULK1 phosphorylation sites were identified at Ser316 and Thr317, but these are not well conserved between species (Dunlop et al. 2014).

Additional post-translational modifications include: phosphorylation events on Thr244, Ser298, Ser558, and Ser571 (Sharma et al. 2014; Parker et al. 2015); ubiquitination on lysine residues lys206, lys272 and lys559 (Wagner et al. 2011; Udeshi et al. 2013); and monomethylation at arginine 477 (Larsen et al. 2016) (figure 1.2C). The relevance of these post-translational FLCN modifications have yet to be determined.

1.2 Interacting partners of FLCN

1.2.1 Folliculin-interacting protein 1 (FNIP1)

Due to its lack of homology with known functional domains, efforts to define FLCN's function have shifted from structural studies to looking for interacting partners to define FLCN's role. The first protein partner identified through co-immunoprecipitation studies was 'folliculin interacting protein 1' (FNIP1), a 130 kDa protein also without recognisable functional domains. FNIP1 is expressed in a similar pattern to FLCN (Baba et al. 2006), and binds to FLCN's C-terminus (Baba et al. 2006). FNIP1 was found to interact with AMPK, a heterotrimeric Ser/Thr protein kinase that serves as a critical energy sensor in cells and a negative regulator of mTOR complex 1 (Baba et al. 2006; Shackelford and Shaw 2009). FLCN interacted with the FNIP1/AMPK complex *in vitro* but was not essential for the FNIP1/AMPK interaction. FNIP1 preferentially binds the phosphorylated form of AMPK, and both FLCN and FNIP1 can be phosphorylated by AMPK (Baba et al. 2006). FNIP1 immunoprecipitates are enriched with the phosphorylated forms of FLCN (Baba et al. 2006). Mutation of Ser62 within FLCN does not affect FNIP1 binding to FLCN, but slightly reduces FLCN's binding to the AMPKα1 subunit. Therefore, it is thought that FLCN phosphorylation at Ser62 may stabilise or enhance the association of the AMPK/FNIP1/FLCN protein complex (Wang et al. 2010).

1.2.2 Folliculin-interacting protein 2 (FNIP2)

A second folliculin-interacting protein, FNIP2 was identified through bioinformatic analysis of sequence databases for FNIP1 homologs (Hasumi et al. 2008; Takagi et al. 2008). FNIP2 has 49% identity and 74% similarity to FNIP1 (Hasumi et al. 2008). The tissue expression of *FNIP2* mRNA is similar to both FNIP1 and FLCN, suggesting that both FNIP1 and FNIP2 may have redundant function to regulate FLCN. Preferential *FNIP2* expression is found in fat, liver, kidney and pancreas, which may imply a more specific function of FNIP2 in metabolic tissues (Hasumi et al. 2008). Similar to FNIP1, FNIP2 also interacts with the C-terminus of FLCN and is directly phosphorylated by AMPK (Hasumi et al. 2008; Takagi et al. 2008).

1.2.3 Functional studies in FNIP1/FNIP2-*deficient in vivo models*

Although identified as FLCN-binding partners, FNIP1 and FNIP2 are themselves newly discovered proteins, and studies are ongoing to determine how FNIP1 and FNIP2 function with FLCN. So far, mice knockout models on *Fnip1* show B-cell deficiency due to a block in B-cell development. Two models suggest this phenotype was caused by caspase-induced cell death and was rescued by expression of the anti-apoptotic protein Bcl2 (Baba et al. 2012; Siggs et al. 2016). A third mouse model showed *Fnip1* deficiency resulted in increased AMPK and peroxisome proliferator-activated receptor gamma coactivator 1 alpha (PGC1α) expression leading to increased mitochondrial biogenesis and dysregulation of pre-B cells (Park et al. 2012). Furthermore, *Fnip1*-deficient mice were also reported to develop cardiomyopathy (Hasumi et al. 2015; Siggs et al. 2016). A switch from type 2 "fast twitch" to type 1 "slow twitch" skeletal muscle fibre, and an increase of AMPK activation and expression of its target PGC1α leading to increased mitochondrial biogenesis (Reyes et al. 2015) was also observed. The significance of these findings remains uncertain. BHD patients with germline F*LCN* mutations do not develop B-cell or muscle tissue manifestations highlighted by the *Fnip1*-deficient mice, suggesting FNIP1 has function independent of FLCN.

Mice with kidney-targeted *Fnip1* and *Fnip2* double inactivation develop cystic kidneys, that express elevated levels of PGC1α and display increased mitochondrial biogenesis (Hasumi et al. 2015), mimicking the phenotype of kidney-targeted *Flcn* knockout mice (Baba et al. 2008; Chen et al. 2008). In addition, both heterozygous inactivation of *Fnip1* or homozygous inactivation of *Fnip2* causes renal tumours in mice. Therefore, at least within the kidney, these proteins are somewhat redundant in function (Hasumi et al. 2015).

Interestingly, FNIP1 and FNIP2 were shown to form homodimers and heterodimers with each other. FLCN and AMPK subunits were present in all immunoprecipitates containing these FNIP1/FNIP2 multimeric complexes (Hasumi et al. 2008). The functional significance of the varying FNIP1/FNIP2 multimeric complexes awaits further investigation to clarify their impact on FLCN function, and on cellular signalling.

1.3 Pathways and cellular processes associated with folliculin function

Since its identification in 2002, several genetic and biochemical studies have attempted to understand the molecular function of FLCN. To date FLCN has been implicated in a number of diverse cellular processes; however, there are inconsistencies in the roles found for FLCN. Therefore, the tumour suppressor function of FLCN remains unclear. Recognised functions of FLCN are discussed below.

1.3.1 Membrane trafficking and GTPases function

Initial studies suggested FLCN may have a role in membrane trafficking. Collectively, X-ray crystallography, fold recognition, and structure prediction software identified a DENN-like domain in the C-terminal of FLCN (Nookala et al. 2012). DENN domains are found within the Rab guanine exchange factor (GEF) protein family whose members function as regulators of membrane trafficking (Marat et al. 2011). GEFs activate Rab proteins by mediating the exchange of GDP for GTP. *In vitro*, the C-terminal domain of FLCN was shown to have GEF activity towards Rab35 (Nookala et al. 2012).

FLCN has also been linked to another GTPase protein family; the Rag GTPases. These play an important role in amino acid signalling and FLCN was shown to interact with Rag proteins at the lysosome (Petit et al. 2013; Tsun et al. 2013). Interestingly, FLCN may have a dual function, as it can also act as a GEF and a guanine activating protein (GAP) to members of the Rag GTPase family. One study suggested FLCN may have GEF activity for Rag A (Petit et al. 2013), while another showed FLCN may act as a GAP for Rag C/D (Tsun et al. 2013). FLCN's role with Rag GTPases is discussed in section 1.3.2.1. Additionally, FLCN's C-terminal domain has also been shown to bind with Rab7A, and wild-type FLCN is able to stimulate Rab7A GTP hydrolysis (Laviolette et al. 2017). Rab7A plays a central role in endosomal recycling and lysosomal degradation of epidermal growth factor receptor (EGFR). FLCN loss resulted in slower endocytic trafficking and an accumulation of EGFR in early endosomes, where the ligand-stimulated EGFR signalling cascade can still be active. EGFR activation is also observed in FLCN-deficient mouse tumours and BHD-associated kidney tumours (Laviolette et al. 2017). FLCN has also been shown to interact directly, via its C-terminal domain, with the Rab34 effector RILP. This interaction promotes

the loading of active GTP-bound Rab34 onto RILP during nutrient withdrawal and causes peri-nuclear clustering of lysosomes (Starling et al. 2016). Collectively, the experimental evidence to date reveals that FLCN likely has dual functionality, acting as both a GAP and GEF for small GTPase in order to regulate vesicle trafficking linked to nutrients.

1.3.2 mTOR signalling pathway

The mammalian target of rapamycin (mTOR) signalling pathway serves as a central regulator of cell metabolism, proliferation, and survival. It is commonly dysregulated in many cancers (Rad et al. 2018). FLCN's involvement in mTOR signalling is complicated and the literature has contradictory findings. *Flcn* heterozygous knockout mice develop kidney tumours with a long latency (> 10 months) only after having lost the wild type *Flcn* allele. Within these FLCN deficient tumours, increased activation of AKT, a substrate of mammalian target of rapamycin complex 1 and 2 (mTORC1 and mTORC2) can be observed (Hasumi et al. 2009). When *Flcn* knockdown is targeted to mice kidneys, mice die by 3 weeks of age due to enlarged polycystic kidneys and renal failure (Baba et al. 2008; Chen et al. 2008). When analysed, the renal cysts displayed elevated levels of phosphorylated AKT (p-AKT), phosphorylated mTOR (p-mTOR) and phosphorylated ribosomal protein S6 (p-RPS6, a downstream effector and surrogate marker of mTOR activity) demonstrating hyperactivation of the mTORC1 pathway in *Flcn*-deficient mice kidneys (Baba et al. 2008; Chen et al. 2008). Furthermore, when targeted exclusively to the proximal tubules in the kidney of mice, FLCN deletion led to renal cysts and early onset renal neoplasms (≥ 6 months) with high tumour penetrance (Chen et al. 2015). These growths also displayed elevated levels of p-AKT, p-mTOR, and p-RPS6. Furthermore, treatment with the mTOR inhibitor rapamycin limited the cystic formations and tumour growths in mice (Baba et al. 2008; Chen et al. 2008; Chen et al. 2015). In humans, renal tumours from BHD patients with germline *FLCN* mutations also present hyperactivated mTORC1 signalling (Baba et al. 2008; Hasumi et al. 2008). Increased p-mTOR and p-RPS6 were found in cyst-lining epithelial cells from BHD patient lungs, and increased p-RPS6 protein levels were seen in human lung-derived cells with *FLCN* knockdown (Khabibullin et al. 2014).

Collectively, these data support a role for FLCN in suppressing mTORC1 activation. Nonetheless, there also exists evidence to suggest FLCN may have an activating role in the mTORC1 pathway. In the yeast model, *Schizosaccharomyces pombe* (*S. pombe*), deletion of the *Flcn* homolog, *bhd*, resulted in hypersensitivity to rapamycin suggesting that *bhd* activates the yeast Tor (van Slegtenhorst et al. 2007). In mice, two *in vivo Flcn* knockdown models showed additional evidence that FLCN may positively regulate mTORC1 signalling. In the first model, mice developed micro-cysts and presented with a low frequency of oncocytic tumours. These oncocytic tumours displayed a reduction in their p-RPS6 immunostaining, suggesting less mTORC1 activity (Hartman et al. 2009). The second *in vivo Flcn* knockdown model developed numerous renal cysts and adenomas over a wide age range. p-RPS6 immunostaining was variable and depended on cyst size and number; showing elevated expression in large, multilocular cysts and weak to no p-RPS6 staining in small, single cysts (Hudon et al. 2010). Reduced p-RPS6 has also been observed in several mammalian cell lines with transient downregulation of FLCN (Takagi et al. 2008; Hartman et al. 2009; Bastola et al. 2013).

This conflicting data suggests FLCN loss, particularly with the regards to renal tumours, is more complex than a simple activation of mTORC1, and may depend upon cell type and knockdown method (Khabibullin et al. 2014). Mice models that revealed that FLCN inhibits mTORC1 signalling where created using a Cre/LOX system, whereas models supporting an activating role were created using gene trap vector technology. It could also be dependent on nutritional/energy status of cells (See section 3.2.1 for more information) (Hudon et al. 2010; Tsun et al. 2013). Equally, FLCN loss may affect additional signalling pathways, such as Raf-MEK-ERK signalling, that in turn can affect mTORC1 signalling (Baba et al. 2008).

1.3.2.1 Interaction with Rag GTPases for amino acid-dependent mTORC1 activation on lysosomes

FLCN is selectively recruited to the lysosome after amino acid starvation and may have a role in nutrient-dependent lysosome-associated regulation of mTORC1 (Petit et al. 2013; Tsun et al. 2013). mTORC1 integrates cellular signals from nutrients, growth factors and energy to drive cellular proliferation and inhibit nutrient scavenging. Nutrients, such as amino acids, glucose and lipids, drive the recruitment of mTORC1 to the lysosomes via

the Rag GTPases (Bar-Peled and Sabatini 2014). The 'inactive' combination of guanosine diphosphate (GDP)-loaded Rag A/B and guanosine triphosphate (GTP)-loaded Rag C/D cannot bind to mTORC1, which remains indolent in the cytoplasm. The 'active' GTP-loaded Rag A/B and GDP-loaded Rag C/D complex, on the other hand, engage mTORC1 to the lysosomal surface (Bar-Peled and Sabatini 2014).

FLCN's interacting partners, FNIP1 and FNIP2, have been shown to interact with Rag proteins and are necessary for starvation-induced localisation of FLCN to the lysosomes. In turn, the FLCN-FNIP1/2 complex allows the dissociation of mTORC1 from the lysosomes (Tsun et al. 2013). It is unclear if FLCN functions as a GAP or GEF, and how FNIP1/2 are required for this process. *In vitro* purified FLCN-FNIP2 complexes stimulated GTP hydrolysis by Rag C and Rag D, but not by Rag A or Rag B (Tsun et al. 2013) suggesting FLCN-FNIP2 acts as a GAP complex for Rag C/D and promotes mTORC1 localisation to the lysosomal surface. However, another study reports that FNIP1, not FNIP2, facilitated this process (Petit et al. 2013). Furthermore, FLCN has been shown to preferentially bind the inactive or GDP-loaded Rag A through its GTPase domain (Petit et al. 2013). This is a property commonly seen in GEFs, suggesting it may function as a GEF towards RagA/B. In both cases, FLCN was selectively recruited to the lysosome after amino acid depletion and interacted with Rag GTPase heterodimers. These data underscore the role of the FNIP proteins in facilitating the nutrient-dependent lysosome association of FLCN. Consistently, FLCN was required for the recruitment and activation of mTORC1 in response to amino acids. However, taking into account previous work on mTOR signalling, it is still not clear if FLCN's ability is to either inhibit or activate mTORC1.

Furthermore, the cellular signals that send FLCN to the lysosome under nutrient-depleted conditions remain uncertain. In Hela and *FLCN*-deficient/*FLCN*-restored UOK257 renal tumour cells, FNIP1 and FNIP2 are thought to be unstable when nutrients are abundant and mTORC1 is active (Nagashima et al. 2017). Given that FNIP1/FNIP2 were shown to be necessary for starvation-induced localisation of FLCN on the lysosomes and for dissociation of mTORC1 from the lysosomes, FLCN nutrient-dependent lysosomal association is likely facilitated by the FNIP proteins.

1.3.3. Adenosine monophosphate (AMP)-activated protein kinase (AMPK) pathway signalling

Similar to mTOR, AMPK is considered a master regulator of energy homeostasis within the cell. AMPK directly regulates energy by phosphorylating metabolic enzymes and nutrient transporters, and indirectly regulates energy production by promoting the transcription of genes involved in mitochondrial biogenesis and function. AMPK acts upstream of mTOR, which both function as energy sensors responding to and maintaining energy balance within tissues. AMPK phosphorylates and activates ULK1, which is a negative regulator of mTOR (Dunlop et al. 2014). Furthermore, AMPK can directly phosphorylate Tuberous Sclerosis Complex 2 (TSC2) (Inoki et al. 2003), which switches Rheb to an inactive GDP-bound state to turn off mTOR (Tee et al. 2003). The interplay of AMPK and mTOR allows cells to coordinate an appropriate response to environmental conditions and helps the cell maintain energy homeostasis. Activated AMPK turns on catabolic pathways to enhance ATP production, while turning off anabolic pathways that consume ATP. mTOR responds to energy availability through AMPK, and in turn determines the rate of cell growth and proliferation. Cellular levels of ATP increase mTOR signalling, as AMPK is switched off.

FLCN has been shown to interact with AMPK through its protein partners FNIP1 and FNIP2 (Baba et al. 2006; Hasumi et al. 2008; Lim et al. 2012; Possik et al. 2014). Both FLCN and FNIP1 serve as substrates for AMPK *in vitro* (Baba et al. 2006). The association of FLCN, FNIP1/2, and AMPK in immunoprecipitates from multiple cell types suggests that they exist in a complex. As previously mentioned, investigations into the functional relationship between FLCN, FNIP1/2 and AMPK *in vitro* and *in vivo* have been ambiguous (see section 2). FLCN deficiency has been shown to facilitate AMPK activation in a variety of models including; nematodes, FLCN-null thyroid carcinoma cells, mouse embryonic fibroblasts (MEFs), the kidneys of mice and in BHD-associated renal tumours (Possik et al. 2014; Yan et al. 2014) Loss of *FLCN* results in the activation of AMPK and, through Hypoxia Inducible Factor (HIF) signalling, leads to large metabolic changes consistent with the Warburg effect (Possik et al. 2014; Yan et al. 2014). AMPK is a key regulator of glycogen metabolism. Acute activation of AMPK leads to the phosphorylation and inhibition of glycogen synthase, and favours glycogen degradation for supply of short-term energy (Wojtaszewski et al. 2002; Miyamoto et al. 2007). However, chronic AMPK activation results in glycogen accumulation

via glucose-6-phosphate-dependent allosteric activation of glycogen synthase bypassing the inhibitory effect of the AMPK-mediated phosphorylation (Hunter et al. 2011). An important role for glycogen is in organismal survival during stress. Indeed, *flcn-1* deficiency in nematodes supported a higher resistance to hyperosmotic stress due to increased glycogen storage by AMPK (Possik et al. 2014). Glycogen is often used by tumour cells to survive harsh microenvironments, such as hypoxia (Favaro et al. 2012; Zois et al. 2014). Indeed, glycogen accumulation occurs in many cancer types (Zois et al. 2014).

Conversely, FLCN loss has also been shown to decrease AMPK signalling. *FLCN*-deficient UOK257 cells, *Flcn*-null primary mouse alveolar epithelial cells (AEC), and siRNA-induced *Flcn* knockdown in mouse epithelial NMuMG cells all display reduced AMPK activation under nutrient deprivation (Goncharova et al. 2014). Within the lungs of mice, loss of FLCN results in cell apoptosis as a result of impaired AMPK activation and increased cleavage of caspase3. Treatment with AICAR, an AMPK activator, or constitutively active AMPK-mutant improved cell survival, lung surface tension and reduced an inflammatory response (Goncharova et al. 2014). Nevertheless, FLCN has been shown to have highly cell-type-specific outcomes. In the same study, knockdown of FLCN in human bronchial epithelial (HBE) cells decreased the phosphorylation of acetyl-CoA (p-ACC), a marker of AMPK activation, while downregulation of FLCN in small airway epithelial (SAEC) cells increased the activity of AMPK (Khabibullin et al. 2014). Collectively, the majority of the published literature supports FLCN acting as a negative regulator of AMPK. While it remains unclear exactly how FLCN regulates AMPK, FLCN appears to be required for a cell to respond appropriately to energy supply, where loss of function of FLCN can lead to metabolic transformation.

1.3.3.1. PPARGC1A/PGC1α regulation and mitochondrial biogenesis driven by AMPK signalling

AMPK activates signalling pathways that promote mitochondrial biogenesis and energy bioavailability, such as peroxisome proliferator–activated receptor gamma coactivator–1α (PGC-1α). PGC-1α is the principal transcription factor for mitochondrial biogenesis, and transactivates nuclear respiratory factors 1 and 2 (NRF1 and NRF2). In turn NRF1 and NRF2

increase the expression of the transcription factor A (TFAM), leading to mitochondrial gene transcription (Marin et al. 2017).

Loss of FLCN in MEFs results in elevated PGC-1α expression, mitochondrial biogenesis and ATP production though the increased activity of AMPK. This leads to reactive oxygen species (ROS)-dependent activation of HIF-1α and a metabolic switch to aerobic glycolysis (Yan et al. 2014). Furthermore, *Flcn* knockdown in *Ampk*-deficient MEFs did not change PGC-1α expression or ROS levels, suggesting AMPK activation is the driving force for the PGC-1α-initiated metabolic switch following the loss of FLCN (Yan et al. 2014). Similarly, chronic hyperactivation of AMPK *in vivo* sequentially lead to PGC-1α-driven mitochondrial biogenesis, which then enhanced oxidative metabolism and metabolic reprogramming (Yan et al. 2016a). When targeted to mouse adipose tissue, *Flcn* inactivation led to a "browning" of white adipose tissue due to AMPK-dependent PGC-1α-, TFE3-, and mTORC1-dependent transcriptional control of energy metabolism (Wada et al. 2016; Yan et al. 2016a). When targeted to mouse kidney and muscle, *Flcn* inactivation again led to elevated PGC-1α gene expression, an increased number of mitochondria, and enhanced flux through the Krebs cycle (Hasumi et al. 2012). Notably, inactivation of PGC-1α reversed the PGC-1α driven metabolic phenotypes, and limited cystic growth in *Flcn*-deficient mice kidneys (Hasumi et al. 2012). When targeted to mice heart cells, *Flcn* inactivation caused dilated cardiomyopathy and mice die by 3 months of age. However, the *Flcn*-deficient hearts display increased mitochondria, ATP levels, and PGC-1α levels (Siggs et al. 2016). BHD-associated renal tumours demonstrate upregulation of both PGC-1α and TFAM transcription factors, along with a subset of PGC-1α regulated genes, all of which are known drivers of mitochondrial biogenesis (Klomp et al. 2010).

Collectively, the evidence emphasises a central role for FLCN as a negative regulator of PGC-1α and mitochondrial biogenesis and suggests that AMPK activity causes an enhanced metabolic state upon the loss of FLCN. Tumour development in BHD may be driven, at least in part, by dysregulation of the PGC1α-TFAM axis.

1.3.4 Regulation of cell-cell adhesion, cell polarity, and RhoA activity

FLCN has been linked to cell-cell adhesion through a direct interaction with p0071 (PKP4/plakophilin) (Medvetz et al. 2012; Nahorski et al. 2012; Khabibullin et al. 2014). p0071 is a member of the armadillo repeat containing protein family that also includes beta-catenin (β-catenin). p0071 binds E-cadherin at adherens junctions and regulates the activity of the small GTPase RhoA in the cytoplasm (Hanna and El-Sibai 2013). RhoA signalling controls cytoskeletal remodelling, and regulation of focal adhesion that is required for cell migration (Hanna and El-Sibai 2013). FLCN has been shown to regulate RhoA signalling in a number of cell lines, where loss of FLCN enhanced cell-cell adhesion (Medvetz et al. 2012; Nahorski et al. 2012; Khabibullin et al. 2014). This suggests the FLCN-p0071 protein complex acts as a negative regulator of cell-cell adhesion. Interestingly, FLCN-deficient thyroid cancer cells displayed a more migratory phenotype when compared to wild-type controls, whereas data from BHD-RCC derived kidney cells suggested a migratory delay. Furthermore, FLCN was shown to negatively regulate cell-cell adhesions in three-dimensional cell cluster assays (Medvetz et al. 2012). Despite conflicting roles as to whether loss of FLCN upregulates or down regulates RhoA signalling, the data supports a role for the interaction of FLCN and p0071 in the regulation of cell-cell adhesion.

FLCN knockdown in polarised mouse inner medullary collecting duct (IMCD-3) cells resulted in a reduction of E-cadherin immunostaining (Nahorski et al. 2012). These cells had a delay in tight junction formation, which led to a disruption of cell polarity. A reduction in E-cadherin has also been noted in primary mouse lung AECs, (Goncharova et al. 2014). Interestingly, loss of E-cadherin is a common event in epithelial cancers, and loss of the RCC tumour suppressor gene, *Von Hippel-Lindau*, is associated with the down-regulation of E-cadherin expression (Esteban et al. 2006).

1.3.5. Regulation of autophagy

Autophagy is a highly controlled process of degrading and recycling damaged organelles and macromolecules to replenish cellular energy and amino acid supply. Within the cytoplasm, materials are sequestered in specialised double membrane vesicles

called autophagosomes. Autophagosomes then fuse with lysosomes and the material is enzymatically degraded (Choi et al. 2013).

FLCN knockdown in a human kidney cell line (HK2), *FLCN*-deficient MEFs and BHD-associated kidney tumour tissue all show an accumulation of the autophagic marker sequestosome1 (SQSTM1/p62), which can be reversed with FLCN reintroduction (Dunlop et al. 2014). In addition, increased endogenous levels of GABA(A) receptor-associated protein (GABARAP), a component of mature autophagosomes, was observed in *FLCN*-deficient HEK293 and HK2 cells, along with impaired maturation of autophagosomes (Dunlop et al. 2014). The FLCN-GABARAP interaction in mammalian cells was shown to be dependent on FNIP1 and FNIP2 association but displayed a preference for FNIP2. In addition, Unc-51 like autophagy activating kinase 1 (ULK1) is an activator of the autophagic process and a GABARAP interactor. ULK1 was shown to phosphorylate FLCN at three serine sites; Ser406, Ser537, Ser542 and the kinase activity of ULK1 was required for FLCN-FNIP2 dissociation from GABARAP (Dunlop et al. 2014). Furthermore, BHD-patient derived FLCN mutations interacted more strongly with ULK1 than the wild type FLCN protein, showed impaired binding to GABARAP, and were not able to reverse SQSTM1/p62 levels as efficiently as wild-type FLCN (Dunlop et al. 2014) suggesting FLCN may be a positive modulator of autophagy.

On the other hand, studies exploring the relationship between AMPK and FLCN in the *flcn* deficient *Caenorhabditis elegans* model, *flcn-1*(*ok975*), support an opposing role of FLCN in autophagy. In this model, loss of *flcn-1* increased numbers of autophagic vacuoles and elevated resistance to oxidative stress through the AMPK ortholog, aak-2 (Possik et al. 2014). This resistance was shown to be from increased autophagy and not ROS-related pathways. Furthermore, higher autophagic activity was shown to be *aak-2* dependent and required for resistance to oxidative stress. *Flcn-1* mutants showed an autophagy-driven increase of ATP levels which, in turn, protected against apoptosis. Similar findings have been noted in *Flcn −/−* MEFs and in thyroid carcinoma cells lacking *FLCN* (Possik et al. 2014). Overall, loss of FLCN in worm, mouse and human *in vivo* models resulted in activation of AMPK, elevated autophagy and increased ATP levels conferring resistance to metabolic stress. More in-depth studies will be required to understand these divergent results

regarding a role for FLCN in regulating autophagy. In addition, it is unclear how impaired autophagy may contribute to the BHD syndrome phenotype.

1.3.6. Ciliogenesis and cilia-dependent flow sensory mechanisms

Patients with both von Hippel-Lindau (VHL) and tuberous sclerosis complex (TSC) diseases have similar clinical manifestations to those with BHD, and all are susceptible to renal tumour growths. Both VHL and TSC have previously been linked to dysfunctional primary cilia (Esteban et al. 2006; Hartman et al. 2009). Therefore, a possible role for FLCN in cilia formation was explored. Cilia function as flow sensors and down regulate mTORC1 signalling through flow-mediated activation of Liver Kinase B1 (LKB1). LKB1 in turn phosphorylates and activates AMPK, which negatively regulates mTORC1 via phosphorylation and activation of TSC2 (Boehlke et al. 2010). FLCN was demonstrated to localise to primary cilia in several cell types, with both wild type and mutant forms of FLCN binding to the basal body during early ciliogenesis (Luijten et al. 2013). FLCN knockdown resulted in delayed development of cilia in serum starved cells (Luijten et al. 2013). Primary cilia restrict canonical Wnt signalling by sequestration of β-catenin in the basal body (Lancaster et al. 2011), and abnormal Wnt/β-catenin signalling has been attributed to renal cyst formation (Kotsis et al. 2013). Elevated levels of un-phosphorylated (active) β-catenin and its downstream targets were observed in cultured mouse *Flcn*-deficient cells, suggesting *Flcn* deficiency may lead to kidney and lung cyst formation through defective ciliogenesis, resulting from an inappropriate activation of the canonical Wnt/β-catenin pathway (Luijten et al. 2013). In addition, FLCN was shown to recruit LKB1 to cilia and induce its association with AMPK for activation in response to flow stress (Zhong et al. 2016). Flow stress has been shown to reduce mTORC1 signalling in FLCN–expressing HKC-8 and FLCN-restored UOK257 cells in a cilium-dependent manner, but not in FLCN-deficient cells (Zhong et al. 2016). In the FLCN-deficient cells, increased AMPK activity and AMPK-mediated phosphorylation of TSC2 were attributed to mTORC1 inhibition. Furthermore, Kinesin Family Member 3A (KIF3A) has been identified as a FLCN-interacting protein(Zhong et al. 2016). KIF3A is one of two motor subunits that make up the kinesin-2 motor required for primary cilium assembly and maintenance (Kim and Dynlacht 2013). These results support a role for FLCN as part of the mechanosensory machinery that

controls LKB1 and AMPK activation resulting in mTORC1 pathway inhibition through primary cilia.

1.3.7 Regulation of gene transcription

FLCN is thought to have negative regulatory effects on a broad range of gene transcription (Hong et al. 2010a; Betschinger et al. 2013; Gaur et al. 2013; Petit et al. 2013). In Drosophila, dBHD interacts with Rpt4, a known regulator of ribosomal RNA (rRNA) transcription (Gaur et al. 2013). Loss of dBHD resulted in upregulation of rRNA synthesis. Whereas an overexpression of dBHD reduced rRNA transcription by preventing the association of Rpt4 with the ribosomal DNA locus (Gaur et al. 2013). Similarly, Rpt4 knockdown impedes the growth of FLCN-deficient human renal cancer cells in mouse xenografts (Betschinger et al. 2013).

FLCN has been linked to two key members of the MiT/TFE transcription factor family, TFEB and TFE3 (Hong et al. 2010a; Petit et al. 2013). The MiT/TFE transcription factor family are regulators of cell survival and energy metabolism, through the promotion of genes involved in lysosomal regulation, oxidative metabolism and the oxidative stress response (Slade and Pulinilkunnil 2017). TFEB and TFE3 are considered oncogenes and are often implicated in the development of sporadic renal cell carcinomas (RCC), clear cell sarcomas, and malignant melanoma (Argani et al. 2003; Kauffman et al. 2014). Specifically, TFEB is a master regulator of lysosomal biogenesis (Raben and Puertollano, 2016). Loss of FLCN results in an increase of nuclear TEFB (Petit et al. 2013). Previous work shows the nuclear localisation of TFEB is controlled by mTORC1-dependent phosphorylation of TFEB on serine 211 (Ser211) and inhibits its nuclear localisation when lysosome function is sufficient. TFEB Ser211 phosphorylation was reduced in FLCN-deficient cells, and along with elevated nuclear levels of the protein, an increase in lysosomal proteins was identified (Petit et al. 2013). Furthermore, FLCN has also been shown to be important for the cellular localisation of TFE3. Similar to TFEB, FLCN-deficient cells display a decrease in phosphorylation and elevated nuclear accumulation of TFE3, resulting in the increased expression of target genes (Hong et al. 2010a). In addition, expression of GPNMB, a surrogate for TFE3 activity, was found to be high in BHD-associated kidney tumours and in

kidney tumours from *Flcn* heterozygous knockout mice (Hong et al. 2010a; Furuya et al. 2015). The nuclear sequestration of TFE3 in FLCN-deficient cells is thought to be due to the loss of mTORC1-dependent phosphorylation of TFE3 allowing localisation to the nucleus and activation of its target genes (Wada et al. 2016). FLCN's roles in the regulation of gene transcription seem to centre around the trafficking of transcription factors, ensuring nuclear shuttling only when appropriate.

1.3.8 Summary

In addition to the known functions of FLCN described above, a number of published reports support roles for FLCN in other signalling pathways and cellular processes and include: JAK/STAT signalling (Singh et al. 2006), TGF-β signalling (Singh et al. 2006; Hong et al. 2010b; Cash et al. 2011), Matrix Metalloproteinase signalling (Hayashi et al. 2010; Pimenta et al. 2012), regulation of HIF-1α transcriptional activity (Preston et al. 2011; Yan et al. 2014), the cell cycle (Kawai et al. 2013; Laviolette et al. 2013), and an interaction with HSP90α (Woodford et al. 2016). Collectively, these studies suggest a multitude of cell-type- and/or tissue-specific functions for FLCN that are highly dependent on biological context. As such, FLCN is perhaps better thought of as a globalised regulator of cellular homeostasis rather than having a distinct cellular purpose.

1.4 About Birt-Hogg-Dubé

1.4.1 Epidemiology

Birt-Hogg-Dubé (BHD) syndrome, is a rare genetic disorder resulting from the loss of function of FLCN (Schmidt et al. 2005; Toro et al. 2008) and is characterised by fibrofolliculomas (benign skin tumours), pulmonary cysts, spontaneous pneumothorax (lung collapse), and a predisposition to develop RCCs. As of January 2017, it is conservatively estimated that 613 families worldwide have been diagnosed with BHD. The true incidence of BHD is not known. Due to its rarity and the highly variable penetrance of clinical manifestations, it is speculated to be underdiagnosed (Steinlein et al. 2018). At present there is no clear evidence of a genotype-phenotype correlation between *FLCN* mutations and the symptoms of BHD (Schmidt et al. 2005; Toro et al. 2008). Limited evidence suggests

a correlation between mutation location and pneumothoraces. Mutations within exon 9 and exon 12 are associated with an increase in lung cyst size and number (Toro et al. 2007). Furthermore, mutations within the splice-site of intron 9 (thought to cause skipping of exon 9) have been linked with a higher frequency of renal tumours (Schmidt et al. 2005). These two independent studies suggest that exon 9 may have functional importance, however, more work is needed to confirm these observations.

1.4.2 Diagnosis

Initially, BHD was defined by the presence of at least 5 to 10 fibrofolliculomas, of which at least one papule was diagnosed histologically. The identification of *FLCN* defects in families with BHD led to new insights into the penetrance and clinical variability of this syndrome. Diagnostic criteria are based on DNA testing for FLCN mutations in addition to clinical manifestations. It is worth noting, of those who satisfy diagnostic criteria, 7–9 % do not have an identifiable *FLCN* mutation (Tong et al. 2018). Any individual with early-onset renal cancer, unexplained cystic lung disease (with or without a history of pneumothorax), a familial history of cystic lung disease or renal cancer, or any combination of spontaneous pneumothorax and kidney cancer within the family are recommended for a clinical assessment, pedigree analysis, and FLCN genetic mutation analysis. Mutational assessment is recommended even when the clinical diagnosis of BHD is unambiguous. Detection of a pathogenic *FLCN* mutation not only confirms the diagnosis in the index patient, but also permits pre-symptomatic testing of at-risk relatives. Due to the clinical variability of BHD, genetic testing is imperative; adult at-risk relatives without fibrofolliculomas or pulmonary symptoms can carry the familial mutation. Surveillance in *FLCN* mutation carriers usually begins at 20 years of age. In most centres, pre-symptomatic diagnosis is postponed until the age of 16–18 years to allow for counselling and informed consent before genetic testing. However, earlier testing and surveillance might be used in rare circumstances; for example, families with a history of very early onset of pneumothorax or renal cancer (Tong et al. 2018).

1.4.3 Clinical manifestations

1.4.3.1 Fibrofolliculomas

Around 90% of BHD patients develop benign skin tumours, clinically known as fibrofolliculomas. These appear as small, whitish papules, primarily on the face and neck, usually after 20 years of age (Menko et al. 2009). The number of fibrofolliculomas per individual can range from less than ten to over a hundred (Toro et al. 1999) and likely arise from sebaceous glands (Vernooij et al. 2013). Almost 25% of BHD carriers do not have skin symptoms at the time of diagnosis (Nikolaidou et al. 2016). This is especially true in Asian BHD carriers, where more than half do not report having cutaneous lesions (Furuya et al. 2016). The lesions do not cause any physical problems. Patients, however, often report a psychological burden from having numerous facial lesions.

1.4.3.2 Pulmonary cysts and pneumothorax

Around 90% of BHD patients develop pulmonary cysts and have an increased risk of pneumothorax (spontaneous lung collapse) (Zbar et al. 2002; Predina et al. 2011). Lung anatomy in BHD patients appears normal, and despite the presence of multiple cysts, lung function is not often affected (Toro et al. 2007; Tobino et al. 2012). The size of pulmonary cysts can vary from a few millimetres to over 2cm, and from 30-400 in number (Agarwal et al. 2011; Tobino et al. 2012). Cysts are thought to arise due to defects in cell-cell adhesion in the absence of FLCN leading to repeated respiration-induced stress and, over time, expansion of alveolar spaces (Kennedy et al. 2016).

BHD patients have a 50-fold increase in the risk of pneumothorax and a mean age for the first event of 36 years (Houweling et al. 2011). Pneumothoraces have been reported in BHD patients as young as seven and as old as 73; suggesting the age of onset is highly variable (Bessis et al. 2006; Gunji et al. 2007; Okura et al. 2013; Johannesma et al. 2014b). Pneumothorax is strongly correlated with the number of lung cysts present, and it is thought that the pulmonary cysts increase the risk of pneumothorax by rupturing and releasing air into the chest cavity (Furuya and Nakatani 2013; Johannesma et al. 2014a). Pneumothorax typically occurs in the lower regions of the lung in BHD patients, it is thought that the cysts in the lower region of the lung have more chance of rupturing due to it being a region of

high mechanical stress (more compression) and can be instigated by changes in air pressure, such as flying and scuba-diving.

1.4.3.3 Renal Cell Carcinoma

The most life threatening complication of BHD is predisposition to RCC, where renal cancer is 7-fold more likely to occur in a BHD patient than the general population (Zbar et al. 2002). Haploinsufficiency is enough for the benign skin lesions and lung cysts to develop; however a 'second-hit' in the other FLCN allele is required for RCC to develop (Vocke et al. 2005). This suggests, at least in the kidneys, that FLCN acts as a classical tumour suppressor.

BHD-associated RCC has an average diagnosis age of 50.7 years, 10-15 years earlier than sporadic cases (Pavlovich et al. 2005; Toro et al. 2008; Houweling et al. 2011). Around a third of BHD patients will develop RCC. Estimates of RCC prevalence among BHD patients, however, are varied between reported studies. A study on a small Dutch cohort reported that 12% of BHD patients developed renal cancer and further analysis of 22 BHD families of Dutch origin suggest a lifetime risk for RCC to be 16% (Houweling et al. 2011), however, two larger American cohorts found a prevalence of RCC to be 27% and 34% respectively (Pavlovich et al. 2005; Toro et al. 2008). Similarly, a more recent French study found the prevalence to be 27% (Benusiglio et al. 2014). The difference in these estimates may be due to population differences between cohorts, or, more likely, ascertainment bias. The patients in the Dutch study were recruited via dermatology clinics, whereas the cohorts in the American and French studies were recruited via dermatology and urology clinics. Due to these differences, the Houweling *et al* estimation is likely to be low, whilst the Pavlovich *et al*, Toro *et al* and Benusiglio *et al* estimations may be high. Therefore, the risk of developing RCC is estimated to be between 12-34%.

RCC is not a single disease; it has a number of specific subtypes of renal tumours that can occur within the kidney. Each subtype has a different histology that is used as a diagnostic tool to help define them. The renal tumour subtypes response to different therapies as they are often associated with mutations in specific tumour suppressors and oncogenes (Linehan 2013). Unlike other genetic disorders predisposing individuals to renal

tumours, those associated with BHD are histologically diverse (table 1.1). BHD patients are susceptible to all renal tumour subtypes. BHD-associated tumours often display hybrid histologies, are multifocal, and can affect both kidneys (bilateral) (Pavlovich et al. 2002; Houweling et al. 2011; Benusiglio et al. 2014). Most renal tumours in BHD are hybrid tumours comprised of features from both renal oncocytoma and chromophobe RCC (HOCT, 50%), but other BHD-associated sub-types are chromophobe renal cell carcinoma (34%), clear cell renal cell carcinoma (9%), oncocytoma (5%) and papillary renal cell carcinoma (2%) (Hasumi et al. 2015). Tumour progression is usually slow, and tumours rarely metastasise. Nevertheless, 12 deaths have been reported in BHD patients due to metastatic renal cancer (Pavlovich et al. 2005; Toro et al. 2008; Houweling et al. 2011; Hasumi et al. 2015). Given the high percentage of chromophobe tumours, it was initially believed that tumours arise from the distal nephron (Pavlovich et al. 2002). Subsequent research in mice, however, demonstrated *Flcn* expression in the proximal tubules of murine kidneys, which are now regarded as the site of origin for BHD-associated RCC (Chen et al. 2008; Hudon et al. 2010).
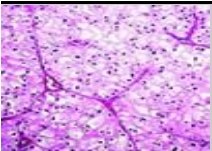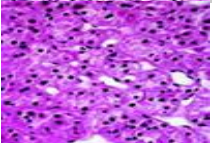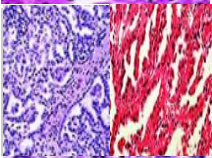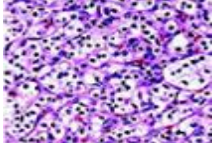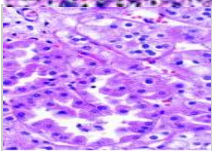
Photomicrograph	RCC subtype	% BHD associated RCC	% subtype of sporadic RCC
	Chromophobe RCC	34%	5%
	Oncocytoma	5%	3-5%
	Papillary RCC (type 1 & 2)	2%	10%
	Clear cell	9%	75%
	HOCT	50%	<5%

Table 1.1 Summary of BHD-associated renal cell carcinoma (RCC) histological subtype prevalence. Information obtained from (Pavlovich *et al*., 2002, Pavlovich *et al 2005,* Linehan WM 2004).

1.4.3.3.1 Sporadic kidney cancer

RCC is the seventh most common cancer in men, tenth in women, and the tenth most common cause of cancer-related deaths worldwide (Wong et al. 2017). It constitutes 90–95 % of all kidney neoplasms (Ljungberg et al. 2011), and 25–30 % of patients have metastatic disease upon diagnosis (Gupta et al. 2008; Wong et al. 2017). The majority of RCC are sporadic. Factors such as smoking, obesity, and hypertension are known to contribute to its development. Somatic *FLCN* mutations have been reported in 3-7 % of sporadic RCC cases (Khoo et al. 2003; Gad et al. 2007) indicating that *FLCN* mutations may cause a small percentage of sporadic RCCs.

While BHD-associated renal tumours are histologically diverse, there is a marked difference in prevalence of each subtype when compared to sporadic cases (table 1.1). A marker panel to discriminate BHD tumours from sporadic RCC is currently ongoing (Table 1.2). BHD-associated hybrid tumours show decreased expression of CK7 compared to sporadic chromophobe RCCs but increased expression of Ksp-cadherin and CD82 compared to sporadic oncocytomas (Iribe et al. 2015). Tumours from BHD patients show increased expression of Transmembrane glycoprotein NMB (GPNMB)(Furuya et al. 2015) and BHD-chromophobe RCC and HOCTs retain chromosome 17 disomy unlike sporadic tumours which are typically monosomic (Kato et al. 2016). So far, these markers are only able to distinguish between some of the sporadic and BHD-associated tumour subtypes. The identification of further markers will allow for greater understanding of the underlying biology but also more accurate RCC subtype diagnoses and, hopefully, a more targeted therapy for the treatment of BHD.

Sporadic RCC subtype	BHD-associated RCC subtype	Distinguishing markers
Chromophobe RCC	Chromophobe RCC	↓FLCN*, ↑GPNMB*, 17q/2p/6p disomy**
Chromophobe RCC	HOCT	↓CK7***, ↓FLCN*, ↑GPNMB*, 17q/2p/6p disomy**
Oncocytoma	HOCT	↑Ksp-Cadherin***, ↑CD82***, ↓FLCN*, ↑GPNMB
Papillary RCC	papillary RCC	↓FLCN*, ↑GPNMB*

Table 1.2 Summary of current work to generate a biomarker panel to distinguish BHD-associated renal tumours from sporadic renal tumours. Reference code *Furuya et al 2015, ** Kato et al 2016, ***Iribe et al 2001

1.4.3.4 Other clinical manifestations

Fibrofolliculomas, pulmonary cysts, pneumothorax and RCCs are the only recognised clinical features of BHD syndrome. Emerging evidence suggests *FLCN* mutations could also play a role in several other manifestations, including an increased risk of other types of cancer. These additional risk factors associated with BHD have yet to be confirmed in bigger case studies, as many reports have only a very limited amount of clinical evidence with a small cohort of patients. Nevertheless, they are summarised in table 1.3, and briefly discussed below.

1.4.3.4.1 Melanoma

Melanoma has been associated with BHD in numerous cases studies (Toro et al. 1999; Khoo et al. 2002; Menko et al. 2009; Cocciolone et al. 2010; Houweling et al. 2011; Mota-Burgos et al. 2013). However, studies attempting to prove a definitive link have been too small in patient numbers and failed to prove a correlation. FLCN negatively regulates the mTOR pathway through FNIP1, FNIP2 and AMPK complexes, to limit cell proliferation and tumour growth (Karbowniczek et al. 2008; Takagi et al. 2008; Cocciolone et al. 2010). The dysregulation of the mTOR pathway is associated with the benign and malignant tumours found in BHD but is also commonly activated in melanomas (Mota-Burgos et al. 2013). Whether patients with BHD have a greater risk of melanoma or it is just a coincidence is hard to establish; skin cancer is very common, and BHD is a rare disease.

Clinical manifestation	Reference
Benign	
Multinodular goiter	(Schmidt et al. 2005)
Parathyroid adenoma	(Chung et al. 1996)
Colorectal polyp and adenoma	(Le Guyadec et al. 1998; Khoo et al. 2002; da Silva et al. 2003)
Neural-tissue tumour	(Hornstein and Knickenberg 1975)
Trichoblastoma	(Chung et al. 1996)
Connective-tissue nevus	(Liu et al. 2000)
Focal-cutaneous mucinosis	(Lindor et al. 2001)
Adenoma of adrenal gland	(Toro et al. 2008; Kunogi et al. 2010)
Lipoma	(Toro et al. 1999)
Angiolipoma	(Chung et al. 1996)
Cutaneous leiomyoma	(Imada et al. 2009)
Rhabdomyoma	(Toro et al. 2008; Bondavalli et al. 2015)
Myoma	(Kunogi et al. 2010)
Thyriod nodules	(Kluger et al. 2010; Benhammou et al. 2011)
Ovarian cyst	(Godbolt et al. 2003)
Malignant	
Breast cancer	(Toro et al. 2008; Kunogi et al. 2010)
Colorectal cancer	(da Silva et al. 2003)
Sarcoma of the leg	(Menko et al. 2009)
Squamous cell carcinoma	(Toro et al. 2004)
Tonsillar cancer	(Warren et al. 2004)
Lung cancer	(Gunji et al. 2007; Furuya and Nakatani 2013; Nishida et al. 2015)
Melanoma	(Toro et al. 1999; Khoo et al. 2002; Cocciolone et al. 2010; Houweling et al. 2011; Mota-Burgos et al. 2013)
Basal and squamous-cell skin cancer	(Leter et al. 2008; Toro et al. 2008)
Dermatofibrosarcoma protuberans	(Menko et al. 2009)
Hodgkin lymphoma	(Toro et al. 2008)
Uterine cancer	(Toro et al. 2008)
Prostate cancer	(Toro et al. 2008)
Cutaneous leiomyosarcoma	(Toro et al. 2008)
Adrenal carcinoma	(Raymond et al. 2014)

Table 1.3 Reported tumours noted in the literature that may be associated with BHD and/or FLCN loss of function. A direct or causative relationship between FLCN and these tumours have <u>NOT</u> been conclusively demonstrated**.** Adapted from (Menko et al. 2009)**.**

1.4.3.4.2 Pulmonary cancer

A handful of case studies where BHD patients have developed pulmonary tumours have been reported (Gunji et al. 2007; Furuya and Nakatani 2013; Nishida et al. 2015). These however correlate to a history of smoking and no heterozygous loss of *FLCN* was reported.

1.4.3.4.3 Colorectal cancers

Initial studies suggested a link between BHD and colorectal neoplasis due to a high occurrence of colorectal polyps and colorectal cancer in BHD patients (Birt et al. 1977; Schulz and Hartschuh 1999; Khoo et al. 2002). Interestingly, one study noted that BHD patients who developed colonic polyps had mutations within the exon 11 (c.1285delC) hotspot (Khoo et al. 2002). Furthermore, somatic frameshift mutations in the FLCN exon 11 C8 mononucleotide tract were detected in 23% of sporadic colorectal cancers with microsatellite instability, suggesting that FLCN inactivation might contribute to colorectal tumorigenesis (Nahorski et al. 2010). However, subsequent studies containing a larger cohort of patients failed to confirm an association between BHD and colonic polyps or colorectal cancer (Zbar et al. 2002).

1.4.3.4.4 Thyroid and Parotid

Two case studies have described BHD patients with thyroid cancer (Benusiglio et al. 2014; Yamada et al. 2015). Both report a loss of heterozygosity of FLCN in the tumour, but state other genetic lesions that may have contributed to the development of thyroid cancer. Therefore, causality between FLCN and thyroid cancer cannot be established. A study of French families with BHD noted 65 % of cases exhibited thyroid nodules or cysts (Kluger et al. 2010). No thyroid carcinomas were detected. The high prevalence of thyroid nodules in this study is interesting, but the study lacked an appropriate control group and the authors were not able to assess the significance of these results.

To date, eight cases of parotid tumours have been reported in patients with a germline *FLCN* mutation (Liu et al. 2000; Schmidt et al. 2005; Maffe et al. 2011; Lindor et al. 2012; Pradella et al. 2013). Interestingly, the parotid tumours were oncocytic, a trait frequently seen

in BHD kidney tumours, however, there is not sufficient statistical evidence to associate parotid tumours with BHD syndrome.

1.5 Management and current therapies

There is currently limited treatment available for BHD syndrome, and none are curative. More clinical research and a better understanding of the basic biology involved in FLCN loss will facilitate the development of therapies to treat BHD and its symptoms. Screening drug libraries could identify novel therapeutic compounds already known to target a relevant pathway (such as mTOR signalling) or those used in a phenotypically similar disorder could be tested. Once demonstrated effective, FDA-approved drugs could be rapidly repurposed. Granted, therapies that target the mTOR pathway have not been successful in treating BHD-associated fibrofolliculomas, lung cysts, or pneumothorax (Gijezen et al. 2014). mTOR inhibitors have, however, shown early promise with regards to BHD-associated RCCs (further information in section 1.5.3). Gene therapy is a promising treatment for a vast variety of genetic disorders. Preliminary studies show FLCN function can be successfully restored in *FLCN*-null cells (Wong and Harbottle 2013). In the future it may be possible to re-introduce a functional copy of the *FLCN* gene into *FLCN*-null or -heterozygous cells, either preventatively or curatively. These technologies are still very much in their infancy, and there is currently only one FDA-approved gene therapy, Glybera, to treat lipoprotein lipase deficiency, which is currently available. However, a great number of gene therapy clinical trials are currently ongoing.

1.5.1 The skin

Therapies for fibrofolliculomas are very limited and current options include ablative laser, electrocoagulation and excision, and are highly invasive. After such abrasive therapies, regrowth of the fibrofolliculomas is common. This high recurrence rate (typically returning within 2-3 years) is one issue with therapy and there are also significant risk of complications such as scaring, inflammation, and hypo- or hyperpigmentation (Gambichler et al. 2000; Jacob and Dover 2001; Kahle et al. 2001; Gijezen et al. 2014). Given that the animal models demonstrate deregulation of mTOR signalling, topical treatment using a clinically effective

mTOR inhibitor, rapamycin, was trialled for fibrofolliculoma, but found no cosmetic improvement in BHD patients (Gijezen et al. 2014).

1.5.2 The lungs

The management of BHD pulmonary symptoms largely focuses on the treatment of pneumothoraces. BHD lung cysts typically do not result in respiratory failure, however periodic measurement of pulmonary function and CT monitoring of cysts are recommended (Gupta et al. 2013). Although limited, data on smoking and the risk of pulmonary cysts and pneumothorax in BHD suggest smoking may increase the risk of these manifestations and should be avoided (Fabre et al. 2014; Park and Lee 2017).

1.5.3 The kidneys

Due to the high prevalence of RCC, BHD patients with a confirmed germline mutation, and at risk relatives in families with clinical BHD, undergo kidney surveillance. There are no widely established guidelines for BHD-associated RCC surveillance. The age to start surveillance, how regularly patients are monitored, and the method of examination can vary between establishments (Toro et al. 2008). Most institutes start surveillance at around 20 years of age, as BHD-associated RCC typically present between the ages of 25-75. This also allows the individual to receive genetic counselling at an appropriate age. Common methods used include, renal ultrasonography, computed tomography (CT), and magnetic resonance imaging (MRI). Each approach has its strengths and weaknesses as discussed by Choyke *et al*. (Choyke et al. 2003); briefly, ultrasonography is relatively insensitive, detecting only 58 % of small lesions (15–20 mm) when compared to CT and MRI, which detects 100 % of similar sized lesion. Frequent CT scanning, however, would lead to unacceptably high cumulative radiation dose, and MRI, while radiation free, is not widely available at all centres (Hall and Brenner 2008; Sodickson et al. 2009). Annual renal ultrasonography is offered to those with germline confirmed FLCN mutations. Even though the sensitivity of this method in detecting small renal tumours is limited, renal growth removal isn't recommended until lesions are sized 25–30 mm. These size tumours can be readily detectable by ultrasonography, which is available at the majority of healthcare centres (Choyke et al. 2003).

There are no BHD-associated RCC specific treatments. When diagnosed, patients follow the treatment options available for sporadic RCC cases. Complete removal of tumour lesions by partial or full nephrectomy is the best course of action, with partial removal being preferred, allowing surgery to be as nephron sparing as possible. BHD patients, however, are at risk of synchronous and multiple kidney cancers throughout their lifetime. Therefore, the balance of oncological eradication and postoperative renal function is one of the most critical elements for the quality of life and overall survival of BHD patients. Tumour size at the time of removal is essential for minimising the number of surgeries in a lifetime, as well as post-operative renal function. Therefore, it is common practice to operate on BHD-associated renal tumours when the diameter of the largest tumour reaches 3 cm (Ather and Zahid 2018). This concept parallels that of Von Hippel-Lindau (VHL) and Tuberous Sclerosis Complex (TSC)-associated renal tumours.

In recent years, there have been attempts to find specific chemotherapeutics for BHD-associated RCC. The antibiotic mithramycin, for example, was shown to inhibit the growth of *FLCN*-null RCC cells (Lu et al. 2011). Likewise, a combination of autophagy inhibition and Paclitaxel treatment selectively promoted apoptosis in *FLCN*-null cells (Zhang et al. 2013). The mTOR inhibitor, rapamycin, effectively reduced the number and size of renal tumours in *Flcn*-deficient mouse models (Baba et al. 2008; Chen et al. 2008; Wu et al. 2015). Furthermore, a handful of case studies have reported a good response in BHD patients with metastatic RCC who have been treated with systemic small molecule tyrosine kinase and/or mTOR inhibitors (summarised in (Benusiglio et al. 2014)). The mTOR inhibitor everolimus, which is a rapamycin analogue, went into a clinical trial in 2015 (NCT02504892). Everolimus is an approved treatment for sporadic metastatic RCC but has not been specifically trialled in BHD-associated and sporadic chromophobe RCC. The phase 2 trial was terminated April 2018 due to slow, insufficient accrual.

1.6 DNA damage overview

Genome instability is described as one of the hallmarks of cancer and the most universal characteristic of tumour cells (Hanahan and Weinberg 2011). Human DNA is continuously challenged by a host of processes that can alter cellular DNA (Jackson and Bartek 2009). Cells have evolved a complex series of mechanisms that govern genomic integrity. These mechanisms - known collectively as the DNA damage response (DDR) - can be divided into a set of distinct, but functionally overlapping pathways; defined mainly by the type of DNA lesion they repair (Jackson and Bartek 2009; Ciccia and Elledge 2010). A summary of the types of DNA damage, their causing factors, and dedicated repair mechanisms are outlined in figure 1.4.

1.6.1 Types of damage

DNA can be subjected to a large array of insults, both exogenous and endogenous in origin (Jackson and Bartek 2009). Exogenous sources of DNA damage are environmental agents external to the cell, such as ultraviolet light (UV), ionising radiation (IR), and chemicals, including those in cigarette smoke and chemotherapeutics. Endogenous causes of DNA damage arise internally from cellular activities, such as metabolism that produces reactive oxygen species (ROS), or errors from faulty DNA replication. Damage to DNA includes mismatched base pairs, insertion or deletion of nucleotides (indels), the addition of bulky adducts, inter- and intra-strand links, single-strand DNA breaks (SSBs), and double-strand DNA breaks (DSBs) (Jackson and Bartek 2009).

Type of DNA damage	Single-strand DNA break	Base oxidation Base hydrolysis	DNA adducts Strand cross links Base dimers	Mis-matched base pairs	Double-strand break repairs	
Causes	Replication stress	ROS UV	Carcinogen UV	Replication stress ROS	IR Replication stress ROS	
Mechanisms of repair	Base excision repair (BER)		Nucleotide excision repair (NER)	Mis-match repair (MMR)	Homologous recombination (HR)	Non homologous end joining (NHEJ)
Key proteins for repair	OGG1 PARP1 PARP2 ↓ XRCC1 ↓ Pol β PCNA FEN1 ↓ Ligase III		GG-NER TC-NER ↓ ↓ XPD Pol β XPC CSA XPE CSB ↘↙ ERCC1/XPF ↓ PCNA Pol δ Pol ε ↓ Ligase I	MSH2/MSH6 MLH1/PMS2 ↓ EXO1 PCNA RCF ↓ Pol δ ↓ Ligase I Ligase IV	ATM MRN complex ↓ RPA BRAC2/FANCD RAD51 FANCF ↓ Pol δ Pol ε ↓ Ligase I	KU70 KU80 ↓ DNA-PKcs Artemis XRCC4-XLF ↓ Pol μ ↓ Ligase IV

Figure 1.4 Summary of the types of DNA damage, their usual causes, repair mechanisms, and key proteins involved in DNA repair. Various types of DNA damage can occur within cells, caused by both endogenous and exogenous agents. These agents can cause base modifications, helix-distorting lesions or DNA strand cross-links, and single-stranded, or double-stranded DNA breaks, that are repaired by biochemically distinct DNA repair pathways. (Ciccia and Elledge 2010; O'Connor 2015). Abbreviations; UV, ultraviolet radiation; ROS, reactive oxygen species; IR, ionising radiation; GG-NER, global genome-nucleotide excision repair; TC-NER, transcription coupled-nucleotide excision repair.

1.6.2 DNA damage repair

In response to DNA lesions, cells activate an elaborate signalling network, the DDR. DDR can be divided into three main phases that translate the signal of DNA damage into an integrated cellular response (Jackson and Bartek 2009). In the first phase, the "sensors" of DNA lesions detect abnormally structured DNA and initiate the signalling response. The key DDR sensors known to date in mammalian cells are DNA-dependent protein kinase (DNA-PK), ataxia telangiectasia-mutated protein kinase (ATM), and ATM-Rad-3-related protein kinase (ATR). Upon activation, these sensors phosphorylate "mediator" proteins that further recruit "transducer" proteins, such as p53, checkpoint kinase 1 (Chk1) and checkpoint kinase 2 (Chk2), to amplify the DDR signal. Once activated, the transducer kinases phosphorylate "effector" proteins who elicit multiple mechanisms of cell fate including DNA repair, cell cycle arrest, and/or cellular death (Marechal and Zou 2013; Yan et al. 2016b).

There are several distinct repair pathways, specialised for different types of DNA lesions (summarised in figure 1.4). Base excision repair (BER) corrects small, non-helix-distorting base lesions, by the removal of the damaged base only. This covers damage which arises from hydrolysis, alkylation or oxidation of nucleotides, that could otherwise cause mutations by mispairing or lead to DNA breaks during replication (Krokan and Bjoras 2013). Nucleotide excision repair (NER), on the other hand, co-ordinates the repair of DNA adducts. Large helix-distorting base lesions, intercalated agents, and strand cross links are removed by the excision of a short string of nucleotides and replaced as directed by the undamaged template strand. Recently NER has been divided into two distinct modes; global genome NER (GG-NER) and transcription coupled NER (TC-NER). GG-NER repairs damage in both transcribed and un-transcribed DNA strands throughout the genome and is initiated by XPC-RAD23B. CT-NER focuses on repairing lesions within the transcribed strand of active genes and is initiated by RNA polymerase at a stalled replication fork (Scharer 2013). Mismatch repair (MMR) detects non-commentary base pairings, errors that commonly occur due to polymerase mis-incorporation, or chemical and/or physical damage to nucleotides (for example, oxidation or deamination) (Jiricny 2013).

DSBs are among the most destructive DNA lesions and are repaired through two pathways; homologous recombination (HR) and non-homologous end-joining (NHEJ). HR is

an accurate process that uses information from genetically identical DNA molecules to repair damaged DNA. Several genes with tumour-suppressor activity are crucial to this process, including *BRCA1, BRCA2, PALB2* and *RAD51*, and their functioning is essential for an error-free repair (Moynahan and Jasin 2010). NHEJ, on the other hand, recruits DNA-PK to bring about the direct ligation of two dsDNA molecules, regardless of whether the ends come from the same chromosome. As such, NHEJ is far more error-prone and has increased mutagenic potential. NHEJ itself is therefore a potential source of carcinogenic transformation within cells.

Typically, it is the phase of the cell cycle that determines the dominant pathway of DSB repair. Highly compact chromatin restricts access to homologous sequences. As such, it is thought NHEJ is the dominant DSB repair pathway when cells aren't replicating and during early phases of the cell cycle (Branzei and Foiani 2008). Cell cycle checkpoints occur at the G1/S and G2/M cell cycle boundaries to prevent cells from proliferating in the presence of DNA damage (figure 1.5). Co-ordination of DNA repair within cycling cells is controlled through cyclin-dependent kinases (CDKs). CDKs regulate cell cycle transitions by inducing degradation of inhibitory proteins and are systematically activated by their regulatory cyclin subunits, which are differentially expressed in a phase dependant manner (Branzei and Foiani 2008).
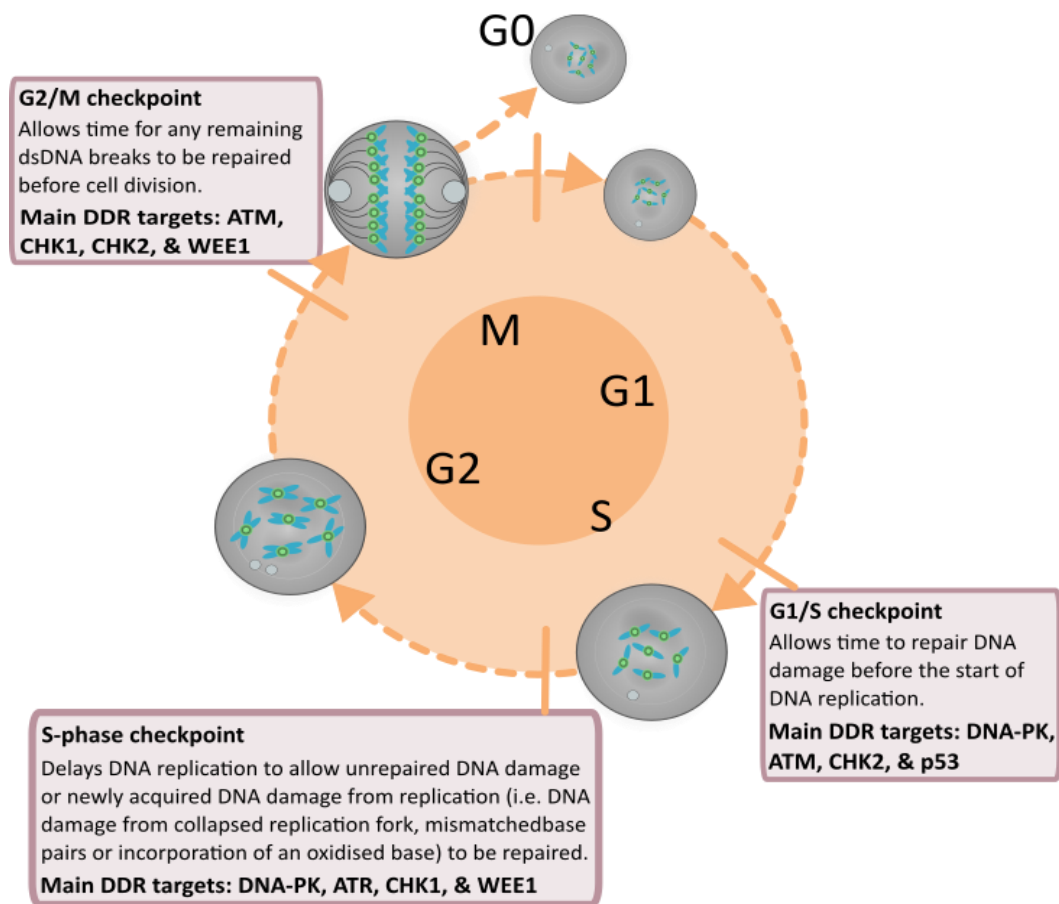
Figure 1.5 The DNA damage response (DDR) key proteins during the cell cycle. DDR targets are shown for each cell-cycle checkpoint. Adapted from (O'Connor 2015). Abbreviation; DNA-PK, DNA-dependent protein kinase ATM, ataxia-telangiectasia mutated; ATR, ataxia-telangiectasia and Rad3-related; CHK1, Checkpoint kinase 1; CHK2, Checkpoint kinase 2; WEE1, Wee1-like protein kinase. G1, gap/growth phase 1; S, DNA replication phase; G2, gap/growth phase 2; M, mitosis (cell division phase).

1.6.3 Telomere maintenance

Telomeres are specialised nucleoprotein complexes. They protect the natural ends of linear chromosomes from being recognised as intra-chromosomal DSBs and exposure to the DDR (Longhese 2008). Telomere shortening occurs with each round of DNA replication. In the absence of a compensatory mechanism this results in unmasked chromosome ends. As a consequence, DDR will activate and define the fate of cells; either engaging replicative senescence or apoptosis (Fumagalli et al. 2012). Dysfunctional telomeres are associated with an increased cancer risk. They promote tumorigenesis through chromosomal instability and influence tumour cell plasticity (Plentz et al. 2007; Tomasetti and Vogelstein 2015; Gunes et al. 2018).

1.6.4 Genomic instability in cancer

Defects in DDR are associated with increased mutational load and genomic instability. They are well-established causes of neoplastic transformation and drive a variety of hereditary and sporadic tumours (Halazonetis et al. 2008; Negrini et al. 2010; Hosoya and Miyagawa 2014). Both activation and inactivation of the DDR are found in various cancers. For example, *TP53* (p53) is one of the most frequently altered genes in human cancers. While the reported occurrences of *TP53* mutation vary among the different types of cancer, it is estimated that more than half of cancers involved inactivated p53 due to mutation, deletion, loss of heterozygosity, or decreased expression of the gene (Brosh and Rotter 2009; Hosoya and Miyagawa 2014). Inactivating mutations are also commonly observed in *ATM*, *BRCA1*, and *BRCA2* (Grasso et al. 2012; Koboldt et al. 2012; Cremona and Behrens 2014), and cancers often display a decreased expression of *ATM, Chk2, and RAD51* suggesting aberration of the DDR is common feature of cancers (Angele et al. 2003; Verlinden et al. 2007; Dzikiewicz-Krawczyk 2008; Hosoya and Miyagawa 2014). On the other hand, inappropriate activation of DDR can also have tumorigenic effects and is linked to worse prognosis or therapy resistance (Ciccia and Elledge 2010). An increase in the gene expression of *Chk1*, *Chk2*, *CDC25A*, *CDC25B*, and *CDC25C* have been reported in numerous tumours (Boutros et al. 2007; Verlinden et al. 2007; Dzikiewicz-Krawczyk 2008; Hosoya and Miyagawa 2014). Furthermore, overexpression of DNA-PKcs, RAD51, BRCA1, and PARP1 have all been associated with resistance to therapy in a variety of cancers (Taron et al. 2004; Kase et al. 2011; Bouchaert et al. 2012; Hosoya and Miyagawa 2014).

DNA damage occurs daily by endogenous and exogenous sources. Erroneous repair or replicative bypass of these lesions can result in DNA mutations and chromosomal aberrations. When mutations affect tumour suppressor genes or oncogenes, cells may transform into cancer cells. DNA repair is therefore essential for preventing tumour development. However, once a cancer has developed, DNA damage can be exploited to reduce cancerous growth and evoke apoptotic demise of cancer cells.

1.7 Aims and objectives of this thesis

Dispite numerous advances to understand its tumour suppressive function, FLCN is still a poorly characterised protein. To better define the cellular role(s) of FLCN in renal tumorigenesis, an unbiased protein-protein interaction study was performed. Manual evaluation found multiple associations between FLCN and components involved in DNA repair. From this, it was hypothesised that FLCN may preserve DNA integrity through the interaction and regulation of proteins involved in DNA damage repair.

The aim of this study was to examine the role of FLCN in the context of genome maintenance. To do this the following objectives were carried out:

- Analysis of the FLCN interactome and validation of novel FLCN interactors

- Analysis of the transcriptomic effect of FLCN knockdown

- Characterise the role of any novel FLCN interacting proteins and explore the effect of FLCN knockdown on DNA damage signalling pathways

- Explore the effect of FLCN knockdown on cell cycling.

Chapter 2: Methods and Materials

2.1 Mass spectrometry sample preparation, sequencing, and analysis

An unbiased protein-protein FLCN interaction screen was performed to analyse proteins co-purifying with FLCN. GST-FLCN was expressed in HEK293 cells, purified and run on an agarose gel. GST-FLCN and interacting proteins were stained and divided into 8 sections based on molecular weight. Protein identification was performed using liquid chromatography-tandem mass spectrometry (LC-MS/MS). GST-FLCN pull-down was previously carried out by Dr Elaine Dunlop, with LC-MS/MS analysis performed by Peter Doubleday and Dr Bryan Balliff (University of Vermont)

Sample preparation and analysis were performed as follows: Protein gel bands were excised and reduced with 10 mM DTT for 30 min at 50 ˚C and then alkylated with 12 mM iodoacetamide at room temperature in the dark for 1 h. Gel pieces were then washed three times with a 50:50 mixture of 100 mM ammonium bicarbonate and acetonitrile. Gel pieces were then rehydrated with 100 mM ammonium bicarbonate and 150 ng of trypsin was added. Tryptic digest proceeded overnight at 37˚C. Peptides were extracted by the addition of 50 % [v/v] acetonitrile (MeCN)/ 5 % [v/v] formic acid (FA) followed by 90 % [v/v] MeCN / 5 % [v/v] FA. Peptides were dried by vacuum centrifugation.

For LC-MS/MS analysis, dried peptides were re-suspended in 2.5 % [v/v] MeCN, 2.5 % [v/v] FA and were loaded for nanoscale microcapillary LC–MS/MS in a LTQ-Orbitrap mass spectrometer (Thermo Electron, Waltham, MA) fitted to a Finnigan Nanospray II electrospray ionization source, a Surveyor HPLC pump plus, and a Micro AS autosampler (all from Thermo Electron, Waltham, MA). After isocratic loading for 15 min in solvent A (2.5 % [v/v] MeCN, 0.15 % [v/v] FA), peptides were separated on an increasing MeCN gradient (2.5–35 %) containing 0.15 % [v/v] FA from 15 to 60 min on a 100 μm internal diameter, in-house prepared, 13 cm long, MagicC18 reverse phase column (5 μm, 200 Å; Michrom Bioresources, Auburn, CA). Data acquisition was performed with a full scan (365-2000 m/z) followed by data-dependent scans on the 10 most abundant precursors. Dynamic exclusion was enabled with a repeat count of 3 and a repeat cycle of 120 s. Lock mass was enabled

and set to calibrate on the mass of a polydimethylcyclosiloxane ion [(Si(CH3)2O)5 + H+]+, m/z = 371.10120.

Mass spectra were searched using SEQUEST (Thermo Electron V26.12) against the human forward and reverse IPI database (human IPI v3.60) using a target-decoy approach and allowing for variable oxidation of methionine (+15.99429), and the fixed modification of carbamiodomethylation to cysteine (+57.02146 Da). Peptide quantification was performed using Vista-based software taking the integral values of the chromatographic monoisotopic peaks generated from full MS1 scans. MS runs were pooled and filtered below a 0.5% false discovery rate using an automated linear discriminant analysis weighted by XCorr, ΔCn2, MS2 ion intensity, missed tryptic cleavages, precursor ppm and peptide length.

2.2 Construction of the FLCN-bound interactome

The STRING protein–protein interaction database (Szklarczyk et al. 2017) was used to create a FLCN interactome. Of the 650 FLCN interacting proteins identified by LC-MS/MS, 613 were successfully mapped within the network. Enrichment analysis of Gene Ontology biological processes (GO-BP) was then used to classify the identified proteins into 8 major functional categories. The following categories were chosen as they have either not previously been or are only weakly associated with FLCN; telomere maintenance, chromatin structure, ubiquitination, DNA damage repair and response, DNA replication, cell cycle, transcription and translation, and other. Enrichment in Gene Ontology cellular component (GO-CC) was also produced in STRING. The interactome was then imported into Cytoscape (v3.6.1,(Lopes et al. 2010) making use of the aesthetic freedom of the software to produce a more informative network.

2.2.1 Topological analysis of the FLCN interactome

The topological analysis of the FLCN interactome was performed using the Network Analyzer plugin (v2.7) for Cytoscape. The following topological properties of the network were analysed, where a node refers to a protein and an edge denotes the interaction between two proteins. The degree (k) represents the connectivity of a node or the number of other nodes that it is connected to, *i.e.*, the number of interactions a protein has to other proteins within the network. The clustering coefficient signifies the connectedness of a node

to other nodes and represents the overall tendency of the nodes to form clusters. The average clustering coefficient of all the nodes in the network is represented as the network clustering coefficient. The shortest path length is measured by the number of edges occurring within the shortest path between two nodes averaged over all pairs of nodes in a network, *i.e.*, the fewest steps between any two proteins within the network. It corresponds to the typical separation between two proteins in a network and is indicative of the navigability of the network. The network diameter is defined as the maximum length of the shortest path between two nodes. Closeness centrality (CC) indicates nodes with the minimum average distance to all other nodes. It is defined as the inverse of the average lengths of the shortest paths to and from all other nodes in the network. Betweenness centrality (BC) is a fundamental parameter of the network. It is measured by the fraction of shortest paths that pass through a node and corresponds to the number of times that a node lies on the shortest path between two other nodes. In essence, it measures how often a node acts as a bridge between other nodes.

2.2.2 Creation of a backbone network

To identify proteins integral to the flow of information through the FLCN interactome, proteins that have a k and BC value more than two standard deviations from mean values were extracted from the giant network to form a backbone network.

2.3 RNA sample preparation, sequencing, and analysis

RNA sample preparation and sequencing were performed by Dr Elaine Dunlop (Cardiff University, UK) in conjunction with Wales Gene Park (Cardiff University, UK).

For each cell line, cells were cultured in separate 60mm plates. Three plates were grown per cell line (n=3). After plates reached ≥90% confluency, media was removed, and cells were washed with phosphate buffered saline (PBS). Plates were treated with 0.5 ml of RNAprotect® (QIAGEN) reagent to stabilise RNA, plates were then scraped, and the mixture pipetted into separate eppendorfs. RNA extraction was performed using the RNeasy® Plus Mini kit (QIAGEN), with the homogenisation step being performed with QIAshredder® (QIAGEN). Purified RNA was stored at -80°C. Maintenence of *FLCN* knockdown was

confirmed by real time PCR prior to RNA sequencing. Total RNA quality and quantity was assessed using RNA Nano 6000 kit and 2100 Bioanalyser™ (both Agilent Technologies, Waldbronn, Germany). 100-900 ng of total RNA with a RIN value >8 was used as the input and the sequencing libraries were prepared using the Illumina® TruSeq® RNA sample preparation v2. (Illumina Inc.). All steps where followed as described by the manufacturer's instructions.

Differentially expressed transcripts were identified using DeSeq2 package in R (Love et al. 2014). Analysis was carried out on all pairwise comparisons in the dataset. *P*-values were corrected for multiple testing using the Benjamini–Hochberg false discovery rate (FDR) method. Differential gene expression was performed by Dr Marc Naven (Wales Gene Park, Cardiff, UK).

Genes where split into biological processes using gene lists generated from the following GO list; GO:0006974 (Cellular response to DNA damage stimulus); GO:0007049 (Cell cycle); GO:0006351 (Transcription, DNA-templated); GO:0006412 (Translation); GO:0006260 (DNA replication); GO: 0016567 (Protein ubiquitination); GO:0006302 (Double-strand break repair); GO: 1902807 (Negative regulation of cell cycle G1/S phase transition); GO: 1902808 (Positive regulation of cell cycle G1/S phase transition) from AmiGo 2 (Ashburner et al. 2000). The E2F target gene list was taken from (Bracken et al. 2004). AMPK gene list was gifted from Dr Henry McCann.

All heatmaps were creating using the R pHeatmap package (Kolde 2019). Density plot was produced in R using the ggplot2 package (Ginestet 2011). All other graphical visualisation (bar graphs, scatter plot and volcano plots) were produced using GraphPad Prism 4.00.

2.3.1 Correlation of log2 fold change between FLCN knockdown cell lines

To explore the effects of differentially expressed genes (DEGs) upon FLCN knockdown four pairwise comparisons were made; (1) low passage wild type vs low passage knockdown cells (LP-WT vs LP-KD), these represent the direct effect of FLCN knockdown; (2) high passage wild type vs high passage knockdown cells (HP-WT vs HP-KD), these represent the effect of FLCN knockdown in aged cells; (3) low passage wild type vs high passage wild type cells (LP-

WT vs HP-WT), these represent changes that normally occur upon cellular aging; and (4) low passage knockdown vs high passage knockdown cells (LP-KD vs HP-KD), these represent changes occurring due to continuous FLCN knockdown. Where indicated Pearson's correlation coefficient (PCC) was performed, using GraphPad Prism 4.00, to understand the statistical relevance of gene correlation.

2.3.2 Functional analysis of differentially expressed genes

To investigate the biological mechanisms related to the DEGs, enrichment analysis was performed using REACTOME online resource tool (Fabregat et al. 2017). Figures were adapted using Inkscape v0.92.4.

2.4 Validation of RNA sequencing

2.4.1 Reverse transcription

Reverse transcription of purified RNA to create cDNA was undertaken using QuantiTect® Reverse Transcription Kit (QIAGEN). 1 μg of template RNA was used per sample. Temperature and length of reactions on heat block were as follows: 2 min at 42 °C for genomic DNA elimination reaction, 30 mins at 42 °C for reverse transcription reaction and 3 min at 95 °C to inactivate Quantiscript® Reverse Transcriptase (QIAGEN). cDNA was stored at -20 °C until needed.

2.4.2 Real-time quantitative Polymerase Chain Reaction (qPCR)

qPCR was carried out using Taqman® chemistry (Applied Biosystems). For each gene being assayed, 20 μL reactions per sample were set up in triplicate on a 96-well PCR plate. Each reaction consisted of 10 μL of Taqman Master Mix (2X), 1 μL primer/probe mix, 1 μL of cDNA and 8 μL of RNase-free water. RNase-free water was used in place of cDNA as a negative control. Plates underwent a qPCR reaction using a 7500 Real Time PCR system (Applied Biosystems). The thermal cycling conditions were as follows: 2 min at 50 °C, 10 min at 95 °C, then 40 cycles of both 15 s at 95 °C and 1 min at 60 °C. ACTB (β-actin) was used as the control gene which C_T values were normalised against. Genes were assayed in five

experiments. The following primer/probe mixes were sourced from Applied Biosystems; CCND1 (Assay ID= Hs00765553_m1), TP53 (Assay ID= Hs01034249_m1), FOXN3 (Assay ID= Hs00758121_m1), ACTB (Assay ID= Hs01060665_g1), RPA (Assay ID= Hs00161419_m1), JUN (Assay ID= Hs01103582_s1), TGFA (Assay ID= Hs00608187_m1), PPARGC1A (Assay ID= Hs00173304_m1). qPCR of FLCN, CCND1, TP53 and FOXN3 were carried out by Mr Jesse Champion under my guidance. qPCR of FLCN, RPA, JUN, TGFA, and PPARGC1A were carried out by Dr Elaine Dunlop.

2.6 Cell culture and treatment

Human embryonic kidney 293 (HEK293) and human proximal epithelial kidney (HK2) cell lines were propagated in Dulbecco's modified Eagle's medium (DMEM; Life Technologies, 11995065) and supplemented with 10 % [v/v] foetal calf serum (Life Technologies, 10270-106), 100 U/ml penicillin and 100 µg/ml streptomycin (Life Technologies, 15070- 063) in a humidified incubator containing 5 % CO_2 at 37 °C.

FLCN shRNA plasmid (pLKO.1-puro-shRNA5968, Sigma-Aldrich-Aldrich) and non-target shRNA plasmid (pLKO.1-puro-NonTaget, Sigma-Aldrich) used to generate stable FLCN knockdown in HK2 cells. HK2 are a non-disease associated human proximal kidney cell line and were chosen as the proximal tubules are thought to be the origin cells of BHD associated renal tumours (Chen et al. 2008; Hudon et al. 2010). 'Low passage' refers to cells grown in culture for less than 2 months, while 'high passage' signifies cells gown continuously for one year. Cells where kept under selection with 2 µg/ml puromycin (Gibco™).

All transfections were performed using Lipofectamine 2000 according to the manufacturer's protocol (Life Technologies, 11668019). Where specified, cells were exposed to ionising radiation (IR) using Gammacell 1000 Elite (Nordion International Inc).

2.7 Cell lysis

HEK293 cells were lysed in 'BHD lysis buffer' (20 mM Tris, 135 mM NaCl, 5 % [v/v] glycerol, 50 mM NaF, 0.1 % [v/v] Triton X-100) containing the protease inhibitors pepstatin (1 ug/ml); antipain (2 uM); leupeptin (10 uM); benzamaidine (1 mM); phenylmethylsulfonyl fluoride (0.1 mM) and the phosphatase inhibitor, sodium orthovanadate (1 mM).

HK2 cells were lysed in 1x NuPAGE LDS sample buffer (Invitrogen) containing 62.8 mM Tris, 10 % [v/v] glycerol, 2 % [w/v] SDS, 0.1 % [w/v] bromophenol blue. 50 mM dithiothreitol (DTT) was added just before use.

2.8 Protein quantification

Where appropriate, protein quantification of cellular lysates was carried out using Bradford protein assay. 750 μl of Bradford reagent was added to 12 μl of lysate, and light absorbances were measured using a Genova life sciences spectrometer (Janeway) at 595 nm.

2.9 GST pull down and co-immunoprecipitation

For GST-pull down assays, HEK293 cells were transfected with either GST-FLCN in pDEST27 empty vector (Life Technologies, 11812013) or pcDNA3.1 empty vector (Invitrogen, V79020). 150 μl of lysate was incubated with pre-blocked Glutathione-Sepharose 4B beads (GE Healthcare) at 4 °C in a rotary shaker for 3 h. Beads were washed five times in BHD lysis buffer in the presents of protease inhibitors with a final NaCl concentration of 300 mM for DNA-PKcs and washes three times with 250 mM NaCl for all other proteins. Bound proteins were eluted using 10 mM glutathione in Rheb storage buffer (20 mM HEPES, 200 mM NaCl, 5 mM MgCl2, pH 8). Bound proteins were stored in 1xNuPAGE LDS sample buffer containing 100 mM DTT with a final volume of 40 μl. Where indicated, aliquots were removed for immunoblots of whole cell lysates.

For co-immunoprecipitation assays of patient-derived FLCN mutations, HEK293 cells were transfected with either HA-FLCN wild type, HA-FLCN Y463X, HA-FLCN H429X in pN3HA

backbone (kindly gifted from Professor Maurice Van Steensel, Maastricht University, Netherlands) or pcDNA3.1 empty vector. 150 µl of lysate was incubated with unblocked protein G-Sepharose beads (GE Healthcare Life Sciences, 17-0618-05) for 1 h at 4 °C in a rotary shaker. This 'pre-clear' step was to remove any tenacious proteins. Lysates were spun down for 3 min, 3,000 rpm at 4 °C to removed unblocked beads. Lysates were then incubated with anti-HA antibodies (1:150, #1186742300; Roche) for 2 h at 4 °C in a rotary shaker before the addition of pre-blocked protein G-Sepharose beads (GE Healthcare Life Sciences, 17-0618-05) for further 2 h. Beads were washed as described for GST-pull downs above. Bound proteins were stored in 40 µl 1xNuPAGE LDS sample buffer containing 100 mM DTT. Where indicated, aliquots were removed for immunoblots of whole cell lysates. Endogenous-endogenous interaction was explored by immunoprecipitating FLCN using Anti-FLCN antibody gifted from Prof Arnim Pause (McGill University, Canada) at 1:50 dilution.

Both Glutathione-Sepharose 4B beads and protein G-Sepharose beads were blocked in 2 % [w/v] BSA in PBS for at least 1 h at 4°C in a rotary shaker.

2.10 *In vitro* DNA-PK kinase assay

To assess if FLCN could be a DNA-PK substrate, DNA-PK Kinase Enzyme System (Promega, #V4106) was used. Following the manufacturer's protocol, 25 Units/reaction of purified DNA-PK holoenzyme, 150 ng/reaction of either purified GST–FLCN or GST-p53, was prepared on ice. p53, a well characterised substrate of DNA-PK (Goodwin and Knudsen 2014), was used as a positive control. ddH$_2$O was used as a substrate negative control. The assay was activated with 100 mM ATP containing 1 µCi γ-[32P] ATP. Reactions were incubated for 45 min at room temperature. Kinase activity was stopped with the addition of 1x NuPAGE LDS sample buffer (Invitrogen) supplemented with 100 mM DTT (Sigma-Aldrich-Aldrich). Samples were separated by SDS-PAGE (Invitrogen). Gels were vacuum-dried and [32P]-incorporation was measured by autoradiography.

2.11 Western blot

Protein samples were separated on SDS-PAGE (Invitrogen) at 150 V for 1 h and 5 min, after which, proteins were electrophoretically transferred to a polyvinylidene difluoride (PVDF) membrane at 25 V for 2 h 10 min. Membranes were blocked with 5 % [w/v] non-fat milk in TBS-T (10 mM Tris, 150 mM NaCl, 0.1 % [v/v] Tween-20, pH7.6) for 1 h at room temperature. Required primary antibodies were diluted (as listed below) in 2 % BSA [w/v] in TBS-T and incubated at 4 °C overnight. After three washes with TBS-T, secondary antibodies conjugated with horseradish peroxidase (HRP) were applied. Membranes were analysed by using enhanced chemiluminescence (Luminata Classic [WBLUC0500], Crescendo [WBLUR0500], Forte [WBLUF0500]; Millipore) as required.

2.11.1 Antibodies

Unless stated otherwise, antibodies were purchased from Cell Signalling Technologies. The following total protein antibodies were used for western blotting;, β-actin (1:1000, #84573 (D6A8)); p53 (1:1000, DO-1; Bethyl); GST (1:1000, #DAM1411332; Millipore); HA (1:1000, #1186742300; Roche); DNA-PKcs (1:250, #D00148436; Calbiochem); p21 (1:1000, 12D1), CDC37 (1:1000, ab108305, Abcam), CDK4 (1:1000, 11026-1-AP, Proteintech), Histone 3 (1:1000, ab1791, Abcam), EGFR (1:1000, #2232), LDHA (1:1000, ab53292, Abcam), SP1 (1:1000, #9389 (D4C3).

The following additional phospho-specific proteins were used; p-ATR s428 (1:1000, #2853p); p-Chk1 Ser345 (1:1000, #2348p (13D3)); p-H2AX Ser139 (1:1000, #9718P (S) (20E3)); p-Chk2 Thr68 (1:1000, #2661P); p-ATM Ser1981 (1:1000, #5883P (D6H9)); p-BRCA1 Ser1524 (1:1000, #9009P); p-p53 Ser15 (1:1000, #9286P (16G8)); p-RB Ser780 (1:1000, D59B7); p-DNA-PK Ser2056 (1:5000, Ab124918; Abcam).

2.12 Cell viability assay

1×10^5 low passage HK2 cells were seeded onto a 60 mm plate and incubated overnight. Cells were subjected to 10 Gy IR, trypsininsed and 10μL of suspended cells were loaded onto a NC-Slide A8™. DNA was stained with Solution 18™ (chemoetic) to identify live vs total cells

and the viability of harvested HK2 cells were measured by using a NucleoCounter NC-3000 (Copenhagen, Denmark), according to the manufacturer's instructions.

2.13 Subcellular fractionation

Cells were treated with either 5 or 10 Gy IR and after 1 hour lysed using the Subcellular Protein Fractionation Kit for Cultured Cells™ (ThermoFisher Scientific) as stated in the manufacturer's protocol. The following proteins were used as fraction controls; lactate dehydrogenase (LDHA) for the cytoplasmic fraction; epidermal growth factor receptor (EGFR) for the membrane-bound fraction; transcription factor Sp1 (SP1) for the soluble nuclear fraction; and histone 3 (His3) for the chromatin-bound fraction.

2.14 Flow cytometry

For all experiments, cells were seeded at $1x10^5$ in 35 mm plates. Where specified, cells were subjected to IR. To quantify DNA content, 20 µM DRAQ5™ (BioStatus) was added to samples 10 min before FACS analysis using a BD FACSCalibur™ (BD Biosciences). Data were quantified by using Flow Jo v10 Software (Tristar).

2.14.1 Cell cycle analysis following DNA damage

Low passage HK2 cells were subjected to 2 Gy IR, after which fresh media was added. Cells were washed once with 1 mL PBS and fixed with ice-cold 70 % [v/v] ethanol on ice for 45 min. Fixed cells were stored at 4 °C in PBS until analysed.

2.14.2 G2/M phase block

Low passage HK2 cells were subjected to 2 Gy IR and fresh media was added containing 60 ng/mL colcemid (Gibco). Cells were washed once with 1 mL PBS and fixed with ice-cold 70 % [v/v] ethanol on ice for 45 min and stored at 4 °C in PBS until analysed.

2.14.3 Quantifying S phase cells

The thymidine analogues; 5-bromo-2'-deoxyuridine (BrdU) and 5-ethynyl-2´-deoxyuridine (EdU), were trialled in an attempt to quantify cells entering S phase.

For Brdu treatment, cells were treated with 30 μM BrdU and fixed with ice-cold 70 % [v/v] ethanol on ice for 45 min. Once fixed, DNA was denatured by incubating cells in 1 mL 3 M HCL at room temperature for 30 min and washed with 1 mL of 0.1 M sodium borate (Sigma-Aldrich-Aldrich) to stop acid depurination. Samples were centrifuged for 10 min at 1000 rpm and supernatant was removed. Cells were re-suspended in 180 μl 0.5 % [v/v] Tween 20 and 1 % [w/v] BSA in PBS and incubated at room temperature for 15 min. 20 μl Anti-BrdU, antibody (clone B44, 347580 Becton Dickinson Biosciences) was added and samples were incubated for 1 h at room temperature. Cells were washed once with 3 mL PBS before being incubated with Alexa 488-conjuated secondary antibody (1:500, Invitrogen) in 100 μl 0.5% [v/v] Tween 20 and 1 % [w/v] BSA in PBS for 1 h at room temperature in the dark. Cells were stored at 4 °C in PBS until analysed.

For EdU treatment, the Click-iT® EdU Alexa Fluor® 488 Flow Cytometry Assay Kit (ThermoFisher Scientific) was used as described in the manufacturer's protocol. The concentration of EdU used was lowered from 10 μM to 8 μM for longer incubation time, as recommended by manufacturer.

2.15 Data handling and statistical analysis

Where appropriate Student's t-test was performed in Microsoft Excel and two-way ANOVA was performed in GraphPad Prism 4.00.

Chapter 3: Analysing the FLCN interactome; a novel FLCN/DNA-PKcs interaction

3.1 Introduction

Cellular functions are not carried out by single proteins, but rather by protein networks that act together. Recent advances in biological techniques such as yeast-2-hybrid, tandem affinity purification, and mass spectrometry, have led to a large amount of publicly available protein-protein interaction (PPI) data. PPI networks represent the cross talk among groups of proteins and provide valuable information to help understand cellular function, biological processes, and mechanisms of disease aetiology (Barabasi and Oltvai 2004; Kann 2007; Safari-Alighiarloo et al. 2017). There are limitations to PPI networks. For instance, PPI networks do not explore spatial or temporal aspects that might influence protein interactions within the network, i.e., due to interactions in different cellular compartments. Consequently, PPI networks may not accurately reflect the actual situation in a cell. Nevertheless, the organisational principles discovered by analysing the topological features in these networks can be used to provide an insight into cellular interactions that exist under defined conditions (Barabasi and Oltvai 2004). Topological characteristics in PPI networks allow you to determine the key elements within a network (Barabasi and Oltvai 2004; Safari-Alighiarloo et al. 2017). Centrality is an important part of the topological characteristics of any given PPI network and there are many centrality parameters are defined for network analysis (Barabasi and Oltvai 2004), some prove more informative than others. 'Degree' (k) and 'betweenness centrality' (BC) are the two most commonly applied topological attributes explored in PPI networks. Proteins with a high number of interactions, as determined by their k value, are known as hubs; while proteins with high BC are termed bottlenecks (Barabasi and Oltvai 2004). Proteins that have both a high number of interactions and a high BC are often referred to as hub-bottlenecks. These proteins are often crucial for the PPI network integrity (Barabasi and Oltvai 2004) and are useful for understanding the flow of information around the network.

To better understand the tumour suppressor role of FLCN, an unbiased protein interaction screen for FLCN was carried out. To do this, GST-tagged FLCN was expressed in HEK293 cells and then purified on glutathione-Sepharose beads. Proteins that co-purified

with GST-FLCN were resolved on SDS-PAGE and subjected to mass spectrometry. This identified over 650 potential FLCN-interacting proteins, 613 of which were successfully mapped to form a FLCN interactome using the STRING protein–protein interaction database (Szklarczyk et al. 2017). The dense protein interaction network was then imported into Cytoscape (v3.6.1 (Lopes et al. 2010) to explore the topology and form a more meaningful network (Figure 3.1A). A full list of proteins identified by mass spectrometry can be found in appendix 1.

A)

B) <u>Colour Key</u>

- 🔵 Telomere maintenance
- 🟣 DNA damage
- 🟡 Transcription & Translation
- 🔴 Chromatin structure
- 🔵 DNA replication
- ⚫ 2 or more functions
- 🟢 Ubiquitination
- 🟠 Cell cycle
- ⚪ Other (function(s) not referenced)
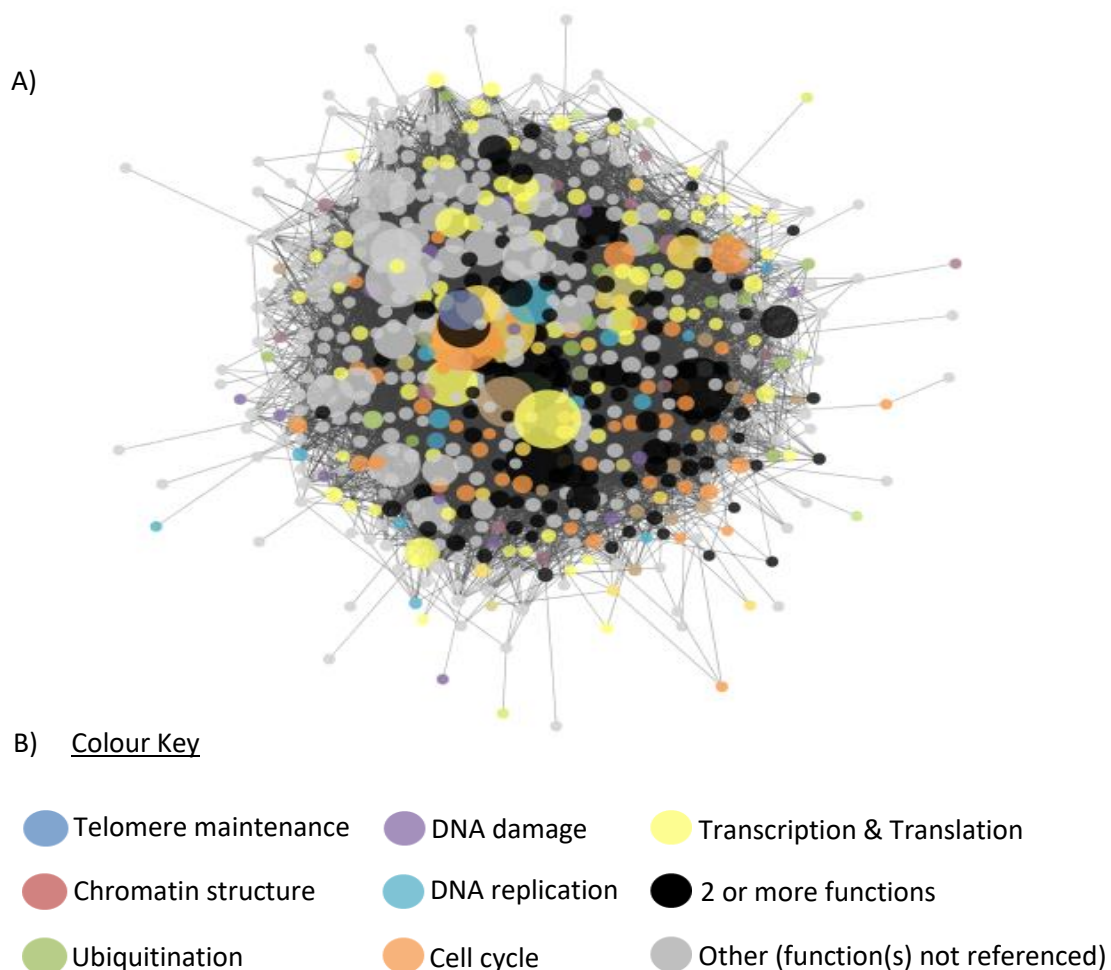
Figure 3.1 Network image of the FLCN interactome. A) FLCN interactome containing all proteins as determined by GST-FLCN pull down. The network contains 613 proteins coloured according to the biological processes they are involved in. Node size corresponds to the number of interactions with other FLCN-bound proteins (k) with larger sized circles representing a higher number of interactions. B) Node colour key indicating what biological process each protein is involved in. A more detailed functional break down of the FLCN interactome can be found in figure 3.4.

3.2 Results and discussion

3.2.1 FLCN interactome network modelling

Within PPI networks, the number of edges that connect to a given node is referred to as its degree (k), *i.e.*, the number of interactions a protein has to other proteins within the network. The largest degree in the FLCN interactome was 169, while the average degree for the network is 32.28 (Figure 3.2A). The degree distribution (Figure 3.2B) of a network is the probability distribution of node degrees over the whole network (Barabasi and Oltvai 2004). Within a biological setting, most proteins within a network participate in only a few interactions, while a few proteins participate in many. These proteins are referred to as hub proteins. Hubs typically represent proteins that have a crucial role for the cell. They function as control centres connecting many cell processes (Barabasi and Oltvai 2004; Han et al. 2004). Depending on the nature of the protein, the degree could indicate a central role in amplification (kinases), diversification and turnover (small GTPases), signalling module assembly (docking proteins), or gene expression (transcription factors). Hubs identified within the FLCN interactome include TP53, HSP90AA1, CDK1, PPP2CA, PPP2R1A, PCNA, and XOP1, and all are involved in DDR, cell cycle regulation, or have been linked to tumorigenesis. These proteins are discussed further in sections 3.3 and 3.5; and summarised in table 3.1.

A) Summary of PPI topological parameters

Parameter	Score
Number of nodes	613
Average Clustering coefficient	0.401
Connected components	1
Average shortest path length	2.475
Maximum node degree	169
Average node degree	32.277
Network density	0.053
Network heterogeneity	0.931
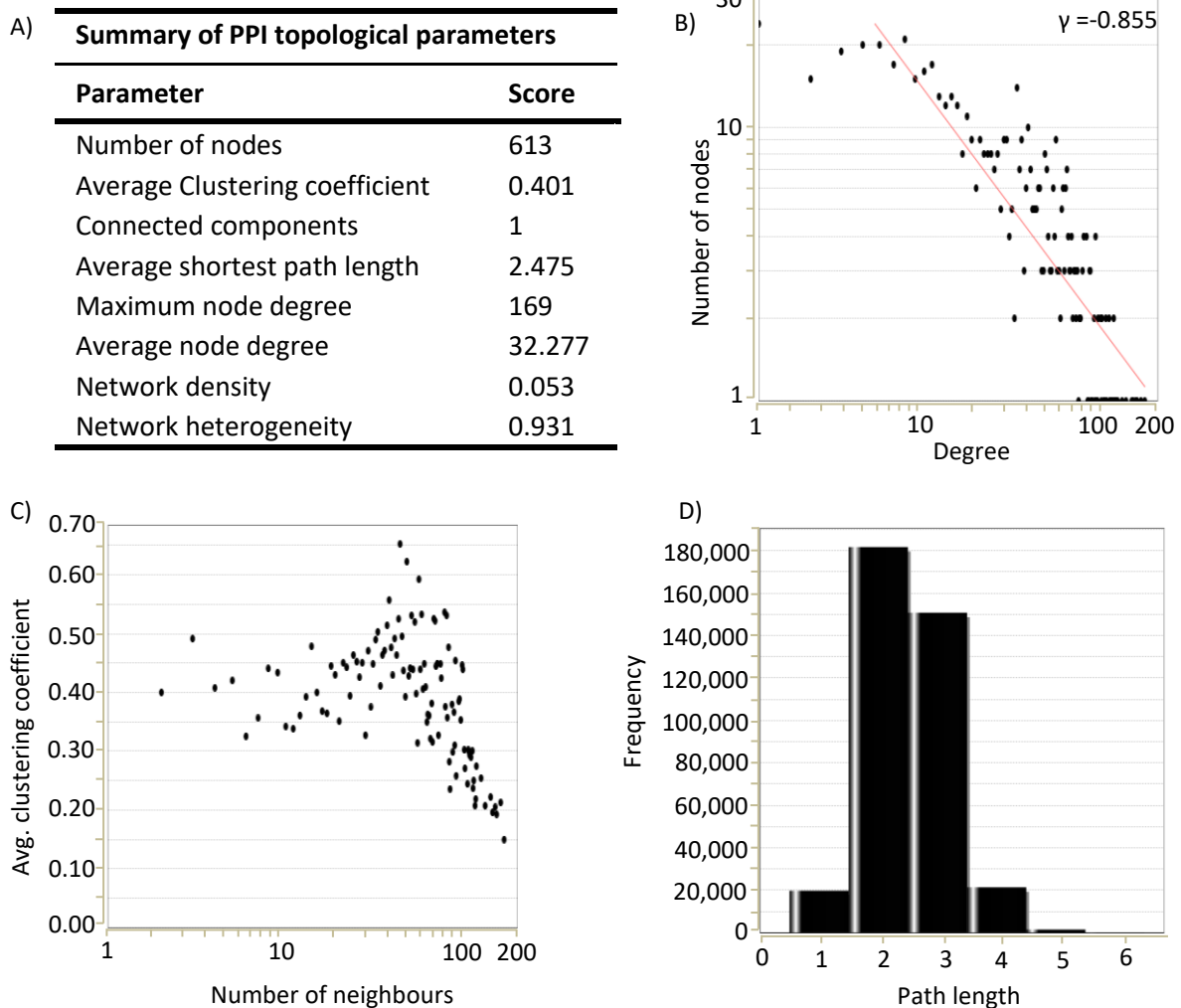
Figure 3.2 Topological parameters of the FLCN interactome. A) A summary of the FLCN protein-protein interaction (PPI) network topological parameters. B) The distribution of node degree within the FLCN interactome. Red line indicates power of fit and has a degree exponent γ =0.-855. C) The distribution of cluster coefficient within the FLCN interactome. D) The distribution of shortest path length within the FLCN interactome.

Within the FLCN interactome, the degree distribution decreases following a power-law (P(k) ~k^γ), where *k* is the number of partner proteins, and γ is the degree exponent (figure 3.2B). This indicates that the network has scale-free properties. Most biological networks are scale-free. In a scale-free network, the probability of a node (protein) being highly connected is statistically more significant than in a random network (Barabasi and Oltvai 2004). In random networks most of the nodes have almost the same number of edges (interactions) (Barabasi and Oltvai 2004). The value of γ can determine characteristics of the

network. The smaller the value of γ, the more important the role of hubs are. For γ>3 the hubs are not relevant, and a scale-free network behaves like a random one. When 2< γ <3 there is a hierarchy of hubs, with the most connected hub being in contact with a small fraction of all nodes. When γ=2, a hub-and-spoke network emerges, with the largest hub being in contact with a large fraction of all nodes. Furthermore, γ<3 networks typically possess a high level of robustness against accidental node failures. This means the network can respond to changes in external conditions or internal organisation while maintaining comparatively normal behaviour (Albert et al. 2000). Within a biological context, disabling an extensive number of proteins will result in a functional dissolution of a network; however, cell signalling networks can withstand the incapacitation of many of their individual components. Even if 80 % of randomly selected nodes fail, the remaining 20 % are usually still able to form a compact cluster with a path connecting any two nodes. On the other hand, the reliance on hub proteins for information flow is an area of vulnerability for scale-free networks. Removing a only few key hub proteins can break the network into small isolated clusters (Albert et al. 2000). Proteins involved in cancer often form hubs and are good examples of the limitations of scale-free networks. p53, for instance, has over 300 protein interactors (Maslon and Hupp 2010). A mutation in any one of these 300 proteins would likely have minimal effect on the cell. However, loss of p53 itself is linked to the deregulation of numerous cell systems and the progression of many cancers (Maslon and Hupp 2010). The FLCN interactome has a degree exponent of 0.855, (figure 3.2B) similar to that of other biological networks following a scale-free distribution (Barabasi and Oltvai 2004). The R^2 value was 0.754, verifying the scale-free property of the network. Together the γ and R^2 value establish an important role for the hub proteins in maintaining the network integrity (Barabasi and Oltvai 2004).

The clustering coefficient, on the other hand, signifies a node's connectedness to other nodes. The clustering coefficient was used to identify the overall organisation of the network (Barabasi and Oltvai 2004). The average clustering coefficient of the nodes decreases as the number of interactions per protein increases, demonstrating the potential of the network to adopt a hierarchical organisation. The average clustering coefficient of the FLCN interactome was 0.401 (figure 3.2C). This parameter was also measured in 100 random networks generated by rewiring edges in the FLCN interactome while preserving the

degrees of the respective nodes. In the random networks, the average clustering coefficient was 0.176 (SD± 0.004), supporting the idea that the FLCN interactome behaves like a real-world network.

The shortest path length describes the distance between two nodes having the minimum edge length, *i.e.*, the shortest route between any given two proteins. The shortest path length distribution can indicate small-world properties, the information transfer efficiency, and the overall navigability of the network (Barabasi and Oltvai 2004). In the FLCN interactome, the average shortest path length was 2.475. The shortest path length distribution (Figure 3.2D) shows the majority of paths are short (<3) suggesting that information can spread rapidly from any given node to all other nodes in the network.

The overall structure and topological properties of the network indicate that it is a strongly connected, scale-free network. Thus, it represents a solid and specific network of interactions from the human PPI.

3.2.2 Identifying important proteins within the FLCN interactome

The global centrality measures (closeness centrality and betweenness centrality) have been used in many studies to find essential proteins within PPI networks. Closeness centrality (CC) is the average length of the shortest path between the node and all other nodes. The more central a node is, the closer it is to all other nodes. It is a measure of how fast information spreads from a given node to other reachable nodes in the network (Barabasi and Oltvai 2004). CC can be interpreted as the probability of a protein to be functionally relevant for several other proteins within the network, but with the possibility to be functionally irrelevant for few other proteins. The higher a CC value is, the closer it is to all other nodes (figure 3.3A). Recently it has been demonstrated that CC does not reliably deduce the essentialness of a protein within a network, and instead betweenness centrality (BC) should be favoured (Raman et al. 2014). BC measures how frequently nodes are on the shortest pathway between any two nodes (figure 3.3B) (Barabasi and Oltvai 2004). The BC of a node reflects the amount of control that a node exerts over the interactions of other nodes in the network (Yoon et al. 2006). Nodes with a high BC are of interest because they function as bottlenecks, i.e., they lie at the intersection of communication paths and can control

information flow. In biology, these nodes represent important proteins in signalling pathways (Girvan and Newman 2002; Barabasi and Oltvai 2004; Han et al. 2004). Within the FLCN interactome the node with the highest BC was TP53, a major tumour suppressor that is heavily mutated in cancer progression.

A backbone network was constructed from nodes with both a high degree and high BC, termed hub-bottleneck nodes. These were determined by values that are 2 standard deviations above respective means. A total of 18 hub-bottleneck nodes were identified in the FLCN interactome (Figure 3.3C), whose functions are summarised in table 3.1. Of these, p53, HSP90AA1, CDK1, PPP2CA, PPP2R1A, PCNA, and XPO1 have all been previously been linked to DDR and cell cycle control and are often altered in tumorigenesis.
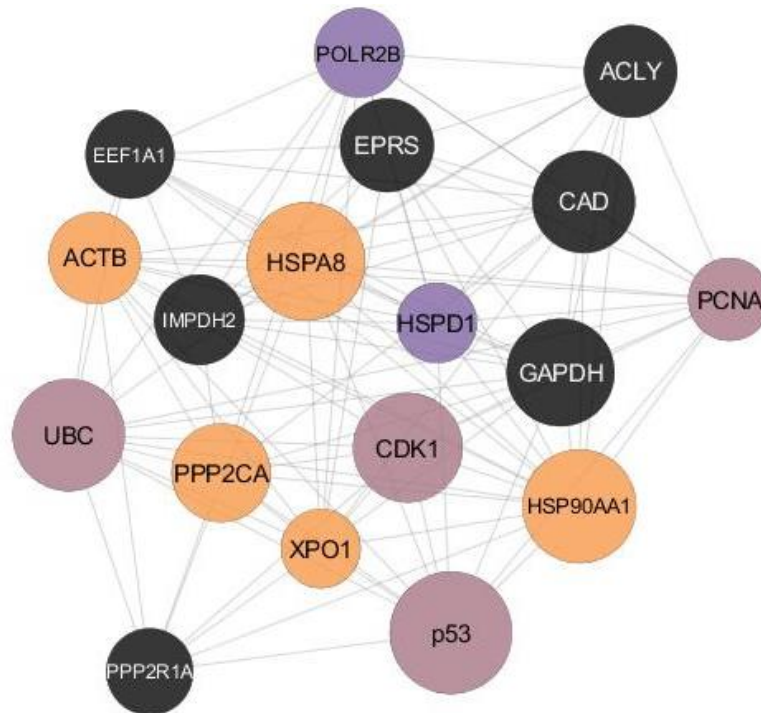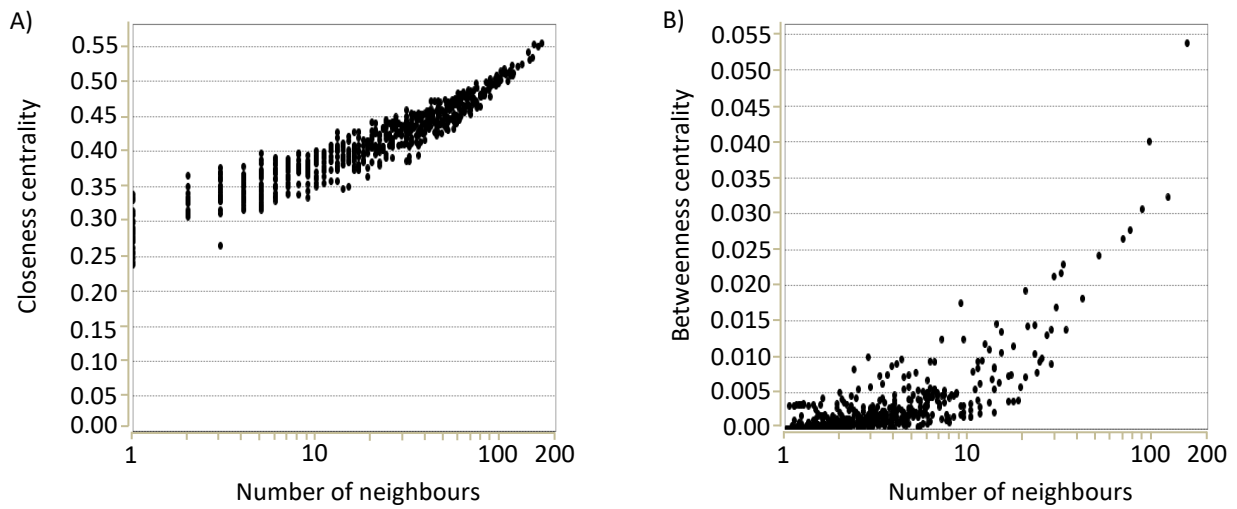
Figure 3.3 Important proteins within the FLCN interactome. A) Distribution of closeness centrality (CC) scores within the FLCN interactome. B) Distribution of betweenness centrality (BC) scores within the FLCN interactome. C) The backbone network of the FLCN interactome showing proteins that contain both a high degree (k) and high a BC score as determined by values that are 2 standard deviations above their respective means. These are considered hub-bottleneck nodes. Purple nodes = proteins with a role in the DNA-damage response (DDR); orange nodes = proteins with a role in the cell cycle; mauve nodes = proteins with a role in both DDR and cell cycle; black nodes = have either 3+ functions, or do not function in DDR and/or cell cycle.

Protein Name	Function	k	BC
p53	Tumour suppressor; induces growth arrest or apoptosis depending on the physiological circumstances and cell type. Negatively regulates cell cycle regulation. Involved in signal transduction following DNA damage.	169	0.05376
HSPA8	Molecular chaperone for in a wide variety of cellular processes. Ensures correct folding of newly synthesized polypeptides. Activates proteolysis of misfolded proteins. Acts in response to stress.	161	0.03225
HSP90AA1	Molecular chaperone that promotes the maturation, structural maintenance and proper regulation of specific target proteins involved in cell cycle control and DNA damage response signal transduction.	153	0.0401
UBC	Polyubiquitin-C has a role in a diverse range of biological processes, including DNA repair.	150	0.03059
CDK1	Plays a key role in cell cycle control. Regulates G1 progression and G1-S transition. Also promotes G2-M transition.	145	0.02768
GAPDH	Modulates cytoskeleton. Has a role in glycolysis. Participates in nuclear events including transcription, RNA transport, DNA replication and apoptosis. Nuclear functions are due to the nitrosylase activity; nuclear target proteins include SIRT1, HDAC2 and **DNA-PKcs**.	142	0.02650
CAD	This protein is a "fusion" protein encoding four enzymatic activities of the pyrimidine pathway (GATase, CPSase, ATCase and DHOase)	132	0.02412
PPP2CA	PP2A is the major phosphatase for microtubule-associated proteins (MAPs). PP2A can modulate the activity of phosphorylase B kinase casein kinase 2, mitogen-stimulated S6 kinase, and MAP-2 kinase. Can dephosphorylate p53. Activates pro-proliferation pathways via RAF1.	125	0.01821
EPRS	Multifunctional protein, primarily part of aminoacyl-tRNA synthetase multienzyme complex. Is an effector of the mTOR signalling pathway.	118	0.01377
ACLY	ATP-citrate synthase is responsible for the synthesis of cytosolic acetyl-CoA in many tissues. Has a central role in de novo lipid synthesis.	117	0.02287
ACTB	B-actin involved in various types of cell motility, major component of the cytoskeleton.	116	0.02172
IMPDH2	Catalyses inosine 5'-phosphate (IMP) to xanthosine 5'-phosphate (XMP). Regulates of cell growth. Possible role in malignancy and progression of some tumours.	114	0.01698
POLR2B	DNA-dependent RNA polymerase catalyses the transcription of DNA into RNA.	113	0.02123
EEF1A1	This protein promotes the GTP-dependent binding of aminoacyl-tRNA to the A-site of ribosomes during protein biosynthesis.	112	0.01379
PPP2R1A	The PR65 subunit of protein phosphatase 2A serves as a scaffolding molecule to coordinate the assembly of the catalytic subunit and a variable regulatory B subunit. Required for proper chromosome segregation and for centromeric localization of SGO1 in mitosis.	110	0.01305
PCNA	Auxiliary protein of DNA polymerase delta. Involved in controlling DNA replication. Plays a key role in DNA damage response (DDR) coordinating DNA replication with repair at the replication folk. Acts as a loading platform to recruit DDR proteins.	105	0.01447
HSPD1	Chaperone implicated in mitochondrial protein import and macromolecular assembly.	102	0.01438
XPO1	Mediates the nuclear export of cellular proteins bearing a leucine-rich nuclear export signal (NES) – such as cyclin D1	101	0.01931

Table 3.1 Table summarising the backbone network of the FLCN interactome. Listed proteins contain both high degree and high betweenness centrality (BC), as determined by values that are 2 standard deviations above their respective means and are considered hub-bottleneck nodes. The proteins are ordered based on degree values (*k*), highest value first.

3.2.3 Functional role of the FLCN interactome

To gain insights into the biological roles of the components of the FLCN interactome, gene ontology (GO) category enrichment was analysed using the STRING-db. The GO categories; cellular component (GO-CC) and biological process (GO-BP) were used to organise the constituents of the FLCN interactome and indicate possible functions for FLCN. GO-CC terms describe subcellular structures and macromolecular complexes and may be used to annotate cellular locations of gene products, and by extension give clues as to its biological function. GO-CC term enrichment for the FLCN interactome suggest FLCN interacts with proteins that function in every aspect of the cellular substructures (figure 3.4), but suggest the nucleus may be the most important compartment of FLCN interactors (Roncaglia et al. 2013).
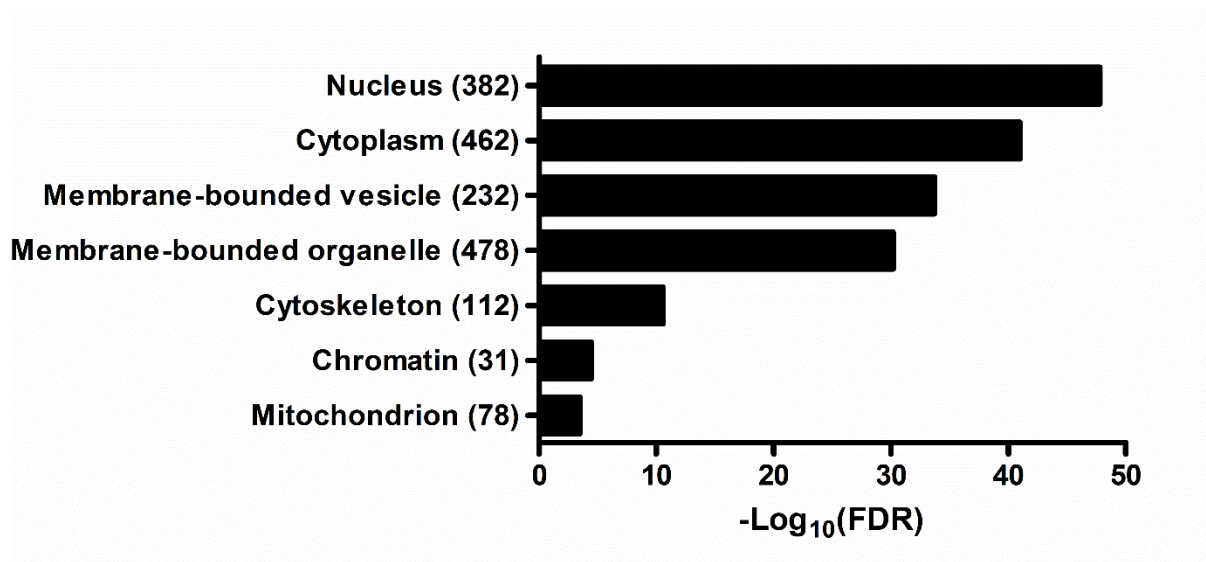
Figure 3.4 Cellular component enrichment of the FLCN interactome. Bar graph showing enrichment *P*-values corrected to multiple testing (FDR) for subcellular compartments in which components of the FLCN interactome function. Number of proteins in each compartment are bracketed.

Using a threshold of FDR<0.05, a total of 743 significant GO-BP terms were enriched (see appendix 2 for a full break down of terms and FDR corrected *P*-values). GO is a large bioinformatic initiative to unify the attributes of genes across all species. The project aims to maintain and develop a controlled vocabulary of gene attributes, and to assimilate and disseminate annotation data to enable functional interpretation of experimental data (Ashburner et al. 2000; Harris et al. 2008). GO is not static; additions, alterations, and corrections are advocated by both those directly involved in the GO project, and members of the research community (Harris et al. 2008; Lovering 2017). Over the years, similar and overlapping terms have emerged, giving a level of redundancy to the GO annotations. This can be considered a good thing as specific association between a GO term and gene can be made stronger by the availability of multiple annotations that reproduce an association using evidence from independent sources of data. However, GO term-gene associations are sometimes based on the same primary data and can result in a false impression, giving more emphasis on the association. Numerous 'GO term/gene product' associations can cause an annotation dataset to become unnecessarily large and cumbersome for data manipulation. For example, within the FLCN interactome the terms; cell cycle (GO.0007049, FDR 6.05E-32), mitotic cell cycle (GO.0000278, FDR 7.56E-35), mitotic cell cycle process (GO.1903047, FDR 7.3E-34), and cell cycle process (GO.0022402, FDR 3.91E-33) are all vastly enriched, but all overlap in function and cover the same biological process. As such, GO terms where combined into 8 broad categories. These were telomere maintenance, chromatin structure, ubiquitination, DNA damage, DNA replication, cell cycle, and, transcription and translation. Everything else is categorised under 'other' (figure 3.5A). These categories were chosen as they either have no or very limited evidence linking FLCN to the biological process.

Interestingly, there is a large degree of functional overlap between each category. Proteins within the FLCN interactome often have roles in multiple biological processes (figure 3.5B). This supports the concept that FLCN functions in co-coordinating multiple cellular responses and global homeostasis, rather than a defined cellular role.
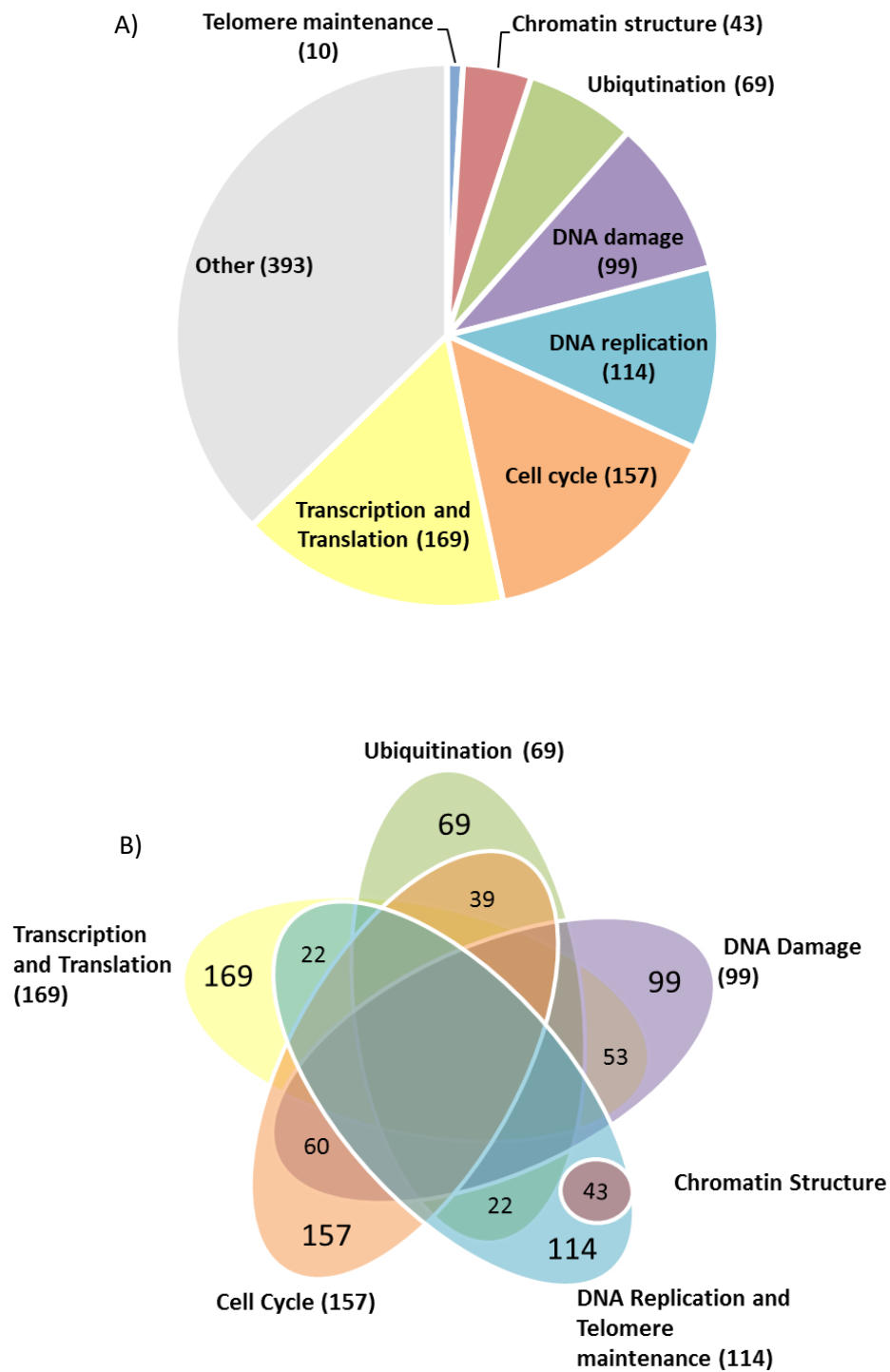
Figure 3.5 Functional break down of the FLCN interactome. A) Pie chart showing merged Gene Ontology biological processes (GO-BP) terms enriched within the FLCN interactome that have either not previously been linked to, or only weakly associated with, FLCN. As determined by string-db.org. B) Venn diagram showing functional overlap of the FLCN PPI network.

3.2.4 A closer look at DDR and cell cycle components of the FLCN interactome

Functional analysis of the FLCN interactome highlighted a role for FLCN in DDR and the cell cycle (figure 3.6). 99 proteins where identified to function within DDR, 157 within the cell cycle and 60 have a role in both (figure 3.6A). As previously stated, a large proportion of proteins highlighted as integral for the function of the FLCN PPI network (figure 3.6B); p53, HSP90AA1, CDK1, PPP2CA, PPP2R1A, PCNA, and XPO1, have been linked to both DDR and the cell cycle. These are discussed in-depth below.

3.2.4.1 Tumour suppressor p53

TP53 gene encodes the tumour suppressor protein p53. p53 accumulates at times of cellular or genotoxic stress, when it functions to regulate transcriptional control at the G1/S phase checkpoint and promote cell cycle arrest, to co-ordinate DNA repair, to initiate and maintain senescence, or to promote apoptosis if the normal cellular conditions are not restored (Brosh and Rotter 2009). It functions to prevent conditions arising within the cell that can lead to the establishment of mutations and tumorigenic transformation of cells. More than 50 % of human cancers have a mutation in p53 that allow cells to escape from p53-driven apoptosis and senescence. Interestingly, TP53 gene expression has been shown to correlate with the transition from precancerous lesions to malignancy (Bartkova et al. 2005; Halazonetis et al. 2008; Brosh and Rotter 2009). Furthermore, overexpression of TP53 relates to poor patient prognosis in different cancer types (Haitel et al. 1999). Specifically in RCC, TP53 gene overexpression has been reported in up to 40% of tumours (Shiina et al. 1997; Haitel et al. 1999), but the role of TP53 overexpression in RCC is still debated (Zigeuner et al. 2004). Interestingly, data suggests that mutations within TP53 gene may not be linked to patient outcome, or progression in renal cancer, and that TP53 up-regulation is not caused by gene mutation in most cases of RCC. Thus, the defect in TP53 leading to its up-regulation in RCC likely reflects indirect and compensatory effects during the course of cancer progression (Noon et al. 2010).
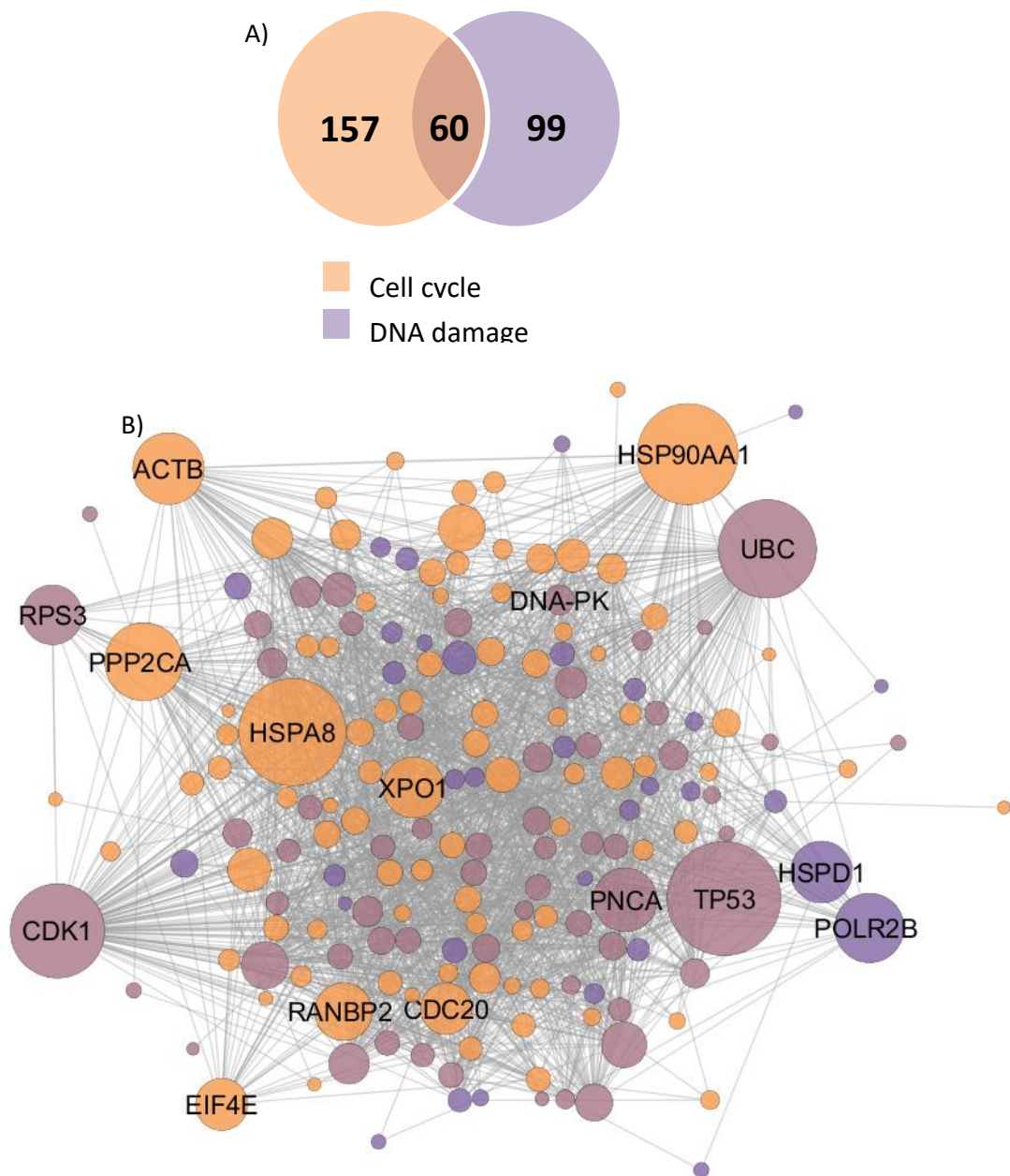
Figure 3.6 A novel role of FLCN involved in DDR and the cell cycle. A) Venn diagram showing the number of proteins within the FLCN interactome that function within the DNA damage response (DDR) or the cell cycle. B) Network image showing proteins within the FLCN interactome that have a functional role in the DDR and/or cell cycle. Purple nodes = proteins with a role in the DDR; orange nodes = proteins with a role in the cell cycle; mauve nodes = proteins with a role in both DDR and cell cycle. Node size reflects the degree of each node.

3.2.4.2 Heat shock protein 90α

Heat shock protein 90-alpha (Hsp90α) is a molecular chaperone required for correct protein folding. Unlike other chaperones, Hsp90α is not required for *de novo* protein folding, but rather facilitates the final maturation of specific proteins. Only once in the correct three-dimensional native conformation can proteins successfully interact with their binding partners. As such, the Hsp90α chaperone machinery plays a key role in orchestrating the spatial and temporal order of protein interactions (Taipale et al. 2010; Makhnevych and Houry 2012). Protein specificity is facilitated through adapter co-chaperones *such as* Cdc37.

The majority of identified Hsp90α protein clients are involved in signal transduction, and HSP90α has been heavily linked to DDR and the cell cycle (Burrows et al. 2004; Pennisi et al. 2015). HSP90α can be considered a regulator of the diverse DDR pathways as multiple components of the DNA DSBR machinery, including BRCA1, BRCA2, Chk1, DNA-PKcs, and p53, have all been described as HSP90α clients. Inhibition of HSP90α has been shown to lead to the altered stabilisation and localisation of DDR proteins after DNA damage (Pennisi et al. 2015). Interestingly, HSP90α has been shown to facilitate telomere maintenance by regulating the switch between its capping and extending structures (DeZwaan et al. 2009). Inhibition of HSP90α was shown to decrease the activity of telomerases (Toogun et al. 2008). Other clients include the cyclin-dependent kinases, CDK4, CDK6, and CDK2, which are essential to cell cycle G1/S phase progression. HSP90α mRNA levels are typically increased at G1/S phase transition and inhibition of HSP90 often leads to G1 cell cycle arrest (Burrows et al. 2004; Giraldez et al. 2017). Importantly, FLCN has already shown to interact with HSP90α (Woodford 2016).

3.2.4.3 Cyclin-dependent kinase 1

Cyclin-dependent kinase 1 (CDK1) is one of the master regulators of mitosis (Salaun et al. 2008). The expression of CDK1 is constant throughout the cell cycle and regulation of its activity depends on its association with cyclins A and B, as well as on post-translational modifications such as phosphorylation. CDK1 activity is restricted from S-phase until mitosis due to the oscillating protein abundance of cyclins A and B, whose gene transcription, translation, and degradation cycles are highly regulated in a temporal manner (Draetta et al. 1989; Hunt 1989; Salaun et al. 2008). CDK1 is bound to cyclin A during S- and G2-phases

(Draetta et al. 1989). In G2, cyclin B is synthesised, allowing cyclin B-CDK1 complexes to form and activate CDK1 to initiate mitotic entry (Morgan 1995). Hyperactivation of CDK1 has been observed in many cancers and dysregulation of Cdk1 causes abnormal proliferation and genomic instability (Hall and Peters 1996; Malumbres and Barbacid 2009).

3.2.4.4 Protein Phosphatase 2A (PP2A) –Scaffold subunit (PPP2R1A), and catalytic subunit (PPP2CA)

The PP2A family of phosphatases are a major class of serine/threonine phosphatases. They have been associated with many cellular events such as the regulation of cell cycle, cell proliferation, and cytoskeletal remodelling (Janssens and Goris 2001). PP2A is a heterodimeric complex comprised of a scaffolding A subunit and a catalytic C subunit. This A/C unit interacts with a regulatory B subunit producing the PP2A heterotrimeric holoenzyme. To date, two different A (A_α and A_β) and C (C_α and C_β), and four different B subunits (B, B', B", and B"') have been identified. The combination of all subunits (A, B, and C) is predicted to produce over 75 different trimeric holoenzymes depending on cell type. The A and C subunits are both ubiquitously expressed, while certain B subunits are only expressed in a tissue-specific manner and/or at particular stages of cellular development. It is thought that the variability of the B subunit dictates substrate specificity and/or subcellular localisation of a given PP2A holoenzyme (Janssens and Goris 2001).

The scaffold subunit, PPP2R1A (A_α), and catalytic subunit PPP2CA (C_α) were identified within the FLCN interactome, and both were found to be hub-bottleneck proteins. Interestingly, it has been demonstrated that the small GTPases, Rab8 and Rab9, interact with PPP2R1A in a GTP-independent manner. It has previously been suggested that specific members of the Rab GTPase family play a role in the inhibition of the PP2A tumour suppressor. The interaction between Rab8/9 competes with PPP2CA to bind PPP2R1A, and weakens the assembly of the PP2A holoenzyme, resulting in its inactivation. Furthermore, it has been noted that numerous Rab proteins associate with PPP2R1A but not the catalytic subunit PPP2CA. This includes Rab34, Rab35, and Rab7a (Sacco et al. 2014). This is interesting as FLCN has already been shown to function as a GEF and GAP for Rab35 (Nookala 2012), and more recently with Rab7a (Laviolette et al. 2017). Furthermore, the regulatory B subunits identified in the FLCN interactome are

PPP2R5C (B'γ), PPP2R5D (B'δ), PPP2R5E (B'ε). Specifically, the PP2A-B'γ holoenzyme is thought to dephosphorylate and activate p53, and play a role in DNA damage-induced inhibition of cell proliferation (Li et al. 2007).

3.2.4.5 Proliferating cell nuclear antigen

Proliferating cell nuclear antigen (PCNA) acts as a molecular platform to facilitate the numerous protein–protein and protein–DNA interactions that occur at the replication fork and is essential for the faithful replication of DNA. PCNA provides a central role co-ordinating many replication-associated processes, including DNA damage repair, chromatin establishment, and correct sister chromatid cohesion. Due to a large number of proteins competing for a common surface, PCNA is able to modulate well controlled regulatory mechanisms. This allows a responsive interplay between appropriate proteins at different stages of DNA replication and associated processes (Strzalka and Ziemienowicz 2011; Mailand et al. 2013).

3.2.4.6 Exportin 1

Exportin 1 (XPO1, also known as CRM1) is one of the most well understood nuclear exporters. It is involved in the shuttling of over 200 cargo proteins (Xu et al. 2012). Crucially, it is the single nuclear exporter of several important cancer-related proteins (Turner et al. 2012), including tumour suppressor proteins (p53, Rb, and BRCA1) (Jiao et al. 2006; Kanai et al. 2007; Brodie and Henderson 2012) and cell cycle regulators (such as p21 and cyclin D1) (Asada et al. 1999; Alt et al. 2000). XPO1 is elevated in many cancers and correlates with poor patient prognosis (Cheng et al. 2014; Azmi et al. 2015; Muqbil et al. 2016; Azmi et al. 2017). It's likely that the enhanced export of tumour suppressor and regulatory proteins away from their targets due to XPO1 overexpression can lead to aberrant cellular growth signalling and prevents apoptosis (Turner and Sullivan 2008). Furthermore, XPO1 forms a complex with eukaryotic initiation factor 4E (eIF4E) and transports known oncogene mRNAs (such as cyclin D1 and MDM2) to the cytoplasm, promoting the synthesis of oncoproteins (Culjkovic-Kraljacic et al. 2012). FLCN was shown to interact with eIF4E within the FLCN-interactome.

3.2.5 Validation of novel interactors

Several proteins within the FLCN interactome were identified with known roles in maintaining genetic stability (Figure 3.7A). The PIKK family members, DNA-PK, ATM, and ATR were of particular interest as they are critically involved in DDR. All three are serine/threonine kinases and are recruited to the DNA lesion site (Lovejoy and Cortez 2009). DNA-PK was the most significant FLCN-interacting protein, with 66 unique peptides identified during MS (figure 3.7A). DNA-PK was confirmed to interact with GST-FLCN by western blot (figure 3.7B). ATR was not confirmed to interact, and ATM may be a very weak interactor. Limited evidence shows ATM interacted weakly with FLCN in two out of three replicates. For the sake of this thesis, ATM is not considered a true interactor with FLCN.

Another protein of interest is telomere-associated protein RIF1 (RIF1). RIF1 is a key regulator of TP53BP1. It plays a role in promoting the repair of double-strand DNA breaks (DSBs) by non-homologous end joining (NHEJ) (Silverman et al. 2004; Drane et al. 2017). Furthermore, the yeast ortholog of RIF1 has a well-established role in maintaining telomere length (Shi et al. 2013). Mammalian RIF1 telomere function is still under debate (Xu and Blackburn 2004; Shi et al. 2013; Kumar and Cheok 2014). In addition, a number of other proteins involved in telomere maintenance were identified by MS (supplementary figure 1), such as TPP1, an important component of the telomeric shelterin complex. This led to the idea that FLCN may be involved in telomere conservation. While preliminary evidence suggested an increase in telomere length and telomere fusion events upon FLCN loss (supplementary figure 1), both RIF1 and TPP1 failed to be validated as FLCN interactors (figure 3.6C). In addition, time restrictions did not permit the exploration of FLCN in maintaining telomeric integrity.

It is worth noting, overexpressed V5-tagged p53 was also transfected into HEK293 cells alongside GST-FLCN. Upon western blotting the V5-tag could not be detected, nor could p53. This was only briefly explored and is worth further work to confirm if p53 directly interacts with FLCN.

A)

Protein Name		# of Unique Peptides	Total peptides
DNA-PKcs	DNA-dependent Protein Kinase, catalytic subunit	66	
RIF1	Rap1 interacting factor homology	7	
ATM	Ataxia-telangiectasia-mutated	5	147
ATR	ataxia telangiectasia and Rad3-related	2	
CDC37	Cell division cycle 37	6	
CDK4	Cyclin-dependent kinase 4	5	
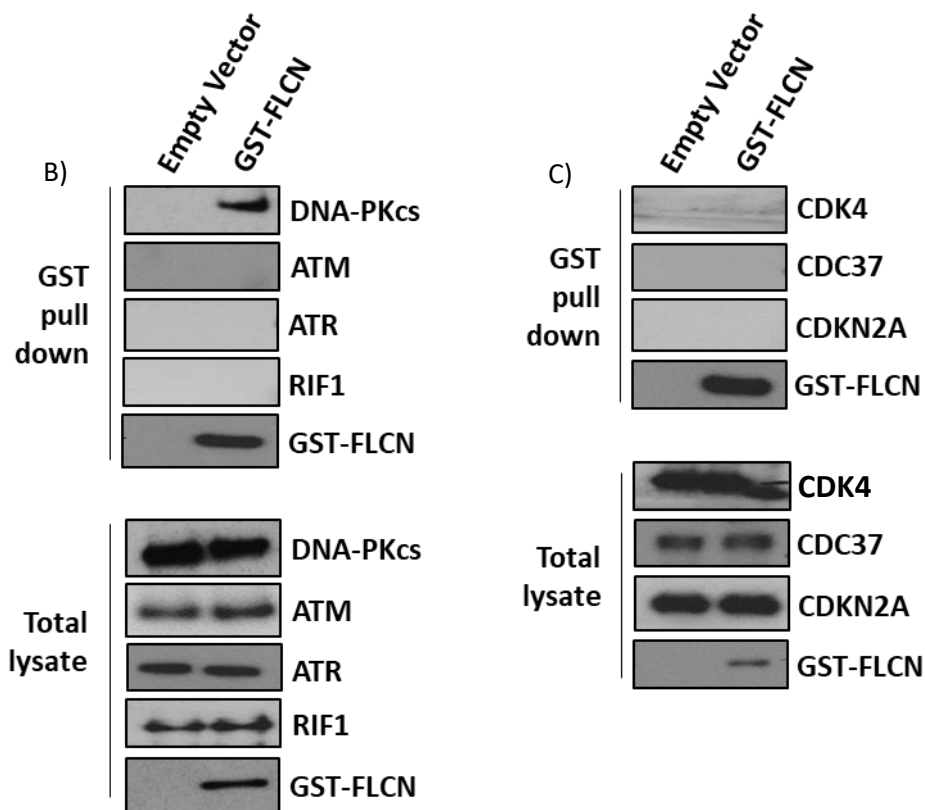
Figure 3.7. Validation of candidate novel FLCN interactors. A) Table of candidate proteins identified by mass spectrometry. B) GST-tagged FLCN was overexpressed in HEK293 cells and used as bait protein to validate a protein interaction between FLCN and endogenously expressed DNA damage components (DNA-PKcs, ATM, ATR). C) GST-tagged FLCN was overexpressed in HEK293 cells and used as bait protein to validate a protein interaction between FLCN and endogenously expressed cell cycle components (CDK4, CDC37, CDKN2A).

Cell cycle associated proteins CDKN2A, CDC37 and CDK4 were also tested as potential FLCN interacting proteins. It's worth noting both CDC37 and CDK4 function as clients of HSP90, a protein already confirmed to interact with FLCN (Burrows et al. 2004; Woodford et al. 2016). However, no evidence was found to validate CDKN2A, CDK4, or CDC37 as FLCN interactors. It's worth noting lysis buffer was changed after this validation attempt. Details are discussed on page 104 but briefly, the lysis buffer used for GST-pull down assays may not sufficiently break down nuclear membrane. Therefore, the lack of biochemical interaction observed for nuclear DDR and cell cycle components such as ATM, ATR, CDK4, CDC37, and CDKN2A may be due to an inadequate lysis protocol. DNA-PKcs, on the other hand, is an extremely abundant protein and is commonly found in the cytoplasm (Anderson 1996; Huston et al. 2008).

To further validate the protein interaction of DNA-PK with FLCN, endogenous DNA-PK co-purified with immunoprecipitated endogenous FLCN (Figure 3.8A). In addition, DNA-PK association was compared with either wild-type FLCN or two patient-derived mutants (Y463X and H429X) (Figures 3.8B). DNA-PK could associate with the two C-terminal truncated patient mutants, indicating that the C-terminus of FLCN is not crucial for DNA-PK binding. DNA-PKcs is a serine/threonine kinase responsible for instigating a DDR against dsDNA breaks. Therefore, DNA-PK's protein interaction with FLCN following IR was explored to better understand the regulation of FLCN binding (figure 3.8C). GST-FLCN expressing HEK293 cells were subjected to IR and showed a marked reduction in association with DNA-PK upon 5 Gy, while no apparent association of FLCN with DNA-PK was observed with the higher dose of IR (10 Gy). DNA-PKcs autophosphorylates at serine 2056 (Ser2056) in response to dsDNA breaks (Smith and Jackson 1999) and phosphorylated H2AX is a well characterised surrogate marker of DSB. Both DNA-PK and H2AX were phosphorylated upon IR, confirming that IR was causing DNA damage.
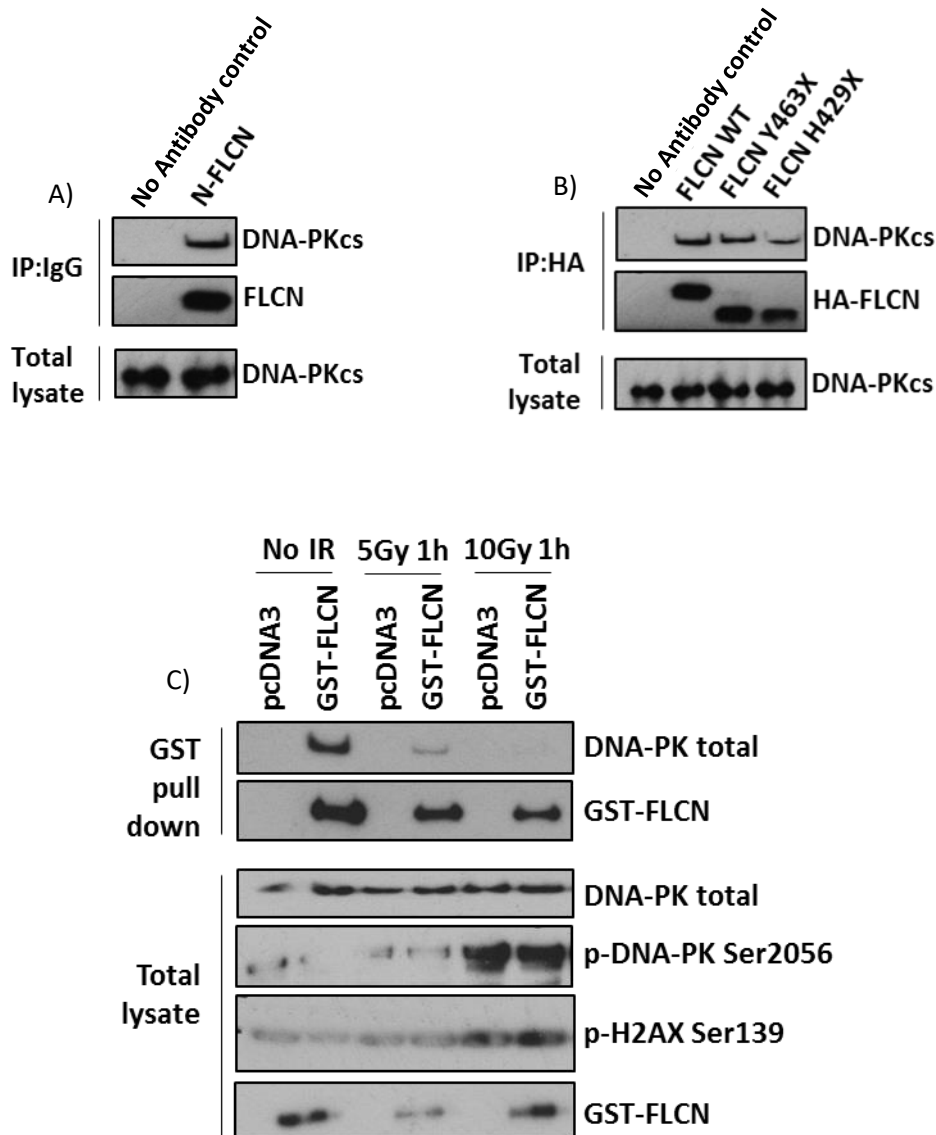
Figure 3.8 Further validation of the novel FLCN/DNA-PKcs interaction. A) Endogenous DNA-PKcs co-immunoprecipitation with endogenous FLCN from HEK293 cells. FLCN was used as the bait protein and immunoprecipitated using an antibody raised against the N-terminal of FLCN. B) Endogenous DNA-PKcs immunoprecipitation with overexpressed HA-tagged FLCN. HA-tagged FLCN constructs consisted of wild type FLCN (WT), and two patient derived C-terminal truncated mutants (Y463X and H429X). C) FLCN/DNA-PKcs interaction following induction of DNA-damage by ionising radiation (IR). GST-tagged FLCN was overexpressed in HEK293 cells and used as bait protein to validate a protein interaction between FLCN and endogenous DNA-PKcs. Cells where subjected to IR (5 or 10 Gy) and left for 1 hour prior to cellular lysis.

3.3 Conclusion

The description of the topological characteristics of a network is often the first step in the analysis of network data (Assenov et al. 2008; Sanz-Pamplona et al. 2012). Proteins that have a large proportion of connections and high centrality measures within the network often play biologically important roles within in the studied system and are essential to the network's viability (Barabasi and Oltvai 2004; He and Zhang 2006; Goh et al. 2007). Proteins that are traditionally associated with cancer tend to be implicated in several cellular processes and signalling pathways; they often work as protein hub-bottlenecks inside PPI networks (Kar et al. 2009). This was observed in the FLCN interactome. The proteins identified as most important for the network organisation and information flow (TP53, HSP90AA1, CDK1, PPP2CA, IMPDH2, PPP2R1A, PCNA, and XOP1) have all previously been linked to DDR, cell cycle control, and/or tumorigenesis (Haitel et al. 1999; Li et al. 2007; Malumbres and Barbacid 2009; Turner et al. 2012; Mailand et al. 2013; Pennisi et al. 2015).

It is necessary to keep in mind that despite huge efforts, the human interactome is not complete. Well studied proteins have a higher probability of being included in such a network, resulting in some selection bias with respect to less studied proteins. Moreover, it is well known that the human interactome contains false positive interactions, so a careful interpretation of results is required (Chua and Wong 2008). Lack of spatial-temporal information is another obstacle to consider in the network elucidation process (Strogatz 2001). Diseases like cancer are complex, consisting of cross-talk between neighbouring cells and the surrounding microenvironment, which is often missed in PPI networks (Kenny et al. 2007; Hanahan and Weinberg 2011) . Despite this, information obtained is often valuable for hypothesis generation.

Several proteins identified in the FLCN interactome have a role in DDR and/or the cell cycle. This led to the hypothesis that FLCN's tumour suppressor functions may extend to genomic maintenance. Moreover, a novel FLCN interactor, DNA-PKcs, was identified and validated. This is an exciting finding. For the first time, FLCN has been linked to a role in genome integrity. The biological reason for this interaction is explored in subsequent chapters.

Chapter 4: Transcriptomic effects of FLCN knockdown

4.1 Introduction

RNA sequencing (RNA-seq) is a high-throughput technology used to provide a comprehensive and unbiased view of the complex nature of the transcriptome (Wang et al. 2009). RNA-seq can be used to identify many features including fusion genes, disease-associated single nucleotide polymorphisms (SNP), and differential gene expression across different groups or treatments (Wang et al. 2009). RNA-seq technology has emerged as a powerful tool for identifying functional genes and pathways in cancer research. Compared to previous hybridisation-based microarray and Sanger sequencing-based methods, RNA-seq provides a higher resolution with less background noise (Wang et al. 2009). In recent years, RNA-seq has become a very widely used technology for profiling transcriptional activity in biological systems. One of the most common uses of RNA-seq is to identify genes or molecular pathways that are differentially expressed between two or more biological conditions (Kukurba and Montgomery 2015). Changes in expression can then be associated with differences in biology and justify further enquiry to uncover mechanisms of action. Indeed, RNA-seq has led to the understanding of the molecular pathogenesis in many cancers (Wang et al. 2019; Zhou et al. 2019). For example, in clear cell RCC, RNA-seq was used to identify novel signalling pathways significantly affected in patient tumour samples (Yang et al. 2014). Similarly, gene expression from RNA-seq data has identified gene signatures that are associated with clear cell carcinoma aggressiveness, prognosis, and overall survival (Tan et al. 2011; Chen et al. 2014; Eckel-Passow et al. 2015; Chen et al. 2016a). RCC is not a single disease. It contains several histologically defined cancers, each with different genetic drivers and therapeutic responses. RNA-seq has been used to evaluate the three major histologic subtypes, clear cell, papillary, and chromophobe RCC to reveal distinctive features of each RCC subtype and provide the foundation to develop subtype-specific therapeutic and management strategies for patients affected with these cancers (Ricketts et al. 2018). RNA-seq has also shown shared features among histological subtypes of RCC. For example, loss of CDKN2A, which encodes p16, was found in 16% of all RCC. Loss of CDKN2A correlated with poor survival in clear cell, papillary, and chromophobe renal cancers (Hamilton and Infante 2016) and demonstrates a universal feature in RCC that

is potentially druggable with CDK4/6 inhibitors that target the downstream effects of p16 loss.

Therefore, transcriptional profiling from RNA-seq of HK2 cells following FLCN knockdown was explored to understand FLCN's tumour suppressive function or to identify potential mechanisms for cellular transformation following FLCN loss. The primary objective of this chapter was to have a broad understanding of transcriptional changes following FLCN loss. RNA preparations were carried out by Dr Elaine Dunlop, Cardiff University. Sequencing of the mRNA was performed by Wales Gene Park, Cardiff. Differentially expressed gene lists were generated by Dr Marc Naven, Cardiff University. It's worth noting RNA-seq was performed using a single clone per cell line in triplicate, therefore results represent means of technical repeats.

4.2 Results and Discussion

4.2.1 Overview analysis of the RNA sequencing data

To get an overview of the effect that FLCN knockdown has on the transcriptome of HK2 cells, a simple analysis compared the total number of significantly differentially expressed genes (DEGs) (figure 4.1A). To do this, FLCN expression was knocked down in a human kidney proximal tubule epithelial cell line (HK2), as the proximal tubules are thought be to the origin cells for BHD-associated RCC (Chen et al. 2008; Hudon et al. 2010). HK2 cells were continually propagated, either with FLCN (wild type, WT) or without FLCN (knockdown, KD), for one year. This BHD cell line model was generated to reflect the effects of long-term loss of *FLCN* in kidney cells present within BHD patients. From this four pairwise comparisons were made; (1) low passage wild type vs low passage knockdown cells (LP-WT vs LP-KD), these represent the direct effect of FLCN knockdown; (2) high passage wild type vs high passage knockdown cells (HP-WT vs HP-KD), these represent the effect of FLCN knockdown in aged cells; (3) low passage wild type vs high passage wild type cells (LP-WT vs HP-WT), these represent changes that normally occur upon cellular ageing; and (4) low passage knockdown vs high passage knockdown cells (LP-KD vs HP-KD), these represent changes occurring due to continuous FLCN knockdown.

A lot of transcriptional dysregulation was detected from FLCN knockdown alone, with 1932 DEGs observed in the LP-WT vs LP-KD cells. Interestingly, this is a higher degree of change than ageing alone (1542 DEGs LP-WT vs HP-WT). Further changes in gene expression occur on ageing with FLCN knockdown with HP-WT vs HP-KD having 4773 DEGs and LP-KD vs HP-KD 4503 DEGs. This is again far above the number seen as part of normal cell ageing (LP-WT vs HP-WT; 1541), suggesting an accelerated deregulation occurs in the absence of FLCN. Next, the direction of the differential expression was explored in response to FLCN knockdown (i.e., are genes up- or down-regulated). Upon normal ageing a similar amount of up regulation and down regulation can be observed (figure 4.1B). In both LP-WT vs LP-KD, and LP-KD vs HP-KD, FLCN knockdown resulted in an increase in the number of upregulated genes (figure 4.1C and 4.1D). However, when comparing the effect of FLCN knockdown in high passage cells to aged matched controls (HP-WT vs HP-KD), an increase in down regulated genes was observed (figure 4.1E).

Typically, a fold change of 1.5 or 2 is considered a true effect in a change of gene expression. It's often argued that small log-fold changes are not biologically relevant, but the exact definition of "small" is open to interpretation, and this thinking typically stems from the idea that larger log-fold changes are more robust and reliably detected across different technologies (e.g., RNA-seq, microarray, and qPCR). Indeed, selecting a threshold on this basis would depend on the sensitivities of the technologies involved (Wang et al. 2009). Several studies have highlighted the functional importance of small gene expression changes (Flintoft 2007; St Laurent et al. 2013; Taugbol et al. 2014). Fold change on its own is not enough to select the DEGs. A log-fold change threshold doesn't tell you much about the error rate, as it doesn't account for the variability of the expression values. Statistics are employed to control the false discovery rate and ensures that the expected proportion of false positives in your data set of DEGs is below a certain threshold (usually 5%). While this itself may be an arbitrary threshold, the choice of this threshold is directly related to the probability of whether the genes are truly differentially expressed or not. The biological significance of a given fold-change is likely to depend on the gene and on the experimental context (McCarthy and Smyth 2009). Therefore, within the HK2 cells, genes were first selected on FDR *P*value<0.05, and all genes were explored in subsequent analysis regardless of their fold change.
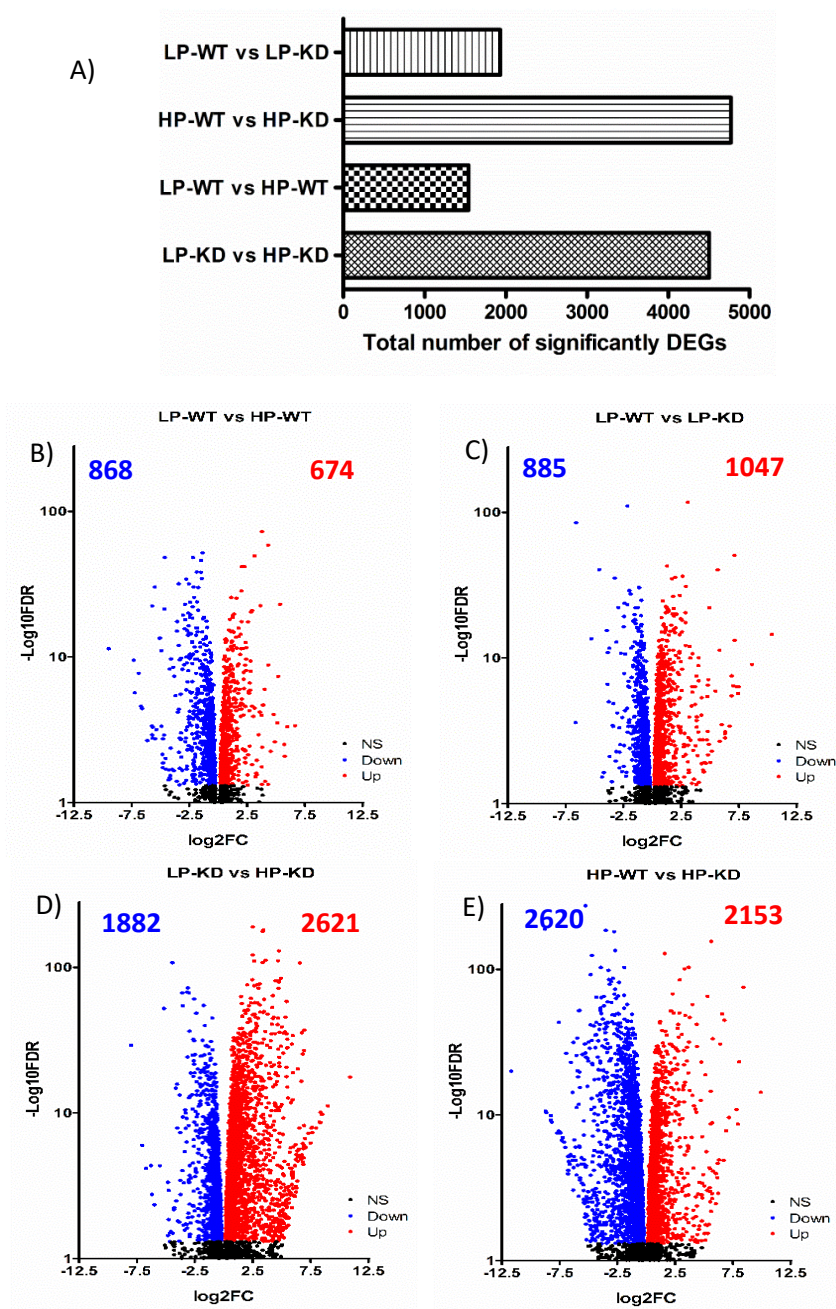
Figure 4.1 Exploring the transcriptomic changes following FLCN knockdown. A) The number of significantly differentially expressed genes (DEGs) in each pairwise comparison of low passage (LP), high passage (HP), wild type (WT), and FLCN knockdown (KD) cells. For each comparison the cell line labelled first represents the control cell line. B) Volcano plot showing normal age-related changes to the HK2 transcriptome (LP-WT vs HP-WT). C) Volcano plot showing upregulated and down regulated genes as a direct response to FLCN knockdown (LP-WT vs LP-KD). D) Volcano plot showing age related changes to the HK2 transcriptome following continued FLCN knockdown (LP-KD vs HP-KD). E) Volcano plot showing upregulated and down regulated genes following a year of continuous cell culture with FLCN knockdown compared to aged matched wild type FLCN cells (HP-WT vs HP-KD). -Log10FDR = log transformed *P*value adjusted for multiple testing using the FDR method. Log2FC = log transformation of gene expression fold change.

The distribution of statistically significant gene expression for each pairwise comparison is summarised in figure 4.2. Interestingly, FLCN knockdown did not produce large transcriptional changes in low passage cells (LP-WT vs LP-KD), only 9% of DEGs have a fold change ±2. The standard deviation of low passage cells was 1.30, meaning 95% of DEGs had a fold change between ±2.60. This increased slightly with normal ageing (LP-WT vs HP-WT, SD 1.50, 95% of DEGs between ±3), and increased again in aged FLCN knockdown cells (HP-WT vs HP-KD, SD 1.72, 95% of DEGs between ±3.44; and LP-KD vs HP-KD, SD 1.75, 95% of DEGs between ±3.5). This suggests that FLCN knockdown may contribute to a larger occurrence of subtle changes, and these changes may become further deregulated with an even longer duration of FLCN knockdown.

A)

B)

All differentially expressed genes				
	Total # DEGs	SD log2FC	# genes log2FC >±2	% genes log2 FC >±2
LP-WT vs LP-KD	1932	1.30	175	9.06
HP-WT vs HP-KD	4773	1.72	763	15.99
LP-WT vs HP-WT	1541	1.50	213	13.82
LP-KD vs HP-KD	4503	1.75	812	18.03
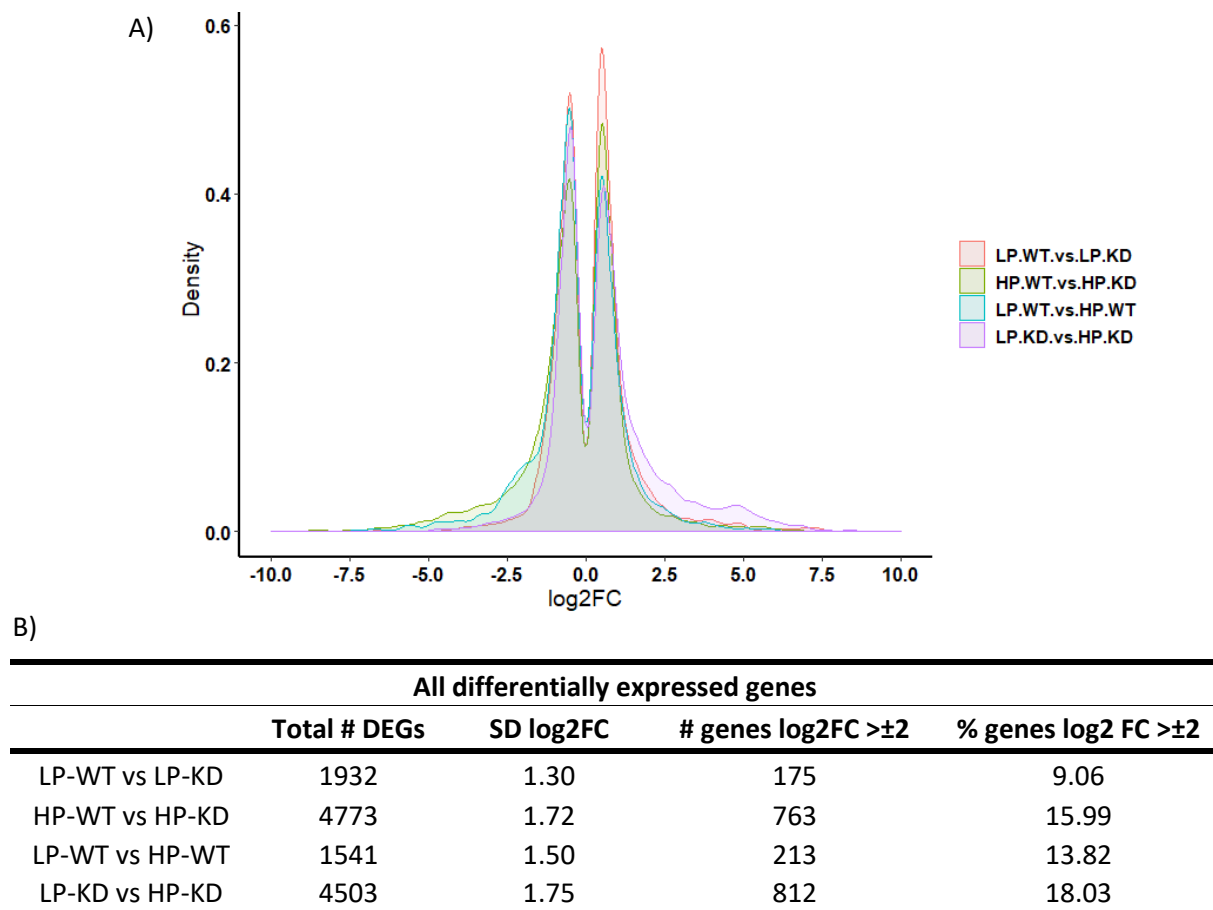
Figure 4.2 Distribution of statistically differentially expressed genes (DEGs) A) Density plot showing the distribution of statistically differentially expressed genes (DEGs) following FLCN knockdown in each pairwise comparison. B) Table summarising the distribution of statistically differentially expressed genes (DEGs) following FLCN knockdown. For each pairwise comparison total number of DEGs, standard deviation (SD) of DEGs, total number of DEGs with a log2 fold change greater or smaller than 2, and percentage of total DEGs with a log2 fold change greater or smaller than 2 are shown. LP = low passage cells, HP = high passage cells; WT = wild type FLCN control, KD = FLCN knockdown.

Gene dysregulation is a hallmark of cancer. Cancer arises from genetic alterations that invariably lead to dysregulated transcriptional programs (Gonda and Ramsay 2015; Vinuela et al. 2018). These dysregulated programs can cause cancer cells to become highly dependent on certain regulators of gene expression (Vinuela et al. 2018). Transcriptional dysregulation arises in cancer from disease-defining genetic alterations, either indirectly via mutation of signalling factors converging on transcriptional control, or directly via genetic alterations in gene control factors themselves. Cancer-associated genetic alterations can affect proteins participating in nearly all levels of transcriptional control, including *trans*-factors (transcription factors, signalling proteins, cofactors, chromatin regulators and chromosome structuring proteins) and *cis*-elements (enhancers, promoters and insulators) (Bradner et al. 2017). Indeed, the FLCN interactome highlighted several proteins with a role in transcription.

Next, transcriptional changes upon FLCN knockdown in low passage cells were compared to their expression in high passage cells, focusing on genes with a role in DDR, cell cycle, and transcription and translation. DEGs were split into biological processes using Gene Ontology (GO) definitions for simplicity (figure 4.3). Blue dots indicate significant DEGs in low passage cells only, green dots indicate significant DEGs in high passage cells only, and black triangles indicate significant DEGs in both low and high passage cells. Genes that are differentially expressed in either low passage or high passage cells were included to highlight any potentially interesting patterns of gene expression changes during cell ageing. For example, in low passage cells, genes related to DDR could be collectively down regulated as a result of FLCN loss. This theoretically could represent a restricted response to DNA damage, enabling an accumulation of genetic mutations. DEGs present in high passage cells but not low passage cells represent acquired alterations due to FLCN knockdown. They may not be directly influenced by FLCN, but they could represent avenues of cellular transformation.

Pearson's correlation coefficient (PCC) calculations were performed to better understand the relationship of gene expression between the age status of the cells following FLCN knockdown. The PCC ranges from −1 to 1. A value of 1 implies that the linear equation describes the relationship between X axis and Y axis perfectly. As X increases, Y increases equally, and all data points lie on a line. A value of −1, on the other hand, implies that all

data points lie on a line for which Y decreases as X increases. A value of 0 implies that there is no linear correlation between the variables. A positive correlation within this data would suggest genes that are upregulated (or downregulated) following FLCN knockdown in low passage cells are also upregulated (or downregulated) in FLCN knockdown high passage cells. These changes in gene expression are likely to be directly, or near directly, influenced by FLCN. A negative correlation suggests genes that are upregulated (or downregulated) in low passage cells, become downregulated (or upregulated) upon ageing. These changes are likely to be indirectly influenced by FLCN or a result of complex feedback mechanisms. A summary of all correlation scores can be found in table 4.1.

When comparing all DEGs no patterns in gene expression change can be seen in low passage cells only (figure 4.3A). However, in aged cells a very weak negative correlation can be observed (PCC -0.24, Pvalue <0.001, R^2 0.057). Interestingly, DEGs in both low and high passage cells show a slightly stronger negative trend (PCC -0.43, Pvalue <0.001, R^2 0.187). This suggests as cells age, over-expressed genes become under-expressed and/or vice versa. These results aren't completely unexpected, as large transcriptional changes are commonly observed during cellular transformation (Bradner et al. 2017). Ultimately, however, this analysis provides little information with regards to molecular changes occurring as a result of FLCN knockdown.
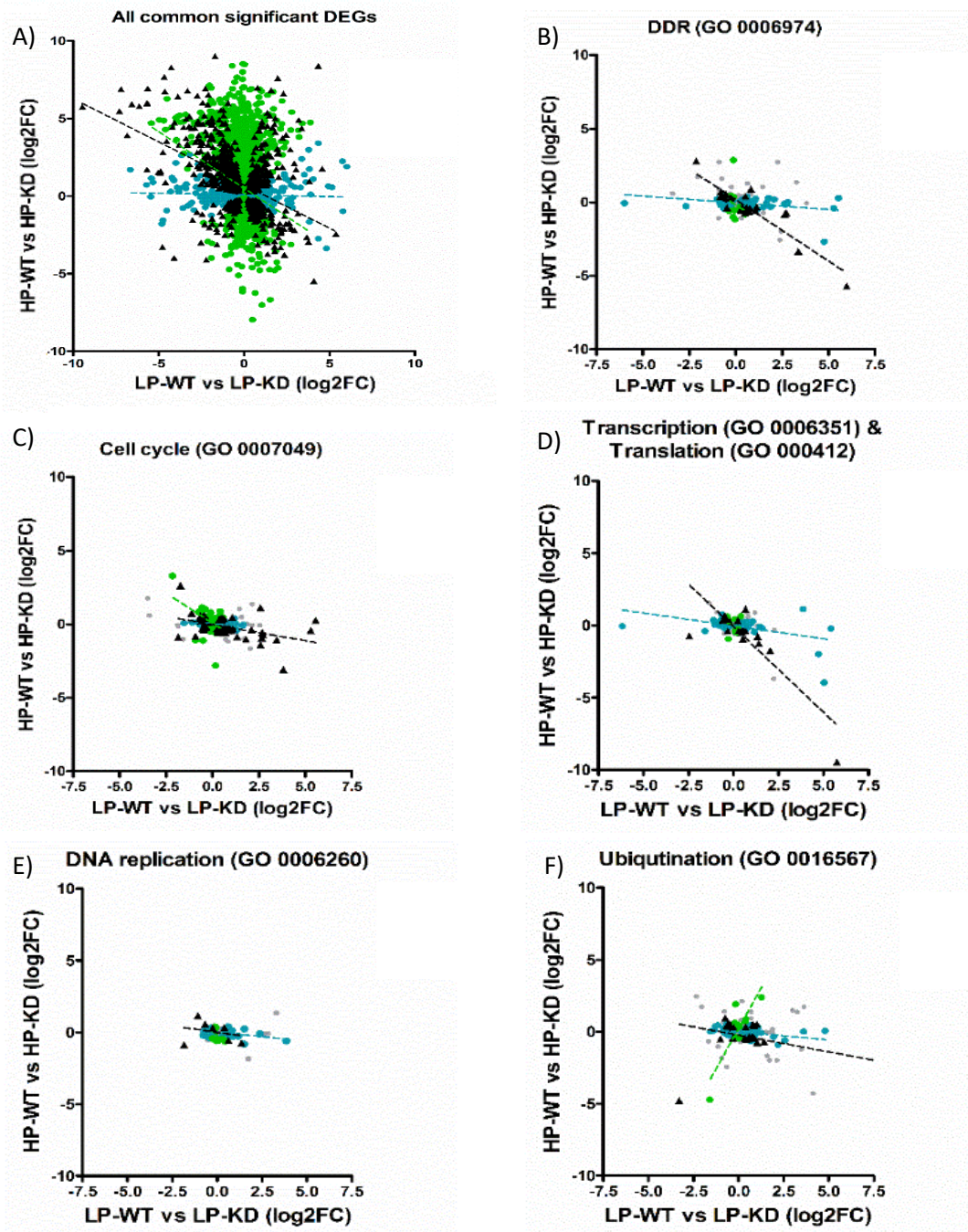
Figure 4.3 Comparison of differentially expressed genes (DEGs) A) All common statistically significantly dysregulated genes. B) Shows transcriptome changes following FLCN knockdown for genes involved in DNA-damage response (DDR), list generated from GO 0006974. C) Shows transcriptome changes following FLCN knockdown for genes involved in cell cycle), list generated from GO 0007049. D) Shows transcriptome changes following FLCN knockdown for genes involved in transcription, and/or translation, list generated from GO 0006351 and GO 0006412 respectively. E) Shows transcriptome changes following FLCN knockdown for genes involved in DNA replication list generated from GO 0006260. F) Shows transcriptome changes following FLCN knockdown for genes involved in ubiquitination list generated from GO 0016567. Where appropriate, grey dots indicate not significant genes (NS), blue dots indicate significant DEGs in low passage cells only, green dots indicate significant DEGs in high passage cells only, and black triangles indicate significant DEGs in both low and high passage cells. Significance is indicated by FDR Pvalue<0.05.

Looking at the DDR genes (figure 4.3B); low passage cells only DEGs displayed a weak negative correlation (PCC -0.37, *P*value 0.0001, R^2 0.14). High passage only DEGs did not display a significant correlation. Collectively, for DEGs in both low and high passage cells, genes are upregulated in low passage cells and become downregulated upon ageing. They display a very strong negative correlation (PCC -0.90, *P*value <0.001, R^2 0.82). It is plausible that upon FLCN knockdown, cells experience an increase to DNA damage or at least an increase in the expression of DDR genes. It is also possible this upregulation in low passage cells may provide cells with a selective advantage where they are better able to tolerate harsh microenvironments (Di Micco et al. 2006; Broustas and Lieberman 2014). This phenomenon is commonly observed in human cancers (Chiang et al. 2003; Winnepenninckx et al. 2006; Kauffmann et al. 2008; Klein 2008; Broustas and Lieberman 2014). However, it's not clear the extent these changes play in the early stages of cellular transformation. Once aged, these genes are expressed less than the aged matched control. Interestingly, it is common in cancer for DDR genes to be downregulated (Curtin 2012,2013). For cell cycle linked genes, on the other hand, FLCN knockdown had a smaller effect on gene expression changes as indicated by genes being more tightly clustered (figure 4.2C). Low passage only (PCC -0.45, *P*value <0.0001, R^2 0.20), high passage only (PCC -0.45, *P*value <0.0001, R^2 0.20), and DEGs in both (PCC -0.45, *P*value 0.0001, R^2 0.20) all display limited correlation. Based on this evidence it's hard to hypothesise the effect on proliferative drive these expression changes have. Differential gene expression of DDR and cell cycle genes are explored more later in this chapter (see figure 4.5-4.8).

For genes involved in transcription and/or translation; high passage only cells display no significant correlation. Low passage only cells have a very weak negative correlation (PCC -0.46, *P*value <0.0001, R^2 0.21), while DEGs present in both have a strong negative correlation (PCC -0.84, *P*value <0.0001, R^2 0.71). For DNA replication, the only significant correlation was found in the low passage cell DEGs with a moderately weak correlation (PCC -0.46, *P*value 0.0004, R^2 0.21). Low passage only DEGs for ubiquitination showed similarly weak negative correlation (PCC -0.44, *P*value <0.0001, R^2 0.19). High passage cells, on the other hand, showed strong positive correlation (PCC 0.83, *P*value <0.0001, R^2 0.69), an increase or decrease in expression correlates well with cell ageing. However, for DEGs in

both low and high passage cells, no significant correlation can be seen, suggesting the changes seen in high passage cells may have more to do with ageing, then FLCN loss per se.

All DEGs			
	Low passage only	High passage only	Both
PCC	-0.06127	-0.2389	-0.4320
*P*value	NS	0.0001	0.0001
R^2	0.00375	0.05710	0.1866
DDR			
	Low passage only	High passage only	Both
PCC	-0.3697	-0.2053	-0.9017
*P*value	<0.001	NS	<0.0001
R^2	0.1367	0.04215	0.8130
Cell cycle			
	Low passage only	High passage only	Both
PCC	-0.4425	-0.4499	-0.4503
*P*value	<0.0001	<0.0001	0.0001
R^2	0.1958	0.2024	0.2028
Transcription/ Translation			
	Low passage only	High passage only	Both
PCC	-0.4632	-0.2298	-0.8446
*P*value	<0.0001	NS	<0.0001
R^2	0.2146	0.0579	0.7133
DNA replication			
	Low passage only	High passage only	Both
PCC	-0.4572	-0.5493	-0.2573
*P*value	0.0004	NS	NS
R^2	0.2090	0.3018	0.06623
Ubiquitination			
	Low passage only	High passage only	Both
PCC	-0.4397	0.8313	-0.3271
*P*value	<0.0001	<0.0001	NS
R^2	0.1934	0.6910	0.1070

Table 4.1 The table shows the Pearson's Correlation Coefficient (PCC) for differentially expressed genes (DEGs) explored in figure 4.3. NS = not significant.

4.2.2 Functional enrichment analysis using REACTOME pathway analysis tool

Upon FLCN knockdown, a lot of small transcriptional changes occur (figure 4.1-4.3). To better understand the biological impact of these transcriptional changes the REACTOME online resource was used to visualise and interpret the DEGs following FLCN knockdown (Fabregat et al. 2017; Fabregat et al. 2018). REACTOME is a curated database of pathways and reactions in biology (Fabregat et al. 2018). Cells function through a complex network of molecular interactions. Molecules are synthesised and degraded, undergo an array of temporary and permanent modifications, are transported from one location to another, and form complexes with other molecules. REACTOME represents these layers of complexity as reactions. These reactions can occur spontaneously or be facilitated by physical entities acting as catalysts, and their progress can be modulated by regulatory effects of other physical entities. Reactions are linked together by shared physical entities; a product from one reaction may be a substrate in another reaction, which in turn may catalyse a third. It is convenient to group such sets of interlinked reactions into pathways. To do this, the REACTOME tool cross-references over 100 different online bioinformatics resources, including NCBI Gene, Ensembl, UniProt and the PubMed literature database, and merges various pathway analysis-related tasks to a single portal (Nardini et al. 2015). REACTOME was chosen over other software, such as Qiagen's Ingenuity Pathway Analysis (IPA) as REACTOME is a freely available, open source database. All DEGs identified by RNA-seq following FLCN knockdown, regardless of cell age, were submitted to REACTOME for functional analysis to produce a genome-wide overview of pathways affected by FLCN knockdown (figure 4.4). REACTOME pathways are arranged in a hierarchy. The centre of each of the circular "bursts" is the top level pathway, for example "DNA Repair". Each step away from the centre represents the next level, lower in the pathway hierarchy; i.e., a specific repair pathway. The dark yellow lines indicate that at least one gene within that pathway is differential expressed as a result of FLCN Knockdown. This illustration shows a globalised dysregulation upon FLCN Knockdown.
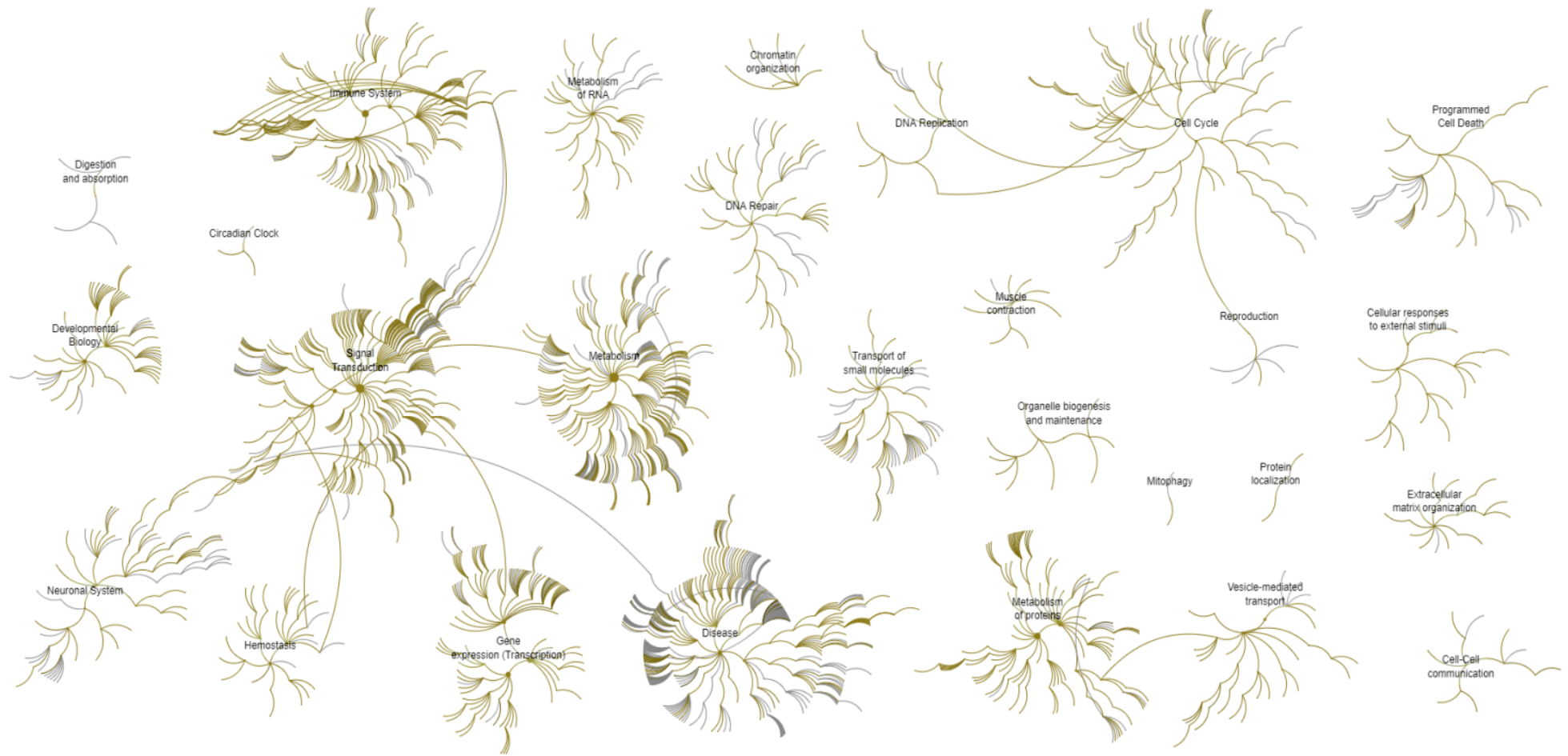
Figure 4.4 An overview of pathways hit by differentially expressed genes following FLCN knockdown. The coloured segments indicate pathways that have at least 1 gene significantly differentially expressed upon FLCN loss, regardless of age status, as generated by REACTOME pathway analysis tool.

Next, REACTOME was used to perform a functional enrichment analysis of the DEGs. REACTOME's pathway analysis tool uses an over-representation analysis. This is a statistical test that determines whether certain pathways are over-represented (or enriched) in the submitted data. It answers the question; does the list of genes contain more genes for pathway 'X' than would be expected by chance? REACTOME produces a probability score, which is corrected for false discovery rate using the Benjamani-Hochberg FDR method. Enrichment analysis was done on DEGs identified between age matched cell lines (LP-WT vs LP-KD and HP-WT vs HP-KD). When analysing all DEGs in low passage cells, no pathways were deemed statistically significant once corrected for multiple testing (figure 4.5A). In high passage cells, however, six pathways were noted as enriched, including Ub-specific processing of protease (FDR Pvalue $2.96E^{-04}$), post-translation protein modification (FDR Pvalue 0.009) and Neddylation (FDR Pvalue 0.009). The enrichment of neddylation is worth noting. Neddylation is a type of post-translation modification that involves the conjugation of the ubiquitin-like protein NEDD8 to a protein substrate. Levels of neddylation enzymes are elevated in many human cancers (Xie et al. 2014; Barbier-Torres et al. 2015; Brown and Jackson 2015; Hua et al. 2015; Chen et al. 2016b; Zhou et al. 2018). Moreover, overexpression of the neddylation modifying enzymes is associated with cancer progression and a worse overall patient survival (Li et al. 2014; Barbier-Torres et al. 2015; Chen et al. 2016b). Neddylation has been linked to cell cycle regulation and DDR. NEDD8 has been shown to localise to sites of DSBs (Ma et al. 2013). Moreover, neddylation of H2AX negatively regulates ubiquitylation of H2AX and blocks the recruitment of the damage response proteins, such as BRCA1 (Li et al. 2014). Neddylation also seems to be an inhibitor of DNA-end resection and HR (Jimeno et al. 2015). In addition, neddylation has been linked to cell cycle regulation (Rizzardi and Cook 2012). An increase in NEDD8 conjugation in human oral carcinoma cells led to an abnormal increase in cell proliferation (Chairatvit and Ngamkitidechakul 2007). Conversely, inhibition of NEDD8 has been shown to lead to cell cycle arrest. Interestingly, the induction of cell cycle arrest, via chemical inhibition of neddylation, can occur in different phase of the cell cycle in a cell line dependent manner. For example, the S phase arrest was observed in GCB lymphoma cells, whereas in ABC lymphoma cells the arrest occurs in G1 phase (Milhollen et al. 2010; Zhou et al. 2018). At this stage, the impact of FLCN knockdown on neddylation is unclear. Neddylation is a complex modulator of multiple cellular signalling pathways. Given its links to the topic of

this thesis, namely DDR and cell cycle control, NEDD8 and associated neddylation pathways linked to DDR and cell cycle control may be worth following up at a later date. Equally, it's worth stating that over-representation analysis assumes pathways are independent from each other, which is contrary to the acknowledgment that many pathway overlap (Barabasi and Oltvai, 2004). Therefore, due to its function in numerous cellular processes, the enrichment of neddylation within this gene list could also be an artefact of over-representation analysis.

Surprising, a lot of DEGs have been linked to immunity, with the most significantly enriched processes being antigen processing: ubiquitination and proteasome deregulation (FDR *P*value 2.31E^{-09}), Class I MHC mediated antigen processing and presenting (FDR *P*value 2.40E^{-07}), and adaptive immune system (FDR *P*value 6.14E^{-04}). In addition, the Immune system just outside significance (FDR *P*value 0.06). Interestingly, almost all RCCs are associated with immune dysfunction (Florek et al. 2005; Alikhan et al. 2017). RCCs are rich in immune infiltrates consisting of T cells, natural killer cells, and macrophages (Santoni et al. 2014; Murphy et al. 2015). While the functions of some of these cells are still elusive, others have well-defined roles in tumour progression. For example, tumour-associated macrophages (TAMs) are known for their immunosuppressive action, which is associated with the secretion of inhibitory cytokines, the generation of reactive oxygen species, and the induction of angiogenesis (Daurkin et al. 2011; Santoni et al. 2014; Ricketts et al. 2018). Very recently, FLCN has been linked to immune regulation, where loss of FLCN was shown to promote AMPK induction of TFEB/TFE3-dependent pro-inflammatory cytokine expression (El-Houjeiri et al. 2019). While interesting, this activity was considered out of scope for this thesis, and therefore wasn't pursued further.
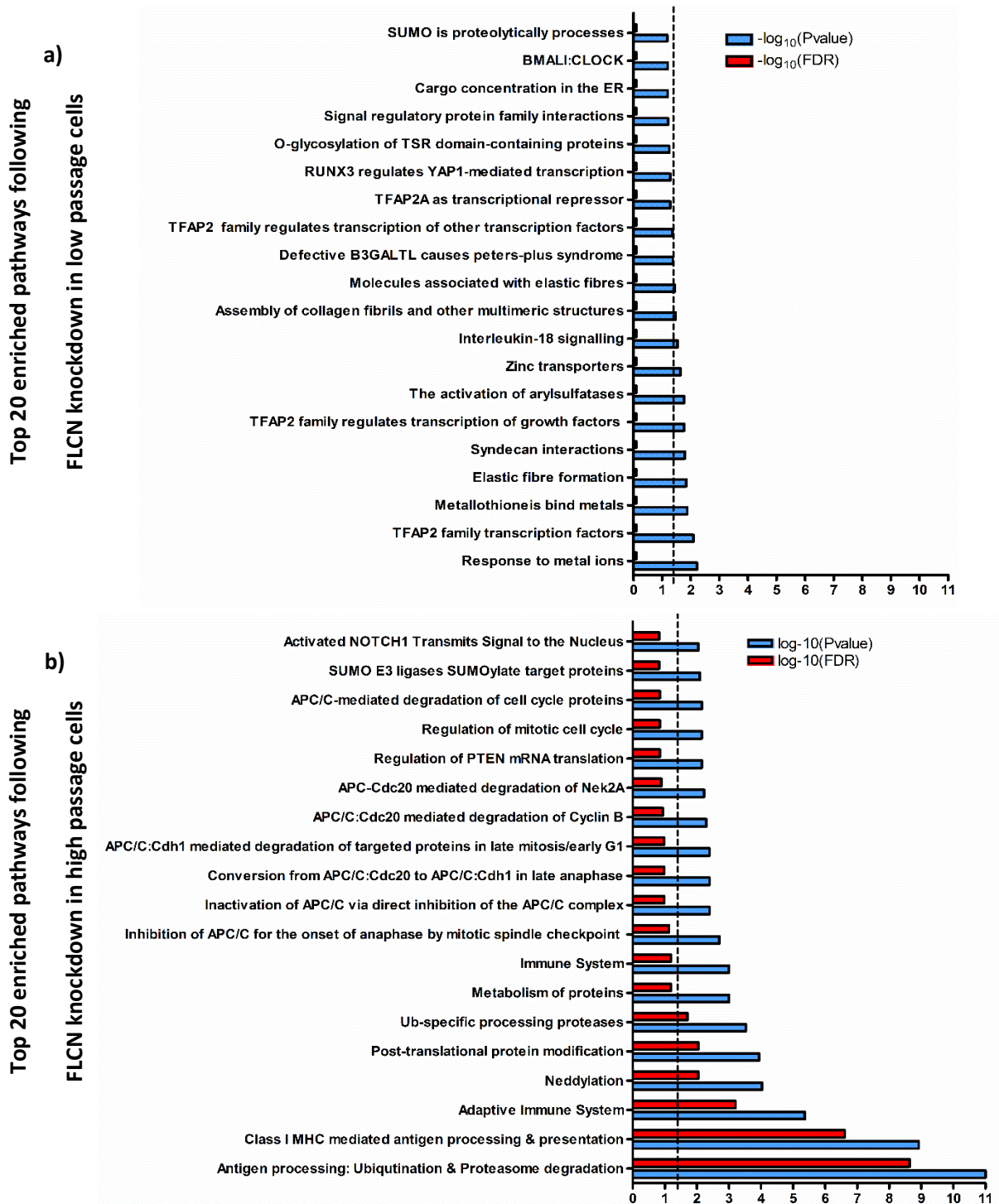
Figure 4.5 REACTOME function enrichment analysis of significantly differentially expressed genes (DEGs) following FLCN knockdown. A list of all DEG names were analysed for functional enrichment using REACTOME online resource. A) Graph shows top 20 pathways that are enriched in low passage HK2 cells following FLCN knockdown (LP-WT vs LP-KD) B) Graph shows top 25 pathways that are enriched in high passage HK2 cells following FLCN knockdown (HP-WT vs HP-KD). Blue bars = log$_{10}$(Pvalue) as determined by REACTOME hypergeometric distribution test; Red bars = -log$_{10}$(FDR), represent pathway enrichment Pvalue corrected for multiple testing using the Benjamani-Hochberg method.

One of the biggest limitations of over-representation analysis is that it only uses the number of genes and ignores how strongly those genes are associated with whatever is being studied. Furthermore, you must arbitrarily decide what is classed as significant. If an FDR *P*value threshold of 0.05 and fold change cut-off of 2 is used, genes with a fold change of 1.95 or FDR *P*value 0.051, which are arguably as important as the genes within the arbitrary cut-off, will not be counted. Pathway analysis methods that are classified as 'Functional Class Scoring' (such as gene set enrichment analysis (GSEA) or Qiagen's IPA) use the fold change in gene expression, in addition to the number of genes present within a list, to compute an enrichment score (Subramanian et al. 2005). Furthermore, it is well appreciated that large changes in individual genes can have significant effects on pathways; however, weaker but co-ordinated changes in a set of functionally related genes can also have significant biological effects (Subramanian et al. 2005; Kukurba and Montgomery 2015). Functional Class Scoring analysis allows a better understanding of the weaker effects of gene dysregulation (Subramanian et al. 2005). Nevertheless, resources to do such analysis are hidden behind paywalls, or require additional skill sets and/or time. As such, this type of analysis was not performed.

Subsequently, an altered and slightly biased approach was taken. The analysis used a list of genes known to function within the DNA-damage response (GO 0006974) or cell cycle (GO 0007049) that are differently expressed upon FLCN knockdown. This changed the question from 'Are there any functional pathways over-represented in the list of genes?' to 'Within this list of genes is a particular aspect of a known functional process over-represented?' It is important to stress that neither DDR and the cell cycle groups where enriched in the unbiased analysis and that *P*value significance sited in this section may be artificially inflated. Instead, the *P*values are used to compare 'sub-categories' between cell lines. To do this the four previously mentioned pairwise comparisons were used; LP-WT vs LP-KD, HP-WT vs HP-KD, LP-WT vs HP-WT, and LP-KD vs HP-KD.

When looking at DEGs with a DDR role following FLCN knockdown (figure 4.6) nucleotide excision repair (NER) was the most enriched repair pathway (FDR *P*value 3.57×10^{-5}) in low passage FLCN knockdown cells. NER is a versatile repair pathway. It is known to eliminate the broadest range of structurally unrelated DNA lesions, including: cyclobutane–pyrimidine dimers and pyrimidine–pyrimidone photoproducts, which are

the caused by UV radiation; numerous bulky chemical adducts; intra-strand crosslinks; and ROS-generated cyclopurines. Defects in NER commonly lead to cancer, particularly skin cancer due to UV induced pyrimidine–pyrimidone photoproducts. Interestingly, studies have shown reduced expression of NER genes are associated with increased risk in cancer (Cheng et al. 2000; Cheng et al. 2002; Latimer et al. 2010). The increased susceptibility to internal tumours is presumably due to the accumulation of endogenously induced DNA lesions (for example, cyclopurines that are caused by ROS) (Marteijn et al. 2014).

In aged cells (HP-WT vs HP-KD), FLCN knockdown resulted in a marked increase in the enrichment of genes involved specifically in the repair of DSB (DSBR) (FDR Pvalue 1.55×10^{-14}). Furthermore, in cells aged following FLCN knockdown (LP-KD vs HP-KD), DSBR genes are further enriched (FDR Pvalue 9.44×10^{-15}). This is interesting as the previous chapter validated DNA-PKcs to interact with FLCN. DNA-PKcs is the apical protein in NHEJ repair of DSBs. Over-representation analysis, however, is non-directional and does not take into account upregulation or downregulation of gene expression. Therefore, the potential transformative effects this has on the cells are unclear. For example, Does DSBR gene expression increased following FLCN knockdown, indicating that these cells are responding to an increase in DNA damage? Or are these genes downregulated in response to FLCN knockdown, which would suggest FLCN plays a role to ensure transcription of repair genes in order to prevent genomic instability?
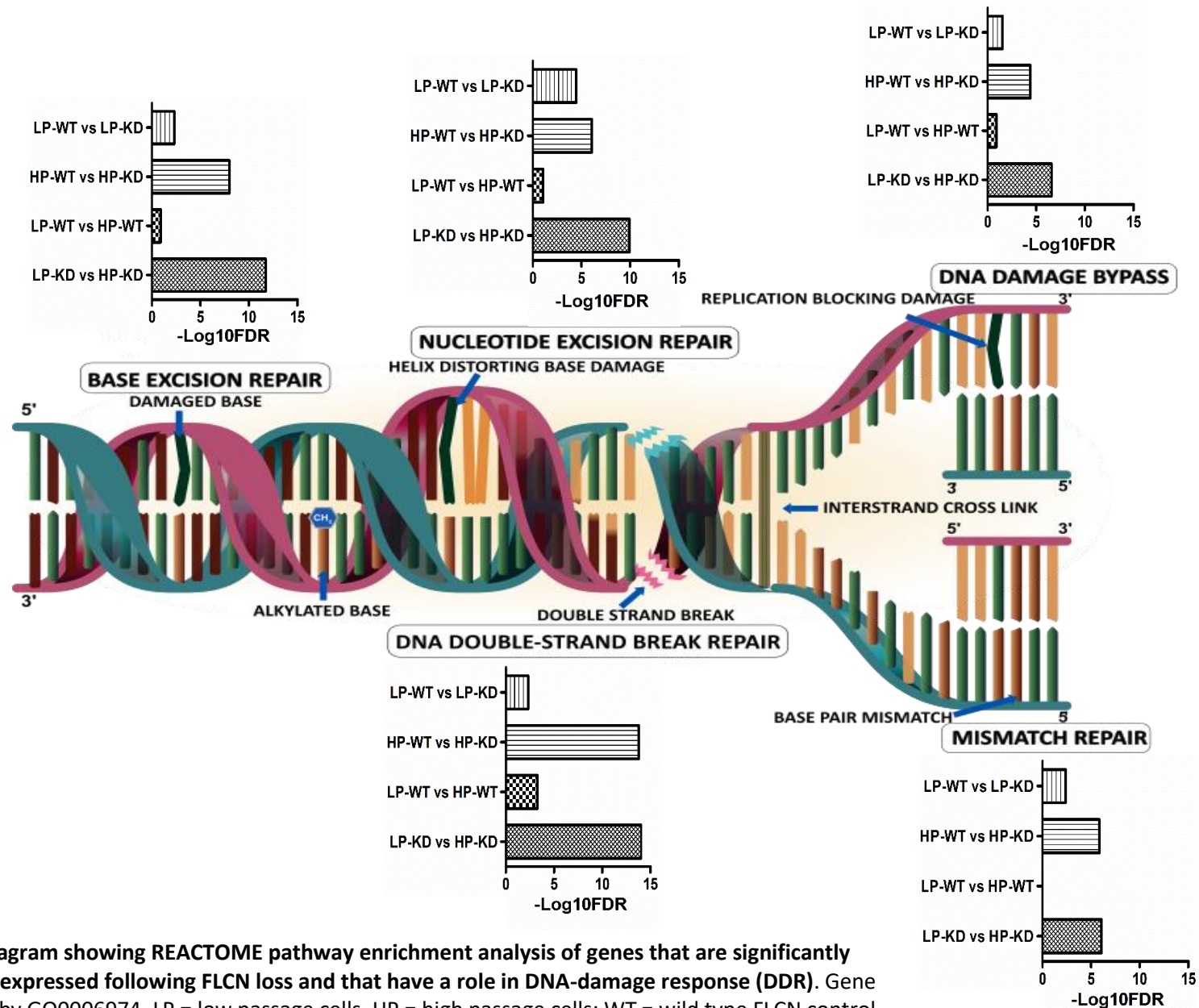
Figure 4.6. Diagram showing REACTOME pathway enrichment analysis of genes that are significantly differentially expressed following FLCN loss and that have a role in DNA-damage response (DDR). Gene list identified by GO0006974. LP = low passage cells, HP = high passage cells; WT = wild type FLCN control, KD = FLCN knockdown

Therefore, a heatmap was generated from the top 23 genes identified to function in DSBR by REACTOME (figure 4.7). In low passage cells (LP-WT vs LP-KD) while expression changes are minimal (less than 1 log2 fold change), they are universally downregulated (figure 4.7). Confoundingly, in aged cells many of these genes become upregulated. These cells display a decrease in DSBR gene expression as a part of normal cell ageing (LP-WT vs HP-WT). Perhaps the increase in these genes are an artefact of comparing HP-WT to HP-KD where in both cell lines a decrease gene expression is observed due to ageing, however such age-related expression changes are smaller in aged FLCN knockdown cells when compared to aged wild type cells. Equally this may be a result of compensatory mechanisms where more DNA damage is present in FLCN knockdown cells.

Of special note is the gene, APBB1. APBB1 encodes Amyloid Beta Precursor Protein Binding Family B Member 1. It is a nuclear adaptor protein most known for interacting with the amyloid precursor protein responsible for Alzheimer's disease. APBB1 thought to specifically recognise and bind to histone H2AX phosphorylated on Tyrosine 142 at DSB. APBB1 is also required for histone H4 acetylation at double-strand breaks (DSBs) permitting a more open chromatin structure and allowing repair molecules access to DSB (Dhar et al. 2017). This gene becomes highly upregulated upon continued growth without FLCN (figure 4.7). However, it's also highly downregulated when compared to the aged matched control, suggesting cells may be trying to respond to an increase in DSB but the response is still suboptimal. Collectively, this evidence could support FLCN being a positive regulator of DSBR, however, how FLCN may regulate DSBR is unclear.
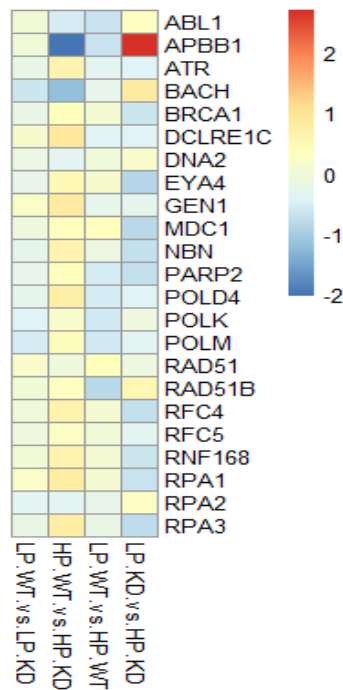
Figure 4.7 Heatmaps of the top 23 DSBR response genes that are differentially expressed following FLCN knockdown. Scale is based on log2 fold change, red = over-expressed genes, blue = under-expressed genes.

Next DEGs involved in the cell cycle (identified by GO 0007049) were explored in REACTOME to see if any phase of the cell cycle is enriched upon FLCN knockdown (figure 4.8). Transcriptional changes can be seen at all stages at the cell cycle upon FLCN knockdown, however, G1-G1/S phase has by far the largest amount of gene enrichment (figure 4.8). This suggests FLCN may be involved in cell cycle progression or checkpointing at the G1/S phase boundary. FLCN has previously been linked to the cell cycle. In fact, FLCN has been linked to nearly all aspects of the cell cycle. *In vitro* studies have suggested that wild type FLCN delays cell cycle progression through late S and G2/M phase (Laviolette et al. 2013). FLCN has also been shown to bind to γ-tubulin at centrosomes at the basal body of cilia and mitotic spindle (Luijten et al. 2013), important for planar cell polarity, microtubule function, and chromosome segregation in anaphase, and therefore could play a role in mitosis. Finally, FLCN has been linked to G1/S phase where it was shown to inhibit cyclin D1 expression (Baba et al. 2008; Kawai et al. 2013). In zebra fish embryos upon re-introduction of wild type FLCN the number of cells in G1 increased (Kenyon et al. 2016). Furthermore, FLCN has been found to regulate RhoA signalling, which is also involved in the G1 to S phase transition of the cell cycle and regulates cyclin D1 activity (Mammoto et al. 2004; Watts et al. 2006).
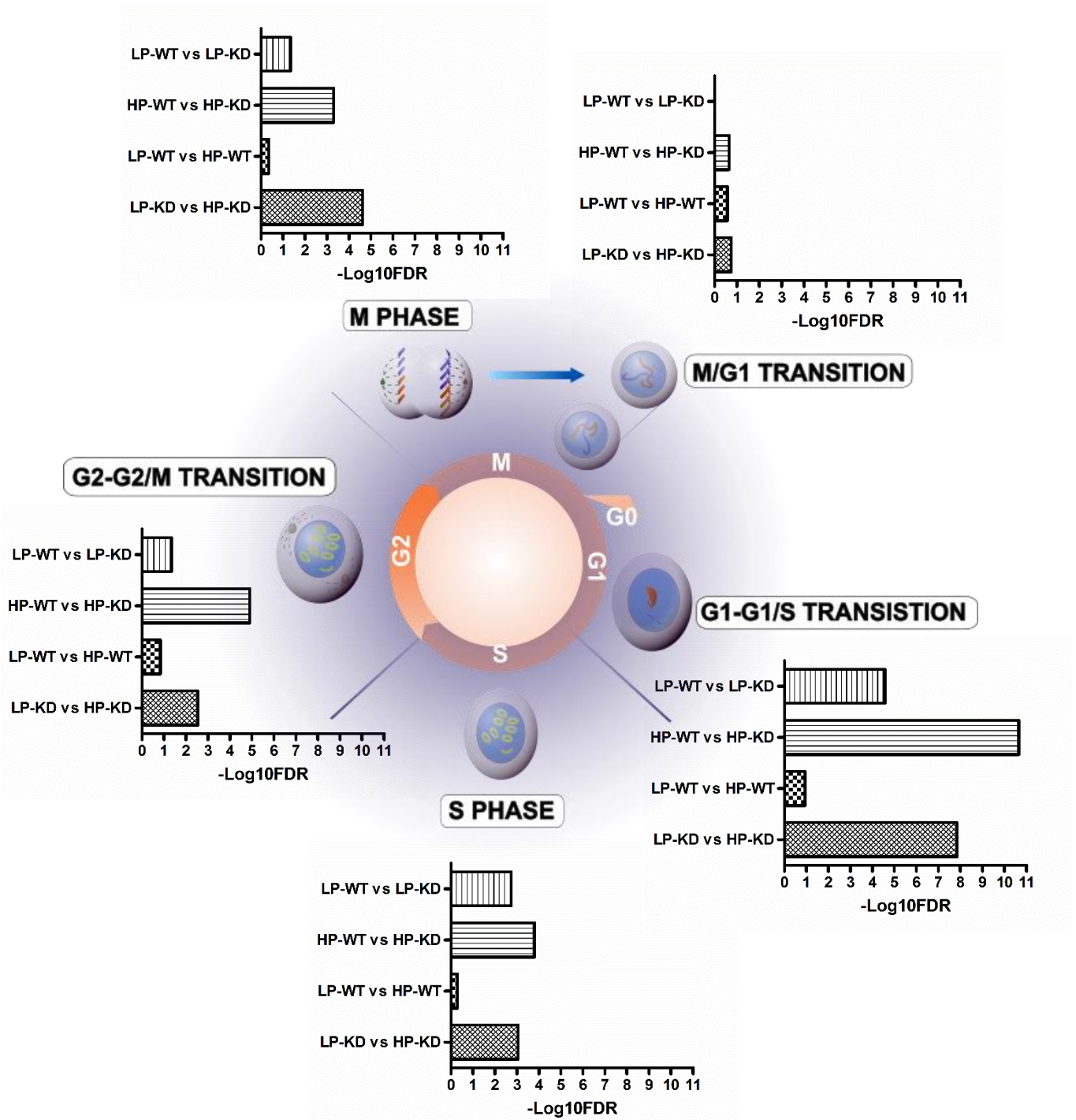
Figure 4.8. Diagram showing REACTOME pathway enrichment analysis of genes that are significantly differentially expressed (DEGs) following FLCN loss and that have a role in the cell cycle. Gene list identified by GO0007049. LP = low passage cells, HP = high passage cells; WT = wild type FLCN control, KD = FLCN knockdown.

To explore this further, genes involved in G1/S phase transition were segregated into positive and negative regulators of cell cycle as indicated by gene ontology lists GO 1902807 and GO 2000134 respectively (figure 4.9). The most dysregulated genes (largest log2 fold change) are highlighted. These include genes known to contribute to cancer progression or aggressiveness. For example, GPNMB is a transmembrane glycoprotein that regulates a variety of physiologic processes in a cell-type dependent manner. In immune cells, for example, GPNMB was shown to block entry into the S phase of the cell cycle in T-cells (Chung et al. 2009). While GPNMB overexpression in macrophages led to an increased Cyclin A expression and a shortened S phase (Guo et al. 2019). GPNMB is overexpressed in numerous cancers including RCC (Kuan et al. 2006; Taya and Hammes 2018; Trail et al. 2018), and its expression often correlates with increased proliferation, migration, invasion, and decreased tumour cell apoptosis. Indeed, its overexpression is a prognostic indicator for RCC (Qin et al. 2014; Taya and Hammes 2018) . In addition, it has been demonstrated that upon FLCN inactivation, GPNMB gene expression is upregulated in renal cancer cells, mouse embryonic fibroblast cells, and human renal cell carcinomas (Hong et al. 2010a). In accordance with this, both low (2.93 log2FC, Pvalue 1.3×10^{-31}) and high (0.98 log2FC, Pvalue 0.0004) passage FLCN knockdown HK2 cells displayed elevated expression of GPNMB (figure 4.9). Another interesting gene is FHL1, which has an inhibitory effect on cell growth. FHL1's activity was associated with both G1 and the G2/M cell cycle arrest. This was indicated by a marked inhibition of cyclin A, cyclin B1 and cyclin D as well as the induction of the cyclin dependent kinase inhibitors p21 (WAF1/CIP1) and p27 (Kip1) (Niu et al. 2012). Its gene expression has been shown to be downregulated several cancers, including breast, kidney, prostate, and lung (Asada et al. 2013). Similarly, both low (-0.76 log2FC, Pvalue 2.9×10^{-09}) and high (-0.92 log2FC, Pvalue 2.8×10^{-14}) passage FLCN knockdown HK2 cells displayed decreases in FHL1 gene expression (figure 4.9).

TERT forms the catalytic component of the telomerase holoenzyme complex essential for countering telomere attrition (Wang et al. 2014; Hosen et al. 2015). Like most cancers, RCCs exhibit widespread telomerase re-activation, and a close correlation between TERT expression and telomerase activity is well documented (Kanaya et al. 1998; Wang et al. 2014; Hosen et al. 2015). An increase in TERT expression is associated with more advanced forms of malignant diseases (Heidenreich et al. 2014; Liu et al. 2014; Wang et al.

2014; Hosen et al. 2015; Simon et al. 2015). However, studies looking specifically into RCC overexpression of TERT show underwhelming results. One study looked at 188 tumours from patients with clear cell RCC and found only twelve tumours (6.4%) carried a mutation that could result in TERT overexpression (Hosen et al. 2015). Another study explored 109 patients with RCC (96 clear cell RCC, and 8 chromophobe RCC tumours) with only 9/96 (9.3%) clear cell RCC tumours and 1/8 (13%) chromophobe RCC tumours contained overexpressed TERT (Wang et al. 2014). Both studies, however, linked TERT overexpression to poor patient outcome, and increased tumour aggression. TERT is overexpressed in both low and high passage FLCN knockdown cells, log2FC 1.34 and 1.24 respectively, however neither are statistically significant (figure 4.9).
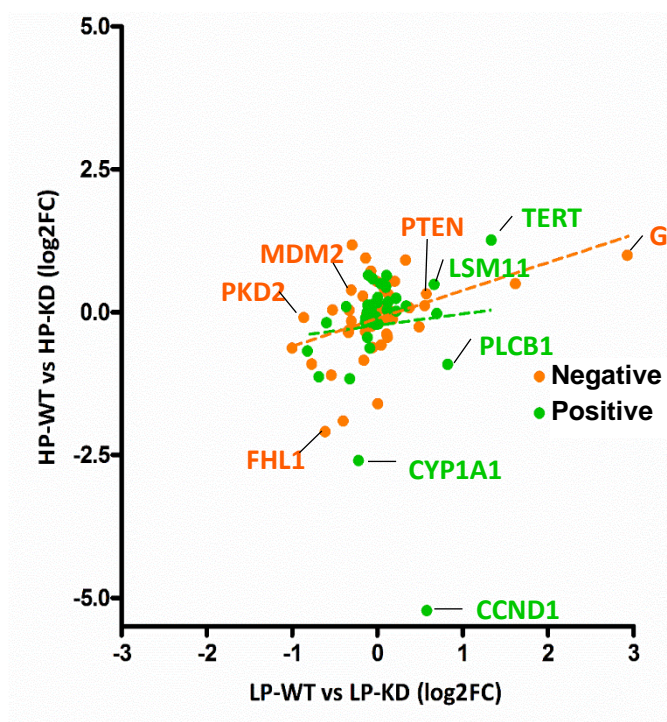
Figure 4.9 Comparison of genes that are significantly differentially expressed in aged-matched FLCN knockdown HK2 cells (LP-WT vs LP-KD and HP-WT vs HP-KD). Orange = negative G1/S transition regulators (GO 1902807); green = positive G1/S transition regulators (GO 1902808).

Cytochrome P450 1A1 (CYP1A1) is part of the cytochrome P450 superfamily of enzymes that play major roles in the detoxification, activation and metabolism of several endogenous and exogenous substances. CYP1A1 catalyses the oxidation of pro-carcinogens to carcinogenic reactive intermediates (Badal and Delgoda 2014; Go et al. 2015). As a result, the expression of CYP1A1 is an important contributor to carcinogenesis. Indeed, CYP1A1 is

overexpressed in many human tumours (Androutsopoulos et al. 2013; Li et al. 2018). More importantly CYP1A1 was shown to regulate breast cancer cell proliferation and survival via suppression of AMPK signalling. Additionally, CYP1A1 has been shown to be involved in β-catenin signalling contributing to cancer metastasis (Braeuning et al. 2011; Kasai et al. 2013). As a result, constitutive expression of CYP1A1 in tumours may not only directly influence cancer progression via activation of carcinogenic compounds, but also via biological pathways are linked to the functional role of this enzyme. However, in both low and high passage FLCN knockdown cells, CYP1A1 expression is downregulated (-0.21 log2FC, low passage; -2.6 high passage (figure 4.9). Furthermore, differential expression is only significant for high passage cells (*P*value 0.005).

Additionally, Phospholipase C, β1 (PLCB1) is a G-protein coupled receptor that plays critical roles in intracellular transduction important to tumorigenesis. Deregulation of signal transduction pathways frequently elicits survival advantages to tumours. Once activated, PLCB1 triggers a series of events culminating in an increase in intracellular calcium and the activation of cell proliferation (Ngoh et al. 2014). In addition, PLCB1 can positively target cyclin D3, and PKC α-mediated cell proliferation pathways to regulate the cell cycle (Bavelloni et al. 2015). Overexpression of PLCB1 is found to be sufficient to drive Swiss 3T3 cell into the S phase of the cell cycle (Martelli et al. 1992; Manzoli et al. 1997). In addition, PLCB1 could reduce cell damage under oxidative stress (Guo and Scarlata 2013). As such, PLCB1 is upregulated in several cancer cells, and their increased expression is associated with with poor overall survival and metastatic relapse (Tan et al. 2015; Li et al. 2016; Zhang et al. 2019). Curiously, in low passage FLCN knockdown cells PLCB1 expression is upregulated (0.83 FC; FDR *P*value, 0.019), while in high passage cells it is down regulated (-0.92 FC; FDR *P*value 0.005).

Perhaps the most striking DEG is CCND1. This gene belongs to the highly conserved cyclin family, whose members are categorised by a periodicity in protein abundance throughout the cell cycle. Cyclins function as regulators of cyclin-dependent kinases (CDKs). Cyclin D1 forms a complex with CDK4 or CDK6 and is required for the G1/S transition in the cell cycle. Cyclin D1 overexpression correlates with early cancer onset and tumour progression (Diehl 2002). RNA-seq analysis suggests that cyclin D1 is overexpressed in low passage cells (0.58 log2FC, *P*value 4.64×10^{-06}), however, becomes markedly down regulated

in high passage cells (figure 4.9; -5.23 log2FC, *P*value 3.01×10^{-272}). This was validated by qPCR (figure 4.10). Nevertheless, it's unclear at this stage why a dramatic change in CCND1 expression is seen upon ageing with FLCN knockdown. The previous study looking at CCND1 expression following FLCN loss did so in transiently knocked-down Hela cells (Kawai et al. 2013). Cyclin D1 is explored in detail in chapter 6.

The overall trend in expression of positive and negative regulators of G1/S transition suggests that upon FLCN knockdown, the negative regulators (orange) show a moderately weak positive correlation with gene expression upon ageing (PCC 0.4325, *P*value 0.01, R^2 0.1871). Negative regulators of G1/S transition are generally upregulated in both low and high passage cells. However, most genes only reach a significant level of differential expression in high passage cells suggesting age contributes to the up-regulation G1/S negative regulators, and not exclusively FLCN. Interestingly, positive regulators (green) of G1/S transition also follow a similar but extremely weak pattern, but this is not significant (PCC 0.07527, *P*value NS, R^2 0.005665). Based on this data it should be concluded that upon FLCN knockdown in both low and high passage cells there is a globalised dysregulation of expression for genes involved in G1-G1/S cell transition.

4.2.3 Validating RNA sequencing data

To validate the results of RNA-seq, quantitative real-time PCR (qPCR) was performed on 8 genes; FLCN, CCND1, TP53, FOXN3, PGC1A, TGFA, JUN, and RPA1 (figure 4.10). These genes were selected has they are the more highly dysregulated genes, and each plays a role in DDR and/or G1/S transition. qPCR validation was performed by Mr Jesse Champion (FLCN, CCND1, TP53, and FOXN3) and Dr Elaine Dunlop (FLCN, PGC1A, TGFA, JUN, and RPA1). Each gene was validated by 3-5 independent qPCR assays. A high PCC between RNA-seq and qPCR expression data revealed a strong correlation (PCC 0.82, *P*value<0.0001, R^2 0.6655; figure 4.10A) indicating the reliability of the RNA-seq analysis. The slight difference in expression levels between RNA-seq and qPCR data is most likely due to the different methods of normalisation for each technique. In qPCR a reference gene is used for gene expression normalisation. The expression for the reference gene is assumed to be constant for all samples, and the expression of the experimental gene is relative to the expression of the

reference gene. In RNA-seq data, however, we assume each sample has the same total expressed mRNA. Expression is read as read count per million mapped reads or transcripts per million and represents an absolute count. qPCR validation of FLCN knockdown was of limited use as FLCN was always detected in the negative control. This may explain the restricted amount of FLCN knockdown in high passage cells (figure 4.10B). Prior to RNA-seq, however, FLCN knockdown was confirmed by western blot (data not shown, Dr Elaine Dunlop).

In addition to CCND1 (discussed previously), it is worth mentioning PPARGC1A. This gene encodes the transcription cofactor PGC-1α and is considered the master regulator of mitochondrial biogenesis (Mastropasqua et al. 2018). It's well documented that upon FLCN knockdown PGC-1α expression is elevated (Klomp et al. 2010; Wada et al. 2016; Yan et al. 2016a). This observation was also shown in the RNA-seq data and validated by qPCR (figure 4.10E). Additionally, FOXN3 is the only gene to have conflicting results between RNA-seq and qPCR. FOXN3 is a member of the forkhead/winged helix transcription factor family and promotes DNA damage-inducible cell cycle arrest at G1 and G2 (Huot et al. 2014). This gene was highlighted as a gene of interest by undergraduate student Mr Jesse Champion due to FOXN3 being downregulated in a number of human cancers (Basso et al. 2005; Chang et al. 2005; Markowski et al. 2009). Upon validation, FOXN3 expression was not statistically valid in low passage cells, due to inconsistences between replicates. Furthermore, RNA-seq suggests this gene is down regulated in low passage cells, while qPCR failed to validate this, and suggests that FOXN3 expression is instead marginally upregulated (figure 4.10F). However, upon ageing it is statistically downregulated, agreed by both RNA-seq and qPCR. The effects of CCND1 and PGC-1α that are observed upon FLCN knockdown in the RNA-seq data are mirrored in FLCN literature (Klomp et al. 2010; Kawai et al. 2013; Wada et al. 2016; Yan et al. 2016a). This supports the use of the HK2 knockdown cells, suggesting they are representative of FLCN loss.
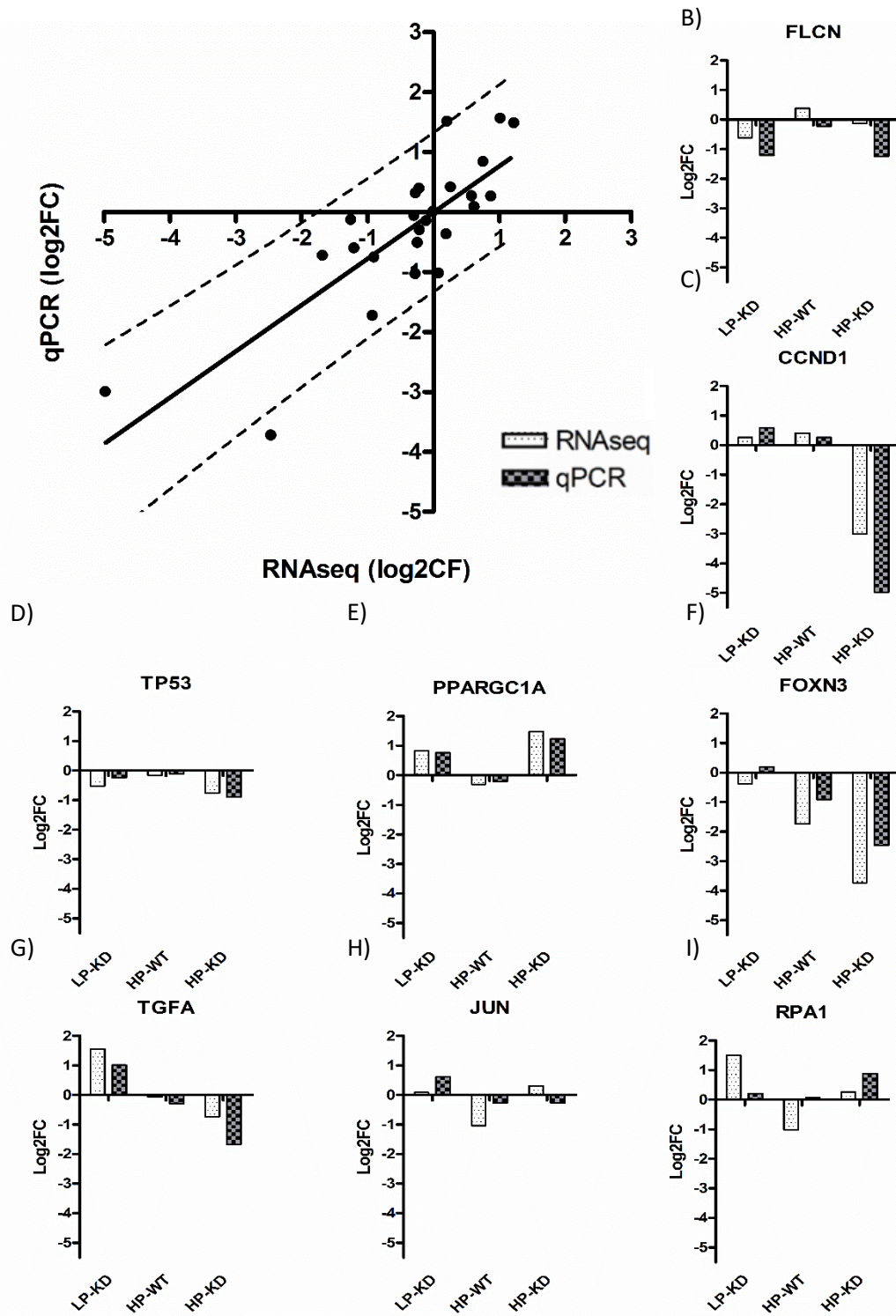
Figure 4.10 Validation of RNA sequencing (RNA-seq) by quantitative real-time PCR (RT-qPCR). A) Correlation between RNAseq and quantitative real-time PCR (RT-qPCR). Pearson's correlation Coefficient (PCC) was calculated to show the reliability of the gene expression analysis from the RNA-seq. PCC 0.82, Pvalue<0.0001, R^2 0.6655. Dashed line indicates the 95% prediction band, this is the area in which it is expected 95% of all data points will fall. B-I) Comparison of log2 fold change of 8 genes obtained by RNA-seq and RT-qPCR. Real-time PCR was performed using the amplified cDNA from each RNA-seq sample for 3 independent qPCR assays. An additional 2 biological repeats were used so qPCR log2FC are calculated from a total of 5 independent repeats. All samples are compared to low passage wild type cells (LP-WT). Statistics and graphs were produced in GraphPad Prism4.

4.3 Conclusion

Collectively, these data show a transcriptional dysregulation following FLCN knockdown. It would be interesting to see how this global dysregulation translated at the protein level. mRNAs levels do not always represent an over- or under- abundance of protein (Schwanhausser et al. 2013). For example, most housekeeping genes including those coding for ribosomal, glycolytic and TCA cycle proteins mostly have stable mRNAs and are translated faithfully into stable proteins. On the other hand, transcription factors, signalling genes, chromatin modifying genes, and genes with cell cycle specific functions usually have unstable mRNA and unstable protein. Therefore, it's likely the most important and interesting regulators of DDR and/or cellular division have a poor correlation between mRNA and protein levels. In many cases mRNA translation is regulated by microRNAs (Catalanotto et al. 2016). In addition, cells have a multitude of post-translational mechanisms for controlling protein turnover and abundance that have been well described (Karve and Cheema 2011; Cajee et al. 2012; Stintzing and Lenz 2014; Brown and Jackson 2015; Santos and Lindner 2017). As such mRNA levels cannot be used as surrogates for corresponding protein levels without verification. Therefore, it's hard to conclude the true biological implications of the gene dysregulation observed in these HK2 cells in response to FLCN knockdown (McCarthy and Smyth 2009; Schwanhausser et al. 2013). In an attempt to understand the functional impact of this transcriptional dysregulation, DDR and cell cycle control was explored in more detail. Both were found to be perturbed. Thus, from this, the effects of FLCN knockdown on DDR in HK2 cells was explored further in chapter 5 of this thesis, while G1/S checkpoint regulation was explored in chapter 6.

Chapter 5: Exploring the role of FLCN in the DNA-damage response

5.1 Introduction

The accumulation of mutations and the resulting genomic instability lie at the origin of cancer (Jackson and Bartek 2009). To maintain genomic integrity, cells have developed a multifaceted network of mechanisms in order to respond to and repair DNA damage (DDR) (Bartkova et al. 2005; Branzei and Foiani 2008; Shrivastav et al. 2008; Jackson and Bartek 2009). Once DNA lesions are identified, cellular pathways can promote a number of outcomes depending on the severity of the damage in order to limit the deleterious consequences of the lesions. Damage to DNA can result in mismatched base pairs, insertion or deletion of nucleotides (indels), the addition of bulky adducts, inter- and intra-strand links, single-strand DNA breaks (SSBs), and double-strand DNA breaks (DSBs) (Jackson and Bartek 2009). DSBs are considered the most harmful lesions and can lead to cell death if not repaired (Mills et al. 2003; Scott and Pandita 2006). If mis-repaired they can cause large deletions, translocations, and fusions in the DNA. These consequences are collectively referred to as genomic rearrangements, and are hallmarks of human cancers (Negrini et al. 2010). DSBs can result from exogenous agents such as ionizing radiation (IR) and chemotherapeutic drugs, or endogenous processes, such as the production of reactive oxygen species (ROS) or the collapse of stalled DNA replication forks (Jackson and Bartek 2009).

In chapter 3, it was demonstrated that FLCN interacts with the catalytic subunit of the serine/threonine kinase, DNA-PKcs. Following DNA damage, DSBs are rapidly bound by the Ku heterodimer (Ku70 and Ku80) which, in turn, loads and activates DNA-PKcs to the site of damage (Mahaney et al. 2009). This holoenzyme is responsible for initiating NHEJ repair of DSB by stabilising break ends in order to prevent exonucleolytic degradation. Binding to DNA promotes the activation of DNA-PKcs kinase activity, although the exact mechanism underlying this event remains poorly understood. Once activated, DNA-PKcs phosphorylates and alters the activity of proteins that mediate NHEJ, which include Ku70, Ku80, Artemis, the X-ray cross complementing protein 4 (XRCC4), XRCC4-like factor (XLF), and DNA ligase IV (LigIV) (Mahaney et al. 2009; Ciccia and Elledge 2010; Roberts et al. 2010). Activated DNA-

PKcs also phosphorylates Ser139 on histone variant H2AX (γH2AX) both directly, and indirectly through AKT/GSK3β signalling (An et al. 2010). γH2AX is a well-established marker of DSBs (Sak and Stuschke 2010). It aids in the recruitment of repair factors to break site (Paull et al. 2000) and coordinates the signalling cascades required for efficient repair (Lukas et al. 2004). This chapter will attempt to understand the role of FLCN in DDR and explore the implications of FLCN deficiency on DDR pathways.

5.2 Results and discussion

5.2.1 DNA-PK in vitro kinase assay

As a well-established serine/threonine kinase, DNA-PKcs has 47 characterised substrates, covering a range of functions from DDR to metabolism (Chung 2018). Therefore, to explore the biological relevance of the FLCN/DNA-PKcs interaction, an *in vitro* kinase assay was performed in the first instance (figure 5.1). It's worth noting, FLCN has a potential DNA-PKcs phosphorylation site; serine 302 (Ser302, figure 5.1A), and the kinase responsible for the phosphorylation of this residue is unknown. DNA-PKcs preferentially catalyses the transfer of a phosphate group to the oxygen atom of serine when followed by a glutamine (S/G). The Ser302 on FLCN is serine followed by glutamate (S/E). DNA-PKcs has, however, previously been demonstrated to phosphorylate S/E residues both *in vitro* and *in vivo* (figure 5.1A) (Wong et al. 2009; Wang et al. 2013). Furthermore, the p-FLCN Ser302 is maximally phosphorylated during the G1 phase of the cell cycle, where NHEJ is the repair mechanism of choice for DSBs (Dephoure et al. 2008).

GST-FLCN or GST-p53 was overexpressed in HEK293 cells and a GST-pull down assay was performed to purify the protein substrates of interest. p53 is a well characterised substrate of DNA-PK (Leesmiller et al. 1992) and was used as a positive control. Incorporation of radiolabelled phosphate [^{32}P] was determined in the presence of short dsDNA to mimic DSBs. The kinase assay suggests FLCN is not a *bona fide* substrate of DNA-PKcs in response to DSBs (figure 5.1B and 5.1C). The kinase activity of DNA-PK is 5-10 fold higher in the presence of dsDNA (Jette and Lees-Miller 2015), which was observed in the GST-p53 control. FLCN may be phosphorylated independently of DSBs, as incorporation of

radiolabelled phosphate [^{32}P] is consistently observed; however, the experiment lacks a non-DNA-PKcs peptide substrate control for reference. Therefore, based on these results, FLCN is not considered a substrate of DNA-PKcs.

A)

Protein	Site	Sequence	
p53	S9-p	EEPQsDP**s**VEPPLsQ	
p53	S15-p	PsVEPPL**s**QEtFsDL	
p53	T18-p	EPPLsQE**t**FsDLWkL	
p53	S20-p	PLsQEtF**s**DLWkLLP	Confirmed DNA-PKcs phosphorylation sites
p53	S37-p	NVLsPLP**s**QAMDDLM	
p53	S46-p	AMDDLML**s**PDDIEQW	
USF1	S262-p	RQSNHRL**s**EELQGLD	
FLCN	S302-p	ESEsWDN**s***E*AEEEEK	Potential DNA-PKcs phosphorylation site

B)

C)
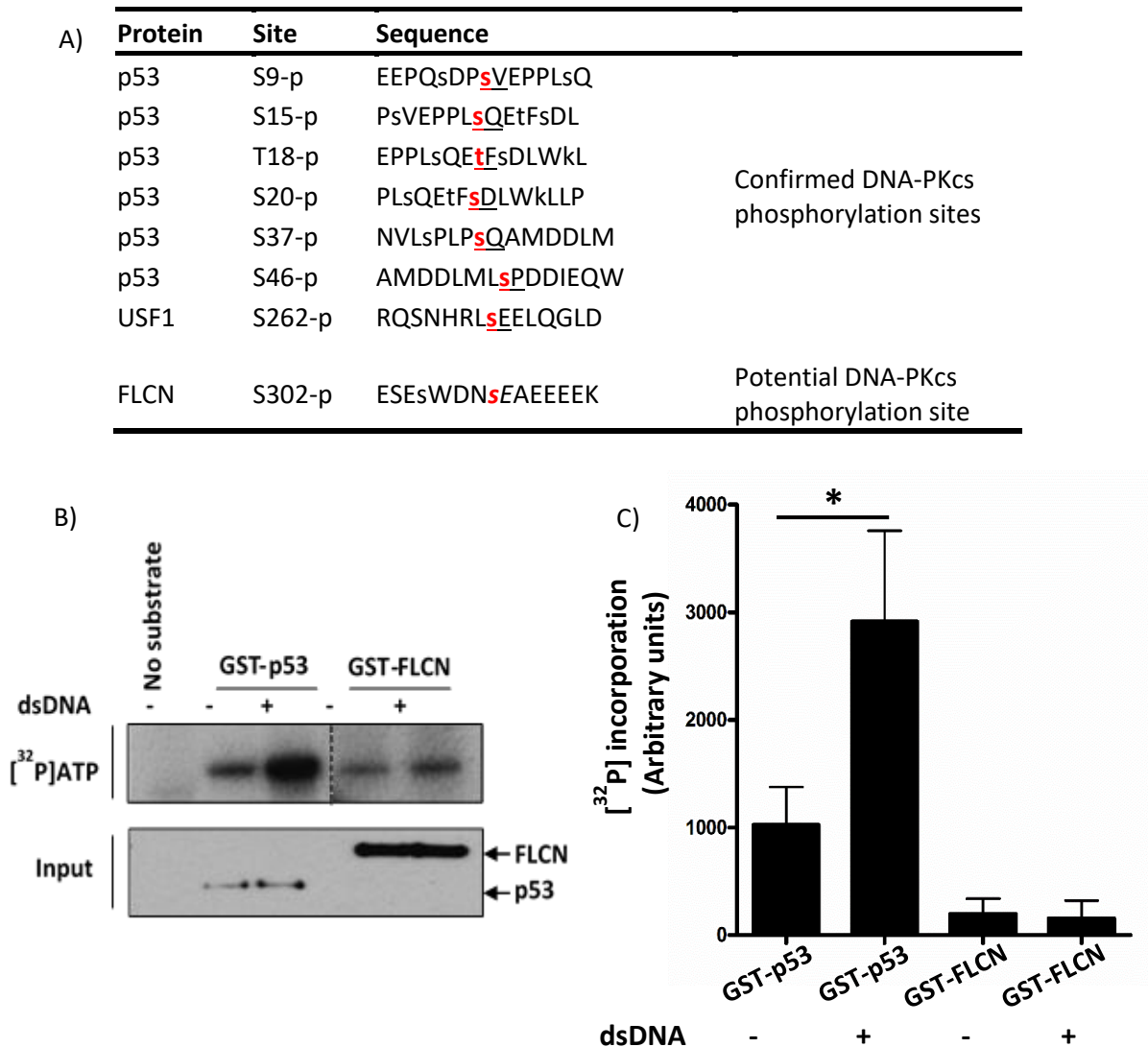
Figure 5.1 *In vitro* DNA-PK kinase assay. A) Table showing confirmed DNA-PKcs phosphorylation sites on p53 and USF1, and the potential DNA-PKcs phosphorylation site on FLCN. Phosphorylation sites were identified using PhosphositePlus® online resource. B) GST-FLCN or GST-p53 was overexpressed in HEK293 cells and GST-pull down was performed to purify the proteins of interest. Incorporation of radiolabelled phosphate [^{32}P] was determined in the presence of short double-strand DNA (dsDNA) to mimic dsDNA breaks. GST-p53 used as a positive control. The blot shown is representative of at least 3 independent experiments, with the exception of GST-FLCN with no dsDNA which had two independent values. C) Densitometry of DNA-PKcs *in vitro* kinase assay. For each tagged protein pixel intensity was normalised against no substrate control. Error bars indicate standard error of mean, SEM. * = *P*value <0.05.

5.2.2 Exploring the effect of FLCN knockdown on DNA-damage signalling

Given that FLCN is unlikely to be a DNA-PK substrate, and that the FLCN interactome described in chapter 3 indicates a number of proteins which function within the DDR, the effect of FLCN loss on DNA damage signalling pathways was explored next. To begin with, etoposide was used to induce DSBs (figure 5.2). Etoposide is a topoisomerase II inhibitor that prevents the re-ligation of DNA strands after helix unwinding. During DNA replication this leads to DSBs (Montecucco et al. 2015). Preliminary results suggested phosphorylation of DNA-PKcs at serine 2056 (Ser2056) was down in aged knockdown cells (HP-KD cells), while phosphorylation of Chk1 and H2AX were up in aged cells (figure 5.2A), with γH2AX being up in basal as well as damage-induced FLCN knockdown cells (figure 5.2A and 5.2B). During this initial analysis, however, western blots demonstrated large inconsistences, where biological replicates were vastly different (data not shown). Etoposide requires a round of replication to introduce DSBs; given that FLCN is suspected to have a role in the cell cycle (Chapter 3 figure 3.5, chapter 6, (Kawai et al. 2013; Laviolette et al. 2013; Kenyon et al. 2016) the method of DSB induction was changed to ionising radiation (IR). IR directly affects DNA structure to induce DSBs (Scott and Pandita 2006). It does not require cells to be replicating and damage occurs throughout all phases of the cell cycle. Therefore, IR presents a more reliable and consistent DNA damage induction method.
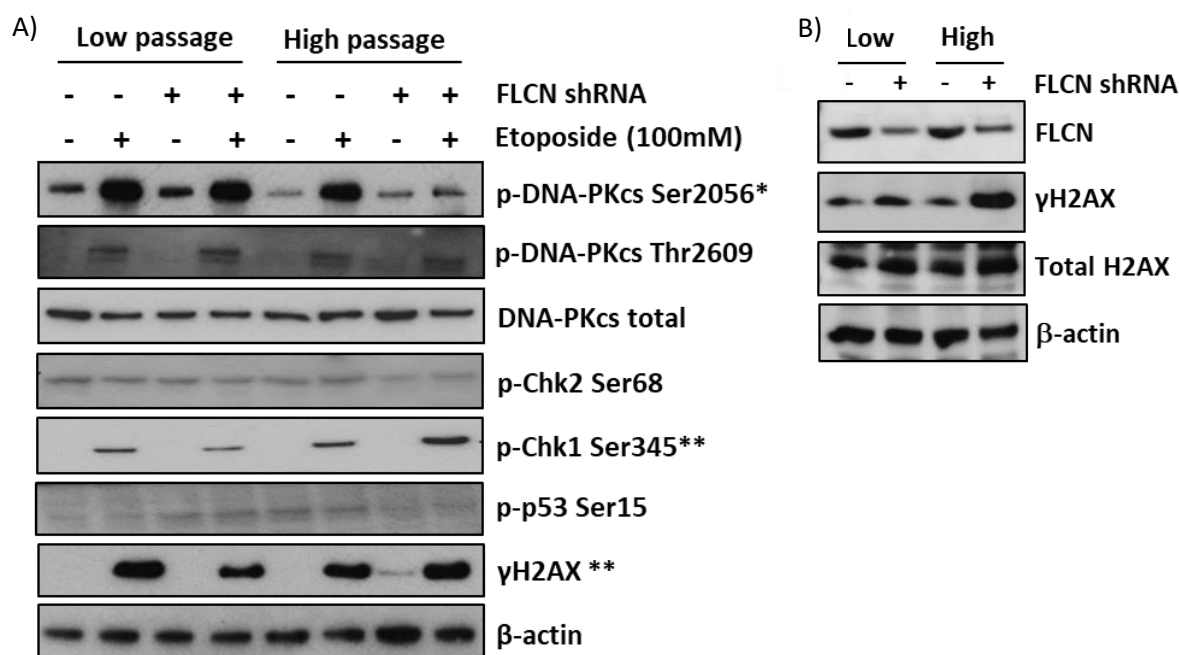
Figure 5.2 Initial analysis of the DNA damage response in FLCN knockdown. A) HK2 cells were treated with 100mM etoposide for 24 hours and immunoblotted for a response to DDR. Image is compiled of up to 4 independent experiments. Each replicate varied, and consensus with repeats could not be achieved. It is worth noting not all proteins where probed for in each experiment. *probed in 2 experiments, **probed in 4 experiments. B) Phosphorylation of histone variant H2AX (γH2AX), a marker of dsDNA breaks was assessed under basal condition in HK2 cells, blot is representative of 3 independent experiments and carried out by Dr Elaine Dunlop.

To ensure appropriate experimental conditions, increasing doses of IR (1-10Gy) were tested for different lengths of time in the low passage wild type HK2 cell line (LP-WT). H2AX is a key molecule in the repair of damaged DNA and its phosphorylation at serine 139 (γH2AX) is commonly used as a marker of DSBs (Kuo and Yang 2008). After the induction of DNA damage, H2AX at the site of DSBs is rapidly phosphorylated allowing the DNA damage signal to spread along the chromatin surrounding each DSB lesion (Kinner et al. 2008). It functions to provide a platform for the recruitment of proteins that participate in DDR. γH2AX form within seconds after strand breakage, but since they are initially quite small and difficult to visualise, they are more reliably examined starting 15–30 min after damage (Lobrich et al. 2010). Other DNA repair-enabling proteins, such as 53BP1, Nbs1, Rad50, Rad51, and BRCA1 that are thought to be more technically challenging to detect because of their limiting sensitivity or more regulated occurrence (Polo and Jackson 2011). For

example, while γH2AX can be detected in all phases of the cell cycle, other proteins, such as Rad51, are restricted to S- and G2-phases, being specific for homologous recombination repair of DSBs. Within the LP-WT control cells used, γH2AX was not observed following 1 Gy or 2 Gy dose. It was, however, observed after 5 Gy and 10 Gy. The signal was seen from 30 min to up to 48 h after IR, with the signal generally weakening over time, as excepted. Breaks induced by the higher dose took longer to repair as indicated by higher levels of γH2AX at the later time points, again as expected (figure 5.3A). Given that the objective is to see how FLCN knockdown cells respond to DNA damage, the lower dose was chosen to better mimic a more realistic damage risk found in FLCN-deficient patients. For this reason, an IR dose of 5 Gy with samples lysed at 1 h after IR was chosen (figure 5.3A). This enabled somewhat more consistent results with exploring DDR in FLCN knockdown cells, however, there were still inconsistencies between replicates (data not shown). Therefore, the lysis buffer was adapted next (figure 5.3B).
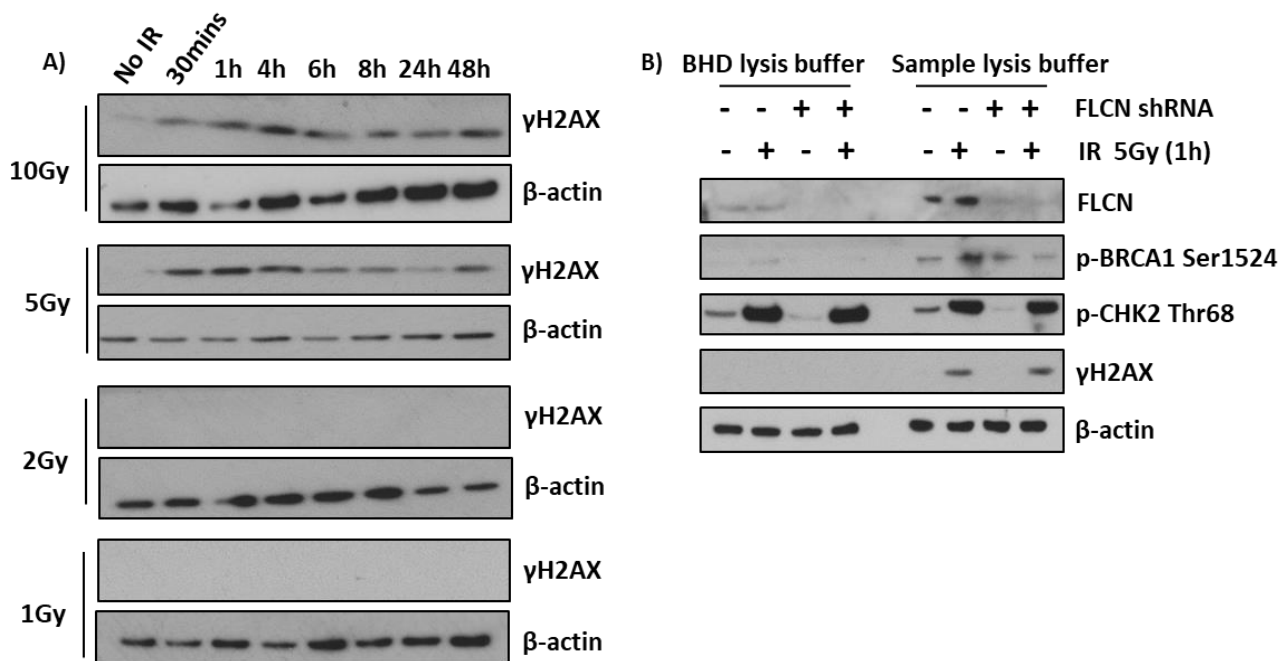
Figure 5.3 Troubleshooting western blot analysis of DNA damage response. A) Optimising the use of ionising radiation (IR) treatment to induce DNA damage. Phosphorylation of H2AX (γH2AX) was used as a marker of double-strand DNA breaks. The blot is representative of 2 independent experiments. B) Optimising cellular lysis buffer. 'BHD lysis buffer' contains triton-X (0.1 % [v/v]) and protease inhibitors, while for the 'sample lysis buffer' cells were lysed directly in 1x LDS sample buffer in the presence of high SDS (0.1 % [w/v]) and DTT (50mM). For both lysis buffers, samples were washed once with cold PBS prior to the addition of lysis buffer and left for 30 minutes on ice. All samples were subjected to two 30 s rounds of sonication.

The lysis buffer (referred to as BHD lysis buffer) initially used contained the detergent Triton X-100, to break down cellular membranes. Triton X-100 is a non-ionic detergent, and is considered a milder, less denaturing detergent. The cell membrane encloses the cytoplasm and the cell organelles; it consists of a lipid bilayer. The nuclear membrane, on the other hand, encloses the nucleus and is made up of double lipid bilayer (Capell and Collins 2006). The DDR proteins being explored are primarily active and located within the nucleus. One idea for the inconsistencies is that Triton X-100 is not stringent enough to reliably break down the double lipid bilayer of the nuclear envelope. Therefore, 'sample lysis buffer' was used as an alternative method of lysis. In the sample lysis buffer, cells were lysed directly in 1x LDS sample buffer (NuPage, Invitrogen) in the presence of high SDS and DTT concentrations (as previously used within the lab (Dodd et al. 2015). The high SDS concentration ensures efficient dissolution of cellular and nuclear membranes. While the high DTT concentrations were used to ensure reduction of proteins to diminish interaction with nuclear membrane, trafficking skeletons, and DNA, to limit proteins of interest being sequestered out of solution in the debris pellet (to exclude this becoming a source of inconsistency). For both buffers, cells were washed once with PBS prior to the addition of lysis buffer. Plates were kept on ice for 5 min before contents were scraped and transferred to ice-cold Eppendorf tubes. Samples were kept on ice for a further 30 min and subjected to two 30 s pulses of sonication at full power. Cells were centrifuged at 10,000 rpm for 8 min at 4°C to pellet the non-soluble parts of the cell. Samples were stored at -20 °C until needed. Proteins to test were selected based on size, ensuring maximum amount of membrane coverage from a single gel, to minimise time and resources used for troubleshooting. Sample lysis buffer showed proteins were more readily detectable in this solution (figure 5.3B). From this point on, all cells where lysed in 'Sample lysis buffer'.

As previously mentioned, γH2AX promotes the repair of DSBs, through the recruitment of DDR proteins to the site of damage and is considered a molecular marker for DSBs. Within weeks of FLCN knockdown (low passage knockdown cells), γH2AX levels were enhanced (Figure 5.4A). The degree of phosphorylation was elevated further upon long-term FLCN knockdown (high passage cells). Both the basal and IR-induced level of γH2AX was higher in the FLCN-deficient HK2 cells (Figure 5.4A), suggesting that loss of FLCN results in an increase in DSBs.
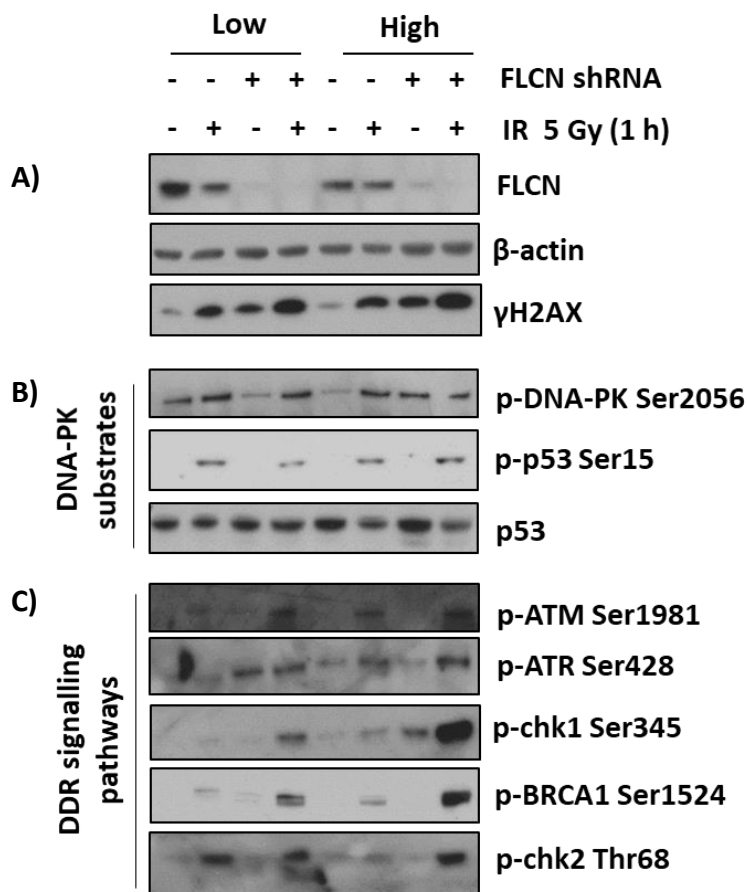
Figure 5.4 FLCN knockdown cells show elevated levels of DNA damaging signalling following ionising radiation (IR). Western blot analysis of wild type and FLCN knockdown HK2 cells 1 h following 5 Gy IR. A) Showing control blots (FLCN and β−actin), and surrogate marker of dsDNA breaks (pH2AX). B) Showing the response of DNA-PKcs and a downstream substrate, p53, to IR. C) Exploring cellular response to DNA damage through 'classical' DNA damage signalling molecules. Blots are representative of 3 independent experiments.

To determine whether FLCN influences DNA damage signalling pathways, FLCN knockdown cells where subjected to 5 Gy IR and lysed after 1 h and immunoblotted for a panel of DNA damage signalling molecules (figure 5.4B and 5.4C). Given that FLCN has been shown to interact with DNA-PKcs (see chapter 3), DNA-PK's ability to autophosphorylate was explored in the first instance (Figure 5.4B). DNA-PKcs autophosphorylation is essential for the appropriate regulation of DNA strand end processing, enzyme inactivation, and complex dissociation from DNA (Chan et al. 2002). The best characterised autophosphorylation sites of DNA-PK occur at Ser2056 (PQR cluster) and Thr2609 (ABCDE cluster) (Meek et al. 2008). It is generally considered that phosphorylation of the Ser2056

blocks access to DNA ends, representing DNA-PK bound to DNA ends, tethering them together (Meek et al. 2007), while phosphorylation at Thr2609 leads to DNA-PK complex dissociation and allows repair molecules access to DNA ends (Meek et al. 2008). Both Ser2056 and Thr2609 were explored in FLCN knockdown cells. No change was observed at the Ser2056 site (figure 5.4B), and the Thr2609 site was difficult to blot, containing a high level of background (data not shown). As no convincing difference was observed with Ser2056, the Thr2609 site was not explored further. These post-translational modifications in DNA-PK are well understood, more than 40 phosphorylation sites have been identified for DNA-PK *in vitro* (Wang and Lees-Miller 2013), and the impact of each on DNA-PKcs function seems to be complex. It is unclear which sites are critical for tumour-associated activities. Pharmacologic inhibition of DNA-PK kinase activity results in inefficient repair and hypersensitivity to double-strand break–inducing agents (Zhao et al. 2006), therefore it is clear DNA-PKcs is required for direct ligation of broken DNA ends, rendering it a critical factor in NHEJ. However, the order of recruitment and function of both processing and ligation factors involved in NHEJ after binding of Ku remain poorly defined, and the process is likely dynamic. The results presented in figure 5.4B suggest FLCN is unlikely to impact on DNA-PK's ability to autophosphorylate, and by extension function. The impact this has further downstream in the NHEJ process, however, may still be interesting to study, especially as γH2AX indicates an increase in DBS (Goodwin and Knudsen 2014).

As previously mentioned p53 is a well characterised substrate of DNA-PK (Leesmiller et al. 1992). It is also the most frequently mutated gene presented in human cancers (Zigeuner et al. 2004; Brosh and Rotter 2009; Noon et al. 2010). Therefore, p53 phosphorylation upon FLCN knockdown was explored next. Under normal conditions p53 is continuously expressed but is maintained at low levels by Mdm2-mediated ubiquitination and proteasomal degradation. Under stress conditions p53 undergoes phosphorylation at numerous sites which stabilise the protein. Serine 15 phosphorylation of p53 is a major focal point in the activation of p53. Serine 15 is the primary target on the p53 protein in response to DNA damage and is phosphorylated by DNA-PK, ATM and ATR protein kinases under genomic stress. Interestingly, it can also be activated by AMPK in response to metabolic stress/glucose starvation (Jones et al. 2005). As expected, phosphorylation of p53 at Ser15 was induced under IR within the HK2 cells, however no differences were observed when

comparing FLCN knockdown with wild type cells (figure 5.4B). Furthermore, the aging of cells didn't affect the phosphorylation of p53. Transcriptional analysis shows TP53 mRNA is significantly downregulated in high passage FLCN knockdown cells (chapter 4, figure 4.10). Interestingly FLCN loss did not affect basal levels of p53, nor did DNA damage change the total level of p53 within HK2 cells, regardless of FLCN status. The disconnect between mRNA and protein levels in FLCN deficient cells is likely to not impact on cellular response, neither total protein level nor phosphorylation at Ser15 of p53 was altered upon FLCN loss (figure 5.4B). Stress responding proteins, transcription factors, signalling genes, chromatin modifying genes, and genes with cell-cycle specific functions tend to have unstable mRNA and unstable protein. The most important regulators of the cellular stress response are expected to have a poor correlation between mRNA and protein, as is the well documented case with p53 (Lavin and Gueven 2006). Indeed, a lot of evidence suggests mRNA levels cannot be used as surrogates for corresponding protein levels without verification (Schwanhausser et al. 2011,2013)

To get a broad overview of DNA damage signalling after IR, a panel of DNA damage response molecules were assessed (Figure 5.4C). Across 3 independent experiments the phosphorylation ataxia-telangiectasia mutated (ATM) and ATM and RAD3-related (ATR) phosphorylation did not seem to be affected by FLCN loss (Figure 5.4C). As such FLCN loss isn't likely to affect the activity of these kinases. Along with DNA-PKcs, ATM and ATR, are members of the PI3K-like protein kinase (PIKK) family which are involved in the cellular response to genotoxic stress. ATM, ATR and DNA-PK have similar substrate specificities *in vitro* (SQ/TQ), and partially overlapping substrate specificities *in vivo*. Recent studies have identified several hundred proteins containing the PIKK phosphorylation motif, the phosphorylation of which is induced in response to ionising radiation (IR) (Matsuoka et al. 2007; Bennetzen et al. 2010). However, it is difficult to estimate the contribution of individual PIKKs, as IR induces various types of DNA lesion and also damages other cell components, leading to the activation of numerous signalling kinases (Bensimon et al. 2010). Interestingly, DNA-PKcs can also be phosphorylated by ATM during the DNA damage response (Meek et al. 2008; Davis et al. 2014). Furthermore, the Thr2609 cluster on DNA-PKcs is primarily phosphorylated by ATM or ATR under different cellular stresses (Chen et al. 2007; Meek et al. 2008). As the Thr2609 site is responsible for complex dissociation from

the DNA, it's likely ATM functions as a regulatory component, ensuring DNA-PK dissociates not only when appropriate, but when DNA-PKcs fails to release, allowing strands to be ligated even if DNA-PK is compromised.

ATM is best known for its role as an apical activator of the DNA damage response in the face of DSBs. ATM controls a complex signalling network by phosphorylating a multitude of substrates in numerous network branches including p53, BRCA1, FANCD2, Chk2, and Nbs1 to induce late-S phase and G2 checkpoints. ATM primarily stimulates the repair of DSBs through homologous recombination (HR). DSB resection is induced in the S and G2 phases of the cell cycle, when sister chromatids can be used for template driven HR (Guleria and Chandna 2016). Upon DNA damage, ATM autophosphorylates on residue serine 1981 resulting in an active ATM molecule (Kozlov et al. 2011; Cremona and Behrens 2014; Ahmed et al. 2016). ATR, on the other hand, responds to single strand breaks that are typically generated at the sites of stalled replication forks. ATR is unable to interact with DNA directly, and depends on nucleofilaments that are formed between the replication protein A heterotrimer (RPA) and ssDNA for DNA binding (Zou and Elledge 2003). The phosphorylation site serine 428 is required to induce enzymatic activity of the kinase. While the apical responders to DDR (DNA-PK, ATM, ATR) activity was not altered by loss of FLCN, downstream responders were. An increase in Breast cancer type 1 susceptibility protein (BRCA1), Checkpoint kinase 1 (Chk1) and Checkpoint kinase 2 (Chk2) phosphorylation was seen in FLCN-deficient cells and, similar to γH2AX, this effect was more pronounced in high passage cells (Figure 5.4C). However, in the case of Chk1 and Chk2, variation was seen in this data. Further work is required to validate if there is an increase in phosphorylation of Chk1 and Chk2 following FLCN knockdown.

BRCA1 relocates to DNA damage sites and promotes HR to repair DSBs (Livingston et al. 1997; Scully et al. 1997). BRCA1 has two key roles; facilitating end processing of messy DNA ends, and inhibiting NHEJ (Wong et al. 1998; Zhong et al. 1999; Sartori et al. 2007; Kass and Jasin 2010). Numerous DNA damage-induced phosphorylation sites on BRCA1 have been identified, including Serine 988, 1189, 1387, 1423, 1457, 1524, and 1542. The site explored in this experiment is Ser1524. It has been demonstrated that IR induces BRCA1 Ser1524 phosphorylation in S phase (Okada and Ouchi 2003) and that this phosphorylation

is required for the formation of the IR-induced G2/M checkpoint (Xu et al. 2001; Xu et al. 2002a). BRCA1 Ser1524 phosphorylation has also been linked to with the regulation of cell growth after IR; HCC1937 cells re-expressing wild type BRCA1 can grow after IR damage, whereas cells expressing a phosphorylation-deficient mutant of Ser1524 residue showed growth retardation under the same condition (Cortez et al. 1999; Okada and Ouchi 2003). As FLCN knockdown HK2 celled showed elevated P-Ser1524 after DNA damage (Fig 5.4C), they may have a proliferative advantage after IR. Interestingly, claspin was found to control BRCA1 phosphorylation at Ser1524. Furthermore, BRCA1 and claspin then function to activate the tumour suppressor Chk1. Unexpectedly, claspin was found to have a second, positive role in control of the cell cycle as claspin overexpression increased cell proliferation. This is noteworthy as FLCN loss was previously cited to increase the expression of claspin (Seabra et al. 2010). It would be interesting to test the effect of FLCN knockdown on other phosphorylation sites of BRCA1. For example, P-Ser1423 is responsible for the G2/M checkpointing (Xu et al. 2001; Ouchi 2006), P-Ser1387 is required for the S phase checkpoint but not the G2/M checkpoint, and P-Ser308 is responsible for mitotic entry (Xu et al. 2002b).

Chk1 and Chk2 are both serine/threonine kinases that play a pivotal role in maintaining DNA integrity. Mechanistically, Chk1 becomes activated by ATR through phosphorylation of serine 317 and serine 345 (Petermann and Caldecott 2006). As a substrate of ATR, Chk1 activation is an important response to single-strand DNA break sensing (Zhao and Piwnica-Worms 2001; Gupta et al. 2018). Chk1 can also be phosphorylated by many other proteins, such as ATM, BRCA1, MCPH1 and p300/CBP (Yarden et al. 2002; Yoo et al. 2006). Chk1 activation results in the initiation of cell cycle checkpoints; late S phase and G2/M cell cycle arrest (Zhao et al. 2002; Brown and Baltimore 2003; Petermann and Caldecott 2006). In the FLCN knockdown cells, ATR activation was unchanged, while Chk1 may be hyperphosphorylated (figure 5.4C). As it stands, evidence suggests DNA damage is not likely to be caused by replication stress and/or faulty replication forks; but the increase in Chk1 phosphorylation may represent an increase in DNA-damage burden in the FLCN knockdown cells. Chk2, on the other hand, is primarily activated by ATM through phosphorylation at residue threonine 68 which induces Chk2 dimerisation and autophosphorylation of the kinase domain (Zannini et al. 2014). As a downstream kinase of ATM, Chk2 participates in the early steps of DSB repair

phosphorylating both BRCA1 (Lee et al. 2000) and BRCA2 (Bahassi et al. 2008), and promoting HR over error prone-NHEJ during the G2/M checkpoint. Chk2 was hyperphosphorylated in high passage, but not low passage FLCN knockdown cells suggesting these cells may be accumulating damage upon aging (figure 5.4C).

It's important to state that despite best efforts to troubleshoot a reliable protocol, results still contained large inconsistences, making interpretation of results difficult. For this reason, confidence is only given to increased levels of γH2AX, and BRCA1, as these were the most consistent. Inconsistent results are not unusual when studying FLCN (Tee and Pause 2013; Chen et al. 2015). For example, FLCN has been shown to both inhibit and promote mTOR signalling in multiple contexts. One idea is that FLCN functions in a lot of processes and as such inconsistencies may arise from stoichiometric pressure. This is particularly interesting with regards to the HK2 knockdown cells used in this thesis. Total FLCN knockout is not viable and, as such, work is done in cells that still express a small amount of FLCN. Therefore, inconsistencies may arise where a finite pool of FLCN can only do so much and random chance is involved in detecting a robust observation.

Collectively, these results suggest FLCN-deficient cells have more DSBs, and elevated DDR signalling. Immunoblotting measures the total levels of γH2AX in whole cell lysates. While it is the easiest to perform, and relatively inexpensive; it is not the most informative method to explore the nature of DSBs. Immunostaining can be used to quantify the damage and to visualise co-localisation with DDR molecules. It is also more sensitive than immunoblotting, as each γH2AX foci represents a single break (Kuo and Yang 2008). It also allows for the study of induction of breaks and repair kinetics. However, it is more laborious and costly. Flow cytometry, on the other hand, allows for accurate and fast analysis of γH2AX, and by extension, quantification of DSBs within individuals cells. Furthermore, γH2AX can be quantitated relative to DNA content, and as such by which phase of the cell cycle damage occurs. It would be interesting to compare how long it takes FLCN KD cells to repair from DSBs, if there is a stage of the cell cycle where damage occurs, or repair differs from wild type cells. Another idea would be to further explore BRCA1 phosphorylation. BRCA1 is strongly implicated in promoting HR over NHEJ. Perhaps the increase in BRCA1 is to drive HR as a compensation to insufficient NHEJ in G1. It would

therefore be interesting to explore the efficacy and efficiency of both HR and NHEJ in FLCN deficient cells.

5.2.3 Cell growth and proliferation following DNA damage

One of the most notable observations with regards to the effect of FLCN loss on DDR signalling explored above is the elevation in γH2AX, indicating there is an increase in DSBs upon FLCN loss (figure 5.4A). DSBs are considered the most harmful lesions in genomic DNA (Mills et al. 2003; Scott and Pandita 2006). If not efficiently repaired, they can lead to chromosomal aberrations and apoptosis; in higher eukaryotes, even a single DSB in an essential gene can trigger the apoptotic signalling cascade (Rich et al. 2000; Lips and Kaina 2001). Therefore, cellular proliferation and viability following FLCN loss was explored in low passage HK2 cells to see if FLCN had a role in cellular sensitivity to DNA damage.

Low passage HK2 cells were subjected to 10 Gy IR, trypsininsed after 1 h, and DNA was stained with Solution 18™ (chemoetic), a mixture of Acridine Orange (a membrane permeable dye that stains both living and dead cells) and DAPI (which can't penetrate the membrane and thus only stains dead cells). Cells where then quantified on NucleoCounter NC-3000™. 10 Gy IR was used, instead of 5 Gy previously used, to observed what affect FLCN knockdown would have under high levels cellular stress.

The total cell count of samples was plotted as a quick and simple, but rough output for cell growth in the first instance (figure 5.5). Initial analysis suggests FLCN knockdown cells grow slower, having a lower total cell count at each time point (figure 5.5). However, variation between replicates was observed (figure 5.5). The error bars for figure 5.5 show the standard error of the mean (SEM) and is a measure of precision for an estimated population mean. The SEM error bars for both wild type and knockdown non-irradiated controls reveals the true mean of the cell lines could overlap. As such the differences between these non-irradiated control cell lines (No IR WT and No IR KD) are not statistically different, with the exception of the 96 hour time point (Table 5.1). From this data we cannot conclude a difference in cell number between the non-irradiated wild type and non-irradiated knockdown. Once irradiated however, both wild type and FLCN knockdown cells fail to proliferate (figure 5.5). Interestingly, knockdown and wild type cell numbers remain similar until 96 h post irradiation. Here, knockdown cells start to increase their numbers but

are not statically different from irradiated wild type cells at any time point (figure 5.5, table 5.1). Total cell number was obtained via staining (all living and dead) cells with Acridine Orange (AO). This is a very rudimentary output for cell proliferation. In addition, total cell number gives no information about the health of these cells, for example, while present in solution the cells may be dead, and as such won't be a source of cellular transformation. The most reliable and accurate method of assessing cell proliferation is a measurement of DNA-synthesising cells. Using a thiamine analogue (such as BrdU or EdU) to label cells as they proliferate. Other methods measure the metabolic activity of cells via tetrazolium salts. These salts form a dye when present in a metabolically active environment. The resulting colour change of the media can be quantified in a spectrophotometer, and so indirectly give an indication of the extent of proliferation.
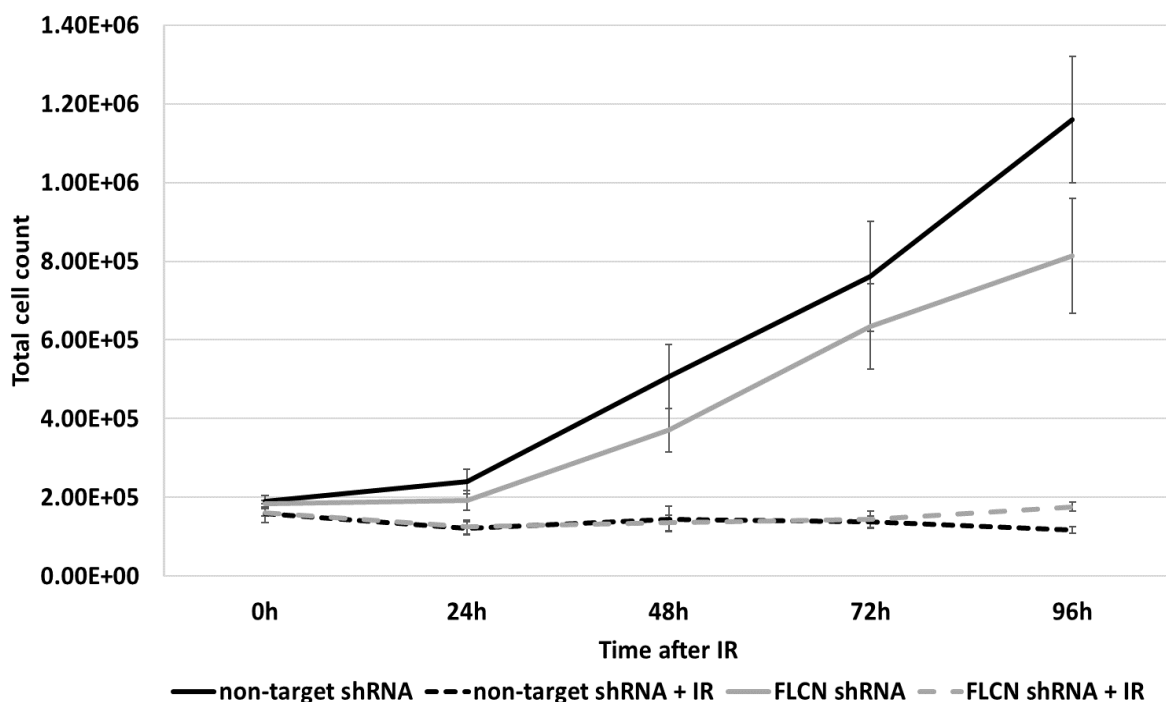
Figure 5.5 Cell growth, as determined by total number of cells, after DNA damage. Low passage wild type (WT) and FLCN knockdown (KD) HK2 cells were subjected to 10 Gy IR and left for up to 96 hours. Graph showing total number of cells at each time point as determined by by staining with acridine orange and analysed via a NucleoCounter NC-3000. Performed over 3 independent experiments, with each experiment containing samples analysed in triplicate. Error bars = SEM.

WT No IR vs KD No IR				
Time (h)	WT No IR (% viable)	KD No IR (% viable)	*P*value	95% CI of diff.
0	189500	183700	P > 0.05	-400500 to 388800
24	240200	192700	P > 0.05	-369800 to 274700
48	507700	371200	P > 0.05	-458700 to 185800
72	761300	634300	P > 0.05	-449200 to 195200
96	1160000	814000	P<0.01	-668500 to -23980

WT No IR vs WT IR				
Time (h)	WT No IR (% viable)	WT IR (% viable)	*P*value	95% CI of diff.
0	189500	159500	P > 0.05	-424600 to 364700
24	240200	120700	P > 0.05	-441800 to 202700
48	507700	145200	P<0.01	-684700 to -40180
72	761300	145200	P<0.001	-938300 to -293800
96	1160000	117100	P<0.001	-1365000 to -720900

WT No IR vs KD IR				
Time (h)	WT No IR (% viable)	WT IR (% viable)	*P*value	95% CI of diff.
0	189500	161500	P > 0.05	-422700 to 366700
24	240200	124800	P > 0.05	-437600 to 206800
48	507700	135000	P<0.01	-694900 to -50380
72	761300	144500	P<0.001	-939100 to -294600
96	1160000	176200	P<0.001	-1306000 to -661800

WT IR vs KD No IR				
Time (h)	WT No IR (% viable)	WT IR (% viable)	*P*value	95% CI of diff.
0	159500	183700	P > 0.05	-370500 to 418800
24	120700	192700	P > 0.05	-250300 to 394200
48	145200	371200	P > 0.05	-96260 to 548200
72	145200	634300	P<0.001	166800 to 811300
96	117100	814000	P<0.001	374700 to 1019000

WT IR vs KD IR				
Time (h)	WT No IR (% viable)	WT IR (% viable)	*P*value	95% CI of diff.
0	159500	161500	P > 0.05	-392700 to 396600
24	120700	124800	P > 0.05	-318100 to 326400
48	145200	135000	P > 0.05	-332400 to 312000
72	145200	144500	P > 0.05	-323000 to 321500
96	117100	176200	P > 0.05	-263100 to 381400

KD No IR vs KD IR				
Time (h)	WT No IR (% viable)	WT IR (% viable)	*P*value	95% CI of diff.
0	183700	161500	P > 0.05	-416800 to 372500
24	192700	124800	P > 0.05	-390100 to 254400
48	371200	135000	P > 0.05	-558400 to 86060
72	634300	144500	P<0.001	-812100 to -167600
96	814000	176200	P<0.001	-960000 to -315500

Table 5.1 Statistical analysis of cell growth, as determined by total number of cells, after DNA damage. Two-way ANOVA was performed to assess the variation in the data. If *P*value<0.05 Bonferroni test was performed post-hoc. Statistical analysis was performed in GraphPad PRISM4.

Next, cell viability was explored to get a better idea of the cellular response to IR. Viability is a measure of the number of living cells in a population. No difference in viability between wild type and FLCN knockdown non-irradiated controls were observed, the viability of HK2 cells is not compromised by FLCN knockdown alone (figure 5.6, table 5.2). Following IR both wild type and FLCN knockdown cells showed a slight decrease in viability over time (figure 5.7). This became statistically different from wild type non-irradiated cells at 48 hours (*P*value<0.01), with both cell lines showing a similar response to IR (figure 5.6). Interestingly, by 96 hours post-irradiation, FLCN knockdown cells were more viable than wild type cells (*P*value <0.001, table 5.2), suggesting cell survival may be increased. Typically, cells that lack key DDR proteins (such as DNA-PKcs, ATM, or BRAC1) become more sensitive to ionising radiation due to their failure to initiate and co-ordinate repair mechanisms (Chistiakov et al. 2008) the opposite, however, is seen in these FLCN knockdown cells. Interestingly, the loss of FLCN has already been linked to increase in stress tolerance. Loss of the *C.elegans FLCN* homologue, *flcn-1*, led to a 21% increase in lifespan under heat stress (Gharbi et al. 2013). This increased longevity was attributed to an increase in HIF signalling (Gharbi et al. 2013) and the induction of autophagy (Schiavi et al. 2013; Possik et al. 2014). Indeed, *flcn-1* deletion led to increased stress resistance through a constitutive activation of the *C. elegans* homologue of AMPK, *aak2*, which led to higher autophagic flux, higher levels of intracellular ATP, and inhibition of apoptosis (Possik et al. 2014). These findings were replicated in mouse embryonic fibroblasts, suggesting that this pathway is evolutionarily conserved in mammals (Possik et al. 2014). Previous work has also suggested FLCN is pro-apoptotic; *FLCN*-null embryonic stem cells and loss of *flcn-1* in *C.elegans* have been shown to have increased resistance to apoptosis (Cash et al. 2011; Possik et al. 2014), and FLCN has been demonstrated to upregulate the expression of a number of pro-apoptotic genes (Verhagen et al. 2002; Martinez-Ruiz et al. 2008; Reiman et al. 2012).
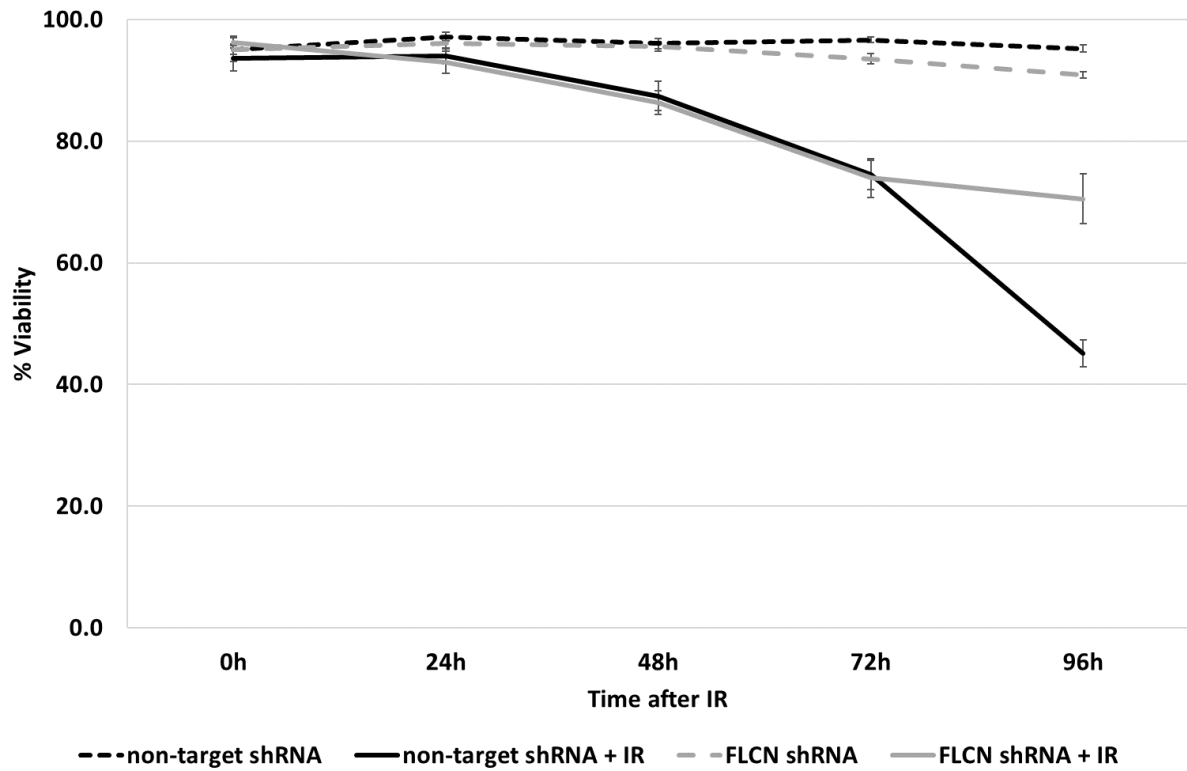
Figure 5.6 Cell viability after DNA damage. Low passage wild type (WT) and FLCN knockdown (KD) HK2 cells were subjected to 10 Gy IR and left for up to 96 hours. Graph showing percentage of viable cells as determined by staining with acridine orange/DAPI and analysed via a NucleoCounter NC-3000. Performed over 3 independent experiments, with each experiment containing triplicate samples. Error bars = SEM.

WT No IR vs KD No IR				
Time (h)	WT No IR (% viable)	KD No IR (% viable)	*P*value	95% CI of diff.
0	95.35	94.65	P > 0.05	-9.596 to 8.196
24	96.93	95.71	P > 0.05	-10.11 to 7.683
48	95.68	95.46	P > 0.05	-9.108 to 8.683
72	96.56	93.40	P > 0.05	-12.06 to 5.733
96	95.15	90.93	P > 0.05	-13.12 to 4.671
WT No IR vs WT IR				
Time (h)	WT No IR (% viable)	WT IR (% viable)	*P*value	95% CI of diff.
0	95.35	93.40	P > 0.05	-10.85 to 6.946
24	96.93	93.25	P > 0.05	-12.57 to 5.221
48	95.68	86.75	P<0.01	-17.82 to -0.02925
72	96.56	74.08	P<0.001	-31.38 to -13.59
96	95.15	44.13	P<0.001	-59.92 to -42.13
WT No IR vs KD IR				
Time (h)	WT No IR (% viable)	WT IR (% viable)	*P*value	95% CI of diff.
0	95.35	96.06	P > 0.05	-8.183 to 9.608
24	96.93	92.26	P > 0.05	-13.56 to 4.233
48	95.68	86.35	P<0.01	-18.22 to -0.4293
72	96.56	73.18	P<0.001	-32.28 to -14.49
96	95.15	71.76	P<0.001	-32.28 to -14.49
WT IR vs KD No IR				
Time (h)	WT No IR (% viable)	WT IR (% viable)	*P*value	95% CI of diff.
0	93.40	94.65	P > 0.05	-7.646 to 10.15
24	93.25	95.71	P > 0.05	-6.433 to 11.36
48	86.75	95.46	P < 0.05	-0.1832 to 17.61
72	74.08	93.40	P<0.001	10.43 to 28.22
96	44.13	90.93	P<0.001	37.90 to 55.70
WT IR vs KD IR				
Time (h)	WT No IR (% viable)	WT IR (% viable)	*P*value	95% CI of diff.
0	93.40	96.06	P > 0.05	-6.233 to 11.56
24	93.25	92.26	P > 0.05	-9.883 to 7.908
48	86.75	86.35	P > 0.05	-9.296 to 8.496
72	74.08	73.18	P > 0.05	-9.796 to 7.996
96	44.13	71.76	P<0.001	18.74 to 36.53
KD No IR vs KD IR				
Time (h)	WT No IR (% viable)	WT IR (% viable)	*P*value	95% CI of diff.
0	94.65	96.06	P > 0.05	-7.483 to 10.31
24	95.71	92.26	P > 0.05	-12.35 to 5.446
48	95.46	86.35	P<0.01	-18.01 to -0.2168
72	93.40	73.18	P<0.001	-29.12 to -11.33
96	90.93	71.76	P<0.001	-28.06 to -10.27

Table 5.2 Statistical analysis of cell viability after DNA damage. Two-way ANOVA was performed to assess the variation in the data. If *P*value <0.05 Bonferroni test was performed post-hoc. Statistical analysis was performed in GraphPad PRISM4.

5.2.4 Exploring the function of the FLCN/DNA-PKcs interaction

Effort was next put into characterising the biological reason for the FLCN/DNA-PKcs interaction. As a DNA damage sensor and moderator of NHEJ, DNA-PKcs is very abundant (Anderson 1996). In addition to the nuclear function, DNA-PKcs is present in the cytoplasm, were emerging evidence suggest DNA-PKcs regulates aging and energy homeostasis, unrelated to DNA repair (Huston et al. 2008; Goodwin and Knudsen 2014; Chung 2018).

Previously, FLCN has been shown to be important for the correct cytoplasmic-nuclear shuttling of transcription factors TFEB and TFE3. Upon FLCN loss, TFEB and TFE3 proteins accumulate within the nucleus, promoting the transcription of gene targets. The literature suggests the nuclear localisation of TFEB and TFE3 is controlled by mTORC1-dependent phosphorylation and FLCNs involvement appears to be co-ordinated with its regulation of mTORC1. A novel idea suggests FLCN may be involved in nuclear-cytoplasmic shuttling of proteins directly, through a functional association with the nucleopore complex. Mass spectrometry analysis identified FLCN interacts with 11 components of the nucleopore complex (RANBP2, NUP205, NUP188, NUP54, NUP35 (NUP53), NUP155, NUP133, NUP160, NUP50, TPR, NUP153), and proteins that are important for nuclear export (XPO1, XPO5, EIF4) (figure 5.7A). FLCN has been demonstrated to interact with NUP155 (data unpublished, Dr Sara Seifan, and Mr Matt Lines), and limited evidence suggests it could be involved in establishing RAN:GTP gradients around the nucleopore required for nuclear export of proteins (unpublished data, M. Van Steensel, Maastricht University). Furthermore, FLCN was shown important for the nuclear export of TDP-43 (Xia et al. 2016). Therefore, the subcellular location of DNA-PKcs was explored following FLCN knockdown and DNA damage (data not shown). Low and high passage of HK2 cells were subjected to 5 Gy and then 10 Gy IR. No difference in DNA-PK localisation was observed upon FLCN loss, or under IR.

Interestingly, however, FLCN may be chromatin bound (figure 5.7C). Subcellular localisation of total FLCN suggests it is primarily cytosolic. However, when phosphorylated at serine 62, FLCN is predominantly chromatin bound (figure 5.7C). FLCN has been shown to be chromatin bound by another group (unpublished data, M. Van Steensel, Maastricht University). Neither total nor phosphorylated FLCN's localisation changed when cells were subjected to IR (figure 5.8C). Therefore, while the observation that FLCN is chromatin bound

is likely a true one, it may not play a direct role in organising repair molecules at the site of DNA lesions.
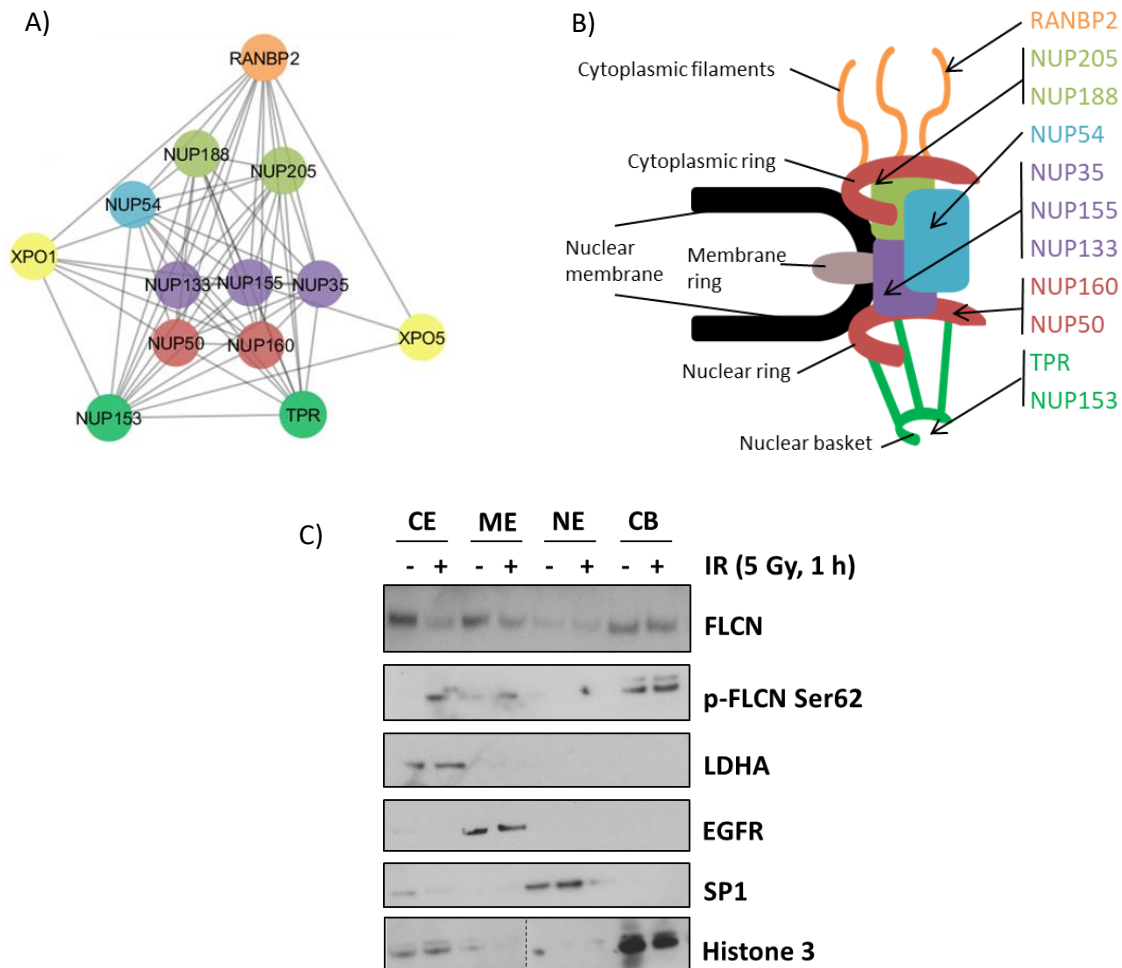
Figure 5.7 Subcellular localisation of DNA-PK following FLCN loss. A) Interaction network visualising members of the nucleopore complex that were identified in the FLCN interactome via mass spectrometry. B) Diagram of the nucleopore complex, with members that are present in the FLCN interactome highlighted. C) Low passage wild type FLCN HK2 cells (LP-WT cells) were subjected to 5 Gy IR and fractionated using the Thermo Scientific subcellular protein fractionation kit as directed by the manufacturer's protocol. CE = cytoplasmic extract, ME = membrane extract, NE = nuclear extract, and CB = chromatin bound. Blots are representative of 2 independent experiments.

Another possible reason for the FLCN/DNA-PKcs interaction could be related to the regulation of heat shock protein 90 α (HSP90α). HSP90α is a molecular chaperone involved in maintaining the stability and activity of numerous signalling proteins under stress conditions. HSP90α plays a key role in DNA damage signalling, repair, and cell cycle control. Multiple components of the DNA double strand break repair machinery, including BRCA1,

BRCA2, Chk1, DNA-PKcs, FANCA, and the MRE11/RAD50/NBN complex, have been described as client proteins of HSP90α. Additional HSP90α clients worth mentioning include cyclin dependent kinase 1 (CDK1), CDK2, CDK4, and CDK6 (and by association their cyclin counterparts cyclin B, cyclin D, and cyclin E). All of these proteins are important components at the G1/S boundary of the cell cycle (Burrows et al. 2004). Inhibition of HSP90α actions leads to the altered localisation and stabilisation of DDR proteins after DNA damage (Sreedhar et al. 2004; Pennisi et al. 2015).

Recently, DNA-PKcs was shown to phosphorylate HSP90α at threonine 5 and 7 (t5,7) both *in vitro* and *in vivo* (Quanz et al. 2012; Park et al. 2017). This phosphorylation decreases HSP90α ability to interact with its clients, and is thought to inhibit HSP90α-directed folding of client proteins (Park et al. 2017). In rhesus monkey skeletal cells, it was demonstrated that age-related increases in DSBs can facilitate the suppression of mitochondrial biogenesis, by activating DNA-PKcs driven inhibition of HSP90α. This prevents the correct folding of AMPK and its upstream regulator LBK1 (Park et al. 2017). It is thought this mechanism is to limit further internal sources of DNA damage (i.e., to limit ROS production). In relation to FLCN, this becomes exciting. AMPK activity is upregulated upon FLCN loss, resulting in mitochondrial biogenesis and metabolic transformation in FLCN-deficient cells, primarily through an increase in PPARGC1A expression (Klomp et al. 2010; Hasumi et al. 2012; Possik et al. 2014; Yan et al. 2016a). It is currently unclear what the mechanism is that leads to this AMPK upregulation. Furthermore, HPS90α was noted as an important network protein in the FLCN interactome (Chapter 3). FLCN itself, is thought to be a client of HSP90α (Woodford et al. 2016). Therefore, it was hypothesised that the FLCN/DNA-PKcs interaction observed in chapter 3, may act as a negative regulator for AMPK through HSP90α.

In the FLCN knockdown HK2 cells, AMPK target genes are dysregulated upon FLCN loss (figure 5.8A and 5.8B), as previously shown by multiple studies (Klomp et al. 2010; Hasumi et al. 2012; Possik et al. 2014; Yan et al. 2016a). This includes PPARGC1A (figure 5.8B), which encodes peroxisome proliferator-activated receptor gamma coactivator 1-alpha (PGC1α). PGC1α is a transcriptional coactivator that regulates the genes involved
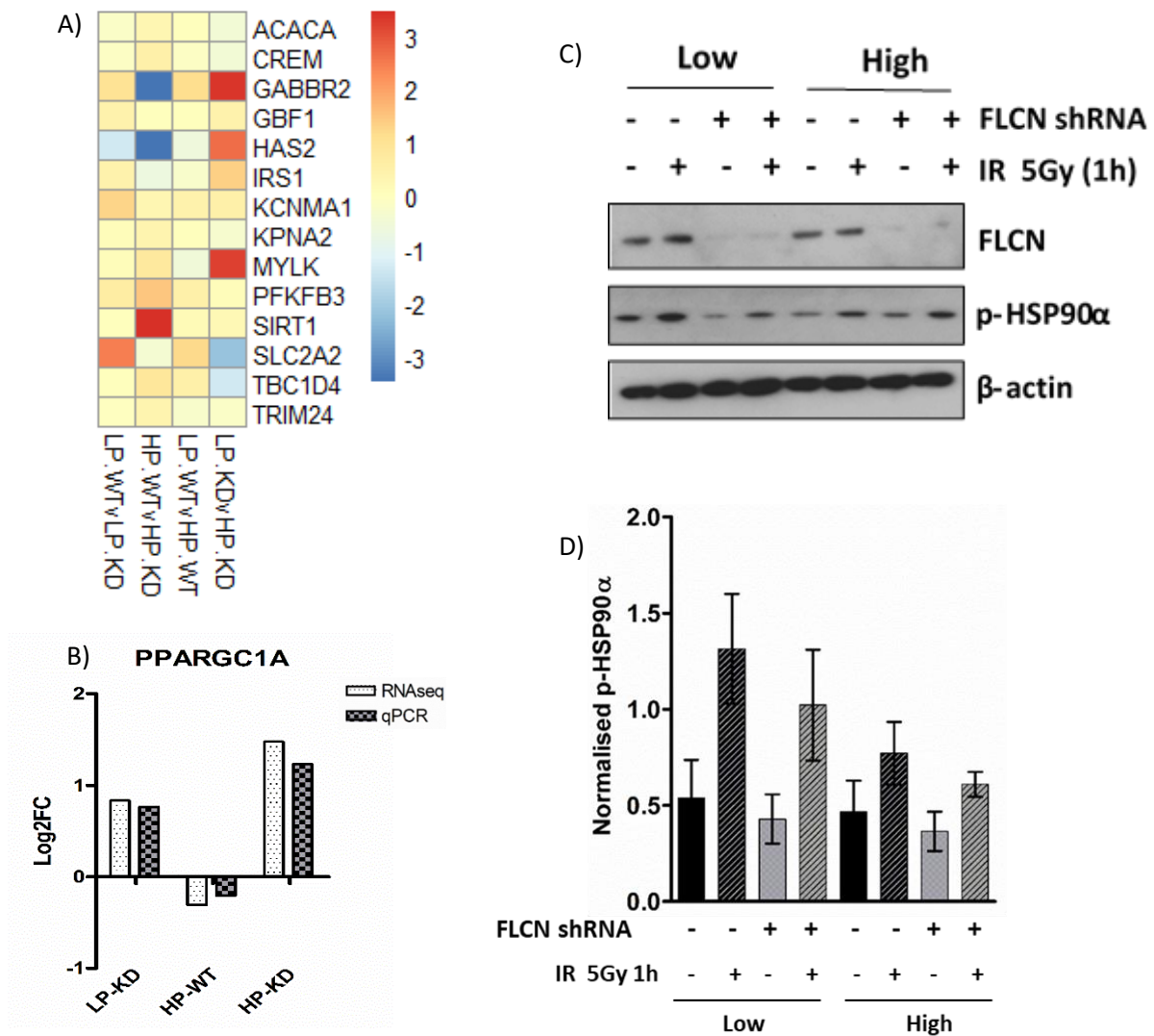
Figure 5.8 Exploring a biological role for the FLCN/DNA-PK interaction: The HSP90α hypothesis. LP-WT = low passage-wild type cells; LP-KD = low passage-FLCN knockdown cells; HP-WT = high passage-wild type cells; HP-KD = high passage knockdown cells. A) Heatmap showing genes under control of AMPK and PGC1α in wild type and FLCN knockdown HK2 cells. B) Bar graph showing log2FC of PPARGC1A gene expression in low passage FLCN knockdown (LP-KD), high passage wild type (HP-WT), and high passage FLCN knockdown (HP-KD). For each, gene expression was compared to low passage wild type (LP-WT). Graph is taken from figure 4.10 C) Western blot analysis of HSP90α DNA-PK dependent phosphorylation in wild type and FLCN knockdown HK2 cells subjected to 5 Gy IR. D) Densitometry of HSP90α DNA-PK dependent phosphorylation. Error bars represent standard error of mean (SEM).

in energy metabolism and is considered the master regulator of mitochondrial biogenesis (Mastropasqua et al. 2018). Collectively, this suggests cells are behaving in accordance with the literature. As a generalised stress responder, HSP90α expression is very low until induced by multiple causes of cellular stress, including DNA damage (Pennisi et al. 2015). To test if FLCN knockdown affected HPS90α phosphorylation, cells were subjected to 5 Gy IR

(figure 5.8C and 5.8D). As expected, in LP-WT control cells, HSP90α phosphorylation (p-HSP90α) increased following IR (figure 5.8C and D). FLCN loss was hypothesised to lessen HSP90α phosphorylation, limiting its ability to regulate mitochondrial biogenesis through AMPK/PGC1α. Following FLCN knockdown in both LP- and HP-KD cells, less p-HSP90α was observed (figure 5.8C and 5.8D), however the findings were inconsistent (figure 5.8D). Therefore, FLCN is unlikely to regulate DNA-PKcs controlled phosphorylation of HSP90α. Furthermore, the initial paper citing DNA-PKcs regulation of p-HSP90α demonstrated, at least in monkey skeletal cells, that phosphorylation of HSP90α increased with age. However, in HK2 cells, it seems to do the opposite, decreasing with age. While it is not exactly clear why HK2 cells respond differently, it is documented that HSP90α has cell-type specific responses (Nollen and Morimoto 2002).

Conclusion

Collectively, the enrichment of DDR proteins in the FLCN protein interactome, the validated interaction between FLCN and DNA-PKcs (both chapter 3), and the possible evidence of deregulated gene expression of damage responders in the transcriptome of FLCN deficient cells (Chapter 4) support the hypothesis that FLCN could be important for maintaining genomic stability. This chapter set out to explore FLCN's role in DDR, and to try and understand the biological implications of FLCN interacting with DNA-PKcs.

The most striking observation of this chapter is the increase in γH2AX (figure 5.4A), a surrogate marker of DSB, upon FLCN knockdown. DNA DSBs are harmful lesions and if left unrepaired can lead to cell death. If imperfectly repaired, they can cause deletions, translocations, and fusions in the DNA. γH2AX elevation is seen in low passage basal cells, suggesting loss of FLCN alone could be enough to promote genomic instability. Interestingly, FLCN knockdown may impart a survival advantage with a higher number of cells tolerating DNA damage (figure 5.6), although this needs further confirmation. An increase in BRCA1 signalling was also observed. It's currently unclear why BRCA1 signalling is up following FLCN loss. However, this could represent a compensatory mechanism, as BCRA1 is largely involved in promoting HR over the error prone NHEJ repair of DSBs (Davis et al. 2014; Isono et al. 2017). An unanticipated observation in the chapter was that FLCN may be chromatin bound. This observation was not affected by IR and is unlikely to represent FLCN having a direct involvement in DNA lesion repair. Nevertheless, it would be interesting to follow up on this. FLCN has no known DNA-binding domains, therefore it's reasonable to assume chromatin localisation of FLCN could be due to protein interactions. For example, FLCN was shown to co-localise with the centrosome maker γ-tubulin, suggesting FLCN may be present at the kinetochore (a complex of proteins associated with the centromere of a chromosome during cell division) and, therefore, could function as a scaffold protein for chromosome alignment and/or correct segregation (Luijten et al. 2013). The biological function of the FLCN/DNA-PK interaction is still unclear. However, cytosolic roles of DNA-PKcs have recently come to light, and novel findings are implicating DNA-PK in metabolism, autophagy, and hypoxia (Bouquet et al. 2011; Park et al. 2017; Chung 2018). Interestingly FLCN is largely implicated in metabolism and autophagy, and FLCN-deficient cells have an increase in HIF

signalling. It is plausible that DNA-PK may function with FLCN in one of these areas. This is discussed further in chapter 7.

Thesis chapter 6: The role of FLCN in cell cycle control

6.1 Introduction

The cell cycle is a tightly regulated and highly organised process that safeguards genetic material and cellular division. Proliferation depends on successful progression through four phases of the cell cycle: G0/G1, S, G2 and M. It is regulated by several cyclin-dependent kinases (CDKs) that act in complex with their cyclin partners. The activity of the CDKs are highly controlled; induced by mitogenic signals and the presence of their cyclins, but inhibited by the activation of cell cycle checkpoints in response to DNA damage (Malumbres and Barbacid 2009).

In most tissues, the majority of cells are in an arrested growth state known as G0 phase. This can be transient (quiescence) or permanent (senescence). Quiescent cells can re-enter the cell cycle once stimulated by mitogenic signals. These signals activate cascades of signalling networks that promote CDK4 and CDK6 (referred to CDK4/6 herein) to drive cell cycle progression from G0 to G1 and eventually into S phase, where DNA replication occurs. CDK4/6 are highly homologous serine/threonine kinases that phosphorylate a largely overlapping set of target proteins (Malumbres and Barbacid 2009; Anders et al. 2011). The activity of CDK4/6 is controlled positively by association with D-type cyclins (cyclins D1–3) and negatively by CDK inhibitors of the INK4 family (Malumbres and Barbacid 2009). Cyclin D–CDK4/6 promote cell cycle progression by phosphorylating the tumour suppressor protein retinoblastoma (Rb). Phosphorylated Rb (p-Rb) then dissociates from the E2F family of transcription factors, enabling E2F to activate the transcription of S phase genes. Among the E2F transcriptional targets is cyclin E, which binds to and activates CDK2. Cyclin E–CDK2 complexes establish a positive feedback loop, further phosphorylating Rb and promotes the transition to S phase. Other E2F gene targets promote DNA replication, chromatin remodelling, chromosome segregation, and spindle assembly. During S phase, cyclin A levels gradually rise. Once DNA has been replicated, cyclin A-CDK1 promotes cell cycle progression into the G2 phase, preventing further replication of DNA and enabling the G2/M checkpoint. Cyclin B-CDK1

complex plays an important role for mitotic entry and during mitosis (Malumbres and Barbacid 2009).

Cell cycle checkpoints are surveillance mechanisms that monitor the order, integrity, and fidelity of the cell cycle. This includes growth to the appropriate cell size, replication of genomic DNA and integrity of the chromosomes, and accurate chromosomal segregation at mitosis (Zhou and Elledge 2000; Foster et al. 2012). Proliferating cells can halt cell cycle progression, allowing repair of any DNA lesions, or, induce apoptosis if the defect is too great. This cell cycle stalling occurs between G1 and S phase before genomic replication (G1/S checkpoint), between S phase and G2 after genomic replication (S phase checkpoint), and between G2 and mitosis (G2/M checkpoint). The G1/S checkpoint is the crucial decision point for a proliferative cell. It is the point at which a cell commits to entering the cell cycle. In a healthy cell, transition into S phase only occurs when internal and external conditions are right for division. These conditions include receiving positive growth signals, sufficient supply of nutrients, energy and macromolecules, and that the integrity of DNA is not compromised. The S phase checkpoint is activated by genotoxic insults and mainly results in reversible inhibition of DNA replication. The G2/M checkpoint prevents cells from initiating mitosis when they have experienced unrepaired DNA damage that was previously inflicted during cell cycle progression through the G1 and S phases (Nyberg et al. 2002). The spindle checkpoint examines whether all the sister chromatids are correctly attached to the spindle microtubules. The separation of the sister chromatids during anaphase is an irreversible step; the cycle will not proceed until all the chromosomes are firmly attached to at least two spindle fibres from opposite poles of the cell. Cells with intact cell cycle checkpoint and DNA damage response (DDR) pathways frequently arrest or die in response to DNA damage, thus reducing the likelihood of cancer progression. Mutations in genes that regulate cell cycle checkpoint, DDR, and/or apoptosis can permit the survival or the continued growth of cells with genomic abnormalities, thereby enhancing the chance of malignant transformation (Zhou and Elledge 2000; Malumbres and Barbacid 2009; Foster et al. 2012).

6.2 Results and discussion

6.2.1 Exploring the p21-cyclin D1-pRb-E2F axis control of G1/S transition in FLCN knockdown cells

Proteomic analysis of the FLCN interactome highlighted a number of potential FLCN interactors that have known roles in the control of the cell cycle (chapter 3, figure 3.5). Interestingly, when these cell cycle associated proteins are plotted based on the phase of the cell cycle in which they are known to function, the G1 and G1/S phase transition are the most common phases associated with the FLCN-interacting proteins (figure 6.1). Complimenting this, transcriptional analysis of the RNA sequencing data showed that the most dysregulated phase of the cell cycle following loss of FLCN is likely the G1-G1/S phase transition (Chapter 4, figure 4.8). Furthermore, CCND1 (cyclin D1) gene expression appears to be highly dysregulated upon FLCN loss (Chapter 4, figure 4.10). Collectively, these data support a novel role for FLCN within the G1-G1/S phase transition of the cell cycle. This chapter will, therefore, explore these new potential links between FLCN function and cell cycle control further.
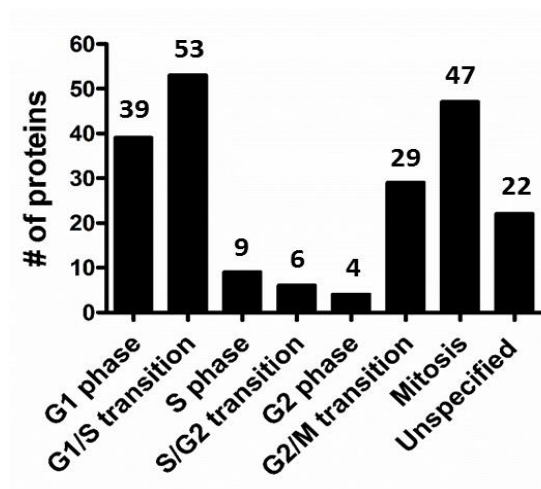
Figure 6.1 Proteomics data suggests a role for FLCN in G1-G1/S cell cycle transition. Graph showing the number of cell cycle functioning proteins found in the FLCN interactome separated by the phase of the cell cycle in which they function.

Given the importance of the G1/S phase of the cell cycle demonstrated in Figure 6.1 and the key role played by CyclinD1-Rb-E2F in control of this checkpoint, this cyclin D1-pRb-E2F signalling axis was explored in HK2 FLCN knockdown cells (figure 6.2). Low and high passage HK2 cells were subjected to 5 Gy IR to induce DNA damage and stall cell cycle

progression. Following DNA damage, cyclin D1 and p-Rb levels are expected to decrease as cells initiate checkpointing to halt their proliferation. This decreased in cyclin D1 and p-Rb was observed for wild type cells. However, the FLCN knockdown cells did not respond in such manner, as observed by retaining high levels of cyclin D1 protein expression and p-Rb hyperphosphorylation, particularly in low passage cells (figure 6.2). Interestingly, cyclin D1 protein levels further increased in aged cells (at high passage). This was a surprising observation as CCND1 mRNA, shown by both RNAseq and qPCR validation, was substantially downregulated in aged FLCN-deficient HK2 cells (chapter 4, figure 4.10). Cyclin D1 protein levels were previously found to be increased upon FLCN loss. Increased cyclin D1 protein expression was observed by immunohistochemistry in FLCN-inactivated mice kidneys, along with Cyclin A1, Cyclin B1, CDK4 (Baba et al. 2008). Transient, FLCN knockdown in HeLa cells show both an increase in CCND1 mRNA and cyclin D1 protein, as seen in LP-KD HK2 cells used in this thesis (figure 6.2). Supporting this, re-introduction of FLCN in NR32 *(FLCN-*deficient renal tumour cell line from the Nihon rat) lowered cyclin D1 protein levels (Kawai et al. 2013). It is worth pointing out that both HeLa and NR32 are derived from already established cancers, where cell cycle regulation may already abnormal. The finding that cyclin D1 is stable in the presence of IR when FLCN is deficient builds on previous published work and suggests that FLCN may be involved in the control of cyclin D1 during DNA damage. It is possible that FLCN loss is associated with an increase in cyclin D1 protein levels and could be a driving force behind RCC development.

The increased levels of cyclin D1 protein in the FLCN-deficient cells may be as a result of reduced nuclear export of cyclin D1, enhanced protein translation or enhanced protein stability. Overexpression of cyclin D1 is observed in a variety of cancers (Hall and Peters 1996; Alt et al. 2000) and suggests that cyclin D1 overexpression provides cells with a distinct growth advantage via enhanced proliferative drive. However, evidence suggests that overexpression of cyclin D1 alone is not sufficient to promote uncontrolled cell growth, but rather its nuclear retention promotes cell transformation. A constitutively nuclear cyclin D1 mutant showed a more transformative phenotype than overexpressed wild type cyclin D1 (Alt et al. 2000). During S phase, the nuclear exclusion of cyclin D1 complexes are critical for the regulation of normal cellular proliferation. GSK-3β phosphorylates Cyclin D1 at threonine 286, which promotes the nuclear-to-cytoplasmic shuttling of cyclin D1 (Resnitzky

et al. 1994; Diehl et al. 1998). Following GSK-3β-mediated phosphorylation, cyclin D1 nuclear export is facilitated by the association of cyclin D1 with the nuclear XPO1 (a FLCN interactor identified by mass spectrometry, see chapter 3). In addition, the FLCN interactome, presented in chapter 3, also highlighted numerous nuclear pore complex proteins as previously discussed (chapter 5, figure 5.7). Interestingly, p21 can also promote the nuclear retention of cyclin D1 and is thought to protect cyclin D1 from cytoplasmic degradation (Alt et al. 2002). Therefore, similar to DNA-PK, the subcellular localisation of cyclin D1 in FLCN knockdown cells was explored under IR. No evidence of dysregulated localisation was found when cells were subjected to 5 Gy IR (n=3, data not shown). However, a follow up study using 10 Gy IR indicates a modest increase in nuclear cyclin D1 level, accompanied by a slight decrease to cytoplasmic levels in FLCN knockdown (n=2, data not shown, performed by Mr Matthew Lines). Due to time limitations, cyclin D1 was only tested in two independent experiments, the second of which does not contain a full complement of analysed controls. Therefore, for the purpose of this thesis, cyclin D1 cytoplasmic-nuclear shuttling is considered to not be affected by FLCN knockdown. Although validation of these findings should be a priority for future work.
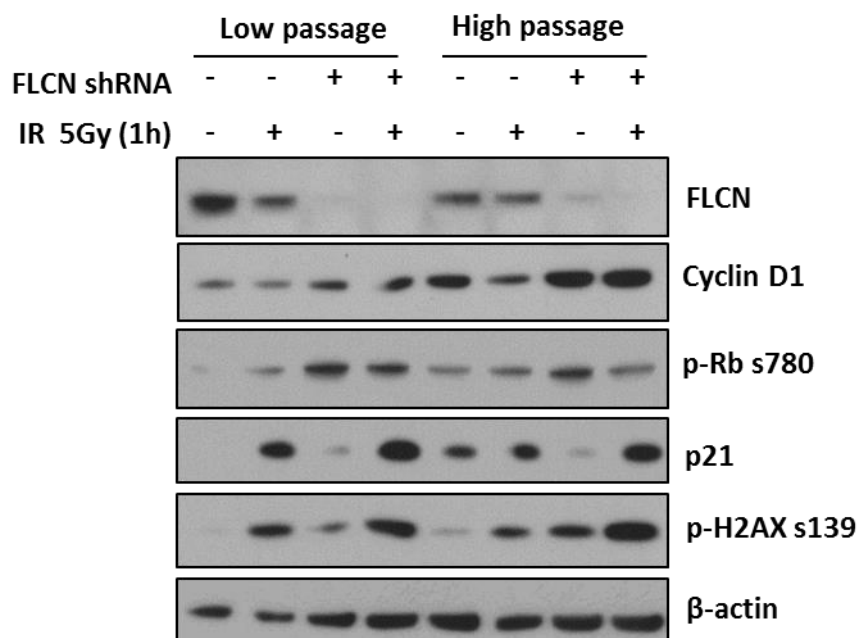
Figure 6.2 Western blot analysis of p21-CylcinD1-retinoblastoma regulation of G1/S transition following IR-induced DNA damage. Wild type and FLCN knockdown cells were subject to 5 Gy IR for 1 h. Cyclin D1 and p21 total protein, and phosphorylated retinoblastoma (p-Rb) and phosphorylated histone marker H2AX (γH2AX) were analysed to see if the G1/S phase transition was activated.

On the other hand, in HeLa cells, it was demonstrated that FLCN negatively regulates cyclin D1 through elements on the CCND1 mRNA. The authors propose that the post-transcriptional regulation of CCND1 expression by FLCN may be associated with microRNA(s) or RNA binding protein(s) that bind to the 3' untranslated region (3'UTR). Interestingly, the mRNA cap-binding protein, eukaryotic initiation factor 4E (eIF4E) was identified in the FLCN interactome. eIF4E is a rate-limiting factor of cap-dependent translation initiation. eIF4E associates and promotes the nuclear export of CCND1 mRNA. The basis of this discriminatory interaction of FLCN with the CCND1 mRNA is an ~100 nucleotide sequence in the 3'UTR of CCND1 mRNA. It is possible that FLCN might be important for the export of CCND1 mRNA but functions as a negative repressor of its translation (Culjkovic et al. 2005).

p21 is a member of the Cip/Kip family of CDK inhibitors and contributes to the regulation of multiple tumour suppressor pathways to promote several anti-proliferative activities (Deng et al. 1995; Abbas and Dutta 2009). p21 inhibits the kinase activity of a broad range of cyclin-CDK complexes, preventing cyclin-dependent progression of the cell cycle. In recent years, the simplistic idea that p21 acts solely as a tumour suppressor has been complicated. For instance, p21 has been shown to exhibit oncogenic activities (Roninson 2002; Gartel 2006); it is often overexpressed in many human cancers, and upregulation of p21 positively correlates with tumour aggressiveness and poor survival (Abbas and Dutta 2009). p21 has been shown to promote the assembly of cyclin D-CDK4/6 complexes, without inhibiting kinase activity (LaBaer et al. 1997; Gartel 2006; Abbas and Dutta 2009). Furthermore, it is thought cyclin D-CDK4/6 sequestration of p21 could facilitate oncogenesis by freeing CDK2 from p21 inhibition (Liu et al. 2007; Abbas and Dutta 2009). In addition to halting cell cycle progression allowing time to repair DNA, p21 can compete for PCNA binding with several PCNA-reliant proteins that are directly involved in DNA synthesis. This interaction is thought to modulate repair processes (Mortusewicz et al. 2005; Walsh and Xu 2006; Abbas and Dutta 2009). For example, p21-PCNA interaction is sufficient for p21 to inhibit mismatch repair (Umar et al. 1996) and PCNA-dependent base excision repair (Tom et al. 2001). The p21-PCNA interaction has also been shown to prevent ubiquitylation (Soria et al. 2006) of PCNA required for translesion DNA synthesis, limiting a cells ability to bypass stalled replication forks.

Nucleotide excision repair (NER) could also be modulated by p21, however the evidence is contradictory. *In vitro*, high p21:PCNA ratios have been shown to block DNA synthesis and NER (Floresrozas et al. 1994; Luo et al. 1995; Podust et al. 1995; Shivji et al. 1998; Soria et al. 2006). *In vivo*, the majority of studies report little or no effect (Chen et al. 1995; Luo et al. 1995; Nakanishi et al. 1995; Lin et al. 1996). One idea is that the p21:PCNA ratio is crucial to inhibit DNA synthesis and NER (Abbas and Dutta 2009). PCNA is an abundant protein, and even the highest physiological levels of p21 might be insufficient to titrate PCNA, as the p21:PCNA ratio likely never exceeds 1:1 *in vivo* (Luo et al. 1995; Gottifredi et al. 2004). The inhibitory effect of the PCNA-interacting domain of p21 on DNA synthesis *in vitro* requires p21:PCNA ratios of 10:1 or higher (Shivji et al. 1998; Gottifredi et al. 2004). Furthermore, the amount of p21 available depends on other events, such as p21 sequestration by cyclin-CDKs and modifications to chromatin accessibility (Abbas and Dutta 2009). It's likely any DNA synthesis or repair modulation activity of p21 derives from its tumour suppressive role, sequestering PCNA to limit DNA synthesis. Perhaps to nullify DNA repair to promote apoptosis. Given the significant role of various DNA repair processes in protecting against cancer, it would be useful to elucidate the extent to which p21 modulates DNA repair processes and whether this activity of p21 contributes to its tumour-suppressing or tumour-promoting activities within FLCN deficient RCC. Collectively, the western blot analysis of the cyclin D1-pRb-E2F axis, suggests that FLCN-deficient cells may be inappropriately transitioning through the G1/S checkpoint; and that the upregulation of pro-proliferative components (cyclin D1 and pRb) occur shortly after FLCN loss (figure 6.2).

6.2.2 Transcriptomic pressure of E2F regulated genes in FLCN knockdown cells

The increase in cyclin D1 and p-Rb levels observed in the FLCN knockdown HK2 cells (figure 6.2) suggest a mechanism of proliferative drive. While the increase in p21 could indicate a compensatory mechanism for increased cyclin D1, or an oncogenic role within the cells. To better understand the proliferative pressure of this cyclin D1-p-Rb axis within the FLCN knockdown cells, the transcription of E2F target genes were explored (figure 6.3).

Transcriptional analysis of 110 E2F-regulated genes revealed 24 were differentially expressed (FDR *P*value<0.05) as a direct consequence of FLCN loss (LP-KD vs LP-WT, Figure 6.3A). This increased upon aging, with 40 genes significantly differentially regulated (HP-KD vs HP-WT, figure 6.3B), suggesting loss of FLCN allows for an acceleration in cell cycle progression. Of interest, pro-growth factors TGFA, PPARGC1A, c-JUN were most upregulated in low passage FLCN knockdown cells. TGFA encodes transforming growth factor α, and is a growth factor that activates cell proliferation. It has been shown to directly act as a specific growth-stimulatory factor for primary renal proximal tubule epithelial cells which are thought to give rise to RCC (Gomella et al. 1989; Humes et al. 1991; De Paulsen et al. 2001). It is commonly upregulated in many cancers, including RCC (Derynck et al. 1987; Mydlo et al. 1989; Petrides et al. 1990; Walker et al. 1991). PPARGC1A, encoding PGC1-α, is the master regulator of mitochondrial biogenesis. It plays an essential role in the co-ordination of an array of genes involved in glucose and fatty acid metabolism, as well as metabolic reprogramming in response to nutrient availability (Mastropasqua et al. 2018). PGC1-α is well characterised to be up regulated upon FLCN loss (Klomp et al. 2010; Hasumi et al. 2012; Hasumi et al. 2014; Yan et al. 2014). Therefore, this result is supported by the literature on FLCN loss and adds to the reliability of the HK2 cells used and how they model this disease. Furthermore, the E2F target gene, PGC1-α, is commonly dysregulated in RCC (Mastropasqua et al. 2018) and has previously been shown to be upregulated in FLCN-null kidney cell lines (Yan et al. 2014). Additionally, in the aged cells, PGC1-α is consistently upregulated upon FLCN loss. This supports the idea of metabolic reprogramming commonly seen in RCC and FLCN-deficient *in vitro* and *in vivo* models (Klomp et al. 2010; Wada et al. 2016; Yan et al. 2016a). An interesting observation when comparing changes in low passage cells to high passage cells is that several key cell cycle promotors (CCND1, CCND3, CCNA1, CCNE1, and E2F1) are upregulated in low passage cells (although only slightly) but become downregulated upon aging. This suggest the old cells still retain the ability to control cell growth, and perhaps represents the cells attempting to compensate for increased pressure to grow in the presents of DNA damage (Chapter 5, figure 5.4).
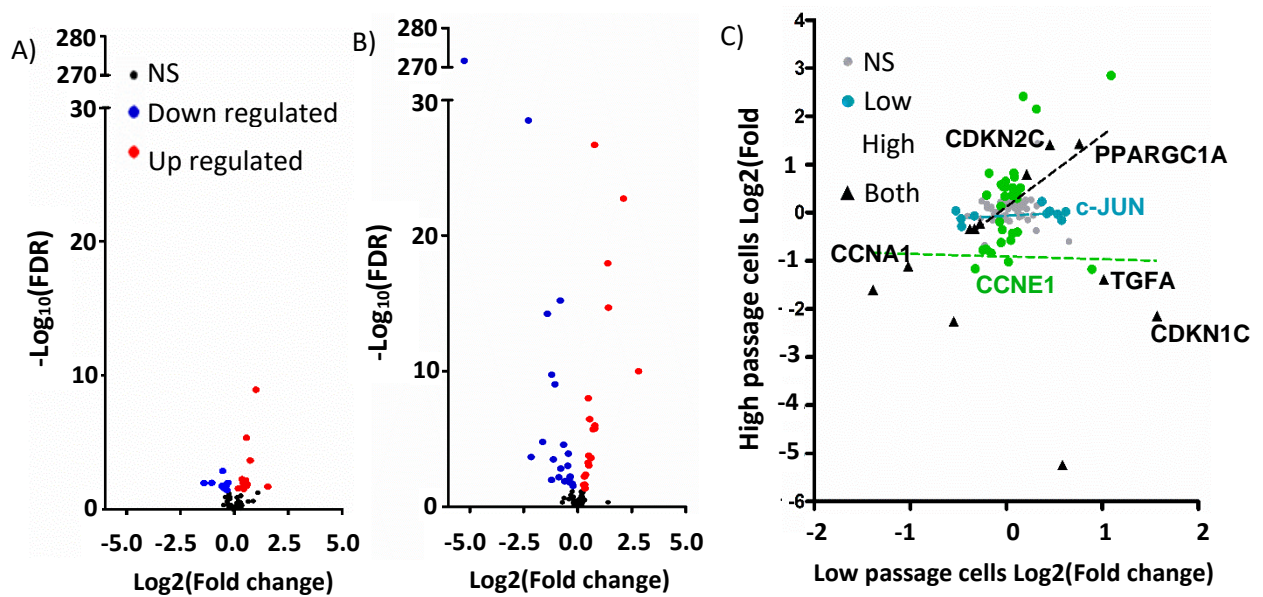
Figure 6.3 Analysis of E2F regulated genes. 110 E2F regulated genes were analysed comparing the effect of FLCN knockdown in low and high passage cells. A) Volcano plot showing differentially expressed E2F genes as a direct response to loss FLCN (LP-WT vs LP-KD). B) Volcano plot showing differentially expressed E2F genes in FLCN-deficient aged cells (HP-WT vs HP-KD). For both volcano plots black dots represent genes in which change in expression was not significant (NS), blue dots are down regulated genes (FDR Pvalue<0.05), and red dots are up regulated genes (FDR Pvalue<0.05). C) Differentially expressed E2F genes, directly comparing changes that occur upon aging in the absence of FLCN. Grey dots represent genes in which change in expression was NS, light blue dots represent significant changes (FDR Pvalue<0.05) in expression between low passage cells (LP-WT vs LP-KD) only, green dots represent significant changes (FDR Pvalue<0.05) in expression between high passage cells (HP-WT vs HP-KD) only; Black triangles represent significant change (FDR Pvalue<0.05) in expression in both low and high passage cells.

Another E2F-target gene, c-Jun, is a proto-oncogene and functions as a key regulatory molecule for cell growth control. c-Jun expression is associated with the recruitment of cells from G0 to G1 (Oya et al. 2005). Altered c-Jun expression is thought to play a critical role in early carcinogenesis lung and oral squamous cancer, and RCC (Szabo et al. 1996; De Sousa et al. 2002). Interestingly, healthy proximal kidney tubules have little to no c-Jun expression, but it has been shown to be ectopically expressed in clear cell and papillary RCC originating from the proximal kidney tubules. c-Jun activation is commonly observed at an early stage of RCC; similarly, c-Jun expression increases were noted in LP-KD

cells (figure 6.3C). The negative regulators of cell proliferation, CDKN1C and CDKN2C, were also some of the most upregulated E2F controlled genes. CDKN1C strongly inhibits several cyclin-CDK complexes including cyclin E-CDK2, cyclin D2-CDK4, cyclin A-CDK2, and, to lesser extent, the mitotic cyclin B-CDK2 complex, to promote a non-proliferative state in cells. CDKN2C inhibits both CDK4 and CDK6; with a preference for the latter. Furthermore, the positive regulators of cell proliferation, CCNE2 (cyclin E2) and CCNA1 (cyclin A1), were down regulated. Cyclin E expression increases just before S phase initiation and represent cells committing to proliferation. Cyclin A expression increases in early S phase and is required for G2/M progression.

In the high passage cells, on the other hand, the most aberrant observation is the upregulation of a selection of homeobox (HOX) genes (HOXA4, HOXA5, HOXA7, and HOXB9). HOX genes comprise a super-family of evolutionarily conserved genes that play essential roles in controlling body plan specification and cell fate determination (Haria and Naora 2013). Overexpression or down-regulated expression of many homeobox genes have been observed in a wide variety of malignancies and have cell specific roles (Abate-Shen 2002; Samuel and Naora 2005; Shah and Sukumar 2010). For example, HOXA4 is reportedly overexpressed in colorectal cancer and epithelial ovarian cancer (Yamashita et al. 2006; Bhatlekar et al. 2014). HOXA4 expression was down-regulated in lung cancer tissues when compared with non-cancerous tissues. Furthermore, overexpression of HOXA4 in lung cancer cell lines decreased the protein expression levels of β-catenin, cyclin D1, and c-Myc, supressing proliferation, migration, and invasion. The expression patterns and functional properties of HOX genes in solid tumours fall into two broad categories. HOX genes that are expressed in embryonic tissues and are 'reactivated' in tumours tend to have oncogenic properties. HOX genes whose expression is normally maintained in differentiated adult tissues but is down-regulated in tumours often exhibit tumour suppressive properties. Less commonly, homeobox genes can be expressed in tumours derived from a lineage in which these genes are not normally expressed during development; these often have tumour-promoting properties. Despite numerous reports of their aberrant expression, the mechanisms of many homeobox genes in tumours are poorly understood.

The E2F transcription factor family consist of seven members (E2F1-7). E2F1-3 function as transcriptional activators; acting as the classical E2F transcription factor enabling expression of S phase genes. E2F4 and E2F5 are repressors and are exported from the nucleus during early G1 (Di Stefano et al. 2003; Bracken et al. 2004). E2F1-5 can bind to and be inhibited by Rb, while E2F6 and E2F7 are thought to act as a transcriptional repressors. E2F7 is induced during early S phase (Stott et al. 1998; Di Stefano et al. 2003), and is thought to repress only a subset of E2F target genes, such as CCNE1 and CDC6. It does not repress later-transcribed genes such as CCNA2 and CDC2 (Di Stefano et al. 2003). It is possible that E2F6 and E2F7 transcription factors function within feedback loops that allow orderly and finely tuned progression through the cell cycle. Very little is known about the function of E2F6. In the absence of ChIP data, it is unclear what E2F responsive genes E2F6 regulates,

or whether this occurs throughout the cell cycle or is restricted to a specific phase (Trimarchi and Lees 2002). Transcriptome analysis of FLCN knockdown cells reveals a generalised dysregulation (figure 6.3C and 6.3D), there isn't a trend in positive and negative regulators of G1/S phase transitioning genes being collectively up- or down-regulated in response to FLCN loss (figure 6.3C and 6.3D; chapter 4, figure 4.9). E2F luciferase assay may be able to provide a more direct idea of the proliferative drive FLCN-deficient cells are under as a result of FLCN knockdown. Unfortunately, time restrictions prevented the use of E2F luciferase assay.

Collectively, E2F regulated gene expression upon FLCN loss is dysregulated. E2F regulation has a multitude of positive and negative feedback loops in addition proliferation driving genes. This allows highly controlled and finely tuned progression through the cell cycle. Examining E2F regulated genes as shown in figure 6.3, it can be concluded that FLCN loss leads to perturbed regulation, however, no obvious promotion or inhibition of G1/S transition can be concluded. Collectively, the results indicate that G1/S cell cycle checkpoint control through E2F is likely dysregulated as a direct consequence of FLCN loss, but further agitated during the ageing process in the continual absence of FLCN.

6.2.3 Exploring cell cycle profile of FLCN knockdown cells

Evidence so far suggests FLCN knockdown cells should be transitioning through the cell cycle irrespective of the presence of DNA damage, inappropriately skipping through the G1/S checkpoint of the cell cycle. DRAQ5 was used to quantify DNA content in order to profile the cell cycling properties of FLCN knockdown cells. DRAQ5 is a fluorescent dye that stoichiometrically stains DNA. As such, fluorescent intensity of a cell can be used to estimate the number of cells in G0/G1, S, and G2. As a cell progresses through the cell cycle, the quantity of DNA increases from 2N (G0/G1 phase) to 4N (G2 phase). Cells with DNA below 2N are typically in apoptosis and are considered debris. While transcriptomic data suggested high passage cells may have a more dysregulated cell cycle, low passage cells were used with the aim of better understanding FLCN loss in establishing renal neoplasms. Low passage FLCN expressing HK2 cells were used to establish IR dose and timings before the effect of FLCN loss was explored (figure 6.4).
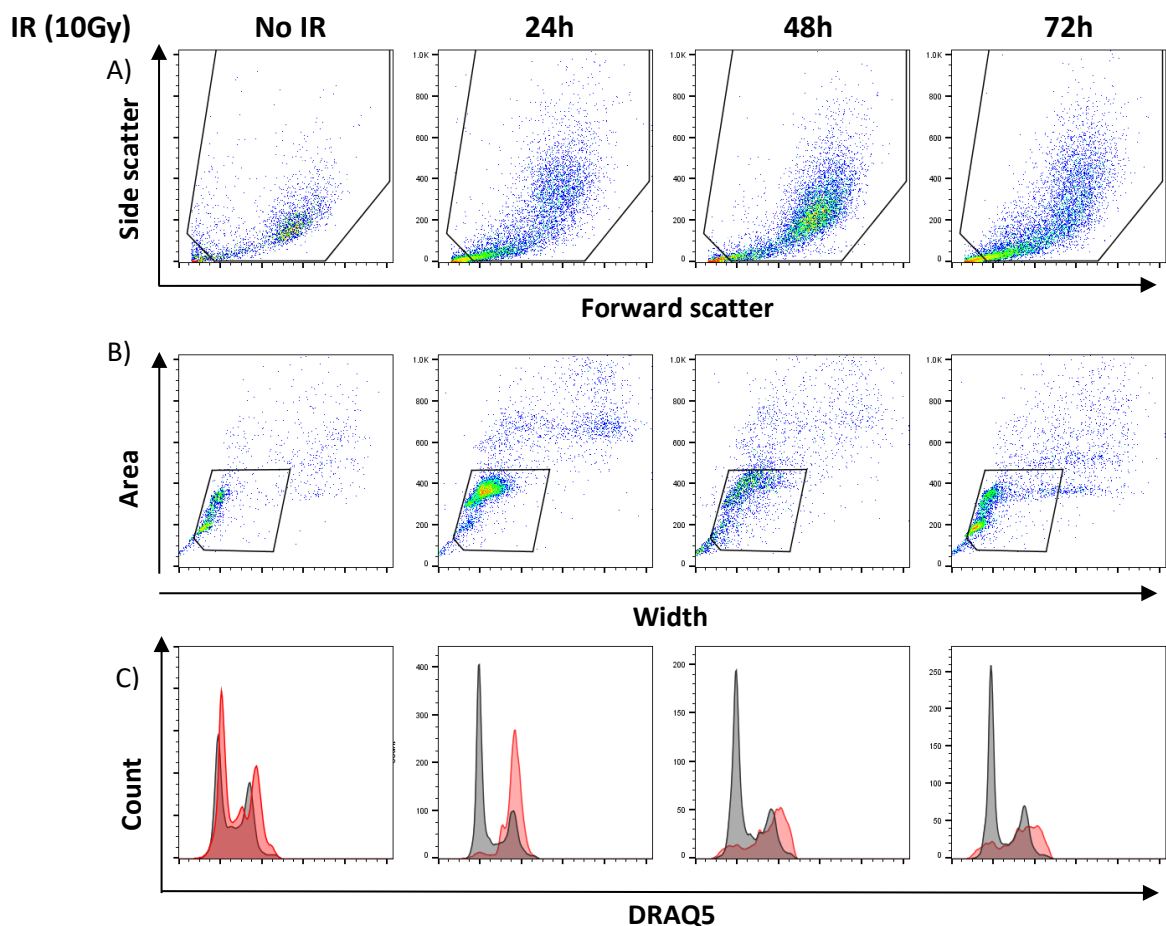
Figure 6.4. Analysis of HK2 cell line cell cycle profile. HK2 LP-WT cells were used to optimise protocol treatments. DRAQ5 was used to quantify DNA content. A-C) Establishing time points to analysis cell cycle profile. Cells were treated with 10Gy IR and left for up to 72 h to establish a maximum treatment time. A) Isolating cells from debris. B) Isolating single cells to removed polyploidy or clumps of cells. C) Comparing the cell cycle profile of irradiated cells (red) versus their time match non-irradiated control (grey). Plots and graph are representative of 2 independent experiments.

For the initial analysis of cells, forward scatter versus side scatter (FSC vs SSC) gating was used to identify cells of interest away from cellular debris. (figure 6.4A). In order to ensure only single cells are being analysed, cells were gated to removed doublets, or cell clumps, as well as polyploid cells (figure 6.4B). Cell cycle profiles were plotted as histograms of fluorescent intensity vs cell count (i.e., DRAQ5 incorporation vs the number of cells at a given intensity; figure 6.4C). In the first instance cells were subjected to 10 Gy IR and left for up to 72 h to establish a maximum time after IR to investigate (figure 6.4C). Although the experiment was only carried out once, it indicates the majority of cells will be in G2 by 24 h. Cells left longer will produce an increase in debris as cells choose to undergo apoptosis, which could impinge or complicate the interpretation of subsequent results. Next, an IR dose-course was performed to better establish a suitable radiation exposure.

The aim was to lightly damage cells, enough to encourage cellular stalling but not enough to induce apoptosis, in order to study the effect FLCN knockdown on cell cycle checkpointing. In the first instance, LP-WT HK2 cells were subjected to 1-10 Gy of IR and DNA content was examined after 24hrs. This dose test was only carried out once and initial analysis supported a 2 Gy IR dose would be an appropriate for experimental requirements. However, due to issues discussed later, 2 Gy IR was later found to not be a suitable dose.

Nevertheless, DRAQ5 staining was used to ascertain cell cycle profiles following 2 Gy IR in LP-WT and LP-KD cells. Single cells were identified, and cell cycle profiles were plotted as described above (figure 6.5A and 6.5B). FlowJo V10 software was used to estimate G0/G1, S phase, and G2/M populations using DRAQ5 signal, to generate a cell profile model. Technically, cell ploidy is visualised rather than a cell's true residence in interphase or mitosis. Therefore, it is more accurate to refer to the G0/G1 and G2/M populations as 2N and 4N respectively. The model assumes Gaussian distributions of the 2N and 4N populations, then a subtractive function is used to identify the S-phase population (figure 6.5C).

Non-irradiated LP-KD cells displayed fewer 2N cells (G0/G1) and more 4N (G2) cells than the wild type controls (figure 6.5D and 6.5E). DNA damage can stall cells at the G1/S and G2/M checkpoints. To see if FLCN knockdown cells have a more proliferative phenotype despite the presence of damage, cells were subjected to 2Gy IR and left for up to 24 h. Generally, LP-KD cells had fewer cells in G1 and more cells in G2 (figure 6.5F and 6.5G). This supports the idea the FLCN-deficient cells slip through G1/S phase. Interestingly, it's been noted that FLCN reintroduction in zebra fish embryos caused a significant drop in S-M phase cells with a corresponding increase in G1 cells (Emma J. Kenyon et al 2016), agreeing with results observed in HK2 cells in figure 6.5. Nevertheless, there are consistently fewer cells at all time points (figure 6.5F and 6.5G). The results may just be from lower cell numbers and not be reflective of the biology. Therefore, the mitosis inhibitor colcemid (figure 6.7) and S phase marks, BrdU and EdU (figures 6.8 and 6.9) were used in an attempt validate findings.
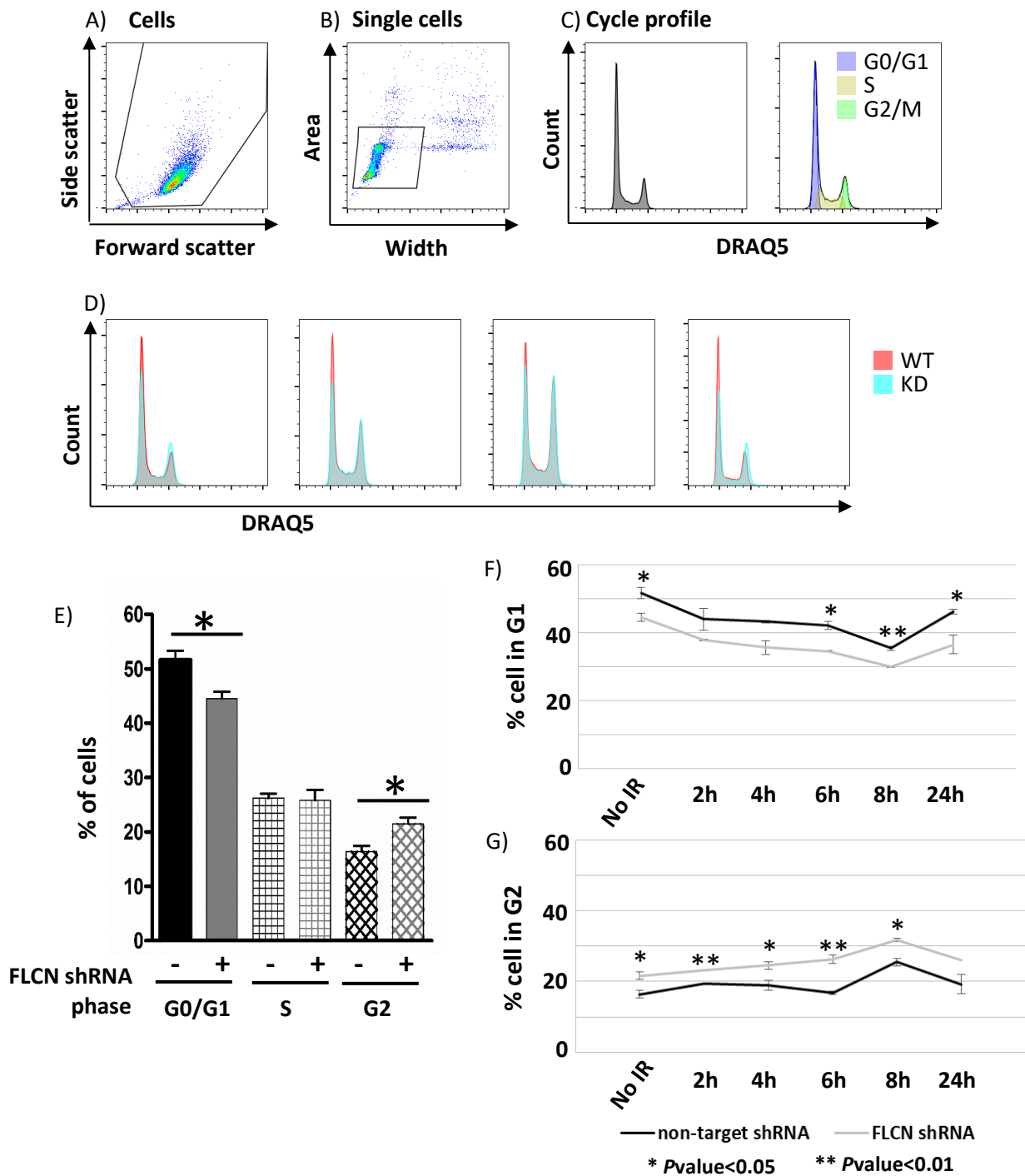
Figure 6.5 Analysis the cell cycle profile in FLCN-deficient cells. Low passage wild type (LP-WT) and knockdown (LP-KD) cells were subjected to 2Gy IR. A) Isolating cells from debris. B) Isolating single cells to removed polyploidy or clumps of cells. C) Histogram of DRAQ5 signal to produce cell cycle profile. D) Cell cycle profile comparison of wild type and FLCN knockdown. E) Percentage of cells at each stage of the cell cycle, as determined by DRAQ5 staining, under basal conditions. F) Percentage of cells in G0/G1 phase following 2 Gy IR G) Percentage of cells in G2/M phase following 2 Gy IR. Percentage of cells in each stage of the cell cycle was determined using FlowJo V10 cell cycle analysis function. Student's T Test was used to determine statistical significance between wild type and knockdown cell lines, and was performed in Microsoft Excel 2013. Plots are representative of 3 independent experiments.

137

Colcemid is a microtubule-depolymerising compound. Colcemid prevents cells from undergoing mitosis and, as such, stalls cells in G2 phase. Using a mitotic inhibitor would prevent cells re-entering the cell cycle, where these cells could otherwise confound results. In the LP-WT control cells, after the addition of 60ng/mL colcemid, cells accumulated overtime (figure 6.6A) with most of the cells in a 4N state (64%); a surrogate indication of G2 (figure 6.6A and 6.6B), demonstrating the conditions of colcemid treatment are sufficient to stall cells in G2. It was expected that LP-KD cells would accumulate in G2 faster than WT cells, however, no difference could be observed between the cell lines (data not shown). FLCN has previously been thought of as a positive regulator of the G2/M phase transition (Lavoittle 2013) and required for mitosis (Kawai et al. 2013). Following IR, the cell lines still had a continuous and equal percentage difference in cells throughout the duration of the experiment, similar to what was previously observed under IR (figure 6.5G).
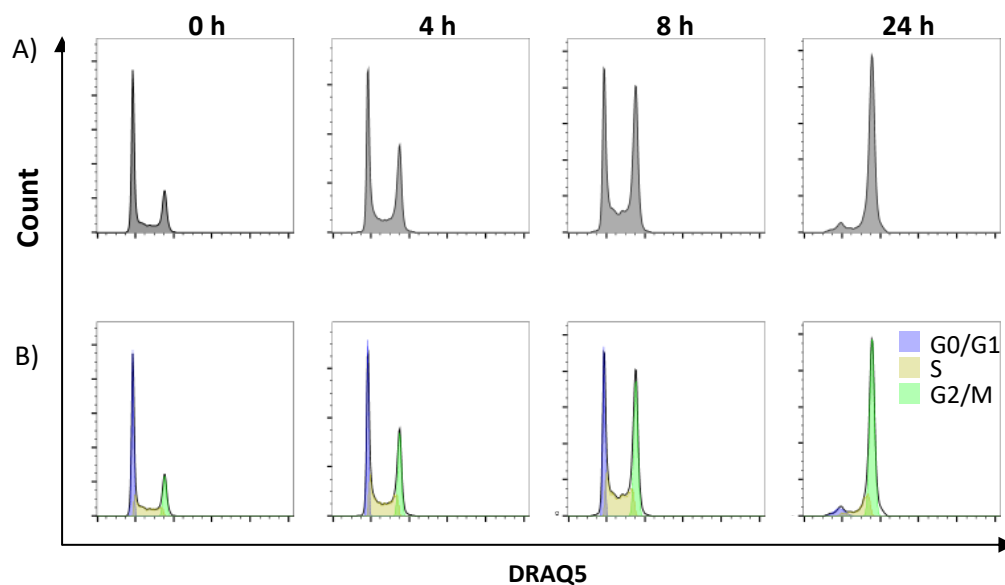
Figure 6.6. Analysis the cell cycle profile in FLCN-deficient cells after treatment with G2/M phase blocker, colcemid. HK2 low passage wild type (LP-WT) and knockdown (LP-KD) cells were treated with colcemid (60 ng/μL) and analysed up to 24 h after treatment. A) Histogram of DRAQ5 signal in LP-WT cells to produce cell cycle profile. B) Percentage of LP-WT cells in each stage of the cell cycle was determined using FlowJo V10 cell cycle analysis function. Plots are representative of 3 independent experiments.

Next, in order to validate the G1/S slippage in FLCN KD cells, genomic DNA was labelled by exposing cells to the thymidine analogue, 5'-bromo-2'-deoxyuridine (BrdU). Interestingly, BrdU incorporation has been evaluated in FLCN-inactivated mouse kidney cells and was measured by immunostaining (Baba et al. 2008). BrdU incorporation was statistically significantly greater in kidney cells from BHDf/d/KSP-Cre mice than BHDf/+/KSP-Cre mice. The study did not quantify DNA content and so the information cannot be used to establish G1-G1/S slippage specifically, but that FLCN-deficient cells hyper-proliferate.

During DNA replication (in S phase), BrdU is incorporated into newly synthesised DNA. Incorporated BrdU is stained with anti-BrdU and fluorescent antibodies, in addition to the DNA dye (i.e., DRAQ5) This allows for a more accurate separation of G0/G1, S , and G2/M phase cells (Rothaeusler and Baumgarth 2007; Kim and Sederstrom 2015). For analysis, DNA was quantified as described above; cells were isolated from cellular debris and polyploidy (figure 6.7A and 6.7B) and plotted to show cell cycle profile (figure 6.7C). Once single cells were identified, and DNA content quantified, BrdU incorporation was analysed. Firstly, background fluorescence was established using an antibody free control (figure 6.7D; black). Then the sample with the largest expected signal (in this case cells exposed to BrdU for 24 h) was used to ensure BrdU incorporation could be detected (figure 6.7D; purple). To confirm the protocol was set up correctly, a secondary antibody only sample was used (figure 6.8E). When compared to the 24 h sample, the secondary antibody only control almost fully overlapped. This suggests wash steps were insufficient, and no conclusion of BrdU incorporation can be drawn. Furthermore, when analysing DRAQ5 staining following BrdU incorporation over time, cells with no exposure to BrdU display a normal cell cycle profile whereas those with BrdU did not (figure 6.7F).

A disadvantage of BrdU incorporation method is that both membrane permeabilisation and harsh DNA denaturation processes are required for antibody penetration to the incorporated BrdU. As an alternative to BrdU, 5-ethynyl-2'-deoxyuridine (EdU) has been developed to overcome these limitations (Salic and Mitchison 2008; Cavanagh et al. 2011; Kim and Sederstrom 2015). After EdU treatment during cell proliferation, incorporation of EdU can be subsequently detected by a fluorescent azide molecule through a copper (I) catalysed reaction which results in a stable triazole ring formation between EdU and fluorescent dye (so called "Click-it" reaction). Since the small-sized fluorescent dye readily penetrates the cell and it easily reacts with EdU even in intact DNA double strand, EdU method is more gentle, highly sensitive, and much faster than a classical BrdU incorporation assay (Salic and Mitchison 2008; Cavanagh et al. 2011; Kim and Sederstrom 2015).
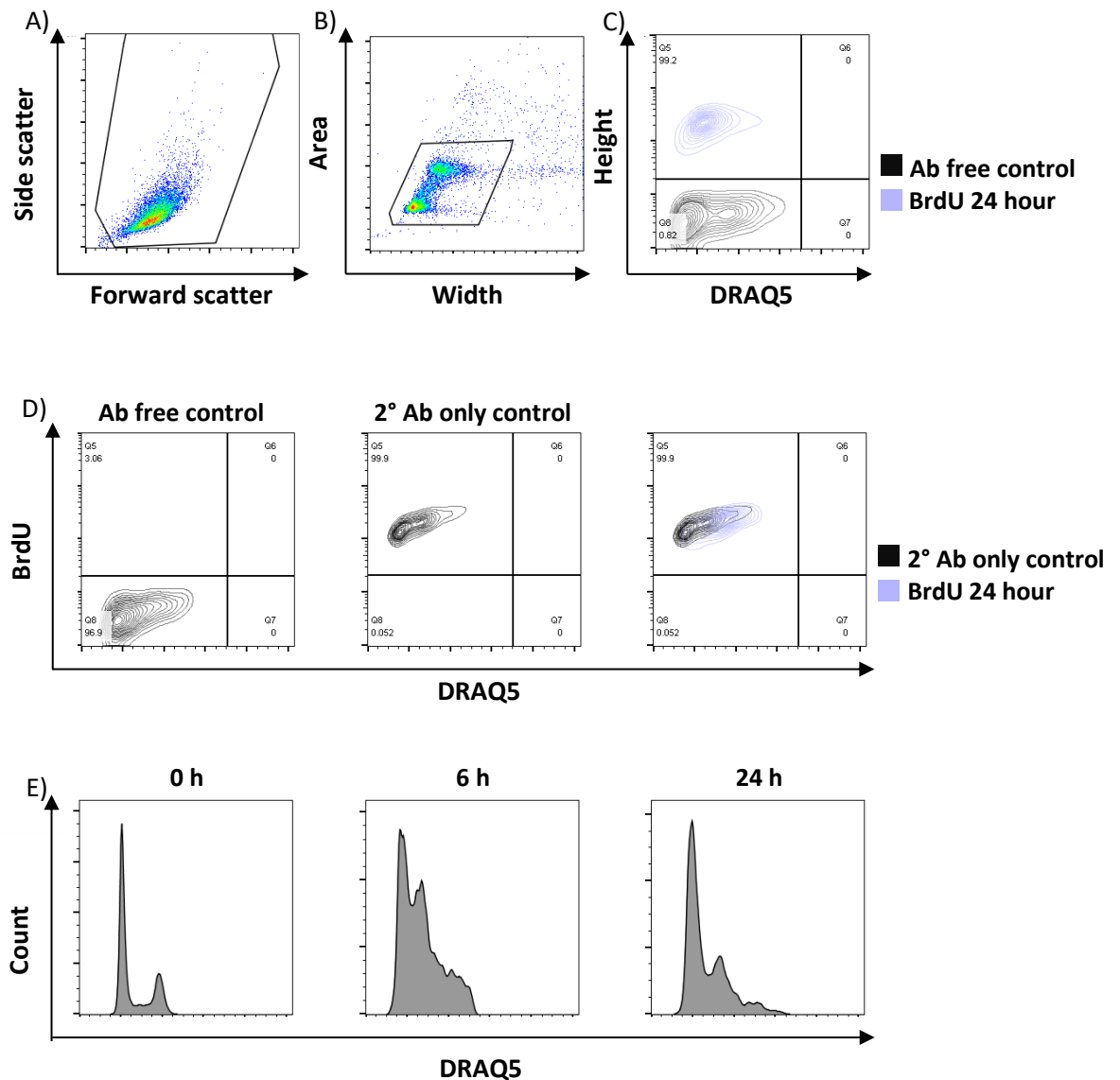
Figure 6.7 Testing BrdU incorporation as a method of quantifying S phase cells. Low passage wild type (LP-WT) cells were treated with 8µM BrdU and left for up to 24 h A) Isolated cells from debris B) Isolating single cells to removed polyploidy or clumps of cells. C) Contour plot showing Brdu incorporation into cells after 24 h (purple), no anti-Brdu antibody (Ab) was used to establish a baseline to remove background florescence from the analysis (black). D) Contour plot showing antibody controls, secondary (2°) antibody only sample (black) shows almost total overlap with 24 h Brdu sample (purple) suggesting insufficient wash steps. E) Histogram of DRAQ5 signal to produce cell cycle profile. Plots are representative of 2 independent experiments.

To test if EdU would be a more suitable S phase maker, low passage wild type cells were treated with 8 µM of EdU and left for either 8 or 24 h. In the absence of EdU, normal cell cycle profiles can be observed with DRAQ5 staining (figure 6.8A). However, similar to BrdU, the presence of EdU lead to abnormal cell cycle profile plots (figure 6.8B). To verify the cells were able to respond correctly, colcemid was used to stall cells at G2 (figure 6.8C). DRAQ5™ is a live-cell permeant dsDNA-specific probe that efficiently and stably labels

nucleated cells. DRAQ5™ binds strongly to the A-T sites at the minor grove of DNA. One explanation could be that as BrdU and EdU are both thiamine analogues, therefore using a DNA binding dye that preference A-T sites has limited use. Furthermore, BrdU influences the fluorescence of many DNA dyes; it incompletely quenches DAPI, Hoechst, and acridine orange dyes; where, similar to DRAQ5, both DAPI and Hoechst are AT-specific (Kubbies and Rabinovitch 1983). BrdU has also been reported to enhance the fluorescence of mithramycin and 7-AAD (GC-specific DNA binding dyes) (Ormerod and Kubbies 1992). Specific information on EdU quenching or enhancing DRAQ5 was not found. Equally information on the effects of EdU with DRAQ5 could not be found. Many publications use propidium iodine (PI) to quantify DNA content alongside the use of thiamine analogues, where PI universally intercalates between base pairs (Sakimoto et al. 2006; Liu et al. 2013a). Based on data presented in figure 6.7 and 6.8, DRAQ5 is unlikely to be compatible with thiamine analogues use.
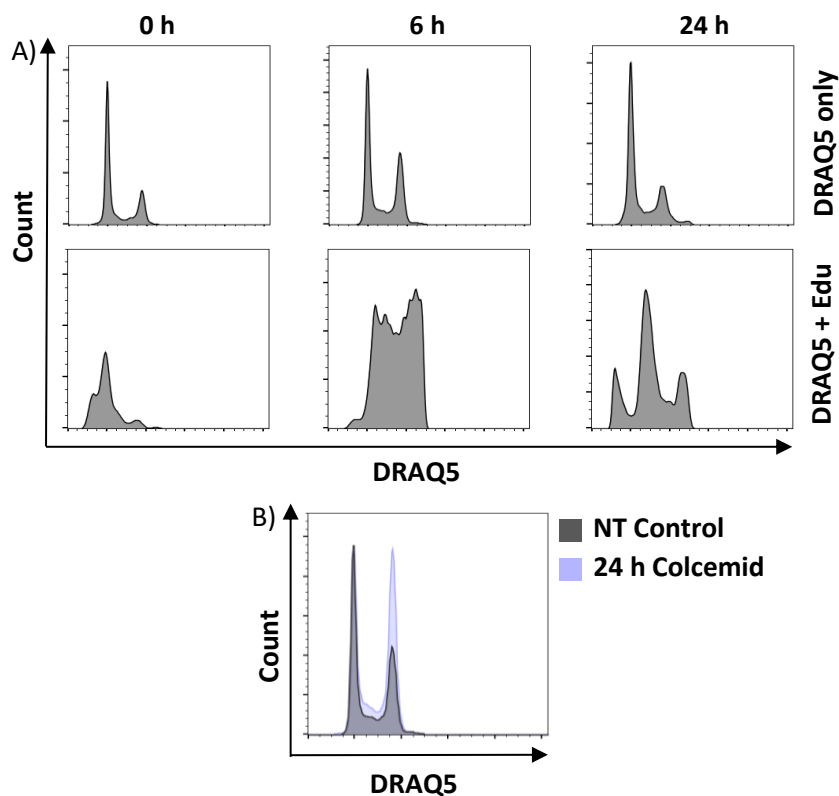
Figure 6.8 Understanding the use of DRAQ5 with thiamine marker. A) Histogram of DRAQ5 signal in Low passage wild type (LP-WT) cells to produce cell cycle profile. Top row, cells treated with 20μM of DRAQ5 for up to 24 h; bottom row, cells treated with 20μM of DRAQ5 and 8μM Edu for up to 24 h. B) LP-WT cells were treated with 60ng/μL colcemid to check cells can respond appropriately. Grey, no treatment (NT) control; purple, cells treated with 60ng/μL colcemid for 24 h. Plots are representative of 3 independent experiments.

EdU incorporation without a DNA marker was explored in order to determine if a difference between the cell lines could be detected, and as such gauge its usefulness before optimising a new DNA binding dye (figure 6.9). Cells were isolated from debris, and a no antibody control was used to establish background florescence (figure 6.10A). EdU incorporation was assessed at 6 and 24 h (figure 6.9B). Over the course of 24 h EdU incorporation increased, with 65.1% (± 4.086 %) of cells staining positive for EdU at the end of 24 h (figure 6.9C). This shows that it is possible to track DNA synthesis within the HK2 cells through incorporation of the thiamine analogue EdU. This was repeated in LP-KD cells after 2 Gy of IR, but no difference was observed between the cells lines (n=2, data not shown). However, when compared to non-irradiated controls, no evidence of cells stalling could be seen. This was further explored in the LP-WT control cell line (figure 6.9C). With increasing dose of IR, it is expected to see a smaller EdU signal at any given time point. This is because upon more DNA damage cells will stall DNA synthesis, although some incorporation of EdU will occur as part of DNA repair, this should be much lower than non-irradiated controls. IR dose was increased incrementally to 50Gy, and EdU incorporation was detected up to 24 h after IR (figure 6.9C). Little difference can be observed, with minor decrease in percentage of cells with EdU incorporation at each time point. R^2 of each of the timepoint trendlines suggest the data doesn't fit the trendline very well (R^2 = 0.37 for 6 hours, and R^2 = 0.58).

Two-way ANOVA was performed to look at the effect of EdU incorporation over time and with increasing IR dose (table 6.1). The effect of IR dose was not significant, accounting for only 1% of variation observed in the data (p=0.6584). Time, however, contributed to 61.83% of variation within the data (p<0.0001). This make sense, more EdU can be incorporated following longer time periods. Within this data, IR did not affect the incorporation of EdU, which implies that IR-induced DNA damage does not cause cell cycle arrest in these HK2 cells. It's worth pointing out that doses 15-50 Gy had only 1 replicate, which limits confidence in the statistical analysis. It is possible that more repeats may support a contribution of the high IR dose to affect EdU incorporation, as suggested by the downward slope on the trendline. This analysis was not expanded upon to due time and resource constraints. Further troubleshooting could involve adapting the times of treatment in which cells are labelled with EdU. One limitation of the current protocol is that EdU is present throughout the whole duration of the experiment and, as such, could be incorporated as part of the DNA repair response. As the DNA content of the cells was not quantified in these experiments by flow, cells could indeed still be stalling (not replicating their DNA). Therefore, it cannot be ruled out that the increase in EdU signal observed in the LP-WT cells aren't simply an artefact of cells repairing their DNA. Instead of adding EdU for the duration of the experiment, it might be better to add EdU for a limited amount of time (e.g. 1 h) prior to DNA damage induction by IR. This would allow for EdU incorporation into the genome but prevent continued increase of signal over time. This shorter 1 h pulse with EdU was briefly attempted n=1 (data not shown) but leads to a similar result to figure 6.9C.

It seems that thiamine analogue inclusion over time alone has limited usefulness, as to understand the cell cycle response to IR in these HK2 cell lines, thiamine analogue signal needs to be co-ordinated with DNA content. To continue this avenue, use of an alternative DNA marker (such as PI) would be required.

Under normal conditions, the fraction of proliferating tubular epithelial cells in the kidney is below 1% (Moonen et al. 2018). This is to cover the casual loss of tubular epithelial cells due to physiological cell death or spontaneous release from the basal membrane into the urine (Moonen et al. 2018). The remaining 99% cells are quiescent, resting in the G0 phase. For the proximal tubular epithelium, however, this is only partly true. Proximal tubule cells have particular high metabolic activity/demand of these cells; there is physiological hypoxia in the medullary region, and these cells experience a high exposure to intra-tubular toxins (Bonventre and Yang 2011). Studies show that stressing the kidney leads to an increase in cellular proliferation, yet, this stress also induces cell cycle inhibitors. It is thought that up to 40% of cells express cyclin D1, suggesting cells are in the mid-to-late G1 phase (Witzgall et al. 1994; Vogetseder et al. 2008; Moonen et al. 2018). Additionally, nearly all these cells were immunoreactive for p27, a cyclin dependent kinase inhibitor that blocks cell cycle progression and keeps cells in the G1 phase (Iwakura et al. 2014). Furthermore, studies looking into acute kidney injury suggest there is a rapid induction of p21, which is thought to contribute to arresting proximal tubule cells in the G1 phase (Price et al. 2009). It is assumed that proximal tubule cells have a physiological G1 arrest that, after toxic insult, ensures cells can initiate proliferation extremely rapidly. Proximal tubule cells in the kidney have a remarkably strong inherent ability to regenerate after injury (Moonen et al. 2018). Replacement of lost proximal tubule cells does not involve specialised progenitors, but the proliferation of proximal tubule cells themselves is the key of renal repair (Humphreys et al. 2011). Perhaps FLCN is important for the priming of these cells to respond to damage faster. In the absence of FLCN the intricate balance between pro- and anti-proliferative signals is tipped in favour of pro-proliferation at the G1/S boundary; reducing available time for DNA repair. The majority of cells proliferate out of damage, however, overtime in the absence of FLCN, the propagation of genetic defects leads to transformation of proximal tubule cells. Only a handful of cell cycle regulators (e.g., p53, p21) have been thoroughly studied during renal repair (Moonen et al. 2018). How and why proximal tubule cells decide to arrest their cell cycle and how this arrest can be overcome remains unanswered and are challenging questions to address.
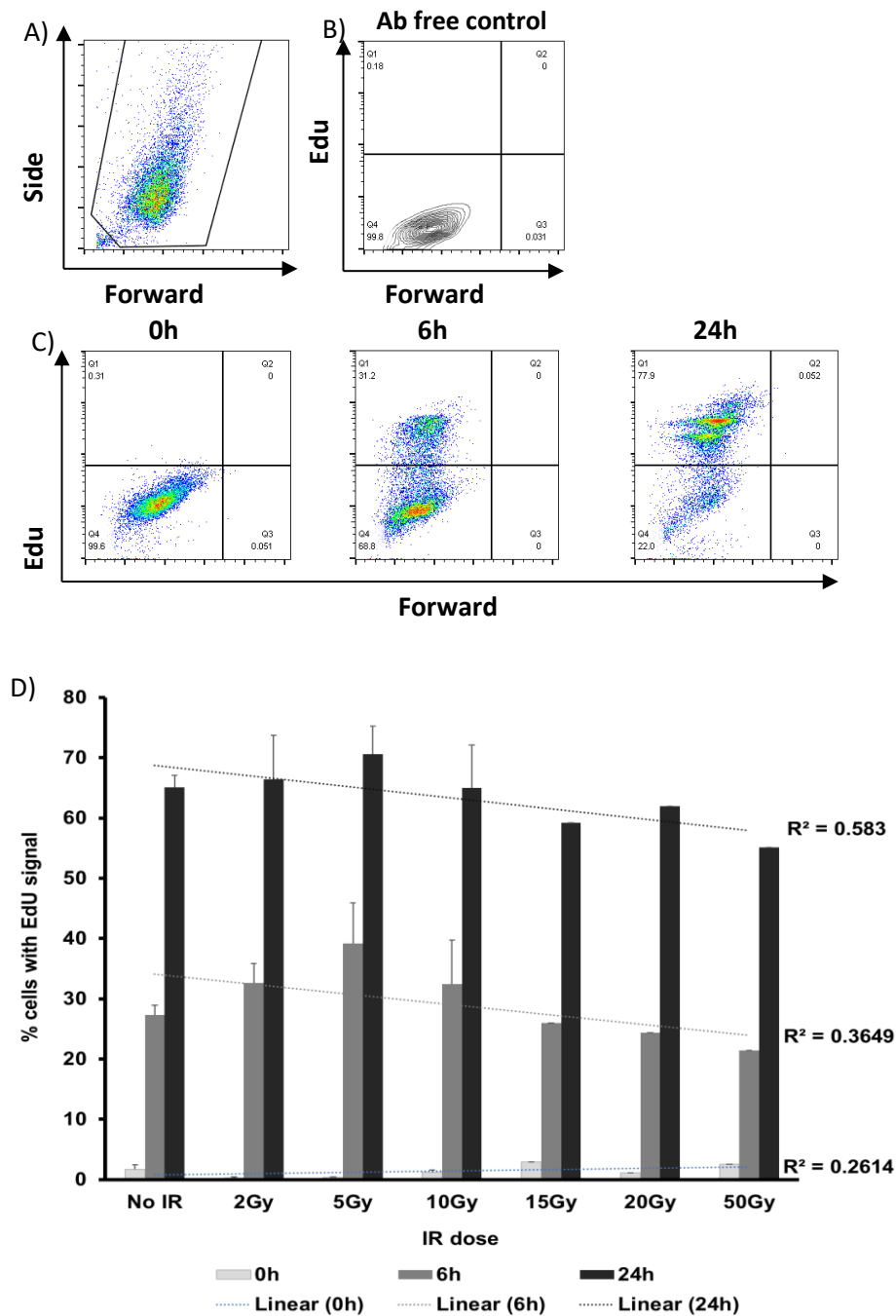
Figure 6.9. Troubleshooting the use of Edu as an S phase marker in HK2 cells. LP-WT cells were treated with 8µM of Edu in the absence of DRAQ5 and left for up to 24 h, were stated cells were treated with IR. A) Cells were isolated from debris B) Antibody free control was used to establish background florescence. C) Graph showing the effect of increasing dose of IR on Edu incorporation in LP-WT cells over 24 h. Data displayed for No IR – 10 Gy IR dose are averages of 3 independent experiments, error bars represent standard deviation; data displayed for 15 – 50 Gy IR is from a single experiment. The trendline and R^2 were calculated in Microsoft excel.

Two-way ANOVA Summary		
Source of variation	% of total variation	Pvalue
Interaction	0.85	0.9852
IR dose	1.00	0.6584
Time	61.83	**P<0.0001**

No IR vs 2Gy				
Time (h)	No IR (% cells Edu)	2Gy (% cells Edu)	Pvalue	95% CI of diff.
0	0.8783	0.2870	P > 0.05	-25.64 to 24.45
6	27.30	32.60	P > 0.05	-19.75 to 30.35
24	65.07	66.40	P > 0.05	-23.71 to 26.38
No IR vs 5Gy				
Time (h)	No IR (% cells Edu)	5Gy (% cells Edu)	Pvalue	95% CI of diff.
0	0.8783	0.3800	P > 0.05	-25.54 to 24.55
6	27.30	39.17	P > 0.05	-13.18 to 36.91
24	65.07	70.60	P > 0.05	-19.51 to 30.58
No IR vs 10Gy				
Time (h)	No IR (% cells Edu)	10Gy (% cells Edu)	Pvalue	95% CI of diff.
0	0.8783	1.173	P > 0.05	-23.13 to 23.72
6	27.30	32.40	P > 0.05	-18.33 to 28.53
24	65.07	65.03	P > 0.05	-23.47 to 23.39
No IR vs 15Gy				
Time (h)	No IR (% cells Edu)	15Gy (% cells Edu)	Pvalue	95% CI of diff.
0	0.8783	2.870	P > 0.05	-33.43 to 37.41
6	27.30	26.00	P > 0.05	-36.72 to 34.12
24	65.07	59.20	P > 0.05	-41.29 to 29.55
No IR vs 20Gy				
Time (h)	No IR (% cells Edu)	20Gy (% cells Edu)	Pvalue	95% CI of diff.
0	0.8783	1.120	P > 0.05	-35.18 to 35.66
6	27.30	24.40	P > 0.05	-38.32 to 32.52
24	65.07	61.90	P > 0.05	-38.59 to 32.25
No IR vs 50Gy				
Time (h)	No IR (% cells Edu)	50Gy (% cells Edu)	Pvalue	95% CI of diff.
0	0.8783	2.500	P > 0.05	-33.80 to 37.04
6	27.30	21.40	P > 0.05	-41.32 to 29.52
24	65.07	55.10	P > 0.05	-45.39 to 25.45

Table 6.1 Two-way ANOVA analysis of Edu incorporation in LP-WT cells subjected to increasing dose of IR (2-50 Gy) over time (0-24 h). Two-way ANOVA analysis was performed in GraphPad Prism4.

6.3 Conclusion

As previously discussed, FLCN has been linked to the cell cycle. This chapter attempted to explore the G1/S phase transition control in more detail in HK2 cells. Similar to previous reports, FLCN knockdown lead to an increase in cyclin D1 levels. Results in this chapter show that the increase in cyclin D1 levels is a direct result of FLCN loss. This data supports previously proposed observations of heightened Cyclin D1 expression shown in HeLa cells and *in vivo* mouse tumour cells (Baba et al. 2008; Kawai et al. 2013), consolidating this as a genuine biological observation; not artefacts of already malignant cells. The cyclin D1 pathway is disrupted in all human cancers leading to increased cell proliferation through shortening of the G1/S checkpoint control (Kim and Diehl 2009). In line with this, the increase in cyclin D1 levels observed in the LP-KD cells coincide with an increase in p-Rb under DNA damage. Furthermore, FLCN knockdown led to a decrease in the percentage of cells in the G1 phase and increased the percentage of cells in the G2 phase of the cell cycle (figure 6.5). These observations again agree with current literature, where it was shown that reintroduction of FLCN in zebrafish embryos lead to a significant decrease in cells in the S-M phase of the cell cycle with a corresponding increase of cells in the G1 phase (Kenyon et al. 2016). In zebrafish, no increase in cyclin D1 levels were observed. However, it does suggest FLCN's roles in G1/S transition is conserved between species and is not exclusive to mammalian models.

Collectively, results indicate that loss of FLCN promotes modest G1/S phase checkpoint skipping, with cells inappropriately committing to cellular division. However, the exact nature of FLCN's control on the cell cycle remains to be determined. It will be interesting to find out how FLCN's role in cyclin D1 inhibition relates to its published role in G2/M phase promotion, and mitotic spindle association; do these studies show snapshots of different portions of a single, large, cell cycle regulatory pathway, or does FLCN function independently in multiple pathways in order to fine tune cell cycle regulation? Perhaps the specific development of kidney cancer in BHD patients is a reflection of the requirement of FLCN to help facilitate DNA damage repair during cell cycle progression in acute conditions of cellular stress that is present in the kidney.

Thesis chapter 7: Overall discussion

The tumour suppressor FLCN has been implicated in a diverse range of cellular processes, including cellular trafficking, energy homeostasis and stress sensing. Collectively, the literature suggests a range of cell-type specific functions for FLCN. Within kidney cells, FLCN has been shown to regulate mTOR and AMPK signalling, mitochondrial biogenesis, cilium formation and cell polarity, and endocytic trafficking (Baba et al. 2008; Chen et al. 2008; Hasumi et al. 2009; Hasumi et al. 2012; Nahorski et al. 2012; Laviolette et al. 2017). FLCN loss is associated with RCC, were metabolic reprogramming is an integral part of cellular transformation (Zhang et al. 2014b). Uniquely, however, FLCN loss can lead to all histological subtypes of RCC, including hybrid tumours. It is currently unclear why such heterogeneity exists as a result of FLCN loss. Work within this thesis aimed to better understand the molecular role of FLCN loss in renal cell transformation. Preliminary work highlighted several potential FLCN interactors that have a role in DNA damage sensing or repair. DNA damage is a common occurrence for all cells and is a substantial risk to genetic stability. Indeed, genetic instability is an underlying driver of tumour development that is perpetuated by failures in the DNA repair processes (Mills et al. 2003; Negrini et al. 2010). As such, the focus of this thesis was to explore a novel role for FLCN within genomic maintenance. Given that FLCN loss exhibits intertumoral diversity it was hypothesised that FLCN plays an important housekeeping role to maintain genetic stability at the level of DNA damage repair.

There are three key findings within this thesis; (1) a novel protein-protein interaction between FLCN and the DNA-damage responder DNA-PKcs was identified (2) FLCN knockdown lead to an increase in DSBs, as indicate by elevated γH2AX, and (3) FLCN knockdown lead to a perturbed G1/S phase transition control. The implications for these roles in the larger context of BHD and RCC, along with future research directions are discussed further within this chapter. A schematic illustration summarising FLCN's currently known cellular roles and how the findings of this thesis might relate can be found in figure 7.1.
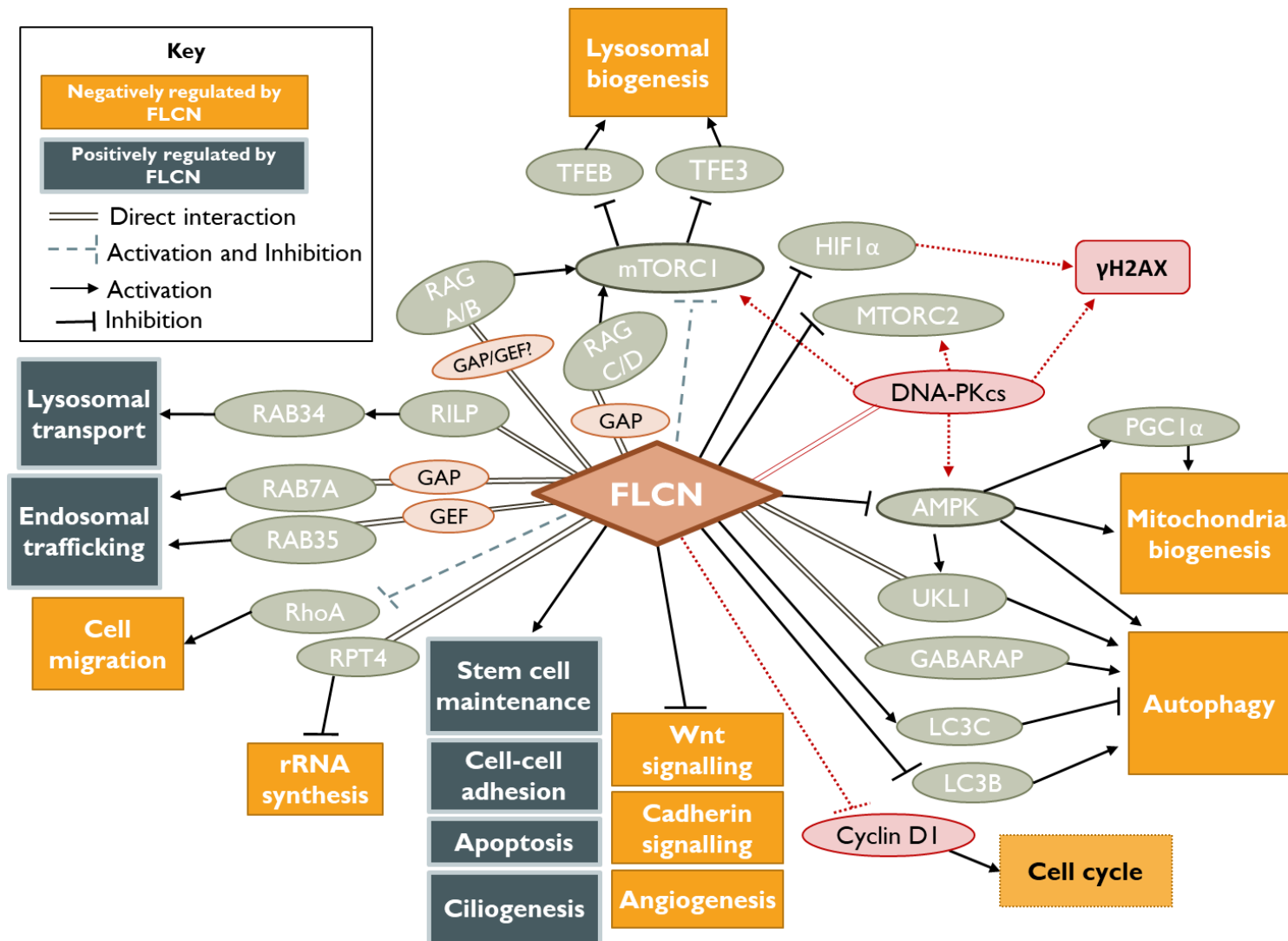
Figure 7.1 A schematic illustration summarising FLCN's currently known cellular roles. Proteins and actions coloured red hypothesise how findings within this thesis might fit within the current FLCN literature. This is discussed in detail within chapter 7.

7.1 A novel protein-protein interaction: FLCN/DNA-PKcs

Perhaps the most exciting finding presented in this thesis is the interaction between FLCN and DNA-PKcs, a DSB sensor and mediator of NHEJ DNA repair. This implicates FLCN in the DDR. Indeed, FLCN knockdown lead to an increase in γH2AX, a marker of double strand breaks, in both basal and irradiated cells (figure 5.4). FLCN is unlikely to be a substrate of DNA-PKcs as incorporation of ^{32}P did not increase upon DNA-PK activation with the addition of short dsDNA (figure 5.1). However, IR did weaken the protein-protein interaction in a dose dependent manner (figure 3.8C), revealing that this interaction is regulated upon IR treatment. FLCN knockdown did not apparently affect DNA-PKcs ability to become activated after DSB damage, as indicated by no change to Ser2056 phosphorylation of DNA-PKcs between wild type and knockdown cells (figure 5.4). Neither did FLCN loss contribute to mis-localisation of DNA-PKcs under both basal and DNA damaged states (data not shown).

DNA-PKcs is an extremely abundant protein. It is estimated that cells contain around 100,000 copies of DNA-PKcs (Anderson 1996). This is far in excess of what is needed for NHEJ, as only one DNA-PKcs binds to each DSB (Sibanda et al. 2017). Furthermore, is has been published that DNA-PKcs is not only present in the nucleus of a cell, but also in the cytoplasm (Huston et al. 2008). To date DNA-PKcs has been linked to various cytoplasmic pathways, including EGFR and NFκB signalling, mRNA metabolism, and the cytoskeleton (Panta et al. 2004; Dittmann et al. 2005; Szumiel 2006; Berglund and Clarke 2009). The most interesting emerging evidence, however, links DNA-PKcs to the regulation of energy homeostasis. While contradictory in the specifics, an overwhelming number of studies into FLCN's cellular function is associated to energy homeostasis, including regulatory roles in metabolic signalling, autophagy, and hypoxia (Baba et al. 2006; Baba et al. 2008; Preston et al. 2011; Dunlop et al. 2014; Yan et al. 2014). Moreover, RCC is considered a metabolic disease, where undergoing metabolic reprogramming is an essential hallmark of carcinogenesis (Choyke et al. 2003; Zhang et al. 2014b; Wettersten et al. 2015; Li et al. 2018). Another point worth mentioning is DNA-PKcs alone cannot bind DNA. Its interaction with the Ku complexes (Ku70/80) at DBS ends is essential for DNA-PKcs DNA binding (Leesmiller et al. 1992; Anderson 1996; Baumann and West 1998). This interaction is strong,

however, neither Ku70 nor Ku80 were identified in the FLCN protein interaction analysis (chapter 3). Collectively, this supports the idea that the FLCN/DNA-PKcs interaction might be independent of DNA damage sensing and/or direct repair.

7.1.1 A role for FLCN/DNA-PKcs in mTOR signalling

Multiple studies have linked DNA-PKcs activity to cellular metabolism. DNA-PKcs itself is regulated by the metabolic state of a cell, where it is active under fed conditions and inhibited during fasting (Wong et al. 2009). DNA-PKcs is thought to be a positive regulator of mTOR signalling, specifically mTORC2. DNA-PKcs has been shown to physically interact with two key components of mTORC2 activation; stress-activated protein kinase interacting protein 1 (SIN1) and rapamycin-insensitive companion of mTOR (Rictor) (Yang et al. 2006; Cameron et al. 2011; Zheng et al. 2016). In RCC, DNA-PKcs is commonly overexpressed and is thought to act as an oncogene by promoting cell proliferation (Zheng et al. 2016). Indeed, when in complex with SIN1, DNA-PKcs was shown to phosphorylate AKT at serine 473 (Zheng et al. 2016). In turn, phosphorylated AKT activates mTORC2 to promote proliferation. DNA-PKcs activity towards mTORC1, on the other hand, is less clear. Evidence suggests it does not interact with components required for mTORC1 activation (raptor, LST8, PRAS40 and deptor) (Zheng et al. 2016), and DNA-PKcs depletion did not change mTORC1 activity under basal conditions or in response to etoposide (Puustinen 2018a). Several studies, however, have shown the usefulness of dual inhibitors that target both DNA-PKcs and mTOR. Targeting DDR and mTOR signalling has a potent anti-tumour activity against a large panel of hematopoietic and solid cancer cell lines resulting in a reliable induction of apoptosis in a subset of cancer lines (Shortt et al. 2013; Mortensen et al. 2015; Munster et al. 2016; Tsuji et al. 2017). The dual DNA-PKcs/mTOR inhibitors explored so far inhibit both mTORC1 and mTORC2, and it's currently not clear if the potency comes from targeting two independent, synthetically lethally, pathways (DNA-PKcs/mTORC1) or synergistically targeting overlapping pathways (DNA-PKcs/mTORC2).

FLCN's function in mTOR is complicated. Collectively, however, the data suggests that in kidney cells FLCN can inhibit both mTORC1 and mTORC2 (Baba et al. 2008; Chen et

al. 2008; Hasumi et al. 2009; Petit et al. 2013; Tsun et al. 2013). However, the mechanism of how FLCN controls both mTORC1 and mTORC2 function is less clear. The most convincing evidence suggests FLCN regulation of mTOR occurs at the lysosome. FLCN was shown to interact with components of the 'ragulator' complex required for mTORC1 activation. Specifically, FLCN was shown to interact with the GTPase domain of RagA when RagA is GDP bound (inactive form). The preferential binding to the GDP-bound form of a small GTPase is a property commonly seen in GEFs, suggesting it may function as a GEF towards RagA/B (Petit et al. 2013). Furthermore, FLCN was also shown to act as a GAP towards RagC/D (Tsun et al. 2013). In recent years, FLCN has also been demonstrated to act as a GAP towards RagA (Meng and Ferguson 2018). It is possible that FLCN binds to RagA/B^{GDP} in a GEF-like manner that does not lead to nucleotide exchange. Rather it allows FLCN to be in close proximity to RagC/D and thus help facilitate GAP activity toward RagC/D (either directly as a GAP, or indirectly via an associated GAP protein). Such a pseudoGEF-GAP function for FLCN toward RagA/B and RagC/D likely helps to tightly coordinate nucleotide status within Rag heterodimers.

Regulation of mTOR activation at the lysosomes, specifically refers to mTORC1. mTORC1 is extremely dependent on cellular energy status, cell type, and FLCN being in complex with either FNIP1 or FNIP2. On the other hand, little is known about FLCNs involvement with mTORC2 activity. The mTORC2 target, AKT has been shown to be hyperphosphorylated at Ser473 in FLCN knockdown cells, and FLCN was demonstrated to physically interact with the mTORC2 regulator SIN (Mathieu et al. 2019). It has been suggested that the FLCN/SIN1 interaction may negatively regulate mTORC2 activity by preventing mTORC2/SIN1 interaction (Mathieu et al. 2019). However, this has yet to be biochemically proven. Given that DNA-PKcs promotes and FLCN likely inhibits mTORC2 by binding to SIN, perhaps the FLCN/DNA-PKcs interaction represents another layer of mTORC2 regulation?

7.1.2 A role for FLCN/DNA-PKcs in autophagy

Autophagy is a complex and highly regulated homeostatic process. Autophagy allows cells to efficiently remove defective organelles and molecules, and to recycle nutrients
for survival under deprived conditions (Levine and Kroemer 2008; Mizushima et al. 2008;

Mizushima et al. 2011). Consequently, dysregulation in the normal rates of autophagy can result in a metabolic imbalance and disease (Levine and Kroemer 2008). Classic autophagy involves a process that uses a ubiquitin-like cascade of autophagy-related (ATG) proteins leading to the formation of double-membrane autophagosomes (Mizushima et al. 2011). Autophagosomes ultimately fuse with lysosomes targeting the cargo for proteolytic degradation (He and Klionsky 2009). An emerging body of evidence has associated autophagy with the DDR and suggest it is an integrated part of the genome surveillance network (Abedin et al. 2007; Katayama et al. 2007; Rieber and Rieber 2008). This overlap of processes likely co-ordinate the turnover of key DDR proteins, remove damage macromolecules, and to regulate the supply of ATP, NAD$^+$, and dNTPs that are necessary to repair DNA (Rello-Varona et al. 2012; Eliopoulos et al. 2016).

DNA-PKcs has been linked to autophagy (Paglin et al. 2001; Yao et al. 2003; Zhuang et al. 2011). DNA-PKcs knockdown or inhibition sensitises cells to IR-induces autophagy response and inhibition of autophagy can block DNA-PKcs dependent autophagic response, suggesting DNA-PKcs may negatively regulate autophagy (Zhuang et al. 2011). However, from these results it's unclear if DNA-PKcs response in autophagy is a general phenomenon or specifically DNA damage induced, or if the DNA-PKcs kinase activity is required for the response. (Paglin et al. 2001; Yao et al. 2003; Daido et al. 2005). On the other hand, DNA-PKcs has been demonstrated to be a positive regulator of autophagy through a direct regulation of AMPK (Amatya et al. 2012; Lu et al. 2016; Puustinen 2018b). DNA-PKcs was demonstrated to interact with the regulatory gamma subunit of AMPK (AMPKγ), where it has been shown to phosphorylated AMPKγ at Ser192 and Thr284. (Amatya et al. 2012; Lu et al. 2016; Puustinen 2018a). Alanine substitutions of these DNA-PKcs-dependent phosphorylation sites in AMPKγ inhibited the lysosomal localisation of AMPK and its starvation-dependent association with LKB1 (Puustinen 2018b). The lysosomal membrane has been recently recognised as an important site for the activation of AMPK (Zhang et al. 2014a; Zhang et al. 2017). In the absence of glucose, LKB1 and scaffold protein AXIN translocate to the lysosomal membrane, where they form a large complex with AMPK, vacuolar H$^+$-ATPase and the ragulator complexes (Zhang et al. 2014b). This super complex serves as the site for LKB1-mediated phosphorylation and activation of AMPK alpha subunit (AMPKα) (Zhang et al. 2014b). Mechanistically, it is thought that the DNA-PKcs-mediated

152

phosphorylation of AMPKγ primes AMPK for lysosomal activation. AMPK is a master regulator catabolic processes, including autophagy. AMPK promotes autophagy through Unc-51 like autophagy activating kinase (ULK1). AMPKγ subunit physically interacts with ULK1 and this interaction is required for the induction of autophagy (Lee et al. 2010). Multiple studies have identified numerous AMPK-dependent phosphorylation sites on ULK1 (Egan et al. 2011; Kim et al. 2011; Shang et al. 2011). These studies often contradict each other as they identify AMPK-dependent phosphorylation sites unique to individual studies with very little consensus between them. Therefore, it's unclear where AMPK phosphorylates ULK1 and mechanistically what the function of these phosphorylation sites maybe (Egan et al. 2011; Kim et al. 2011; Shang et al. 2011). Nevertheless, the evidence agrees that energy deprivation activates AMPK, which in turn activates ULK1 to initiate autophagy.

FLCN's role in autophagy is complicated. FLCN has been shown to inhibit the activity of autophagic transcription factors TFEB and TFE3 (Petit et al. 2013; Martina et al. 2014) and autophagy is increased in *dBHD*-null *Drosophila* (Liu et al. 2013b). Furthermore, FLCN has been shown to inhibit LC3B and stimulate LC3C autophagic activity (Bastola et al. 2013). LC3s are structural proteins of autophagosomal membranes that act as scaffolding proteins. The human LC3 family has three members, LC3A, LC3B and LC3C. LC3B is commonly upregulated in RCC and LC3B-mediated autophagy is often needed for tumour progression. LC3C, on the other hand, has tumour suppressor activity (Mikhaylova et al. 2012). It is currently unclear how LC3C acts as a tumour suppressor. LC3C could be a part of an unidentified autophagic pathway or could participate in a non-autophagic tumour-suppressing pathway. FLCN may therefore inhibit the oncogenic LC3B and promotes the anti-tumour activity of LC3C. Collectively, these results suggest that FLCN usually inhibits autophagy, at least *in vitro* and in *Drosophila*. In contrast, however, autophagic flux was found to be reduced in mice primary cardiac cells, mouse embryonic fibroblasts, HK2 cell lines, and BHD-associated RCC (Dunlop et al. 2014; Hasumi et al. 2014). FLCN was demonstrated to enhance basal autophagic flux through its interaction with the autophagic proteins GABARAP and ULK1, acting as a positive regulator of autophagy in mammalian cells.

The functional relevance of autophagy in tumour formation and progression remains unclear. Autophagy seemingly has a paradoxical role in modulating cancer progression as it has been demonstrated to have both oncogenic and tumour suppressive roles. Collectively, it is thought that the effect autophagy has on tumour cell fate depends on the cancer type, stage, and genetic context (Eisenberg-Lerner and Kimchi 2009; Singh et al. 2018). Autophagy initially safeguards cells by preventing a build-up of toxic cellular waste products and preserve organelle function. However, as cancer progresses, the stress-mitigating properties of autophagy are hijacked by tumour cells to meet the heightened metabolic requirements necessary for tumour survival and rapid proliferation (White 2012; Singh et al. 2018). It would be interesting to see DNA-PKcs effects on AMPK-dependent activation of autophagy, such as ULK1 activation, and if FLCN knockdown alters this. Furthermore, it is well established that AMPK is hyperactive upon FLCN loss. The mechanistic reason(s) for this are unknown to date and AMPK localisation to the lysosomes following FLCN loss has not yet been published, could FLCN be involved in the DNA-PKcs-dependent localisation and activation of AMPK?

7.1.3 A role for FLCN/DNA-PKcs in hypoxic signalling

Another emerging aspect in which DNA-PKcs functions outside of DDR is hypoxia. Hypoxia is defined as the reduction or lack of oxygen in cells. The hypoxic response plays a critical role in cell biology and disease development; particularly in cancer, where solid tumours consume high amounts of oxygen despite inadequate vascularisation.

Hypoxia-inducible factors (HIFs) are the central transcription factors regulating the cellular response to hypoxia. There are three known isoforms of HIF subunits; HIF1α, HIF2α, and HIF3α (Kondo et al. 2002; Yang et al. 2017). The functions of HIF1α and HIF2α are relatively well known, whereas little is known about the specific function of HIF3α due to its late discovery and low expression levels (Yang et al. 2017; Pezzuto and Carico 2018). Overall, HIFs play distinct and overlapping functions in various cell types (Yang et al. 2017). HIFs are commonly over-expressed in numerous cancers where they activate a number of hypoxia-related genes required for adaptation to low oxygen levels (Wenger et al. 2005; Pezzuto and Carico 2018). Interestingly, DNA-PKcs is activated by hypoxia and was shown to positively regulate both HIF1α and HIF2α (Um et al. 2004; Wenger et al. 2005; Bouquet et al. 2011).

154

(Toschi et al. 2008). DNA-PKcs-dependent activation of HIFs was shown to be independent of DSBs (Zheng et al. 2016). Combined, these studies present the novel concept that co-ordinated regulation between DNA-PKcs and the HIF family of transcription factors may influence cellular response to oxygen depletion. It would be interesting to see if FLCN knockdown alters these functions. FLCN is thought to negatively regulate HIF1α and HIF2α as FLCN loss correlates with increase in HIF gene expression (Lu et al. 2011; Preston et al. 2011; Nishii et al. 2013). Indeed, increase in HIF2α is commonly observed in BHD-associated RCC (Lu et al. 2011; Preston et al. 2011). Moreover, HIF2α induces oncogenic CCND1 expression in RCC cell lines, yet CCND1 expression is not hypoxia inducible in non-RCC cancer cell lines (Raval et al. 2005). This could represent a mechanism for cellular transformation unique to RCC.

7.1.4 Conclusion

The understanding of DNA-PKcs' cellular function is moving beyond its classical role as a component of DDR. Recent findings illuminate a multi-faceted role for DNA-PKcs that affect numerous tumour-associated pathways. These effects can be both depend and independent of DNA damage. An interesting observation is that DNA-PKcs seems to promote both mTOR signalling and autophagy. Perhaps then the transformative process in BHD-associated RCC involves inappropriate cell growth via upregulated catabolic processes (mTOR) which are constantly fed via an upregulation of anabolic processes (AMPK, autophagy). Could FLCN act to regulate DNA-PKcs oncogenic tendencies? Given FLCN's extensive links to energy homeostasis, it would be interesting to explore the activity of DNA-PK under nutrient and/or oxygen deprivation following FLCN loss.

7.2 FLCN knockdown results in an increase of DNA double-strand breaks (DSB)

Daily, a wide range of insults damage cellular DNA and continuously challenging genome integrity. These can be physical or chemical insults that directly damage DNA bases, or errors incorporated during DNA replication (Hoeijmakers 2001). To prevent the harmful consequences of genotoxic stress, organisms have evolved a complex network of genome surveillance mechanisms. These are designed to maintain the genomic integrity, or to eliminate hazardous cells when DNA damage is beyond repair (Jackson and Bartek 2009; Ciccia and Elledge 2010). DSB are considered the most lethal DNA insult and can lead to large chromosomal rearrangements if not repaired. FLCN knockdown in HK2 cells lead to an increase in γH2AX, suggesting these cells have an increase in DSBs (figure 5.4). Additionally, FLCN knockdown did not make cells hypersensitive to IR. Suggesting cells can tolerate the increase in DSB observed. Indeed, initial analysis hints that FLCN knockdown cells may recover more readily to DNA insults than wild type cells (figure 5.6).

7.2.1 Exploring the cause of the increase in DSB upon FLCN loss

At present, it is unclear why cells accumulate DSB upon FLCN knockdown. It would be interesting to expand on the increase in γH2AX observed; are they the result of replication stress, increased metabolic burden, or are DSB repair mechanisms compromised as a result of FLCN loss? Below these questions are discussed in more detail.

7.2.1.1 Replication stress as a cause for increase in DSBs

Although replication stress is widely recognised as a significant problem for genome stability, there is currently no unifying description of this phenomenon. Nor is there a clear set of cellular markers which unambiguously characterise this state. The most widely accepted definition considers replication stress as the slowing or stalling of replication fork progression and/or DNA synthesis (Zeman and Cimprich 2014). Replication stress can be generated by a wide range of physical obstacles that usually results in stretches of single-stranded DNA (ssDNA). The ssDNA frequently form when the replicative helicase continue to unwind the parental DNA after the polymerase has stalled (Pacek and Walter 2004). However, DSBs can occur as a result of collapsed replications forks when stalling is not overcome. Many markers that are used to detect replication stress reflect the activation of

the ATR repair pathway, including γH2AX. γH2AX can be generated by numerous kinases, which detect different types of DNA damage throughout the cell cycle. Therefore, it is not a useful marker to isolate replication stress. ATR-dependent phosphorylation of RPA or Chk1, or the direct detection of ssDNA, are more reliable indicators of replication stress (Marechal and Zou 2013; Zeman and Cimprich 2014). Within this thesis ATR activation was not affected by FLCN knockdown, and Chk1 phosphorylation, while possibly elevated in response to IR compared to wild type cells, had an inconsistent response (figure 5.4C). On the other hand, RPA gene expression is increased upon FLCN knockdown. It should be noted that the use of ATR substrates or ssDNA accumulation as markers of replication stress assumes that the stress is sufficient to activate ATR to a high enough level to induce widespread phosphorylation of its downstream targets, or that the stress generates large enough patches of ssDNA that they are readily detectable, neither of which is necessarily true (Koundrioukoff et al. 2013). For example, the cell may experience replication stress at one or a few stalled forks and respond locally, but not globally, to that stress (Koundrioukoff et al. 2013). There is also evidence that replication stress can be induced by protein-DNA complexes or inter-strand DNA crosslinks that do not accumulate ssDNA from helicase-polymerase uncoupling (Marechal and Zou 2013). These structures may be resolved by other repair pathways without activating ATR (Zeman and Cimprich 2014). Therefore, it may be worth co-ordinating the induction of γH2AX with a phase of the cell cycle, in the first instance, to help establish the cause of the DSB observed in response to FLCN loss.

7.2.2 Metabolic burden as a cause for increase in DSBs

7.2.2.1 Reactive oxygen species (ROS)

One of the most cited observations following FLCN loss is the upregulation of mitochondrial biogenesis (Klomp et al. 2010; Lindor et al. 2012; Pradella et al. 2013; Raymond et al. 2014; Wada et al. 2016; Yan et al. 2016a). This is accompanied by an increase in mitochondrial ROS. An increase in ROS has long been associated with cancer (Moloney and Cotter 2018). ROS are primarily oncogenic, causing oxidative damage to DNA, proteins, and lipids (Liou and Storz 2010; Roy et al. 2015; Moloney and Cotter 2018). Overtime, this damage accumulates and promotes cellular transformation. Indeed, high or sustained levels of ROS

contribute to the development of cancer (Martien and Abbadie 2007; Ralph et al. 2010; Verbon et al. 2012), as shown by the inhibitory effects of antioxidants on tumour formation (Zhang et al. 2002). Furthermore, ROS have been demonstrated to generate DSB. Chronic exposure to ROS resulted in oxidative clustered DNA lesions (OCDLs), closely spaced oxidative lesions (within 20bp) that result in the breakdown of double strand interactions. ROS is thought to be the largest cause of DSB during G1 phase of cell cycle. In addition, NHEJ is thought to be the primary repair pathway for oxidative DSBs. Cells become hypersensitive to ROS stress when components of NHEJ (e.g. DNA-PKcs, Ku 70/80, X-ray repair cross-complementing protein 4 (XRCC4), and DNA ligase 4 (Lig IV)) are compromised. This hypersensitivity to ROS is above that observed when HR is prohibited (Karanjawala et al. 1999; Karanjawala et al. 2002; Woodbine et al. 2011; Dolan et al. 2013; Sharma et al. 2016).

A simple explanation, therefore, would be that FLCN loss results in an increase in mutagenic ROS through dysregulation of mitochondria. This promotes DSB via oxidative clustered DNA lesions. Surprisingly, however, it's been reported that the increase in mitochondrial ROS production in FLCN knockdown cells did not increase oxidative DNA bases to a statistically significant level in mouse embryonic fibroblasts (Yan et al. 2014). Instead the authors showed ROS acted as a signalling molecule to enhance HIF transcriptional activity (Yan et al. 2014). OCDLs can have a combination of different DNA lesions including abasic sites, SSBs and oxidative damaged bases. However, the most reliable method for detecting OCDLs is pulse field gel electrophoresis (PFGE). Nevertheless, if the increase in ROS contributed to the aetiology of BHD-associated RCC by causing OCDLs-induced DSB, a notable increase in oxidative DNA indicated by 8-hydroxydeoxyguanosine (8-OHdG) ELISA, as used in the study, theoretically should have been detected. Therefore, current evidence doesn't support the increase in DSBs upon FLCN loss to be caused by ROS.

7.2.2.2 Hypoxia-associated γH2AX

Under hypoxic conditions, several cancer cell lines have been noted to have HIF-dependent accumulation of γH2AX (Economopoulou et al. 2009; Wrann et al. 2013; Goodwin and Knudsen 2014). RNAi knockdown of either HIF-1α or HIF-2α reduced observable γH2AX, which can be further reduced by knockdown of both HIF-1α and HIF-2α. Interestingly, no

detectable levels of DSBs were observed following the HIF-dependent accumulation of γH2AX (Wrann et al. 2013). Suggesting this may be a damage independent mechanism. One idea is that increase in γH2AX allows for more relaxed chromatin and might increase a cancer cell's capacity to repair DNA damage or promote HIF target gene transcription providing cells with a selective advantage in conditions with reduced oxygen (Wrann et al. 2013; Goodwin and Knudsen 2014).

Furthermore, reduced oxygen levels may prohibit effective repair of DSB. Residual DSBs were observed 24 hours after IR under long term hypoxia. Previous studies that have investigated DNA repair during hypoxic irradiation conditions were followed by re-oxygenation, and concluded that the mutation rate and DSB repair rate were not influenced by hypoxia (Olive and Banath 2004; Kumareswaran et al. 2012). However, DNA repair under continued hypoxia leads to decreased repair of G1-associated DSBs (Kumareswaran et al. 2012). NHEJ is the predominant DSB repair pathway in the G1 phase of the cell cycle (Shrivastav et al. 2008). Due to the increase in G1-associated DSBs, it is thought that NHEJ may be compromised under hypoxia. This might, in part, explain the increased genetic instability observed in hypoxic cells that adapt to low oxygen conditions. There are conflicting data in the literature regarding the effect hypoxia has on NHEJ repair. NHEJ-related genes have been shown downregulated at mRNA and protein levels in both normal and malignant hypoxic cells (Meng et al. 2005). By contrast, the apical protein of NHEJ, DNA-PKcs has been demonstrated to have increased activity under hypoxic conditions (Um et al. 2004). However, neither of these studies directly measured DSB repair in chronically hypoxic cells. The mechanism by which hypoxia may alter NHEJ is not known. More studies are required to test whether hypoxia leads to a defect in both DNA-PKcs-dependent and/or DNA-PKcs-independent NHEJ pathways throughout the cell cycle. As previously mentioned, FLCN is thought to inhibit HIF signalling (Preston et al. 2011). It would be tempting to speculate the increase in γH2AX could be HIF-driven. However, γH2AX was observed under normal oxygen conditions. While an upregulation of HIFs seems to promote γH2AX foci, its unclear whether HIFs upregulation alone is enough to drive γH2AX foci or if hypoxic conditions are essential for this. Nevertheless, it may be interesting to explore the increase in γH2AX observed in FLCN knockdown cells under the context of HIF signalling.

159

7.2.3 Defective repair mechanisms as a cause for increase in DSBs

Leading on from the idea of a hypoxia induced comprise to NHEJ repair of DSBs, it would be interesting to explore if DSB repair kinetics are altered in FLCN knockdown cells. DNA-PKcs interaction with FLCN was weakened by IR (figure 3.8C), suggesting there is regulation over their interaction. However, activation of DNA-PKcs is not altered in FLCN knockdown cells (figure 5.4). Due to time constraints, downstream NHEJ components were not investigated. Co-localisation between key NHEJ factors (such as XRCC4 , Lig IV, and XRCC4-like factor (XLF)) and DSB are often used as markers on NHEJ (Costantini et al. 2007; Yano et al. 2008; Chatterjee and Walker 2017). Another common marker for cells undergoing NHEJ repair is p53-binding protein 1 (53BP1). 53BP1 plays an important regulatory role by recruiting the NHEJ components to the DNA break site, and activating checkpoint signalling (Panier and Boulton 2014).

Furthermore, NHEJ is error prone process. It can result in fusing mismatched DNA ends, fusing ends that contains damaged bases, loss of DNA sequence by haphazardly stitching DNA ends together, and even large chromosomal translocations or chromosome fusion (Shrivastav et al. 2008). HR on the other hand, uses an intact sister chromatid as a template. This process is normally accurate but is only available during late S phase and G2/M checkpoint, after DNA replication. The decision of which DSB repair pathway to use is a highly controlled process. Interestingly, one of the key regulators of this decision is BRCA1. Specifically, BRCA1 promotes 53BP1 dephosphorylation and RIF1 release, favouring repair by HR (Ciccia and Elledge 2010; Isono et al. 2017). BRCA1 was found hyperphosphorylated in FLCN knockdown cells in response to DNA damage. Could this represent a compensatory mechanism whereby HR in G2 is working to overcome unrepaired DSB from G1, or as a result of malfunctioning NHEJ? It would be interesting to compare the recruitment of NHEJ components upon FLCN knockdown to see if NHEJ repair is perturbed. In addition, it would be interesting to compare the efficiency of NHEJ and HR repair of DSBs following FLCN knockdown to investigate if FLCN plays a role in repair kinetics.

7.2.3.1 Compromised DNA repair through nuclear accumulation of the autophagic regulator Sequestosome 1 (SQSTM1/p62)

Sequestosome 1 (SQSTM1/p62) is a regulator of autophagy and is often upregulated in RCC (Liu et al. 2015). Interestingly, SQSTM1/p62 is emerging as an important mediator of the effects of autophagy on DNA damage repair. Nuclear SQSTM1/p62 has been shown to bind RNF168, inhibiting its E3 ubiquitin ligase activity toward histone H2A. The accumulation of nuclear SQSTM1/p62, driven by a loss of autophagy, decreases chromatin ubiquitination. In turn, this hinders the recruitment of DNA repair proteins such as BRCA1, RAD51, and RAP80 to sites of DSBs, and thus impacts on their ability to repair damaged DNA (Wang et al. 2016). RAD51 is further regulated by nuclear SQSTM1/p62 through filamin A, which physiologically responds to DNA damage by recruiting RAD51 to DSBs. Inhibition of autophagy increases the interaction of SQSTM1/p62 with filamin A, causing proteasomal degradation of both filamin A and RAD51 (Hewitt et al. 2016). Therefore, nuclear SQSTM1/p62 that accrues from defective autophagy compromises DNA damage repair and genomic integrity. Total SQSTM1/p62 was shown to be increased in FLCN knockdown cells and to become nuclear localised in renal tumours from BHD patients (Dunlop et al. 2014). Preliminary data suggests that SQSTM1/p62 is likely to be increase in the nucleus of FLCN knockdown HK2 cells (n=1, data not shown). It would be interesting to validate the increase in nuclear SQSTM1/p62, if RAD51 levels are altered, and/or if there is a reduction in H2AX ubiquitination upon FLCN loss.

7.2.4 Conclusion

There are many reasons why cells accumulate DSBs. Genetic instability is a hallmark of cancer. It would be useful to mechanistically explore how FLCN knockdown facilitates an increase in γH2AX formation and confirm if this γH2AX represents an increase in DSB. A simple set of experiments would be to examine γH2AX foci via immunofluorescence. Unlike radiation induced γH2AX foci, ROS-induced γH2AX foci (specifically hydrogen peroxide) does not induce the formation of distinct foci but rather a whole nucleus staining pattern with only few separate countable foci (Sharma et al. 2016). In addition, matching the induction of γH2AX foci to a phase of the cell cycle would provide a preliminary indication for which DSB mechanism would be worth investigating. γH2AX foci accumulating in G1 would suggest a

fault in NHEJ, while G2 would represent HR. Equally, accumulation of γH2AX during S phase would advocate replication stress as a cause for DSB following FLCN knockdown.

7.3 FLCN knockdown results in dysregulated G1-G1/S phase transition

There is a growing body of evidence to suggest the cell cycle may be perturbed following FLCN Knockdown (Kawai et al. 2013; Luijten et al. 2013; Kenyon et al. 2016). Indeed, within this thesis numerous proteins involved in G1-G1/S phase transition were identified in the FLCN interactome (figure 3.5) and FLCN knockdown led to an enrichment of differentially expressed genes within in G1-G1/S phase transition (figure 4.8). Elevated levels of cyclin D1 are observed in both low and high passage HK2 cells following FLCN knockdown. Furthermore, cyclin D1 protein level did not change when cells were subjected to IR, unlike wild type control cells whose level of cyclin D1 decreased slightly (figure 6.2). FLCN knockdown also led to a decrease in the percentage of cells in G1 phase, with a corresponding increase in the percentage of cells in G2 phase as indicated by DRAQ5 incorporation (figure 6.6E-G). Similarly, in zebra fish embryos, reintroduction of wild type FLCN led to an increase in G1 cells and a decrease in G2 cells (Kenyon et al. 2016). Collectively, the results implicate FLCN in the G1/S control of the cell cycle, specifically FLCN may have a role in G1/S checkpoint to halt proliferation. However, it is not clear exactly what FLCN may be doing at this checkpoint, or how it contributes to checkpointing. For example, why dose FLCN loss result in the increase in cyclin D1? A previous study reported that FLCN negatively regulates cyclin D1 through elements on the CCND1 mRNA (Kawai et al. 2013). It's worth noting that nearly a third of the FLCN interactome has been linked to transcription and/or translation (figure 3.5). Although it has not been previously explored, protein interactions between FLCN and molecules involved in protein transcription and/or translation were considered out of the confines of this thesis. Given FLCNs association with mTOR signalling, which is heavily implicated in protein synthesis, FLCN may function to restrict cyclin D1 protein translation. This idea is discussed in detail later (see section 7.5.1, future research directions).

7.3.1 An increase in ROS promotes G1/S skipping

Increased levels of ROS are considered tumorigenic (Liou and Storz 2010; Moloney and Cotter 2018). They result in the activation of pro-survival signalling pathways, loss of tumour suppressor gene-function, increased glucose metabolism, adaptations to hypoxia and the generation of oncogenic mutations (Heiden et al. 2009; Sabharwal and Schumacker 2014). As previously mentioned, FLCN loss is documented to increase in mitochondrial ROS which functioned as a signalling molecule to promoted HIF signalling (Preston et al. 2011; Yan et al. 2014). Indeed, ROS has been demonstrated to act as a signalling molecule in many cancers, contributing to abnormal cell growth, metastasis, resistance to apoptosis, and angiogenesis (Sabharwal and Schumacker 2014; Moloney et al. 2017).

Interestingly, a growing body of evidence suggest ROS may have central role in controlling cell proliferation. The amount of ROS present seems to determine the effect of ROS on cell proliferation: low amounts result in correct cell cycle progression whereas high amounts have been associated to uncontrolled cell proliferation (Deshpande and Irani 2002; Boonstra and Post 2004; Stockl et al. 2006; Qin et al. 2011). ROS has also been shown to influence proliferation in the form of secondary messengers in many pathways regulating cell proliferation, such as those involving p21, MAPK, or EGFR (Boonstra and Post 2004). In the example of EGFR, ROS is able to inhibit EGFR internalisation in addition to directly activating EGFR (De Wit et al. 2000; Papaiahgari et al. 2006; Leon-Buitimea et al. 2012). Furthermore, ROS were shown to be important modulators of enzymes that ubiquitinate or phosphorylate cell cycle proteins (Boonstra and Post 2004). In fact accumulating evidence suggests modulating ubiquitination of cell cycle components may be the central mechanism of ROS-mediated cell cycle progression (Havens et al. 2006; Yamaura et al. 2009). Appropriate ubiquitination and subsequent degradation of the cyclin protein family is an integral mechanism controlling the regulation of the cell cycle progression (Boonstra and Post 2004). Furthermore, ubiquitination is essential for the regulation of the expression of cyclin kinase inhibitors, such as p21 (Lu and Hunter 2010; Starostina and Kipreos 2012). ROS can influence ubiquitination by inhibiting Ubiquitin-activating E1 and ubiquitin conjugating E2 enzyme activities. In addition, ROS can also directly inhibit the proteasome, to further decrease ubiquitin-mediated degradation (Boonstra and Post 2004). ROS has also been shown to indirectly influence the ubiquitination of pro-proliferation factors. For example, in

human fibroblasts an accumulation of cyclin A at the end of G1 is necessary for progression into the S phase. Treatment with antioxidants prevents cyclin A accumulation resulting in G1 phase arrest. ROS was demonstrated to promote the inactivation of anaphase promoting complex (APC) via APC phosphorylation (Havens et al. 2006). As such, APC cannot ubiquitinate cyclin A and thus cyclin A is not degraded. Since ubiquitination regulates cell cycle progression, ROS influences ubiquitination, and ROS has already been demonstrated to act as a secondary messenger under the context of FLCN loss, it seems reasonable to suggest that the perturbed cell cycle phenotype observed following FLCN knockdown may be mediated by an increase in ROS. Specifically, the increase in ROS contributes to cell cycle progression in FLCN loss cells by inhibiting the ubiquitination, and thus preventing proteasomal degradation, of pro-proliferative factors. Indeed, hydrogen peroxide has been shown to cause a reversible inhibition of the ubiquitin-proteasome dependent degradation of cyclin D1 in HER14 fibroblasts (Munoz et al. 2001). This may explain the increase in cyclin D1 protein levels shown in this thesis. Especially as in high passage FLCN knockdown cells, elevated cyclin D1 protein is observed alongside a marked down-regulation in CCND1 gene expression, and published work suggest FLCNs negative regulation of cyclin D1 may not be directly at the level of gene transcription (Kawai et al. 2013).

Nevertheless, while the main body of evidence suggest ROS can promote cell cycle progression, ROS has also been noted to cause cell cycle arrest. For example, sublethal doses of hydrogen peroxide caused a transient arrest in NIH 3T3 fibroblasts, while nitric oxide caused a G1 phase arrest in human pancreatic carcinoma cell lines (Gansauge et al. 1998; Barnouin et al. 2002; Boonstra and Post 2004). Ultimately, the effect of ROS on cellular processes is complex. While more work needs to be carried out to understand the specifics, the influence ROS has on cell cycle regulation seems to be dependent upon cell type, location of ROS production, and even the type of ROS produced. (Yamaura et al. 2009). Still, it would be exciting to test the effects of ROS-mediated inhibition of cyclin D1 in the context of FLCN knockdown.

7.4 Potential therapeutic targets based on observation presented within this thesis

Understanding the function of FLCN and the cellular pathways in which it interacts with will inform the development of targeted therapies to treat BHD-associated RCC. For example, recent research indicates that FLCN plays an important role in the EGFR signalling pathway and treatment with the tyrosine kinase inhibitor Afatinib has been shown to inhibit BHD-associated renal tumour growth in a mouse model (Laviolette et al. 2017). Tyrosine kinase inhibitors are usually used within sporadic RCC to combat a metastatic disease, but no tyrosine kinase inhibitor to date has been cleared to specifically treat BHD-associated tumours (Rudresha et al. 2017; Wei et al. 2018). Similarly, despite showing promise in *Flcn*-deficient mouse models, no mTOR inhibitor has passed clinical trials for use with BHD-associated RCC (Baba et al. 2008; Chen et al. 2008; Wu et al. 2015).

Work within this thesis may provide justification for exploring other therapeutic avenues. Defects in the DDR give rise to genomic instability in cells, aiding in cancer initiation and progression by allowing mutations to accumulate. However, this also offers targetable vulnerabilities that are specific to cancer cells which can be exploited for clinical benefit with the use of DDR inhibitors. The identification of the protein-protein interaction between FLCN and DNA-PKcs is exciting. Inhibition of DNA-PKcs, through pharmacological inhibitors or RNAi knockdown, have been shown to significantly reduced RCC cell proliferation *in vitro* and *in vivo (Zheng et al. 2016)*. Therefore, DNA-PKcs might be a valuable target for BHD-associated RCC intervention. Three DNA-PK inhibitors are currently being investigated in phase I/II clinical trials: CC-115, M9831 (VX-984), and Nedisertib (M3814; MSC2490484A). Of these, CC-115 is a small-molecule inhibitor of both DNA-PK and mTOR (Mortensen et al. 2015). CC-115 monotherapy has been evaluated in a phase I clinical study (NCT01353625) with an initial 44 patients treated across 10 dose-escalation cohorts (Munster et al. 2016). Preliminary anti-tumour activity was reported, although it is unclear if these responses are attributable to activity against DNA-PK or mTOR; especially considering that CC-115 led to hyperglycaemia, which is consistent with mTOR inhibition, and that associated pharmacodynamic studies provided evidence in favour of mTORC1 and mTORC2 inhibition (Munster et al. 2016). However,

more work is needed to understand the biological impact of the interaction between FLCN and DNA-PKcs before therapeutic exploitation is seriously considered.

Another interesting therapeutic option worth discussion is the use of CDK4/6 inhibitors. FLCN knockdown lead to an increase in cyclin D1 gene expression and protein abundance (chapter 4 and chapter 6). Furthermore, FLCN knockdown cells cycle through G1/S more readily than wild type controls (Kenyon et al. 2016), figure 6.6). CDK4/6-selective inhibitors, such as Palbociclib, Ribociclib and Abemaciclib, have shown significant benefits in clinical studies (Hamilton and Infante 2016; Eggersmann et al. 2019; Petrelli et al. 2019; Poratti and Marzaro 2019). Global genetic ablation of individual cyclins or inhibition of CDK activity in tumour-bearing mice selectively blocked the progression of cancers driven by oncogenic insults, whilst having limited effects on normal tissues (Deng et al. 1995; Liu et al. 2007). Collectively, studies suggest tumour cells become dependent on specific CDKs depending on the genetic lesions they carry, and hence, CDK inhibition may selectively target cancer cells while sparing normal tissues (Poratti and Marzaro 2019). In some instances, inhibition of CDK activity in mouse cancer models not only led to cell cycle arrest but also triggered tumour cell senescence or apoptosis (Puyol et al. 2010; Otto and Sicinski 2017).

Alternatively, inhibition of cell cycle proteins that are crucial for checkpoint function, such as Chk1 and WEE1, in cancer cells prevents cell cycle arrest during S or G2 phase and enables cell proliferation despite accumulation of DNA damage. This promotes cell death during mitosis by mitotic catastrophe (Castedo et al. 2004). This strategy is particularly useful to cancer cells with compromised G1-checkpoint, as these cells critically depend on the G2-checkpoint, especially in the presence of DNA damage-inducing drugs. FLCN knockdown was shown to result in elevated γH2AX suggesting an increase in DBS. Therefore, combining compounds to inhibit G2 checkpointing with a DNA damaging agent may promote tumour cell death in cancers with FLCN loss. Nevertheless, while it is fun to speculate potential therapeutic options, more research is needed to better understand the mechanistic actions of FLCN with DNA-PKcs, and within G1/S cell cycle regulation.

7.5 Future research directions

Future research directions directly based observations presented within the thesis have already been discussed. Namely, future work should focus on characterising the kinetics of γH2AX; aiming to establish when in the cell cycle they occur, or if repair facilitating binding partners are effected by FLCN knockdown. Co-ordinating γH2AX with the cell cycle will better inform future directions to take the research. For example, an accumulation of γH2AX foci during S phase strongly suggests DSB damage arise as a result of replication stress following FLCN loss. Moreover, exploring the cellular function of the FLCN/DNA-PKcs interaction would be highly informative. DNA-PKcs loss of function has huge consequences for the stability of cellular genomes, while unregulated DNA-PKcs activity has been implicated in multiple oncogenic pathways. Furthermore, DNA-PKcs is an attractive therapeutic target.

Discussed below are additional research directions that either complement or build on results shown within this thesis, and that have not previously been discussed within this chapter.

7.5.1 Eukaryotic translation initiation factor 4E (eIF4E); implicating FLCN in protein translation and/or nuclear export

The eukaryotic translation initiation factor 4E (eIF4E) is an important modulator of cellular growth and is often upregulated in many cancers (Ramaswamy et al. 2003; Pelletier et al. 2015). eIF4E has functions in both the cytoplasm and nucleus. In the cytoplasm, eIF4E is required for cap-dependent translation (Sonenberg and Gingras 1998). Here, eIF4E binds the methyl 7-guanosine (m^7G) cap moiety present on the 5' end of mRNAs and subsequently recruits the mRNA to the ribosome (Sonenberg and Gingras 1998). In the nucleus, eIF4E functions to promote the nuclear export of mRNAs (Culjkovic-Kraljacic et al. 2016). It should be noted that not all translation targets of eIF4E are nuclear export targets. For example, vascular endothelial growth factor (VEGF) mRNA is a translation target of eIF4E, but it's nuclear export does not involve eIF4E (Sonenberg and Gingras 1998). eIF4E was identified in the FLCN interactome (chapter 3). This protein narrowly missed out on being a hub protein as defined by being 2 standard deviation (SD) above mean degree within the whole interactome (eIF4E had a degree of 89, while the 2 SD upon the mean is 92.4) but it was a

bottleneck protein as defined by being 2 SD above mean betweenness centrality (BC) within the whole interactome (eIF4E had a BC of 0.015, 2 SD is 0.012). This suggests it may have an important role with regards to information flow within the interactome. Within the literature, as eIF4E is cited as the least abundant initiation factor and, therefore, is considered the rate-limiting factor for translation (Duncan and Hershey 1983; Galicia-Vazquez et al. 2012; Pelletier et al. 2015).

7.5.1.1 A role for FLCN in protein translation

Translation initiation in eukaryotes commences with the binding of the eukaryotic translation initiation factor 4F (eIF4F) complex to the 5'-cap of mRNAs (Topisirovic et al. 2011). eIF4F consists of the cap-binding subunit, eIF4E, the RNA helicase eIF4A, and the scaffolding protein eIF4G (Sonenberg and Hinnebusch 2009; Jackson et al. 2010). It is thought that eIF4A unwinds the secondary structure present in the 5'-UTR of the mRNA to promote the binding of the ribosome (Sonenberg and Hinnebusch 2009; Jackson et al. 2010). eIF4G interacts directly with eIF4E, eIF4A, eIF3 and the poly (A)-binding protein (PABP) (Sonenberg and Hinnebusch 2009; Jackson et al. 2010). The interaction of eIF4G with the multi-component initiation factor eIF3 is required in mammals for the recruitment of the 43S pre-initiation complex (which consists of the 40S ribosomal subunit and associated initiation factors), via the direct binding of eIF3 to the 40S subunit (Sonenberg and Hinnebusch 2009; Jackson et al. 2010). Following assembly at the cap structure, the 43S pre-initiation complex traverses the mRNA 5'UTR in a 5' to 3' direction, until it encounters the initiation codon where it stops and the 60S large ribosomal subunit joins to form the 80S ribosomal complex (Hinnebusch 2014). This is followed by the translation elongation step (Hinnebusch 2014). Although eIF4E is necessary for cap-dependent translation, its requirement varies dramatically among mRNAs (Bhat et al. 2015). It preferentially stimulates the translation of a subset of mRNAs (Bhat et al. 2015). These mostly encode proliferation and survival-promoting proteins such as cyclin D1, c-Myc, MDM2, VEGF, Survivin and Bcl-2 (Gehrke et al. 1983). In general, mRNAs containing long G/C-rich 5'-UTRs, with the potential of forming stable secondary structures are feebly translated (Gehrke et al. 1983). mRNAs with extensive secondary-structure in their 5'-UTRs are exceedingly dependent on eIF4E and eIF4A activity (Koromilas et al. 1992; Svitkin et al. 2001). Mechanistically the eIF4E-binding region within eIF4G can inhibit eIF4A helicase activity

168

when not bound to eIF4E. This inhibition is alleviated upon eIF4E binding to eIF4G (Feoktistova et al. 2013). In addition to eIF4E, both the eIF4G scaffolding proteins that bridge the mRNA and the ribosome (eIF4G1 and eIF4G2), and the hypoxia-induced eIF4E homologue, eIF4E2 where identified as potential FLCN interactors (appendix 1). Several lines of evidence suggest that human eIF4E2 has a distinct cytoplasmic role in the stress response, (Okumura et al. 2007; Feoktistova et al. 2013; Kubacka et al. 2013). Under genotoxic stress, the ubiquitin-like molecule ISG15 is covalently added to eIF4E2 to increase its cap-binding affinity (Okumura et al. 2007). Additionally, eIF4E2 was identified as an activator of translation initiation during periods of hypoxia (Feoktistova et al. 2013). The eIF4E2 interacts with eIF4A and eIF4G3 to form a hypoxic eIF4F complex that increases translation efficiency independent of mRNA abundance (Ho et al. 2016). Interestingly, the protein levels of eIF4E2, eIF4G3, and eIF4A do not change in hypoxia relative to normoxia (Feoktistova et al. 2013; Ho et al. 2016), suggesting that post-translational modifications or compartmentalisation may play a role in modifying their activities (Melanson et al. 2017).

A number of components of the eukaryotic translation initiation factor 3 (eIF3) were also identified in the FLCN interactome (EIF3A, EIF3E, EIF3G, and EIF3I). The eIF3 complex specifically targets and initiates translation of a subset of mRNAs involved in cell proliferation, including cell cycling, differentiation and apoptosis. eIF3 is the largest and most complex of all eukaryotic initiation factors (eIFs) comprised of five core subunits and seven non-essential subunits. It is though that that non-essential subunits may have regulatory functions (Zhou et al. 2005; Kim et al. 2007; Grzmil et al. 2010; Choudhuri et al. 2013). For example, eIF3A is the largest subunit. It is not required for the general function of eIF3, instead eIF3A regulates the translation of a subset of mRNAs that modulate the cell cycle. Specifically, eIF3A may be the translational regulator for proteins important for entrance into S phase (Saletta et al. 2010). Moreover, the eIF3A mRNA is found elevated in several cancers. Similarly, eIF3E knockdown had no major effect on global translation but numerous genes involved in cell cycle related processes were negatively regulated by eIF3E at the level of translation and inhibition of eIF3E expression has been shown to delay mitotic progression in human cells (Morris and Jalinot 2005). One final noteworthy protein identified in the FLCN interactome worthy of discussion is eukaryotic translation elongation factor 1 alpha 1 (eEF1A1). eEF1A1 was identified as a hub-bottleneck protein

suggesting it plays a significant role with regards to the integrity and function of the FLCN interactome. eEF1A1 has a well-defined role in protein synthesis, it delivers amino-acylated tRNAs to the A site of ribosome during translation elongation in a GTP-dependent manner (Mateyak and Kinzy, 2010; Li et al., 2013). Additionally, eEF1A1 can enter the nucleus to mediate the export of mature tRNAs and proteins. Indeed, eEF1A1 has been shown to function as a component of the nuclear export machinery in mammalian cells and is involved in the nuclear export of specific proteins such as the VHL tumour suppressor and poly(A)-binding protein (PABP1) (Khacho et al. 2008). Furthermore, reduced expression of EEF1A1 is seen in many cancers (breast, lung, gastric, kidney, head and neck) (Khacho et al. 2008). Collectively, FLCN seems to interact with several cell proliferative specific translation factors. It would therefore be interestingly to see if FLCN modulates protein translation in anyway.

7.5.1.2 A role for FLCN in nuclear export

Alternately, through eIF4E, FLCN may have a role in nuclear export. eIF4E export activity has been categorised as independent of ongoing protein synthesis (Culjkovic et al. 2006). At least three reported mRNAs have been characterised for the eIF4E-mediate nuclear export; CCND1 (cyclin D1), MCL1 (Induced myeloid leukemia cell differentiation protein Mcl-1), and ODC (ornithine decarboxylase) (Rousseau et al. 1996; Culjkovic et al. 2005,2006). Interestingly, evidence has linked the mRNA export function of eIF4E to its oncogenic activity. A mutant form of eIF4E (W73A), which results in enhanced eIF4E-dependent cyclin D1 mRNA export was shown to transform cells *in vitro* (Cohen et al. 2001; Topisirovic et al. 2003). Moreover, the W73A eIF4E cannot bind eIF4G and thus cannot act in translation, suggesting cellular transformation was due to mRNA export (Sonenberg and Gingras 1998). eIF4E has been demonstrated to promote nuclear export of cyclin D1 mRNAs via an element in the 3'UTR. This is interesting as previous study on the relationship between cyclin D1 and FLCN suggests FLCN regulates cyclin D1 expression post-transcriptionally by an unknown mechanism, and that the central portion of cyclin D1's 3'UTR is necessary for this regulation. Therefore, could FLCN modulate this eIF4E-mediated nuclear export of cyclin D1? How FLCN would do this, however, is currently unclear.

170

Alternately, FLCN may be involved in nuclear-cytoplasmic shuttling independent of eIF4E. Mass spectrometry analysis identified FLCN interacts with 11 components of the nucleopore (RANBP2, NUP205, NUP188, NUP54, NUP35 (NUP53), NUP155, NUP133, NUP160, NUP50, TPR, NUP153), and proteins that are essential for nuclear export (XPO1, XPO5, EIF4) (figure 5.7A). FLCN has been demonstrated to interact with NUP155 (Dr Sara Seifan, and Mr Matt Lines, data unpublished), where this interaction was strengthened under IR. There is also limited evidence to suggest it could be involved in establishing RAN:GTP gradients around nucleopore required for nuclear export of proteins (unpublished data, Prof. M Van Steensel). Furthermore, FLCN was shown important for cytoplasmic shuttling of TDP-43 (Xia et al. 2016). Two candidate proteins where briefly explored within this thesis; DNA-PKcs and cyclin D1. Neither produced evidence to convincingly say FLCN knockdown alters protein translocation both under basal and IR conditions. However, cyclin D1 required further testing.

7.5.2 Single-cell RNA sequencing (scRNA-seq) of FLCN knockdown cells

To date, there are 7 genes linked to hereditary forms RCC; Von Hippel-Lindau (VHL), tyrosine-protein kinase Met (MET), Fumarate Hydratase (FA), Succinate Dehydrogenase (SD), Tuberous Sclerosis Complex 1 (TSC1), Tuberous Sclerosis Complex 2 (TSC2), and FLCN. Apart from FLCN, each of these genes have relatively well described molecular and aetiological roles with regards to RCC. Furthermore, mutations within these genes typically promote a defined RCC subtype. For example, VHL mutations lead to upregulation of hypoxia inducible factors HIF1α and HIF2α. This facilitates metabolic reprogramming that results in the cytoplasmic accumulation of glycogen and lipids, and an increase in vascularisation to produce a network of small, thin walled blood vessels that are definitive of clear cell RCC (Linehan 2012; Haas and Nathanson 2014). Uniquely, however, FLCN mutations are associated with all RCC histological subtypes. The observed heterogeneity in RCC following FLCN loss could be caused by dysregulated cell cycle checkpoint and increase in DNA damage, coupled with metabolic changes previously observed that collectively push unregulated cell proliferation. This would promote an element of randomness to cellular transformation, thus giving rise to the heterogenous tumour phenotypes represented in BHD. However, it would be informative to investigate if it is possible to predict a cancer subtype that may arise, i.e., what are gene signatures that define a cell's transition into a

171

particular RCC subtype? Until recently, most genomic profiling studies have analysed cell populations. Although, cells of the same 'type' can exhibit substantial heterogeneity, reflecting finer sub-types, regulated functional variation, or inherent stochasticity (Altschuler and Wu 2010; Grun et al. 2015; Zeisel et al. 2015). In addition, colonialism is well documented in cancer (Altschuler and Wu 2010). Rapid technological advances in recent years have enabled genome-wide profiling of RNA, DNA, protein, epigenetic modifications, chromatin accessibility, and other molecular events in single cells (Tang et al. 2009; Navin et al. 2011; Bodenmiller et al. 2012; Farlik et al. 2015; Wagner et al. 2016). The scale and precision of such studies have continued to increase (Macosko et al. 2015). By exploring the identity of an individual cells, large-scale single-cell data allows specific molecular exploration of features without relying on prior definitions, hypotheses, or markers (Wagner et al. 2016). Single-cell RNA sequencing (scRNA-seq) can reveal complex and rare cell populations, uncover regulatory relationships between genes, and even track the trajectories of distinct cell lineages in development (Tang et al. 2009; Zeisel et al. 2015; McGranahan and Swanton 2017; Hwang et al. 2018). Transcriptional profiling of a single cell is a powerful approach to categorise heterogeneous cell states. This would be particularly useful to account for biological variation such as stochastic transcription. For example, over the last two decades, knowledge regarding the transcriptional landscape in RCC has come largely from whole tumour profiling using either microarray or RNA-seq data (Wu and Humphreys 2017). These studies have been highly informative, but they are fundamentally limited to describing a transcriptional average across a cell population. This may hide or skew signals of interest. The use of scRNA-seq within cancer has been used to explored intratumor heterogeneity for which it can reliably detect small sub-populations of tumour cells. These may have previously been masked when analysed alongside other low and high RNA expressing cells within a bulk tumour sample or monolayer of cultured cells (McGranahan and Swanton 2017). Within sporadic RCC, scRNA-seq has been used to identify molecular patterns found within RCC subtypes (Eckel-Passow et al. 2015; Chen et al. 2016a). For example, gene expression signatures have been used to predict tumour aggressiveness and progression within clear cell RCC (Kosari et al. 2005; Chen et al. 2014). Given the heterogeneity found in FLCN associated RCC and the large array of biological processes FLCN has been demonstrated to function in, scRNA-seq may provide a way to study gene expression dynamics that contribute to cellular transformation and inform

172

aetiological parameters of tumorigenesis upon FLCN loss. Exploring the transcriptomic landscape of individual cells over a period of time following FLCN loss (from low passage FLCN knockdown, to high passage or even ultra-high passage knockdown of ~2 years in culture) may even identify molecular signatures that promote the devolvement of one tumour subtype over another. Understanding the molecular and genetic features that characterise the RCC subtypes will provide the foundation for the development of better clinical management of RCC. scRNA-Seq could provide a wealth of knowledge for not just FLCN loss associated RCC, but also sporadic tumorigenesis.

7.5.3 FLCN-interacting proteins 1 and 2 (FNIP1 and FNIP2)

One final thought would be to explore the effect of the FLCN-interacting proteins (FNIP1 and FNIP2) have on the observations presented within this thesis. Both FNIP1 and FNIP2 have been noted to co-ordinate functions with FLCN in a tissue dependent manner. Binding of FLCN to both FNIP1 and FNIP2 is mediated through the C-terminal region of FLCN (Baba et al. 2006; Hasumi et al. 2008; Takagi et al. 2008). In BHD syndrome, the majority of mutations are predicted to result in a protein truncation (Schmidt et al. 2005). This results in the loss of the C-terminus of FLCN and therefore abolishes FLCN's ability to interact with FNIP1/FNIP2. It is generally considered that FNIP1 and FNIP2 are largely functionally redundant, however there maybe cell-type specific FNIP functions (Baba et al. 2012; Park et al. 2012; Reyes et al. 2015). Within the kidneys, FNIP1 and FNIP2 have somewhat interchangeable roles alongside FLCN in tumour suppression. FNIP1 and FNIP2 were found to be functionally redundant, with either able to interact with FLCN and inhibit tumorigenic growth in mouse kidneys (Hasumi et al. 2015). Only a complete loss of both FNIP1 and FNIP2 lead to the development of tumours and aberrant mTOR signalling as seen by FLCN loss (Hasumi et al. 2015). Mechanistically, FNIP1 and/or FNIP2 are required for FLCN's localisation to lysosomes during amino acid starvation, where FLCN interacts with the Rag proteins in order to regulate mTOR signalling (Petit et al. 2013; Tsun et al. 2013). Furthermore, both FNIP1 and FNIP2 have been found in complex with AMPK. Here they function alongside FLCN to inhibit AMPK activity (Preston et al. 2011; Siggs et al. 2016). Interestingly, no detectable phenotype in was observed in *Fnip2* only knockout mice, whereas *Fnip1*-deficiency produced phenotypes similar to those seen in *Flcn*-deficient mice in multiple organs, but not in kidneys. One study showed that absolute *Fnip2* mRNA copy number was low relative to *Fnip1* in mice organs

that showed phenotypes under *Fnip1* deficiency. However, *Fnip2* was comparable to *Fnip1* mRNA copy number in mouse kidney (Hasumi et al. 2015). Collectively this suggests, at least in kidney cells, both FNIPs function equally, and that it is FLCN that dictates biological effects.

Of particular interest, however, would be FNIP2. FNIP2 was shown to be important for O^6 methylguanine induction of apoptosis (Komori et al. 2009; Lim et al. 2012). O^6 methylguanine is an alkylated base that can mis-pair with thymine and cytosine during DNA replication to introduce DNA base mutations (Komori et al. 2009; Lim et al. 2012). This suggest FNIP2 may play a role in mis-match repair. Just as FLCN knockdown did not sensitise cells to IR-induced apoptosis, FNIP2 knockdown did not dramatically affect cells sensitivity to alkylating agents, etoposide, or UV irradiation. Equally, FNIP2 knockdown also lead to an increase in γH2AX (Komori et al. 2009). Therefore, it would be interesting to see if FNIP2 complexes with FLCN to bring about observed results presented within this thesis. For example, like the FLCN/FNIP2/AMPK protein complex, does FNIP2 complex with FLCN/DNA-PKcs.

7.6 Final summary

The molecular role of FLCN is complex. Having cell type, and context dependent functions that may be modulated by numerous protein interactions. As such, FLCN should be considered a generic regulator of cellular homeostasis rather than having a distinct cellular purpose. Nevertheless, this thesis highlights a novel aspect of FLCN's highly convoluted cellular role; implicating FLCN in genomic maintenance. FLCN cited functions can all be linked back to energy homeostasis. Interestingly, the surveillance and repair of DNA, the control of the cell cycle, and energy homeostasis are ever increasing being demonstrated to be highly interlinked processes. Cell division requires the co-ordinated generation of energy for multiple processes, including the synthesis of the machinery required for DNA replication and mitosis. The relationship between energy and the cell cycle is bidirectional, and several cell-cycle checkpoints can sense energy deficits in the cell, thus leading to cell-cycle arrest or exit (Salazar-Roa and Malumbres 2017; Laphanuwat et al. 2018). Thus, it seems sensible for a key cell cycle machinery component such as cyclin D1, to be involved in

energy control during the cell cycle (Laphanuwat et al. 2018). Equally, DNA-repair pathways can be influenced by cellular metabolic status and nutrient availability. DNA repair often requires chromatin remodelling through different histone post-translational modifications—including acetylation, methylation, phosphorylation, and ubiquitination; these are energy extensive processes (Turgeon et al. 2018). Furthermore, cell metabolism can regulate DNA-repair through the regulation of the pool of nucleotides required for repair (Turgeon et al. 2018) Indeed, many different metabolic pathways are involved in *de novo* nucleotide synthesis (Patra and Hay 2014; Turgeon et al. 2018). Again, having a direct impact on energy homeostasis would be beneficial to DDR components such as DNA-PKcs. Nevertheless, FLCN precise role in genomic maintenance is undefined. Further research to should focus on understanding this role from a mechanistic point of view and begin to explore how FLCN's DDR and cell cycle roles integrate with that of energy balance and cellular trafficking. Given that FLCN loss predisposes individuals to all RCC subtypes, understanding the molecular mechanisms of FLCN as a tumour suppressor could reveal new cancer promoting pathways linked to RCC progression. Indeed, while rare themselves, inherited genetic conditions that promote the development of tumours can provide valuable insight into the molecular mechanisms behind tumorigenesis within the general population.

Supplementary figure 1: FLCN knockdown impacts telomeres
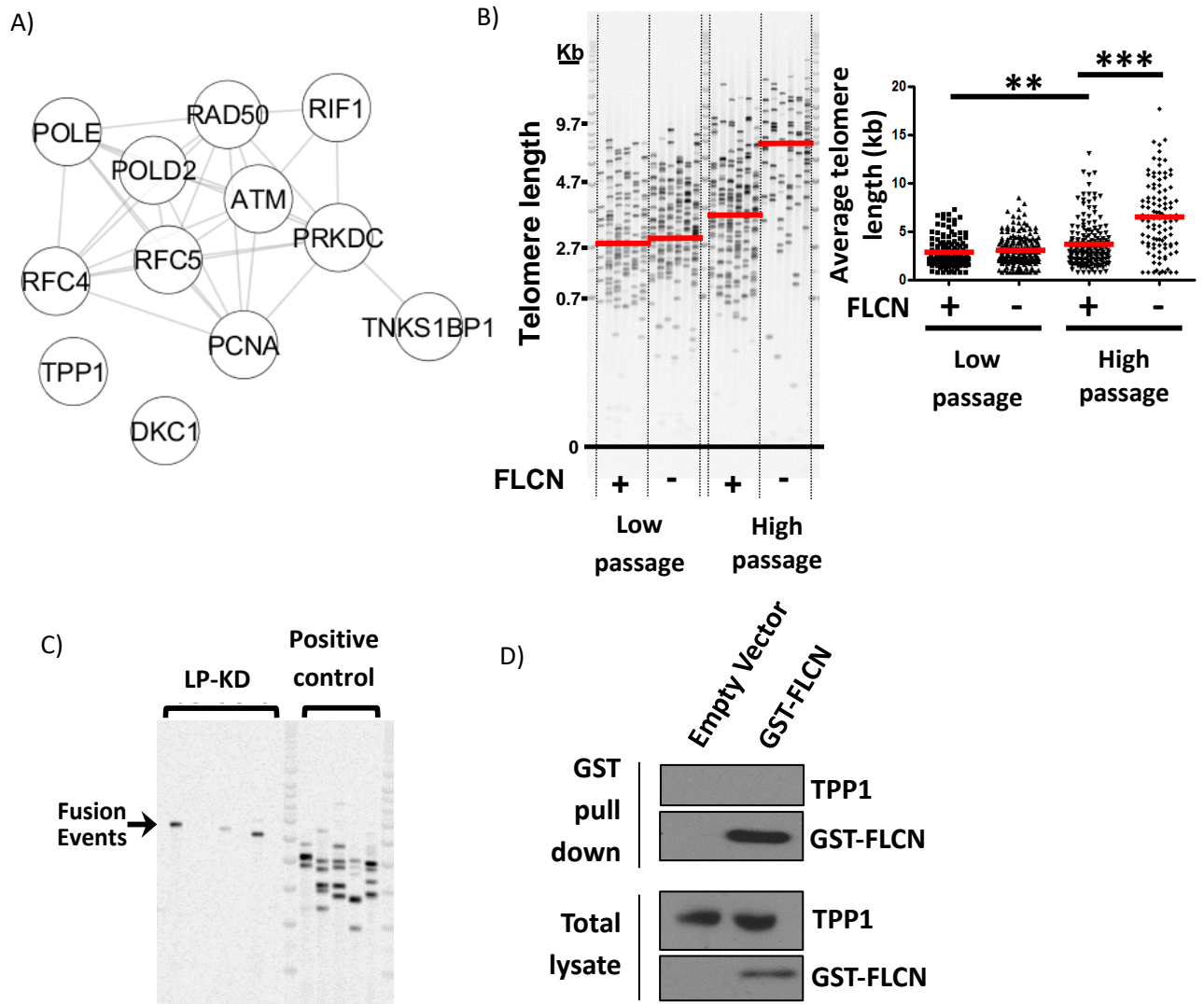
Figure S1 FLCN knockdown impacts telomeres. A) Telomere components found in the FLCN interactome. B) Single telomere length analysis (STELA) shows increase in telomere length following FLCN loss over time. Red line indicates mean length in the gel (left) and graph (right). ** p < 0.01, *** p < 0.001. C) Telomere fusion events were observed in low passage FLCN knockdown cells. Single telomere length analysis (STELA) and telomere fusion analysis was performed by Dr Rhiannon Jones, Cardiff University as described in (Baird et al. 2003; Capper et al. 2007). Figures B and C were taken from the PhD grant application submitted to Tenovus cancer care by Dr Andrew Tee. D) GST-tagged FLCN was overexpressed in HEK293 cells and used as bait to validate interaction between FLCN and endogenously expressed TPP1. Due to time constraints, and a lack of validation of FLCN interacting with telomere components TPP1 and RIF1 (shown in figure 3.6C), telomere dynamics upon FLCN knockdown was not explored further.

Appendix 1: Full list of potential FLCN interactors identified by mass spectrometry

Protein Name	Degree	BC	Protein Name	Degree	BC
AASDHPPT	8	1.57E-04	BAG5	5	2.39E-04
ABI1	11	3.66E-04	BAT1	Not mapped in STRING	
ACACA	91	0.01349732	BAT2	Not mapped in STRING	
ACLY	117	0.02286661	BAT2L	Not mapped in STRING	
ACOT8	Not mapped in STRING		BAX	27	6.39E-04
ACTA2	84	0.01179367	BCCIP	10	2.64E-04
ACTB	116	0.0217231	BCOR	3	6.63E-05
ACTBL2	67	0.00469542	BIRC6	4	1.11E-05
ADSS	18	4.23E-04	BRE	12	5.70E-04
AHCY	19	4.09E-04	BTAF1	8	1.06E-04
AIP	3	3.60E-07	BUB1B	68	0.002048
ALB	74	0.01747427	BUB3	75	0.00324558
ALDH1B1	19	5.63E-04	BZW2	6	1.89E-04
ALDOA	21	0.00145022	C11orf58	2	8.41E-06
ANAPC1	46	0.00159967	C12orf5	17	2.00E-04
ANKHD1	7	9.09E-05	C14orf166	17	4.66E-04
ANKRD17	5	6.66E-06	C1orf174	Not mapped in STRING	
ANXA2	16	0.00171845	C1QBP	32	0.00154119
ANXA2P2	Not mapped in STRING		C20orf117	Not mapped in STRING	
AP1GBP1	Not mapped in STRING		C22orf28	10	9.35E-04
APIP	4	2.61E-05	C22orf9	Not mapped in STRING	
APOOL	4	0.00327557	C3orf75	Not mapped in STRING	
ARCN1	12	3.57E-04	C5orf33	Not mapped in STRING	
ARD1A	Not mapped in STRING		C5orf51	1	0
ARFGAP1	9	4.68E-05	CA2	13	0.00268692
ARFIP2	4	1.18E-05	CACYBP	10	3.57E-04
ARHGAP5	1	0	CAD	132	0.02412087
ASCC3	26	8.08E-04	CALM1	67	0.00530828
ASNS	23	4.65E-04	CALM2	Not mapped in STRING	
ATG2A	7	0.00339191	CALM3	Not mapped in STRING	
ATM	59	0.00447422	CAMSAP1L1	Not mapped in STRING	
ATP5A1	61	0.00442671	CAND1	11	2.95E-04
ATP5B	72	0.00500404	CAP1	16	0.00116887
ATP5C1	36	0.00194902	CAPZA1	16	6.89E-04
ATP6V1B2	21	8.26E-04	CAPZB	17	4.72E-04
ATP6V1D	8	1.47E-05	CARM1	13	1.27E-04
ATP6V1E1	11	4.32E-04	CBR1	7	6.16E-05
ATP6V1H	9	1.02E-04	CBR3	7	6.16E-05
ATR	46	0.00468388	CBS	27	0.00143392
ATXN10	5	1.06E-04	CBWD2	1	0

ATXN2	16	8.30E-04	CCS	10	0.00328105
ATXN2L	7	7.32E-05	CCT2	112	0.00899685
ATXN3	15	0.00189512	CCT3	94	0.00734996
AURKA	83	0.0095123	CCT4	Not mapped in STRING	
BAG4	7	3.07E-05	CCT5	106	0.00786906
CCT6A	72	0.00484691	DHX30	5	2.93E-05
CCT7	107	0.00932019	DHX36	9	1.91E-05
CCT8	41	8.06E-04	DHX9	57	0.00381552
CCT8	Not mapped in STRING		DIAPH1	13	3.38E-04
CDC2	Not mapped in STRING		DIAPH3	11	1.74E-04
CDC20	88	0.00556448	DICER1	55	0.00788685
CDC37	12	2.23E-04	DKC1	52	0.00292496
CDK1	145	0.02768301	DNAJA1	41	0.00622249
CDK3	50	0.00162173	DNAJA2	27	1.62E-04
CDK4	65	0.00313211	DNAJA3	27	2.53E-04
CDKN2A	46	0.0035106	DNAJB11	24	0.00414955
CEP170	Not mapped in STRING		DNAJC7	24	5.46E-04
CEP55	23	6.76E-04	DNMT1	28	0.00462831
CFL1	40	0.00398562	DOCK6	1	0
CHD4	20	3.69E-04	DOCK7	2	0.00326797
CKAP5	52	0.00202422	DOCK9	Not mapped in STRING	
CKB	11	1.22E-04	DPH2	5	6.60E-05
CLASP2	33	2.85E-04	DPM1	13	4.14E-04
CLIC1	8	1.57E-04	DRG1	7	6.71E-04
CLNS1A	12	3.89E-04	DSG1	4	0.0012007
CLTC	40	0.00743698	DSP	3	4.32E-04
CLTCL1	31	0.00555338	DUT	42	0.00208268
CMAS	7	3.20E-04	DYNC1H1	45	0.008754
CNN3	1	0	DYNC1LI2	19	4.99E-04
CNOT1	20	8.88E-04	EDC3	7	4.26E-05
COPA	16	0.00422151	EEF1A1	112	0.01379316
COPZ1	13	4.44E-04	EEF1A2	66	0.00141771
CORO1C	20	5.03E-04	EEF1B2	51	5.12E-04
CPNE1	2	0	EEF1D	50	8.44E-04
CPNE7	1	0	EEF1E1	35	0.00115753
CRKL	7	3.80E-04	EEF1G	95	0.00757227
CROP	Not mapped in STRING		EGLN1	6	0.00332568
CSTB	12	3.09E-04	EIF2S3	60	0.00325508
CTBP2	14	1.67E-04	EIF3A	70	0.00475799
CXorf26	1	0	EIF3E	60	0.0018886
CXorf56	3	2.96E-05	EIF3G	48	7.28E-04
CYFIP1	12	0.00121175	EIF3I	52	0.00409215
DARS	20	9.71E-05	EIF3L	44	9.36E-05
DBNL	22	0.00135874	EIF4E	89	0.0146893

DCAF7	9	1.49E-04	EIF4E2	9	1.49E-04
DCD	Not mapped in STRING		EIF4G1	79	0.0079174
DDB1	36	0.00288404	EIF4G3	15	4.48E-04
DDX49	31	0.00127448	EIF5A2	47	9.22E-04
DDX6	23	0.00510881	ELAVL1	62	0.0048738
DENND4A	Not mapped in STRING		ELP3	16	0.00129349
DGCR14	4	3.11E-05	ELP6	5	2.54E-05
ENO1	88	0.00852909	GSTM4	5	5.57E-06
ENO2	67	0.00366656	GSTP1	14	0.00176789
EPPK1	4	9.72E-06	GTF2I	11	1.01E-04
EPRS	118	0.01377429	GTF3C1	8	1.66E-04
EPX	3	1.02E-04	GTF3C5	4	2.29E-05
ERO1L	4	5.40E-07	HAT1	29	0.00831237
ESYT1	2	9.84E-06	HDAC1	66	0.01252736
EXOSC2	32	0.00130986	HDAC2	54	0.00468868
EXOSC6	26	4.98E-04	HDGF	2	3.37E-06
FAM120B	1	0	HDLBP	11	3.12E-04
FAM62A	Not mapped in STRING		HEATR1	33	6.91E-04
FAM98A	4	1.53E-05	HEATR5A	2	1.08E-06
FANCD2	21	3.00E-04	HECTD1	17	1.60E-04
FANCI	24	3.74E-04	HIST1H1C	5	2.44E-05
FARSA	25	2.88E-04	HIST2H2BE	52	0.00588673
FASN	20	0.00180367	HNRNPA1	91	0.01065132
FKBP4	10	3.65E-05	HNRNPA2B1	57	0.00310668
FLAD1	15	6.18E-05	HNRNPA3	51	0.00180908
FLCN	7	0.00184071	HNRNPAB	34	8.39E-04
FLII	15	2.89E-04	HNRNPCL1	19	2.34E-04
FLNA	31	0.00158237	HNRNPD	58	0.005184
FLNB	18	6.57E-04	HNRNPF	35	5.23E-04
FLNC	20	5.68E-04	HNRNPH1	49	0.00973122
FNIP1	5	9.36E-05	HNRNPK	56	0.00406562
FNIP2	4	8.08E-05	HNRNPL	37	9.75E-04
FNTA	4	0.00327541	HRNR	Not mapped in STRING	
FNTB	1	0	HSD17B10	26	0.00343227
FSCN1	12	2.24E-04	HSD17B12	7	4.01E-05
FTO	1	0	HSP90AA1	153	0.0400851
FTSJ1	22	0.003461	HSP90AA2	Not mapped in STRING	
G6PD	23	3.04E-04	HSP90AB1	105	0.0104931
GAPDH	142	0.02650159	HSPA1A	88	0.00837303
GAPVD1	6	4.50E-05	HSPA1B	Not mapped in STRING	
GART	87	0.00691245	HSPA1L	69	0.00435919
GCLM	8	2.72E-05	HSPA7	Not mapped in STRING	
GCN1L1	23	0.0022618	HSPA8	161	0.03225994
GIGYF2	5	7.16E-05	HSPBP1	11	1.01E-04

GLRX3	11	2.50E-04	HSPC152	Not mapped in STRING	
GNB2L1	82	0.00636729	HSPD1	102	0.01432717
GOPC	5	1.27E-04	HTT	21	7.51E-04
GPKOW	31	1.56E-04	HUWE1	33	0.00302487
GPN1	6	9.33E-06	IARS	46	0.00223831
GRWD1	22	0.00130636	IFIT5	7	1.65E-05
GSR	43	0.00749891	IKBKAP	17	0.00180799
GSTM2	5	5.57E-06	ILF2	35	0.0012066
GSTM3	6	8.74E-05	ILK-2	Not mapped in STRING	
IMPDH2	114	0.01697763	MAP4	9	1.87E-04
INPP5K	3	2.19E-05	MAT2A	27	9.25E-04
IPO5	28	0.0011855	MAT2B	6	1.20E-04
IPO7	16	1.45E-04	MAZ	2	0
IRS2	10	1.22E-04	MCCC2	11	1.52E-04
ISCA2	4	3.29E-05	MDN1	13	0.00141634
ISYNA1	11	3.85E-04	METTL1	10	2.92E-04
KATNA1	3	0	MLLT4	6	9.84E-05
KCTD12	Not mapped in STRING		MNT	2	0
KDM3B	Not mapped in STRING		MPP2	8	8.17E-06
KDM5C	10	1.93E-04	MPP6	13	3.88E-04
KHDRBS1	24	0.00139968	MSH6	37	0.00313329
KIAA0368	42	0.00239671	MTHFD2	14	2.05E-04
KIAA0391	4	1.35E-04	MTMR14	5	6.52E-05
KIAA0664	11	3.00E-04	MTOR	75	0.01252427
KIAA0930	3	0	MYH10	18	0.00148921
KIAA1429	1	0	MYH9	31	0.00115329
KIAA1486	Not mapped in STRING		MYL6	20	5.30E-04
KIF1B	10	2.68E-04	MYO10	15	3.12E-04
KLF4	12	3.70E-05	NAA10	6	2.22E-04
KLHL15	Not mapped in STRING		NACA	37	3.65E-04
KNTC1	49	0.0026243	NADKD1	1	0
KPNA1	27	6.58E-04	NAE1	17	3.69E-04
KPNA2	57	0.00401336	NAMPT	4	4.24E-05
KPNA3	19	2.28E-04	NAP1L1	22	0.00295745
KPNA4	26	5.99E-04	NAP1L4	8	3.81E-05
L2HGDH	2	1.22E-05	NASP	12	2.11E-04
LANCL1	Not mapped in STRING		NCAPD2	23	4.94E-04
LANCL2	Not mapped in STRING		NCAPD3	14	4.84E-04
LARP1	14	1.56E-04	NCAPG	28	4.70E-04
LARS	32	7.62E-04	NDUFAF3	1	0
LCN1	1	0	NEFM	1	0
LDHA	52	0.00187997	NF1	33	6.60E-04
LDHB	55	0.00229064	NIPBL	10	4.85E-05
LGALS7	3	0	NME1	65	0.00349539

180

LGALS7B	Not mapped in STRING		NONO	13	3.34E-04
LOC389842	Not mapped in STRING		NOP58	64	0.00504362
LPCAT1	Not mapped in STRING		NPM1	62	0.0043789
LRPPRC	8	9.72E-05	NT5DC2	Not mapped in STRING	
LRRC59	Not mapped in STRING		NUBP2	10	9.48E-04
LTN1	14	5.60E-05	NUDC	29	8.87E-04
LUC7L2	22	1.94E-04	NUP133	50	0.00227649
LUC7L3	17	4.08E-04	NUP153	41	0.00152142
LYZ	12	0.00335078	NUP155	39	0.00139126
MAP1B	14	0.00215369	NUP160	45	0.00128665
MAP3K7IP1	Not mapped in STRING		NUP188	25	1.23E-04
NUP205	32	7.41E-04	POLR1C	60	0.00510066
NUP35	29	0.00256602	POLR2B	113	0.02123163
NUP50	42	0.00364193	PPA1	38	0.00241027
NUP54	29	5.36E-04	PPAT	18	1.63E-04
ORC5	14	8.10E-05	PPIA	44	0.00296498
ORC5L	Not mapped in STRING		PPM1B	21	8.64E-04
OTUB1	8	0.00330249	PPP1CB	23	4.74E-04
PAICS	86	0.01099495	PPP1CC	52	0.00745493
PAIP1	14	5.94E-04	PPP2CA	125	0.01820768
PBK	38	0.0021062	PPP2R1A	110	0.01305476
PCBP1	46	0.00292856	PPP2R1B	56	0.00159694
PCBP2	39	0.0013708	PPP2R2A	62	0.00194811
PCNA	105	0.01447422	PPP2R2B	34	0.00153929
PCYT1A	3	4.27E-06	PPP2R5C	52	6.94E-04
PDCD2L	Not mapped in STRING		PPP2R5D	58	0.00196229
PDCD4	15	4.88E-04	PPP2R5E	50	5.99E-04
PDCD6	10	5.33E-04	PPP5C	26	5.57E-04
PDIA6	41	0.00249717	PPP6R3	10	4.05E-04
PDS5A	31	3.75E-04	PRDX1	43	0.00195091
PEF1	3	2.22E-05	PRDX4	26	7.04E-04
PELO	9	3.11E-04	PRDX5	16	7.39E-04
PEPD	8	0	PRG2	Not mapped in STRING	
PFAS	81	0.00941427	PRIM2	Not mapped in STRING	
PFDN2	21	9.61E-05	PRKAG1	28	0.00322919
PFN2	18	3.90E-04	PRKDC	61	0.00567711
PGAM5	3	0	PRMT1	31	0.00194359
PGM3	10	1.37E-05	PRPF19	63	0.00932331
PHB	31	0.00183159	PRPF38B	1	0
PHF23	Not mapped in STRING		PRPF8	60	0.00498235
PHGDH	33	0.00123346	PRPS1	22	3.06E-04
PI4KA	16	0.0017761	PRPSAP2	13	1.41E-04
PIK3C2A	25	0.00362704	PRRC2A	4	6.52E-05
PIK3R4	10	5.18E-04	PRRC2B	1	0

181

PIP	Not mapped in STRING		PSMA1	59	0.00324669
PIP4K2C	6	2.52E-04	PSMA4	53	0.00404131
PKM	60	0.00381676	PSMA7	45	4.91E-04
PKM2	Not mapped in STRING		PSMC1	48	0.00291621
PKP4	3	3.08E-05	PSMC2	59	0.00224815
PLCG1	17	0.00197279	PSMC3	53	0.00287866
PLEC	56	0.0054181	PSMC4	52	0.00204496
PLEC1	Not mapped in STRING		PSMC5	53	0.00215172
PM20D2	Not mapped in STRING		PSMC6	64	0.00459512
PNO1	32	9.60E-04	PSMD11	45	6.87E-04
POLD2	21	2.88E-04	PSMD12	45	0.00210698
POLDIP3	24	5.14E-04	PSMD14	81	0.00844395
POLE	59	0.00290838	PSMD3	42	3.82E-04
PSMD6	44	0.0010217	RPL5	94	0.00383517
PSMD8	41	0.00122418	RPL6	74	0.00194139
PSMD9	43	0.001028	RPL7	86	0.00367086
PSME1	38	8.54E-04	RPL7A	81	0.00405323
PSME2	38	9.32E-04	RPL7P32	Not mapped in STRING	
PSME3	40	0.00195273	RPL8	88	0.00233152
PSMF1	36	3.41E-05	RPLP0	101	0.0072243
PSMG1	16	1.01E-04	RPLP2	61	0.00100607
PTBP1	47	0.00167229	RPN2	45	0.00106645
PUM1	7	1.56E-04	RPP30	22	4.66E-05
PURA	3	1.63E-05	RPRD2	5	5.18E-05
PYCRL	3	0	RPS13	82	0.00216
RAD50	40	0.00194645	RPS14	78	0.00167172
RAD54L2	7	9.86E-05	RPS16	78	0.00165818
RAE1	38	0.00189132	RPS17	46	1.11E-04
RANBP2	96	0.01149267	RPS18	71	0.00174118
RAPGEF6	Not mapped in STRING		RPS19	69	8.95E-04
RBBP4	31	0.00127374	RPS2	96	0.00386386
RBBP7	31	0.00152103	RPS20	80	0.00549458
RBM12B	3	5.32E-05	RPS21	60	6.71E-04
RBM16	Not mapped in STRING		RPS24	69	0.00144033
RBM22	33	1.18E-04	RPS27	78	0.00346429
RBM4	13	4.69E-04	RPS27A	Not mapped in STRING	
RBM6	Not mapped in STRING		RPS27L	57	4.68E-04
RC3H1	1	0	RPS3	99	0.00580479
RC3H2	1	0	RPS3A	78	0.00264861
RCC2	26	2.18E-04	RPS4X	82	0.00301733
RCN2	Not mapped in STRING		RPS6	90	0.0063992
RFC2	31	0.00182988	RPS8	75	0.00227805
RFC4	71	0.00464623	RPSAP12	Not mapped in STRING	
RFC5	45	0.00160218	RPSAP15	Not mapped in STRING	

RG9MTD1	Not mapped in STRING		RPSAP55	Not mapped in STRING	
RIC8A	Not mapped in STRING		RTN4IP1	7	1.25E-04
RIF1	7	2.47E-05	RUVBL1	47	0.00242772
RNASE3	2	0	RUVBL2	34	0.00151223
RNF160	Not mapped in STRING		S100A10	7	2.49E-04
RNH1	7	5.38E-05	S100A9	14	6.48E-04
RNMT	9	4.24E-04	SAAL1	Not mapped in STRING	
RPL12	74	0.00321762	SAPS3	Not mapped in STRING	
RPL15	75	0.00162371	SBF1	Not mapped in STRING	
RPL22	58	7.64E-04	SCAF8	6	1.05E-04
RPL23	68	0.00113525	SCLY	10	2.04E-04
RPL27	56	2.33E-04	SDCCAG3	Not mapped in STRING	
RPL36AP37	Not mapped in STRING		SEC16A	4	7.14E-05
RPL38	56	2.92E-04	SEC24B	9	3.10E-04
RPL4	98	0.00391575	SERBP1	13	4.61E-04
SERPINB6	6	2.10E-05	TCP1	108	0.00983764
SF3A3	42	0.00153403	TFCP2	2	0
SF3B1	61	0.00944436	TH1L	9	3.99E-05
SF3B14	33	1.60E-04	THADA	6	0.0033768
SF3B4	35	3.14E-04	THOC2	30	0.0042978
SFRS7	Not mapped in STRING		THOC3	19	0.00106172
SIP1	Not mapped in STRING		THUMPD3	1	0
SKP1	63	0.00548102	TIMM50	9	8.06E-05
SLC25A1	20	0.00172455	TIPRL	10	2.67E-04
SLC25A11	1	0	TMPO	14	1.01E-04
SLC25A3	27	6.63E-04	TNKS1BP1	8	1.13E-04
SLC25A4	15	0.00338487	TNRC6B	7	3.09E-04
SLC25A5	37	3.84E-04	TOE1	5	7.52E-05
SLC25A6	31	4.07E-04	TP53	169	0.05376185
SLC7A9	4	0	TPM1	25	0.00130876
SLK	9	1.79E-04	TPM3	19	4.49E-04
SMARCA4	60	0.00682904	TPM4	24	6.37E-04
SMC2	32	6.96E-04	TPP1	2	1.01E-05
SMC4	36	7.81E-04	TPR	45	0.00305962
SNRNP200	50	0.00559067	TRAF2	31	7.67E-04
SNRPB	64	0.00390637	TRAPPC2L	3	1.49E-04
SNRPC	39	5.56E-04	TRIM65	Not mapped in STRING	
SNRPE	51	0.00129776	TRIP12	35	0.00199184
SNX27	Not mapped in STRING		TRIP13	26	4.83E-04
SPAG9	1	0	TRIP6	12	3.32E-04
SPTAN1	47	0.00907029	TRMT10C	6	1.41E-04
SRM	9	7.48E-05	TRMT11	8	1.00E-04
SRPRB	36	7.54E-04	TRMT112	8	0.00349947
SRSF7	54	0.00246868	TROVE2	2	9.60E-06

Gene	Value1	Value2	Gene	Value1	Value2
STAG2	37	0.00189833	VIM	36	0.00587713
STARD7	1	0	TRRAP	33	0.00245945
STK25	9	3.76E-05	TSC1	21	7.30E-04
STK4	6	8.79E-04	TSC2	27	0.00261116
STRAP	19	8.51E-04	TSNAX	3	6.54E-05
STUB1	36	0.00249913	TTC4	13	9.10E-04
SUGT1	18	2.25E-04	TUBA1A	52	0.00273596
SUPT5H	50	0.00729301	TUBA1C	49	0.00153618
SYNCRIP	33	0.00243678	TUBA3D	31	9.44E-04
SYNRG	4	0	TUBA4A	54	0.00171606
TAB1	11	1.38E-04	TUBAL3	32	3.61E-04
TARBP1	9	3.09E-04	TUBB	57	0.00237986
TARDBP	19	0.00106513	TUBB1	40	6.36E-04
TBC1D4	7	1.66E-06	TUBB2A	51	0.00184416
TBCB	14	2.85E-05	TUBB2C	Not mapped in STRING	
TBCE	15	3.40E-05	TUBB3	36	0.00176117
TCEB2	25	0.00130656	TUBB4	Not mapped in STRING	
TUBB4B	59	0.00252014	TUBB4A	48	9.38E-04
TUBB6	42	8.43E-04	WDR77	16	3.63E-04
TUBG1	37	0.0016588	XIAP	24	8.08E-04
TUFM	59	0.00298755	XPO1	101	0.01931212
TXN	63	0.00555186	XPO5	29	0.00184956
TXNDC5	36	0.00182089	XRN1	26	0.00142999
U2AF1	57	0.00230364	YLPM1	1	0
U2AF2	64	0.00495144	YRDC	2	0
UBA1	39	0.00309404	YWHAB	41	0.00426707
UBAP2	5	1.09E-04	YWHAE	39	0.00185874
UBAP2L	6	2.89E-04	YWHAG	36	0.00185471
UBB	Not mapped in STRING		YWHAQ	37	0.0023876
UBC	150	0.03059425	YWHAZ	46	0.00400644
UBE2L3	27	0.00134361	YY1	30	0.00234145
UBE2O	13	0	ZC3H15	5	0.00337035
UBR4	22	8.48E-04	ZC3HAV1L	Not mapped in STRING	
UBR5	17	6.60E-04	ZCCHC11	5	3.68E-05
UBXN1	9	1.75E-04	ZEB2	6	1.71E-05
UCK2	6	9.41E-06	ZFYVE16	2	9.40E-07
UGCGL1	Not mapped in STRING		ZMYM4	3	0
UGGT1	4	2.05E-05	ZNF318	Not mapped in STRING	
UPF1	66	0.00467004	ZNF362	Not mapped in STRING	
USP24	8	1.25E-04	ZNF609	Not mapped in STRING	
USP34	12	1.90E-04			
USP47	5	3.45E-05			
USP7	35	0.01004796			
USP9X	24	0.00180067			

Appendix 2: Full list of GO term enrichment

Merged name	GO Biological process	Pathway description	Observed count	FRD *P*value
Cell cycle	GO.0007049	cell cycle	129	6.05E-32
Cell cycle	GO.0000278	mitotic cell cycle	105	7.56E-35
Cell cycle	GO.1903047	mitotic cell cycle process	98	7.3E-34
Cell cycle	GO.0022402	cell cycle process	115	3.91E-33
Cell cycle	GO.0031571	mitotic G1 DNA damage checkpoint	27	1.78E-19
Cell cycle	GO.0044770	cell cycle phase transition	50	1.82E-19
Cell cycle	GO.0051439	regulation of ubiquitin-protein ligase activity involved in mitotic cell cycle	29	1.96E-19
Cell cycle	GO.0007093	mitotic cell cycle checkpoint	37	2.64E-19
Cell cycle	GO.1901991	negative regulation of mitotic cell cycle phase transition	36	4.85E-19
Cell cycle	GO.0044772	mitotic cell cycle phase transition	49	5.31E-19
Cell cycle	GO.1901988	negative regulation of cell cycle phase transition	37	5.85E-19
Cell cycle	GO.0072431	signal transduction involved in mitotic G1 DNA damage checkpoint	25	9.73E-19
Cell cycle	GO.0000075	cell cycle checkpoint	41	1.8E-18
Cell cycle	GO.0051437	positive regulation of ubiquitin-protein ligase activity involved in regulation of mitotic cell cycle transition	25	7.17E-18
Cell cycle	GO.0044774	mitotic DNA integrity checkpoint	29	9E-18
Cell cycle	GO.0006977	DNA damage response, signal transduction by p53 class mediator resulting in cell cycle arrest	24	1.05E-17
Cell cycle	GO.0044773	mitotic DNA damage checkpoint	28	1.77E-17
Cell cycle	GO.1901990	regulation of mitotic cell cycle phase transition	42	1.85E-17
Cell cycle	GO.1901987	regulation of cell cycle phase transition	43	3.82E-17
Cell cycle	GO.2000134	negative regulation of G1/S transition of mitotic cell cycle	28	5.44E-17
Cell cycle	GO.0010948	negative regulation of cell cycle process	40	8.25E-17
Cell cycle	GO.0045930	negative regulation of mitotic cell cycle	39	9.24E-17
Cell cycle	GO.0071158	positive regulation of cell cycle arrest	25	1.02E-15
Cell cycle	GO.0051726	regulation of cell cycle	80	1.2E-15
Cell cycle	GO.0045786	negative regulation of cell cycle	52	5.6E-15
Cell cycle	GO.2000045	regulation of G1/S transition of mitotic cell cycle	29	1.44E-14
Cell cycle	GO.0000082	G1/S transition of mitotic cell cycle	32	2.35E-14
Cell cycle	GO.0071156	regulation of cell cycle arrest	26	3.21E-14
Cell cycle	GO.0007346	regulation of mitotic cell cycle	50	2.45E-13
Cell cycle	GO.0010564	regulation of cell cycle process	52	2.56E-12

Cell cycle	GO.0045787	positive regulation of cell cycle	35	1.19E-09
Cell cycle	GO.0090068	positive regulation of cell cycle process	31	1.25E-09
Cell cycle	GO.0007067	mitotic nuclear division	35	1.79E-08
Cell cycle	GO.0007077	mitotic nuclear envelope disassembly	13	2.14E-08
Cell cycle	GO.0051301	cell division	40	2.12E-07
Cell cycle	GO.0000280	nuclear division	36	0.00000139
Cell cycle	GO.0000086	G2/M transition of mitotic cell cycle	19	0.00000382
Cell cycle	GO.0000070	mitotic sister chromatid segregation	9	0.00851
Cell cycle	GO.0007094	mitotic spindle assembly checkpoint	6	0.0111
Cell cycle	GO.0010389	regulation of G2/M transition of mitotic cell cycle	7	0.0163
Cell cycle	GO.0007084	mitotic nuclear envelope reassembly	3	0.0498
Chromatin structure	GO.0006325	chromatin organization	39	0.000541
Chromatin structure	GO.0043044	ATP-dependent chromatin remodeling	10	0.00224
Chromatin structure	GO.0016568	chromatin modification	31	0.00738
Chromatin structure	GO.0032508	DNA duplex unwinding	7	0.0201
Chromatin structure	GO.0006338	chromatin remodeling	13	0.0223
Chromatin structure	GO.0031497	chromatin assembly	11	0.0259
Chromatin structure	GO.0006333	chromatin assembly or disassembly	12	0.0272
DNA damage, repair and surveillance	GO.0006284	base-excision repair	8	0.00299
DNA damage, repair and surveillance	GO.0031571	mitotic G1 DNA damage checkpoint	27	1.78E-19
DNA damage, repair and surveillance	GO.0072422	signal transduction involved in DNA damage checkpoint	26	2.38E-19
DNA damage, repair and surveillance	GO.0072431	signal transduction involved in mitotic G1 DNA damage checkpoint	25	9.73E-19
DNA damage, repair and surveillance	GO.0044774	mitotic DNA integrity checkpoint	29	9E-18
DNA damage, repair and surveillance	GO.0006977	DNA damage response, signal transduction by p53 class mediator resulting in cell cycle arrest	24	1.05E-17
DNA damage, repair and surveillance	GO.0006974	cellular response to DNA damage stimulus	70	1.57E-17
DNA damage, repair and surveillance	GO.0044773	mitotic DNA damage checkpoint	28	1.77E-17
DNA damage, repair and surveillance	GO.0000077	DNA damage checkpoint	32	5.72E-17
DNA damage, repair and surveillance	GO.0031570	DNA integrity checkpoint	33	5.73E-17
DNA damage, repair and surveillance	GO.0072331	signal transduction by p53 class mediator	26	1.45E-12

DNA damage, repair and surveillance	GO.0006281	DNA repair	42	7.74E-10
DNA damage, repair and surveillance	GO.0071478	cellular response to radiation	15	0.00126
DNA damage, repair and surveillance	GO.0042769	DNA damage response, detection of DNA damage	7	0.00205
DNA damage, repair and surveillance	GO.0006289	nucleotide-excision repair	10	0.00372
DNA damage, repair and surveillance	GO.0006297	nucleotide-excision repair, DNA gap filling	5	0.00445
DNA damage, repair and surveillance	GO.0045738	negative regulation of DNA repair	4	0.00613
DNA damage, repair and surveillance	GO.0043517	positive regulation of DNA damage response, signal transduction by p53 class mediator	4	0.0117
DNA damage, repair and surveillance	GO.0006283	transcription-coupled nucleotide-excision repair	7	0.0118
DNA damage, repair and surveillance	GO.2001020	regulation of response to DNA damage stimulus	12	0.0193
DNA damage, repair and surveillance	GO.0006979	response to oxidative stress	21	0.0317
DNA damage, repair and surveillance	GO.0008630	intrinsic apoptotic signalling pathway in response to DNA damage	8	0.034
DNA damage, repair and surveillance	GO.2000780	negative regulation of double-strand break repair	3	0.0388
DNA damage, repair and surveillance	GO.2001022	positive regulation of response to DNA damage stimulus	7	0.0389
DNA damage, repair and surveillance	GO.0006302	double-strand break repair	11	0.0486
DNA replication	GO.0051276	chromosome organization	64	1E-09
DNA replication	GO.0051052	regulation of DNA metabolic process	28	0.00000186
DNA replication	GO.0071103	DNA conformation change	21	0.000077
DNA replication	GO.0006260	DNA replication	20	0.000156
DNA replication	GO.0006323	DNA packaging	15	0.0021
DNA replication	GO.0006310	DNA recombination	17	0.00256
DNA replication	GO.2001251	negative regulation of chromosome organization	11	0.00375
DNA replication	GO.0051053	negative regulation of DNA metabolic process	10	0.00838
DNA replication	GO.0051098	regulation of binding	19	0.00987
DNA replication	GO.0051321	meiotic cell cycle	13	0.0162
DNA replication	GO.0033260	nuclear DNA replication	5	0.0189
DNA replication	GO.0006278	RNA-dependent DNA replication	4	0.0193
DNA replication	GO.0006278	RNA-dependent DNA replication	4	0.0193
DNA replication	GO.0006275	regulation of DNA replication	11	0.023
DNA replication	GO.0071897	DNA biosynthetic process	9	0.023
DNA replication	GO.0051053	DNA biosynthetic process	9	0.023
DNA replication	GO.0070192	chromosome organization involved in meiosis	6	0.0272
DNA replication	GO.0070987	error-free translesion synthesis	4	0.0366

DNA replication	GO.0010032	meiotic chromosome condensation	2	0.0465
Telomere maintenance	GO.0010833	telomere maintenance via telomere lengthening	8	0.000323
Telomere maintenance	GO.0000723	telomere maintenance	10	0.0025
Telomere maintenance	GO.0032201	telomere maintenance via semi-conservative replication	5	0.00896
Telomere maintenance	GO.0000722	telomere maintenance via recombination	5	0.0189
Transcription & translation	GO.0010608	posttranscriptional regulation of gene expression	51	4.98E-19
Transcription & translation	GO.0006417	regulation of translation	43	1.73E-16
Transcription & translation	GO.0045899	positive regulation of RNA polymerase II transcriptional preinitiation complex assembly	7	3.94E-07
Transcription & translation	GO.0010629	negative regulation of gene expression	79	0.000001
Transcription & translation	GO.0045727	positive regulation of translation	12	0.0000539
Transcription & translation	GO.0006446	regulation of translational initiation	12	0.0000834
Transcription & translation	GO.0006367	transcription initiation from RNA polymerase II promoter	23	0.000114
Transcription & translation	GO.0006352	DNA-templated transcription, initiation	24	0.000281
Transcription & translation	GO.0045892	negative regulation of transcription, DNA-templated	58	0.000609
Transcription & translation	GO.1903507	negative regulation of nucleic acid-templated transcription	58	0.00082
Transcription & translation	GO.0006366	transcription from RNA polymerase II promoter	43	0.00218
Transcription & translation	GO.0016441	posttranscriptional gene silencing	7	0.00702
Transcription & translation	GO.0006283	transcription-coupled nucleotide-excision repair	7	0.0118
Transcription & translation	GO.0000122	negative regulation of transcription from RNA polymerase II promoter	38	0.0218
Transcription & translation	GO.0010628	positive regulation of gene expression	70	0.0225
Transcription & translation	GO.0010628	positive regulation of gene expression	70	0.0225
Transcription & translation	GO.0040029	regulation of gene expression, epigenetic	16	0.0272
Transcription & translation	GO.0006357	regulation of transcription from RNA polymerase II promoter	69	0.0311
Transcription & translation	GO.0006369	termination of RNA polymerase II transcription	6	0.0415
Ubiquitination	GO.0031397	negative regulation of protein ubiquitination	34	3.63E-20

Ubiquitination	GO.0051444	negative regulation of ubiquitin-protein transferase activity	29	5.39E-20
Ubiquitination	GO.0051438	regulation of ubiquitin-protein transferase activity	33	7.11E-20
Ubiquitination	GO.0051439	regulation of ubiquitin-protein ligase activity involved in mitotic cell cycle	29	1.96E-19
Ubiquitination	GO.0031145	anaphase-promoting complex-dependent proteasomal ubiquitin-dependent protein catabolic process	27	1.34E-18
Ubiquitination	GO.0051437	positive regulation of ubiquitin-protein ligase activity involved in regulation of mitotic cell cycle transition	25	7.17E-18
Ubiquitination	GO.0051443	positive regulation of ubiquitin-protein transferase activity	27	1.85E-17
Ubiquitination	GO.0031396	regulation of protein ubiquitination	41	3.41E-17
Ubiquitination	GO.2000058	regulation of protein ubiquitination involved in ubiquitin-dependent protein catabolic process	26	5.13E-16
Ubiquitination	GO.0031398	positive regulation of protein ubiquitination	30	3.38E-13
Ubiquitination	GO.0000209	protein polyubiquitination	32	9.09E-13
Ubiquitination	GO.0000209	protein polyubiquitination	32	9.09E-13
Ubiquitination	GO.0043161	proteasome-mediated ubiquitin-dependent protein catabolic process	39	2.08E-12
Ubiquitination	GO.0006511	ubiquitin-dependent protein catabolic process	45	3.02E-11
Ubiquitination	GO.0016567	protein ubiquitination	45	8.53E-08
Ubiquitination	GO.0032435	negative regulation of proteasomal ubiquitin-dependent protein catabolic process	10	0.000323
Ubiquitination	GO.0032434	regulation of proteasomal ubiquitin-dependent protein catabolic process	15	0.000794
Ubiquitination	GO.1901315	negative regulation of histone H2A K63-linked ubiquitination	3	0.00087
Ubiquitination	GO.0070534	protein K63-linked ubiquitination	6	0.0111
Ubiquitination	GO.1902914	regulation of protein polyubiquitination	4	0.0117
Ubiquitination	GO.0036503	ERAD pathway	8	0.0133
Ubiquitination	GO.0030433	ER-associated ubiquitin-dependent protein catabolic process	7	0.0357

References

Abate-Shen, C. 2002. Deregulated homeobox gene expression in cancer: Cause or consequence? *Nature Reviews Cancer* 2(10), pp. 777-785. doi: 10.1038/nrc907

Abbas, T. and Dutta, A. 2009. p21 in cancer: intricate networks and multiple activities. *Nature Reviews Cancer* 9(6), pp. 400-414. doi: 10.1038/nrc2657

Abedin, M. J. et al. 2007. Autophagy delays apoptotic death in breast cancer cells following DNA damage. *Cell Death and Differentiation* 14(3), pp. 500-510. doi: 10.1038/sj.cdd.4402039

Agarwal, P. P. et al. 2011. Thoracic CT Findings in Birt-Hogg-Dube Syndrome. *American Journal of Roentgenology* 196(2), pp. 349-352. doi: 10.2214/ajr.10.4757

Ahmed, M. et al. 2016. ATM mutation and radiosensitivity: An opportunity in the therapy of mantle cell lymphoma. *Critical Reviews in Oncology Hematology* 107, pp. 14-19. doi: 10.1016/j.critrevonc.2016.08.008

Albert, R. et al. 2000. Error and attack tolerance of complex networks. *Nature* 406(6794), pp. 378-382. doi: 10.1038/35019019

Alikhan, M. B. et al. 2017. Primary epithelioid sarcoma of the kidney and adrenal gland: report of 2 cases with immunohistochemical and molecular cytogenetic studies. *Human Pathology* 61, pp. 158-163. doi: 10.1016/j.humpath.2016.09.024

Alt, J. R. et al. 2000. Phosphorylation-dependent regulation of cyclin D1 nuclear export and cyclin D1-dependent cellular transformation. *Genes & Development* 14(24), pp. 3102-3114. doi: 10.1101/gad.854900

Alt, J. R. et al. 2002. p21(Cip1) promotes cyclin D1 nuclear accumulation via direct inhibition of nuclear export. *Journal of Biological Chemistry* 277(10), pp. 8517-8523. doi: 10.1074/jbc.M108867200

Altschuler, S. J. and Wu, L. F. 2010. Cellular Heterogeneity: Do Differences Make a Difference? *Cell* 141(4), pp. 559-563. doi: 10.1016/j.cell.2010.04.033

Amatya, P. N. et al. 2012. A role of DNA-dependent protein kinase for the activation of AMP-activated protein kinase in response to glucose deprivation. *Biochimica Et Biophysica Acta-Molecular Cell Research* 1823(12), pp. 2099-2108. doi: 10.1016/j.bbamcr.2012.08.022

190

An, J. et al. 2010. DNA-PKcs plays a dominant role in the regulation of H2AX phosphorylation in response to DNA damage and cell cycle progression. *Bmc Molecular Biology* 11, doi: 10.1186/1471-2199-11-18

Anders, L. et al. 2011. A Systematic Screen for CDK4/6 Substrates Links FOXM1 Phosphorylation to Senescence Suppression in Cancer Cells. *Cancer Cell* 20(5), pp. 620-634. doi: 10.1016/j.ccr.2011.10.001

Anderson, C. W. 1996. The DNA-activated protein kinase, DNA-PK. *Faseb Journal* 10(6), pp. D17-D17.

Androutsopoulos, V. P. et al. 2013. Expression profile of CYP1A1 and CYP1B1 enzymes in colon and bladder tumors. *PLoS One* 8(12), p. e82487. doi: 10.1371/journal.pone.0082487

Angele, S. et al. 2003. Altered expression of DNA double-strand break detection and repair proteins in breast carcinomas. *Histopathology* 43(4), pp. 347-353. doi: 10.1046/j.1365-2559.2003.01713.x

Argani, P. et al. 2003. Aberrant nuclear immunoreactivity for TFE3 in neoplasms with TFE3 gene fusions - A sensitive and specific immunohistochemical assay. *American Journal of Surgical Pathology* 27(6), pp. 750-761. doi: 10.1097/00000478-200306000-00005

Asada, K. et al. 2013. FHL1 on chromosome X is a single-hit gastrointestinal tumor-suppressor gene and contributes to the formation of an epigenetic field defect. *Oncogene* 32(17), pp. 2140-2149. doi: 10.1038/onc.2012.228

Asada, M. et al. 1999. Apoptosis inhibitory activity of cytoplasmic p21(Cip1/WAF1) in monocytic differentiation. *Embo Journal* 18(5), pp. 1223-1234. doi: 10.1093/emboj/18.5.1223

Ashburner, M. et al. 2000. Gene Ontology: tool for the unification of biology. *Nature Genetics* 25(1), pp. 25-29. doi: 10.1038/75556

Assenov, Y. et al. 2008. Computing topological parameters of biological networks. *Bioinformatics* 24(2), pp. 282-284. doi: 10.1093/bioinformatics/btm554

Ather, H. and Zahid, N. 2018. Recurrent renal cancer in Birt-Hogg-Dube syndrome: A case report. *International Journal of Surgery Case Reports* 42, pp. 75-78. doi: 10.1016/j.ijscr.2017.11.032

Azmi, A. S. et al. 2017. Exportin 1 (XPO1) inhibition leads to restoration of tumor suppressor miR-145 and consequent suppression of pancreatic cancer cell proliferation and migration. *Oncotarget* 8(47), pp. 82144-82155. doi: 10.18632/oncotarget.19285

Azmi, A. S. et al. 2015. Targeting the Nuclear Export Protein XPO1/CRM1 Reverses Epithelial to Mesenchymal Transition. *Scientific Reports* 5, doi: 10.1038/srep16077

Baba, M. et al. 2008. Kidney-targeted Birt-Hogg-Dube gene inactivation in a mouse model: Erk1/2 and Akt-mTOR activation, cell hyperproliferation, and polycystic kidneys. *Journal of the National Cancer Institute* 100(2), pp. 140-154. doi: 10.1093/jnci/djm288

Baba, M. et al. 2006. Folliculin encoded by the BHD gene interacts with a binding protein, FNIP1, and AMPK, and is involved in AMPK and mTOR signaling. *Proceedings of the National Academy of Sciences of the United States of America* 103(42), pp. 15552-15557. doi: 10.1073/pnas.0603781103

Baba, M. et al. 2012. The folliculin-FNIP1 pathway deleted in human Birt-Hogg-Dube syndrome is required for murine B-cell development. *Blood* 120(6), pp. 1254-1261. doi: 10.1182/blood-2012-02-410407

Badal, S. and Delgoda, R. 2014. Role of the modulation of CYP1A1 expression and activity in chemoprevention. *Journal of Applied Toxicology* 34(7), pp. 743-753. doi: 10.1002/jat.2968

Bahassi, E. M. et al. 2008. The checkpoint kinases Chk1 and Chk2 regulate the functional associations between hBRCA2 and Rad51 in response to DNA damage. *Oncogene* 27(28), pp. 3977-3985. doi: 10.1038/onc.2008.17

Baird, D. M. et al. 2003. Extensive allelic variation and ultrashort telomeres in senescent human cells. *Nature Genetics* 33(2), pp. 203-207. doi: 10.1038/ng1084

Bar-Peled, L. and Sabatini, D. M. 2014. Regulation of mTORC1 by amino acids. *Trends in Cell Biology* 24(7), pp. 400-406. doi: 10.1016/j.tcb.2014.03.003

Barabasi, A. L. and Oltvai, Z. N. 2004. Network biology: Understanding the cell's functional organization. *Nature Reviews Genetics* 5(2), pp. 101-U115. doi: 10.1038/nrg1272

Barbier-Torres, L. et al. 2015. Stabilization of LKB1 and Akt by neddylation regulates energy metabolism in liver cancer. *Oncotarget* 6(4), pp. 2509-2523. doi: 10.18632/oncotarget.3191

Barnouin, K. et al. 2002. H2O2 induces a transient multi-phase cell cycle arrest in mouse fibroblasts through modulating cyclin D and p21(Cip1) expression. *Journal of Biological Chemistry* 277(16), pp. 13761-13770. doi: 10.1074/jbc.M111123200

Bartkova, J. et al. 2005. DNA damage response as a candidate anti-cancer barrier in early human tumorigenesis. *Nature* 434(7035), pp. 864-870. doi: 10.1038/nature03482

Basso, K. et al. 2005. Reverse engineering of regulatory networks in human B cells. *Nature Genetics* 37(4), pp. 382-390. doi: 10.1038/ng1532

Bastola, P. et al. 2013. Folliculin Contributes to VHL Tumor Suppressing Activity in Renal Cancer through Regulation of Autophagy. *Plos One* 8(7), doi: 10.1371/journal.pone.0070030

Baumann, P. and West, S. C. 1998. DNA end-joining catalyzed by human cell-free extracts. *Proceedings of the National Academy of Sciences of the United States of America* 95(24), pp. 14066-14070. doi: 10.1073/pnas.95.24.14066

Bavelloni, A. et al. 2015. PLC beta 1a and PLC beta 1b Selective Regulation and Cyclin D3 Modulation Reduced by Kinamycin F During K562 Cell Differentiation. *Journal of Cellular Physiology* 230(3), pp. 587-594. doi: 10.1002/jcp.24776

Benhammou, J. N. et al. 2011. Identification of Intragenic Deletions and Duplication in the FLCN Gene in Birt-Hogg-Dube Syndrome. *Genes Chromosomes & Cancer* 50(6), pp. 466-477. doi: 10.1002/gcc.20872

Bennetzen, M. V. et al. 2010. Site-specific Phosphorylation Dynamics of the Nuclear Proteome during the DNA Damage Response. *Molecular & Cellular Proteomics* 9(6), pp. 1314-1323. doi: 10.1074/mcp.M900616-MCP200

Bensimon, A. et al. 2010. ATM-Dependent and -Independent Dynamics of the Nuclear Phosphoproteome After DNA Damage. *Science Signaling* 3(151), doi: 10.1126/scisignal.2001034

Benusiglio, P. R. et al. 2014. Renal cell tumour characteristics in patients with the Birt-Hogg-Dube cancer susceptibility syndrome: a retrospective, multicentre study. *Orphanet Journal of Rare Diseases* 9, doi: 10.1186/s13023-014-0163-z

Berglund, F. M. and Clarke, P. R. 2009. hnRNP-U is a specific DNA-dependent protein kinase substrate phosphorylated in response to DNA double-strand breaks. *Biochemical and Biophysical Research Communications* 381(1), pp. 59-64. doi: 10.1016/j.bbrc.2009.02.019

Bessis, D. et al. 2006. A novel familial germline mutation in the initiator codon of the BHD gene in a patient with Birt-Hogg-Dube syndrome. *British Journal of Dermatology* 155(5), pp. 1067-1069. doi: 10.1111/j.1365-2133.2006.07449.x

Betschinger, J. et al. 2013. Exit from Pluripotency Is Gated by Intracellular Redistribution of the bHLH Transcription Factor Tfe3. *Cell* 153(2), pp. 335-347. doi: 10.1016/j.cell.2013.03.012

Bhat, M. et al. 2015. Targeting the translation machinery in cancer. *Nature Reviews Drug Discovery* 14(4), pp. 261-278. doi: 10.1038/nrd4505

Bhatlekar, S. et al. 2014. Identification of a Developmental Gene Expression Signature, Including HOX Genes, for the Normal Human Colonic Crypt Stem Cell Niche: Overexpression of the Signature

193

Parallels Stem Cell Overpopulation During Colon Tumorigenesis. *Stem Cells and Development* 23(2), pp. 167-179. doi: 10.1089/scd.2013.0039

Birt, A. R. et al. 1977. Hereditary Multiple Fibrofolliculomas with Trichodiscomas and Acrochordons. *Archives of Dermatology* 113(12), pp. 1674-1677. doi: 10.1001/archderm.113.12.1674

Bodenmiller, B. et al. 2012. Multiplexed mass cytometry profiling of cellular states perturbed by small-molecule regulators. *Nature Biotechnology* 30(9), pp. 858-U889. doi: 10.1038/nbt.2317

Boehlke, C. et al. 2010. Primary cilia regulate mTORC1 activity and cell size through Lkb1. *Nature Cell Biology* 12(11), pp. 1115-U1126. doi: 10.1038/ncb2117

Bondavalli, D. et al. 2015. Is Cardiac Rhabdomyoma a Feature of Birt Hogg Dube Syndrome? *American Journal of Medical Genetics Part A* 167(4), pp. 802-804. doi: 10.1002/ajmg.a.36917

Bonventre, J. V. and Yang, L. 2011. Cellular pathophysiology of ischemic acute kidney injury. *Journal of Clinical Investigation* 121(11), pp. 4210-4221. doi: 10.1172/jci45161

Boonstra, J. and Post, J. A. 2004. Molecular events associated with reactive oxygen species and cell cycle progression in mammalian cells. *Gene* 337, pp. 1-13. doi: 10.1016/j.gene.2004.04.032

Bouchaert, P. et al. 2012. DNA-PKcs Expression Predicts Response to Radiotherapy in Prostate Cancer. *International Journal of Radiation Oncology Biology Physics* 84(5), pp. 1179-1185. doi: 10.1016/j.ijrobp.2012.02.014

Bouquet, F. et al. 2011. A DNA-dependent stress response involving DNA-PK occurs in hypoxic cells and contributes to cellular adaptation to hypoxia. *Journal of Cell Science* 124(11), pp. 1943-1951. doi: 10.1242/jcs.078030

Boutros, R. et al. 2007. CDC25 phosphatases in cancer cells: key players? Good targets? *Nature Reviews Cancer* 7(7), pp. 495-507. doi: 10.1038/nrc2169

Bracken, A. P. et al. 2004. E2F target genes: unraveling the biology. *Trends in Biochemical Sciences* 29(8), pp. 409-417. doi: 10.1016/j.tibs.2004.06.006

Bradner, J. E. et al. 2017. Transcriptional Addiction in Cancer. *Cell* 168(4), pp. 629-643. doi: 10.1016/j.cell.2016.12.013

Braeuning, A. et al. 2011. Coordinate Regulation of Cytochrome P450 1A1 Expression in Mouse Liver by the Aryl Hydrocarbon Receptor and the beta-Catenin Pathway. *Toxicological Sciences* 122(1), pp. 16-25. doi: 10.1093/toxsci/kfr080

Branzei, D. and Foiani, M. 2008. Regulation of DNA repair throughout the cell cycle. *Nature Reviews Molecular Cell Biology* 9(4), pp. 297-308. doi: 10.1038/nrm2351

Brodie, K. M. and Henderson, B. R. 2012. Characterization of BRCA1 Protein Targeting, Dynamics, and Function at the Centrosome a role for the nuclear export signal, CRM1, and aurora A kinase. *Journal of Biological Chemistry* 287(10), pp. 7701-7716. doi: 10.1074/jbc.M111.327296

Brosh, R. and Rotter, V. 2009. When mutants gain new powers: news from the mutant p53 field. *Nature Reviews Cancer* 9(10), pp. 701-713. doi: 10.1038/nrc2693

Broustas, C. G. and Lieberman, H. B. 2014. DNA Damage Response Genes and the Development of Cancer Metastasis. *Radiation Research* 181(2), pp. 111-130. doi: 10.1667/rr13515.1

Brown, E. J. and Baltimore, D. 2003. Essential and dispensable roles of ATR in cell cycle arrest and genome maintenance. *Genes & Development* 17(5), pp. 615-628. doi: 10.1101/gad.1067403

Brown, J. S. and Jackson, S. P. 2015. Ubiquitylation, neddylation and the DNA damage response. *Open Biology* 5(4), doi: 10.1098/rsob.150018

Burrows, F. et al. 2004. Hsp90 activation and cell cycle regulation. *Cell Cycle* 3(12), pp. 1530-1536. doi: 10.4161/cc.3.12.1277

Cajee, U. F. et al. 2012. Modification by Ubiquitin-Like Proteins: Significance in Apoptosis and Autophagy Pathways. *International Journal of Molecular Sciences* 13(9), pp. 11804-11831. doi: 10.3390/ijms130911804

Cameron, A. J. M. et al. 2011. mTORC2 targets AGC kinases through Sin1-dependent recruitment. *Biochemical Journal* 439, pp. 287-297. doi: 10.1042/bj20110678

Capell, B. C. and Collins, F. S. 2006. Human laminopathies: nuclei gone genetically awry. *Nature Reviews Genetics* 7(12), pp. 940-952. doi: 10.1038/nrg1906

Capper, R. et al. 2007. The nature of telomere fusion and a definition of the critical telomere length in human cells. *Genes & Development* 21(19), pp. 2495-2508. doi: 10.1101/gad.439107

Cash, T. P. et al. 2011. Loss of the Birt-Hogg-Dube tumor suppressor results in apoptotic resistance due to aberrant TGF beta-mediated transcription. *Oncogene* 30(22), pp. 2534-2546. doi: 10.1038/onc.2010.628

Castedo, M. et al. 2004. Cell death by mitotic catastrophe: a molecular definition. *Oncogene* 23(16), pp. 2825-2837. doi: 10.1038/sj.onc.1207528

Catalanotto, C. et al. 2016. MicroRNA in Control of Gene Expression: An Overview of Nuclear Functions. *International Journal of Molecular Sciences* 17(10), doi: 10.3390/ijms17101712

Cavanagh, B. L. et al. 2011. Thymidine Analogues for Tracking DNA Synthesis. *Molecules* 16(9), pp. 7980-7993. doi: 10.3390/molecules16097980

Chairatvit, K. and Ngamkitidechakul, C. 2007. Control of cell proliferation via elevated NEDD8 conjugation in oral squamous cell carcinoma. *Molecular and Cellular Biochemistry* 306(1-2), pp. 163-169. doi: 10.1007/s11010-007-9566-7

Chan, D. W. et al. 2002. Autophosphorylation of the DNA-dependent protein kinase catalytic subunit is required for rejoining of DNA double-strand breaks. *Genes & Development* 16(18), pp. 2333-2338. doi: 10.1101/gad.1015202

Chang, J. T. et al. 2005. Identification of differentially expressed genes in oral squamous cell carcinoma (OSCC): Overexpression of NPM, CDK1 and NDRG1 and underexpression of CHES1. *International Journal of Cancer* 114(6), pp. 942-949. doi: 10.1002/ijc.20663

Chatterjee, N. and Walker, G. C. 2017. Mechanisms of DNA Damage, Repair, and Mutagenesis. *Environmental and Molecular Mutagenesis* 58(5), pp. 235-263. doi: 10.1002/em.22087

Chen, B. P. C. et al. 2007. Ataxia telangiectasia mutated (ATM) is essential for DNA-PKcs phosphorylations at the Thr-2609 cluster upon DNA double strand break. *Journal of Biological Chemistry* 282(9), pp. 6582-6587. doi: 10.1074/jbc.M611605200

Chen, D. et al. 2014. Expression and Prognostic Significance of a Comprehensive Epithelial-Mesenchymal Transition Gene Set in Renal Cell Carcinoma. *Journal of Urology* 191(2), pp. 479-486. doi: 10.1016/j.juro.2013.08.052

Chen, F. J. et al. 2016a. Multilevel Genomics-Based Taxonomy of Renal Cell Carcinoma. *Cell Reports* 14(10), pp. 2476-2489. doi: 10.1016/j.celrep.2016.02.024

Chen, J. et al. 2008. Deficiency of FLCN in Mouse Kidney Led to Development of Polycystic Kidneys and Renal Neoplasia. *Plos One* 3(10), doi: 10.1371/journal.pone.0003581

Chen, J. D. et al. 2015. Disruption of tubular FIcn expression as a mouse model for renal tumor induction. *Kidney International* 88(5), pp. 1057-1069. doi: 10.1038/ki.2015.177

Chen, J. J. et al. 1995. Separate domains of p21 involved in the inhibition of CDK kinase and PCNA. *Nature* 374(6520), pp. 386-388. doi: 10.1038/374386a0

Chen, P. et al. 2016b. Neddylation Inhibition Activates the Extrinsic Apoptosis Pathway through ATF4-CHOP-DR5 Axis in Human Esophageal Cancer Cells. *Clinical Cancer Research* 22(16), pp. 4145-4157. doi: 10.1158/1078-0432.ccr-15-2254

Cheng, L. et al. 2000. Reduced expression levels of nucleotide excision repair genes in lung cancer: a case-control analysis. *Carcinogenesis* 21(8), pp. 1527-1530. doi: 10.1093/carcin/21.8.1527

Cheng, L. et al. 2002. Expression of nucleotide excision repair genes and the risk for squamous cell carcinoma of the head and neck. *Cancer* 94(2), pp. 393-397. doi: 10.1002/cncr.10231

Cheng, Y. et al. 2014. XPO1 (CRM1) Inhibition Represses STAT3 Activation to Drive a Survivin-Dependent Oncogenic Switch in Triple-Negative Breast Cancer. *Molecular Cancer Therapeutics* 13(3), pp. 675-686. doi: 10.1158/1535-7163.mct-13-0416

Chiang, Y. C. et al. 2003. c-Myc directly regulates the transcription of the NBS1 gene involved in DNA double-strand break repair. *Journal of Biological Chemistry* 278(21), pp. 19286-19291. doi: 10.1074/jbc.M212043200

Chistiakov, D. A. et al. 2008. Genetic variations in DNA repair genes, radiosensitivity to cancer and susceptibility to acute tissue reactions in radiotherapy-treated cancer patients. *Acta Oncologica* 47(5), pp. 809-824. doi: 10.1080/02841860801885969

Choi, A. M. K. et al. 2013. Mechanisms of disease autophagy in Human Health and Disease. *New England Journal of Medicine* 368(7), pp. 651-662. doi: 10.1056/NEJMra1205406

Choudhuri, A. et al. 2013. Translation initiation factor eIF3h targets specific transcripts to polysomes during embryogenesis. *Proceedings of the National Academy of Sciences of the United States of America* 110(24), pp. 9818-9823. doi: 10.1073/pnas.1302934110

Choyke, P. L. et al. 2003. Hereditary renal cancers. *Radiology* 226(1), pp. 33-46. doi: 10.1148/radiol.2261011296

Chua, H. N. and Wong, L. 2008. Increasing the reliability of protein interactomes. *Drug Discovery Today* 13(15-16), pp. 652-658. doi: 10.1016/j.drudis.2008.05.004

Chung, J. H. 2018. The role of DNA-PK in aging and energy metabolism. *Febs Journal* 285(11), pp. 1959-1972. doi: 10.1111/febs.14410

Chung, J. S. et al. 2009. The DC-HIL/syndecan-4 pathway inhibits human allogeneic T-cell responses. *European Journal of Immunology* 39(4), pp. 965-974. doi: 10.1002/eji.200838990

Chung, J. Y. et al. 1996. Multiple lipomas, angiolipomas, and parathyroid adenomas in a patient with Birt-Hogg-Dube syndrome. *International Journal of Dermatology* 35(5), pp. 365-367. doi: 10.1111/j.1365-4362.1996.tb03642.x

Ciccia, A. and Elledge, S. J. 2010. The DNA Damage Response: Making It Safe to Play with Knives. *Molecular Cell* 40(2), pp. 179-204. doi: 10.1016/j.molcel.2010.09.019

Cocciolone, R. A. et al. 2010. Multiple Desmoplastic Melanomas in Birt-Hogg-Dube Syndrome and a Proposed Signaling Link Between Folliculin, the mTOR Pathway, and Melanoma Susceptibility. *Archives of Dermatology* 146(11), pp. 1316-1318. doi: 10.1001/archdermatol.2010.333

Cohen, N. et al. 2001. PML RING suppresses oncogenic transformation by reducing the affinity of eIF4E for mRNA. *Embo Journal* 20(16), pp. 4547-4559. doi: 10.1093/emboj/20.16.4547

Cortez, D. et al. 1999. Requirement of ATM-dependent phosphorylation of BRCA1 in the DNA damage response to double-strand breaks. *Science* 286(5442), pp. 1162-1166. doi: 10.1126/science.286.5442.1162

Costantini, S. et al. 2007. Interaction of the Ku heterodimer with the DNA ligase IV/Xrcc4 complex and its regulation by DNA-PK. *DNA Repair* 6(6), pp. 712-722. doi: 10.1016/j.dnarep.2006.12.007

Cremona, C. A. and Behrens, A. 2014. ATM signalling and cancer. *Oncogene* 33(26), pp. 3351-3360. doi: 10.1038/onc.2013.275

Culjkovic, B. et al. 2005. eIF4E promotes nuclear export of cyclin D1 mRNAs via an element in the 3 ' UTR. *Journal of Cell Biology* 169(2), pp. 245-256. doi: 10.1083/jcb.200501019

Culjkovic, B. et al. 2006. eIF4E is a central node of an RNA regulon that governs cellular proliferation. *Journal of Cell Biology* 175(3), pp. 415-426. doi: 10.1083/jcb.200604099

Culjkovic-Kraljacic, B. et al. 2012. The Oncogene eIF4E Reprograms the Nuclear Pore Complex to Promote mRNA Export and Oncogenic Transformation. *Cell Reports* 2(2), pp. 207-215. doi: 10.1016/j.celrep.2012.07.007

Culjkovic-Kraljacic, B. et al. 2016. Combinatorial targeting of nuclear export and translation of RNA inhibits aggressive B-cell lymphomas. *Blood* 127(7), pp. 858-868. doi: 10.1182/blood-2015-05-645069

Curtin, N. J. 2012. DNA repair dysregulation from cancer driver to therapeutic target. *Nature Reviews Cancer* 12(12), pp. 801-817. doi: 10.1038/nrc3399

Curtin, N. J. 2013. Inhibiting the DNA damage response as a therapeutic manoeuvre in cancer. *British Journal of Pharmacology* 169(8), pp. 1745-1765. doi: 10.1111/bph.12244

198

da Silva, N. F. et al. 2003. Analysis of the Birt-Hogg-Dube (BHD) tumour suppressor gene (TSG) in sporadic renal cell carcinoma and colorectal cancer. *Journal of Medical Genetics* 40, pp. S73-S73.

Daido, S. et al. 2005. Inhibition of the DNA-dependent protein kinase catalytic subunit radiosensitizes malignant gliorna cells by inducing autophagy. *Cancer Research* 65(10), pp. 4368-4375. doi: 10.1158/0008-5472.can-04-4202

Daurkin, I. et al. 2011. Tumor-Associated Macrophages Mediate Immunosuppression in the Renal Cancer Microenvironment by Activating the 15-Lipoxygenase-2 Pathway. *Cancer Research* 71(20), pp. 6400-6409. doi: 10.1158/0008-5472.can-11-1261

Davis, A. J. et al. 2014. BRCA1 modulates the autophosphorylation status of DNA-PKcs in S phase of the cell cycle. *Nucleic Acids Research* 42(18), pp. 11487-11501. doi: 10.1093/nar/gku824

De Paulsen, N. et al. 2001. Role of transforming growth factor-alpha in von Hippel-Lindau (VHL)(-/-) clear cell renal carcinoma cell proliferation: A possible mechanism coupling VHL tumor suppressor inactivation and tumorigenesis. *Proceedings of the National Academy of Sciences of the United States of America* 98(4), pp. 1387-1392. doi: 10.1073/pnas.031587498

De Sousa, S. O. M. et al. 2002. Immunolocalization of c-Fos and c-Jun in human oral mucosa and in oral squamous cell carcinoma. *Journal of Oral Pathology & Medicine* 31(2), pp. 78-81. doi: 10.1046/j.0904-2512.2001.10012.x

De Wit, R. et al. 2000. Hydrogen peroxide inhibits epidermal growth factor receptor internalization in human fibroblasts. *Free Radical Biology and Medicine* 28(1), pp. 28-38. doi: 10.1016/s0891-5849(99)00199-9

Deng, C. X. et al. 1995. Mice lacking p21(C/P1/WAF1) undergo normal development, but are defective in G1 checkpoint control. *Cell* 82(4), pp. 675-684. doi: 10.1016/0092-8674(95)90039-x

Dephoure, N. et al. 2008. A quantitative atlas of mitotic phosphorylation. *Proceedings of the National Academy of Sciences of the United States of America* 105(31), pp. 10762-10767. doi: 10.1073/pnas.0805139105

Derynck, R. et al. 1987. Synthesis of messenger-RNAs for transforming growth factor-alpha and factor-beta and the epidermal growth-factor receptor by human-tumors. *Cancer Research* 47(3), pp. 707-712.

Deshpande, S. S. and Irani, K. 2002. Oxidant signalling in carcinogenesis: a commentary. *Human & Experimental Toxicology* 21(2), pp. 63-64. doi: 10.1191/0960327102ht211oa

DeZwaan, D. C. et al. 2009. The Hsp82 molecular chaperone promotes a switch between unextendable and extendable telomere states. *Nature Structural & Molecular Biology* 16(7), pp. 711-U742. doi: 10.1038/nsmb.1616

Dhar, S. et al. 2017. The tale of a tail: histone H4 acetylation and the repair of DNA breaks. *Philosophical Transactions of the Royal Society B-Biological Sciences* 372(1731), doi: 10.1098/rstb.2016.0284

Di Micco, R. et al. 2006. Oncogene-induced senescence is a DNA damage response triggered by DNA hyper-replication. *Nature* 444(7119), pp. 638-642. doi: 10.1038/nature05327

Di Stefano, L. et al. 2003. E2F7, a novel E2F featuring DP-independent repression of a subset of E2F-regulated genes. *Embo Journal* 22(23), pp. 6289-6298. doi: 10.1093/emboj/cdg613

Diehl, J. A. 2002. Cycling to cancer with cyclin D1. *Cancer Biol Ther* 1(3), pp. 226-231.

Diehl, J. A. et al. 1998. Glycogen synthase kinase 3 beta regulates cyclin D1 proteolysis and subcellular localization. *Genes & Development* 12(22), pp. 3499-3511. doi: 10.1101/gad.12.22.3499

Dittmann, K. et al. 2005. Radiation-induced epidermal growth factor receptor nuclear import is linked to activation of DNA-dependent protein kinase. *Journal of Biological Chemistry* 280(35), pp. 31182-31189. doi: 10.1074/jbc.M506591200

Dodd, K. M. et al. 2015. mTORC1 drives HIF-1 alpha and VEGF-A signalling via multiple mechanisms involving 4E-BP1, S6K1 and STAT3. *Oncogene* 34(17), pp. 2239-2250. doi: 10.1038/onc.2014.164

Dodding, M. P. et al. 2011. A kinesin-1 binding motif in vaccinia virus that is widespread throughout the human genome. *Embo Journal* 30(22), pp. 4523-4538. doi: 10.1038/emboj.2011.326

Dolan, D. et al. 2013. Systems Modelling of NHEJ Reveals the Importance of Redox Regulation of Ku70/80 in the Dynamics of DNA Damage Foci. *Plos One* 8(2), doi: 10.1371/journal.pone.0055190

Draetta, G. et al. 1989. CDC2 protein-kinase is complexed with both cyclin-A and cyclin-B - evidence for proteolytic inactivation of MPF. *Cell* 56(5), pp. 829-838. doi: 10.1016/0092-8674(89)90687-9

Drane, P. et al. 2017. TIRR regulates 53BP1 by masking its histone methyl-lysine binding function. *Nature* 543(7644), pp. 211-+. doi: 10.1038/nature21358

Duncan, R. and Hershey, J. W. B. 1983. Identification and quantitation of levels of protein-synthesis initiation-factors in crude HeLa-cell lysates by two-dimensional polyacrylamide-gel electrophoresis. *Journal of Biological Chemistry* 258(11), pp. 7228-7235.

200

Dunlop, E. A. et al. 2014. FLCN, a novel autophagy component, interacts with GABARAP and is regulated by ULK1 phosphorylation. *Autophagy* 10(10), pp. 1749-1760. doi: 10.4161/auto.29640

Dzikiewicz-Krawczyk, A. 2008. The importance of making ends meet: Mutations in genes and altered expression of proteins of the MRN complex and cancer. *Mutation Research-Reviews in Mutation Research* 659(3), pp. 262-273. doi: 10.1016/j.mrrev.2008.05.005

Eckel-Passow, J. E. et al. 2015. Assessing the clinical use of clear cell renal cell carcinoma molecular subtypes identified by RNA expression analysis. *Urologic Oncology-Seminars and Original Investigations* 33(2), doi: 10.1016/j.urolonc.2014.07.019

Economopoulou, M. et al. 2009. Histone H2AX is integral to hypoxia-driven neovascularization. *Nature Medicine* 15(5), pp. 553-558. doi: 10.1038/nm.1947

Egan, D. F. et al. 2011. Phosphorylation of ULK1 (hATG1) by AMP-Activated Protein Kinase Connects Energy Sensing to Mitophagy. *Science* 331(6016), pp. 456-461. doi: 10.1126/science.1196371

Eggersmann, T. K. et al. 2019. CDK4/6 Inhibitors Expand the Therapeutic Options in Breast Cancer: Palbociclib, Ribociclib and Abemaciclib. *Biodrugs* 33(2), pp. 125-135. doi: 10.1007/s40259-019-00337-6

Eisenberg-Lerner, A. and Kimchi, A. 2009. The paradox of autophagy and its implication in cancer etiology and therapy. *Apoptosis* 14(4), pp. 376-391. doi: 10.1007/s10495-008-0307-5

El-Houjeiri, L. et al. 2019. The Transcription Factors TFEB and TFE3 Link the FLCN-AMPK Signaling Axis to Innate Immune Response and Pathogen Resistance. *Cell Reports* 26(13), pp. 3613-+. doi: 10.1016/j.celrep.2019.02.102

Eliopoulos, A. G. et al. 2016. DNA Damage Response and Autophagy: A Meaningful Partnership. *Frontiers in Genetics* 7, doi: 10.3389/fgene.2016.00204

Esteban, M. A. et al. 2006. Regulation of E-cadherin expression by VHL and hypoxia-inducible factor. *Cancer Research* 66(7), pp. 3567-3575. doi: 10.1158/0008-5472.can-05-2670

Fabre, A. et al. 2014. Distinguishing the histological and radiological features of cystic lung disease in Birt-Hogg-Dube syndrome from those of tobacco-related spontaneous pneumothorax. *Histopathology* 64(5), pp. 741-749. doi: 10.1111/his.12318

Fabregat, A. et al. 2018. The Reactome Pathway Knowledgebase. *Nucleic Acids Research* 46(D1), pp. D649-D655. doi: 10.1093/nar/gkx1132

Fabregat, A. et al. 2017. Reactome pathway analysis: a high-performance in-memory approach. *Bmc Bioinformatics* 18, doi: 10.1186/s12859-017-1559-2

201

Farlik, M. et al. 2015. Single-Cell DNA Methylome Sequencing and Bioinformatic Inference of Epigenomic Cell-State Dynamics. *Cell Reports* 10(8), pp. 1386-1397. doi: 10.1016/j.celrep.2015.02.001

Favaro, E. et al. 2012. Glucose Utilization via Glycogen Phosphorylase Sustains Proliferation and Prevents Premature Senescence in Cancer Cells. *Cell Metabolism* 16(6), pp. 751-764. doi: 10.1016/j.cmet.2012.10.017

Feoktistova, K. et al. 2013. Human eIF4E promotes mRNA restructuring by stimulating eIF4A helicase activity. *Proceedings of the National Academy of Sciences of the United States of America* 110(33), pp. 13339-13344. doi: 10.1073/pnas.1303781110

Flintoft, L. 2007. Evolution - How small change makes a big difference. *Nature Reviews Genetics* 8(9), pp. 652-653. doi: 10.1038/nrg2180

Florek, M. et al. 2005. Prominin-1/CD133, a neural and hematopoietic stem cell marker, is expressed in adult human differentiated cells and certain types of kidney cancer. *Cell and Tissue Research* 319(1), pp. 15-26. doi: 10.1007/s00441-004-1018-z

Floresrozas, H. et al. 1994. CDK-interacting protein-1 directly binds with proliferating cell nuclear anitgen and inhibits DNA-replication protein-1 directly binds with proflierating cell nuclear anitgen and inhibits DNA-replication catalysed by the DNA-polymerase-delta holoenzyme. *Proceedings of the National Academy of Sciences of the United States of America* 91(18), pp. 8655-8659. doi: 10.1073/pnas.91.18.8655

Fokkema, I. et al. 2011. LOVD v.2.0: The Next Generation in Gene Variant Databases. *Human Mutation* 32(5), pp. 557-563. doi: 10.1002/humu.21438

Foster, S. S. et al. 2012. Cell cycle- and DNA repair pathway-specific effects of apoptosis on tumor suppression. *Proceedings of the National Academy of Sciences of the United States of America* 109(25), pp. 9953-9958. doi: 10.1073/pnas.1120476109

Fumagalli, M. et al. 2012. Telomeric DNA damage is irreparable and causes persistent DNA-damage-response activation. *Nature Cell Biology* 14(4), pp. 355-+. doi: 10.1038/ncb2466

Furuya, M. et al. 2015. Distinctive expression patterns of glycoprotein non-metastatic B and folliculin in renal tumors in patients with Birt-Hogg-Dube syndrome. *Cancer Science* 106(3), pp. 315-323. doi: 10.1111/cas.12601

Furuya, M. and Nakatani, Y. 2013. Birt-Hogg-Dube syndrome: clinicopathological features of the lung. *Journal of Clinical Pathology* 66(3), pp. 178-186. doi: 10.1136/jclinpath-2012-201200

Furuya, M. et al. 2016. Genetic, epidemiologic and clinicopathologic studies of Japanese Asian patients with Birt-Hogg-Dube syndrome. *Clinical Genetics* 90(5), pp. 403-412. doi:10.1111/cge.12807

Gad, S. et al. 2007. Mutations in BHD and TP53 genes, but not in HNF1 beta gene, in a large series of sporadic chromophobe renal cell carcinoma (vol 96, pg 336, 2006). *British Journal of Cancer* 96(8), pp. 1314-1314. doi: 10.1038/sj.bjc.6603733

Galicia-Vazquez, G. et al. 2012. A cellular response linking eIF4AI activity to eIF4AII transcription. *Rna* 18(7), pp. 1373-1384. doi: 10.1261/rna.033209.112

Gambichler, T. et al. 2000. Treatment of Birt-Hogg-Dube syndrome with erbium : YAG laser. *Journal of the American Academy of Dermatology* 43(5), pp. 856-858. doi: 10.1067/mjd.2000.109294

Gansauge, S. et al. 1998. Nitric oxide-induced apoptosis in human pancreatic carcinoma cell lines is associated with a G1-arrest and an increase of the cyclin-dependent kinase inhibitor p21WAF1/CIP1. *Cell Growth Differ* 9(8), pp. 611-617.

Gartel, A. L. 2006. Is p21 an oncogene? *Molecular Cancer Therapeutics* 5(6), pp. 1385-1386. doi: 10.1158/1535-7163.mct-06-0163

Gaur, K. et al. 2013. The Birt-Hogg-Dube tumor suppressor Folliculin negatively regulates ribosomal RNA synthesis. *Human Molecular Genetics* 22(2), pp. 284-299. doi: 10.1093/hmg/dds428

Gehrke, L. et al. 1983. 5'-conformation of capped alfalfa mosaic-virus ribonucleic acid-4 may reflect its independence of the cap structure or of cap-binding protein for efficient translation. *Biochemistry* 22(22), pp. 5157-5164. doi: 10.1021/bi00291a015

Gharbi, H. et al. 2013. Loss of the Birt-Hogg-Dube gene product folliculin induces longevity in a hypoxia-inducible factor-dependent manner. *Aging Cell* 12(4), pp. 593-603. doi: 10.1111/acel.12081

Gijezen, L. C. et al. 2014. Topical Rapamycin as a Treatment for Fibrofolliculomas in Birt-Hogg-Dube Syndrome: A Double-Blind Placebo-Controlled Randomized Split-Face Trial. *Plos One* 9(6), doi: 10.1371/journal.pone.0099071

Ginestet, C. 2011. ggplot2: Elegant Graphics for Data Analysis. *Journal of the Royal Statistical Society Series a-Statistics in Society* 174, pp. 245-245. doi: 10.1111/j.1467-985X.2010.00676_9.x

Giraldez, S. et al. 2017. G(1)/S phase progression is regulated by PLK1 degradation through the CDK1/beta TrCP axis. *Faseb Journal* 31(7), pp. 2925-2936. doi: 10.1096/fj.201601108R

Girvan, M. and Newman, M. E. J. 2002. Community structure in social and biological networks. *Proceedings of the National Academy of Sciences of the United States of America* 99(12), pp. 7821-7826. doi: 10.1073/pnas.122653799

Go, R. E. et al. 2015. Cytochrome P450 1 family and cancers. *Journal of Steroid Biochemistry and Molecular Biology* 147, pp. 24-30. doi: 10.1016/j.jsbmb.2014.11.003

Godbolt, A. M. et al. 2003. Birt-Hogg-Dubé syndrome. *Australas J Dermatol* 44(1), pp. 52-56.

Goh, K. I. et al. 2007. The human disease network. *Proceedings of the National Academy of Sciences of the United States of America* 104(21), pp. 8685-8690. doi: 10.1073/pnas.0701361104

Gomella, L. G. et al. 1989. Expression of transforming growth factor-alpha in normal human adult kidney and enhanced expression of transforming growth factor-alpha and factor-beta-1 in renal-cell carinoma. *Cancer Research* 49(24), pp. 6972-6975.

Goncharova, E. A. et al. 2014. Folliculin Controls Lung Alveolar Enlargement and Epithelial Cell Survival through E-Cadherin, LKB1, and AMPK. *Cell Reports* 7(2), pp. 412-423. doi: 10.1016/j.celrep.2014.03.025

Gonda, T. J. and Ramsay, R. G. 2015. Directly targeting transcriptional dysregulation in cancer. *Nature Reviews Cancer* 15(11), pp. 686-694. doi: 10.1038/nrc4018

Goodwin, J. F. and Knudsen, K. E. 2014. Beyond DNA Repair: DNA-PK Function in Cancer. *Cancer Discovery* 4(10), pp. 1126-1139. doi: 10.1158/2159-8290.cd-14-0358

Gottifredi, V. et al. 2004. Decreased p21 levels are required for efficient restart of DNA synthesis after S phase block. *Journal of Biological Chemistry* 279(7), pp. 5802-5810. doi: 10.1074/jbc.M310373200

Grasso, C. S. et al. 2012. The mutational landscape of lethal castration-resistant prostate cancer. *Nature* 487(7406), pp. 239-243. doi: 10.1038/nature11125

Grun, D. et al. 2015. Single-cell messenger RNA sequencing reveals rare intestinal cell types. *Nature* 525(7568), pp. 251-+. doi: 10.1038/nature14966

Grzmil, M. et al. 2010. An oncogenic role of eIF3e/INT6 in human breast cancer. *Oncogene* 29(28), pp. 4080-4089. doi: 10.1038/onc.2010.152

Guleria, A. and Chandna, S. 2016. ATM kinase: Much more than a DNA damage responsive protein. *DNA Repair* 39, pp. 1-20. doi: 10.1016/j.dnarep.2015.12.009

Gunes, C. et al. 2018. Telomeres in cancer. *Differentiation* 99, pp. 41-50. doi: 10.1016/j.diff.2017.12.004

Gunji, Y. et al. 2007. Mutations of the Birt-Hogg-Dube gene in patients with multiple lung cysts and recurrent pneumothorax. *Journal of Medical Genetics* 44(9), doi: 10.1136/jmg.2007.049874

Guo, K. K. et al. 2019. A Host Factor GPNMB Restricts Porcine Circovirus Type 2 (PCV2) Replication and Interacts With PCV2 ORF5 Protein. *Frontiers in Microbiology* 9, doi: 10.3389/fmicb.2018.03295

Guo, Y. J. and Scarlata, S. 2013. A Loss in Cellular Protein Partners Promotes alpha-Synuclein Aggregation in Cells Resulting from Oxidative Stress. *Biochemistry* 52(22), pp. 3913-3920. doi: 10.1021/bi4002425

Gupta, D. et al. 2018. ATR-Chk1 activation mitigates replication stress caused by mismatch repair-dependent processing of DNA damage. *Proceedings of the National Academy of Sciences of the United States of America* 115(7), pp. 1523-1528. doi: 10.1073/pnas.1720355115

Gupta, K. et al. 2008. Epidemiologic and socioeconomic burden of metastatic renal cell carcinoma (mRCC): A literature review. *Cancer Treatment Reviews* 34(3), pp. 193-205. doi: 10.1016/j.ctrv.2007.12.001

Gupta, N. et al. 2013. Pulmonary manifestations of Birt-Hogg-Dube syndrome. *Familial Cancer* 12(3), pp. 387-396. doi: 10.1007/s10689-013-9660-9

Haas, N. B. and Nathanson, K. L. 2014. Hereditary kidney cancer syndromes. *Adv Chronic Kidney Dis* 21(1), pp. 81-90. doi: 10.1053/j.ackd.2013.10.001

Haitel, A. et al. 1999. Biologic behavior of and p53 overexpression in multifocal renal cell carcinoma of clear cell type - An immunohistochemical study correlating grading, staging, and proliferation markers. *Cancer* 85(7), pp. 1593-1598. doi: 10.1002/(sici)1097-0142(19990401)85:7<1593::aid-cncr22>3.0.co;2-k

Halazonetis, T. D. et al. 2008. An oncogene-induced DNA damage model for cancer development. *Science* 319(5868), pp. 1352-1355. doi: 10.1126/science.1140735

Hall, E. J. and Brenner, D. J. 2008. Cancer risks from diagnostic radiology. *British Journal of Radiology* 81(965), pp. 362-378. doi: 10.1259/bjr/01948454

Hall, M. and Peters, G. 1996. Genetic alterations of cyclins, cyclin-dependent kinases, and Cdk inhibitors in human cancer. *Advances in Cancer Research, Vol 68* 68, pp. 67-108. doi: 10.1016/s0065-230x(08)60352-8

Hamilton, E. and Infante, J. R. 2016. Targeting CDK4/6 in patients with cancer. *Cancer Treatment Reviews* 45, pp. 129-138. doi: 10.1016/j.ctrv.2016.03.002

Han, J. D. J. et al. 2004. Evidence for dynamically organized modularity in the yeast protein-protein interaction network. *Nature* 430(6995), pp. 88-93. doi: 10.1038/nature02555

Hanahan, D. and Weinberg, R. A. 2011. Hallmarks of Cancer: The Next Generation. *Cell* 144(5), pp. 646-674. doi: 10.1016/j.cell.2011.02.013

Hanna, S. and El-Sibai, M. 2013. Signaling networks of Rho GTPases in cell motility. *Cellular Signalling* 25(10), pp. 1955-1961. doi: 10.1016/j.cellsig.2013.04.009

Haria, D. and Naora, H. 2013. Homeobox Gene Deregulation: Impact on the Hallmarks of Cancer. *Cancer Hallm* 1(2-3), pp. 67-76. doi: 10.1166/ch.2013.1007

Harris, M. A. et al. 2008. The Gene Ontology project in 2008. *Nucleic Acids Research* 36, pp. D440-D444. doi: 10.1093/nar/gkm883

Hartman, T. R. et al. 2009. The role of the Birt-Hogg-Dube protein in mTOR activation and renal tumorigenesis. *Oncogene* 28(13), pp. 1594-1604. doi: 10.1038/onc.2009.14

Hasumi, H. et al. 2012. Regulation of Mitochondrial Oxidative Metabolism by Tumor Suppressor FLCN. *Jnci-Journal of the National Cancer Institute* 104(22), pp. 1750-1764. doi: 10.1093/jnci/djs418

Hasumi, H. et al. 2015. Folliculin-interacting proteins Fnip1 and Fnip2 play critical roles in kidney tumor suppression in cooperation with Flcn. *Proceedings of the National Academy of Sciences of the United States of America* 112(13), pp. E1624-E1631. doi: 10.1073/pnas.1419502112

Hasumi, H. et al. 2008. Identification and characterization of a novel folliculin-interacting protein FNIP2. *Gene* 415(1-2), pp. 60-67. doi: 10.1016/j.gene.2008.02.022

Hasumi, Y. et al. 2009. Homozygous loss of BHD causes early embryonic lethality and kidney tumor development with activation of mTORC1 and mTORC2. *Proceedings of the National Academy of Sciences of the United States of America* 106(44), pp. 18722-18727. doi: 10.1073/pnas.0908853106

Hasumi, Y. et al. 2014. Folliculin (Flcn) inactivation leads to murine cardiac hypertrophy through mTORC1 deregulation. *Human Molecular Genetics* 23(21), pp. 5706-5719. doi: 10.1093/hmg/ddu286

Havens, C. G. et al. 2006. Regulation of late G1/S phase transition and APC Cdh1 by reactive oxygen species. *Mol Cell Biol* 26(12), pp. 4701-4711. doi: 10.1128/MCB.00303-06

Hayashi, M. et al. 2010. Birt-Hogg-Dube Syndrome with Multiple Cysts and Recurrent Pneumothorax: Pathological Findings. *Internal Medicine* 49(19), pp. 2137-2142. doi: 10.2169/internalmedicine.49.3670

He, C. C. and Klionsky, D. J. 2009. Regulation Mechanisms and Signaling Pathways of Autophagy. *Annual Review of Genetics* 43, pp. 67-93. doi: 10.1146/annurev-genet-102808-114910

He, X. L. and Zhang, J. Z. 2006. Why do hubs tend to be essential in protein networks? *Plos Genetics* 2(6), pp. 826-834. doi: 10.1371/journal.pgen.0020088

Heiden, M. G. V. et al. 2009. Understanding the Warburg Effect: The Metabolic Requirements of Cell Proliferation. *Science* 324(5930), pp. 1029-1033. doi: 10.1126/science.1160809

Heidenreich, B. et al. 2014. TERT promoter mutations in cancer development. *Current Opinion in Genetics & Development* 24, pp. 30-37. doi: 10.1016/j.gde.2013.11.005

Hewitt, G. et al. 2016. SQSTM1/p62 mediates crosstalk between autophagy and the UPS in DNA repair. *Autophagy* 12(10), pp. 1917-1930. doi: 10.1080/15548627.2016.1210368

Hinnebusch, A. G. 2014. The Scanning Mechanism of Eukaryotic Translation Initiation. *Annual Review of Biochemistry, Vol 83* 83, pp. 779-812. doi: 10.1146/annurev-biochem-060713-035802

Ho, J. J. D. et al. 2016. Systemic Reprogramming of Translation Efficiencies on Oxygen Stimulus. *Cell Reports* 14(6), pp. 1293-1300. doi: 10.1016/j.celrep.2016.01.036

Hoeijmakers, J. H. J. 2001. Genome maintenance mechanisms for preventing cancer. *Nature* 411(6835), pp. 366-374. doi: 10.1038/35077232

Hong, S. B. et al. 2010a. Inactivation of the FLCN Tumor Suppressor Gene Induces TFE3 Transcriptional Activity by Increasing Its Nuclear Localization. *Plos One* 5(12), doi: 10.1371/journal.pone.0015793

Hong, S. B. et al. 2010b. Tumor suppressor FLCN inhibits tumorigenesis of a FLCN-null renal cancer cell line and regulates expression of key molecules in TGF-beta signaling. *Molecular Cancer* 9, doi: 10.1186/1476-4598-9-160

Hornstein, O. P. and Knickenberg, M. 1975. Perifollicular fibromatosis cutis with polyps of colon - cutaneo-intestinal syndrome sui-generis. *Archiv Fur Dermatologische Forschung* 253(2), pp. 161-175. doi: 10.1007/bf00582068

Hosen, I. et al. 2015. TERT promoter mutations in clear cell renal cell carcinoma. *International Journal of Cancer* 136(10), pp. 2448-2452. doi: 10.1002/ijc.29279

Hosoya, N. and Miyagawa, K. 2014. Targeting DNA damage response in cancer therapy. *Cancer Science* 105(4), pp. 370-388. doi: 10.1111/cas.12366

207

Houweling, A. C. et al. 2011. Renal cancer and pneumothorax risk in Birt-Hogg-Dube syndrome; an analysis of 115 FLCN mutation carriers from 35 BHD families. *British Journal of Cancer* 105(12), pp. 1912-1919. doi: 10.1038/bjc.2011.463

Hua, W. et al. 2015. Suppression of glioblastoma by targeting the overactivated protein neddylation pathway. *Neuro-Oncology* 17(10), pp. 1333-1343. doi: 10.1093/neuonc/nov066

Hudon, V. et al. 2010. Renal tumour suppressor function of the Birt-Hogg-Dube syndrome gene product folliculin. *Journal of Medical Genetics* 47(3), pp. 182-189. doi: 10.1136/jmg.2009.072009

Humes, H. D. et al. 1991. Effects of transforming growth-factor-beta, transforming growth factor-alpha, and other growth-factors on renal proximal tubule cells. *Laboratory Investigation* 64(4), pp. 538-545.

Humphreys, B. D. et al. 2011. Repair of injured proximal tubule does not involve specialized progenitors. *Proc Natl Acad Sci U S A* 108(22), pp. 9226-9231. doi: 10.1073/pnas.1100629108

Hunt, T. 1989. Maturation promoting factor, cyclin and the control of M-phase. *Current Opinion in Cell Biology* 1(2), pp. 268-274. doi: 10.1016/0955-0674(89)90099-9

Hunter, R. W. et al. 2011. Molecular Mechanism by Which AMP-Activated Protein Kinase Activation Promotes Glycogen Accumulation in Muscle. *Diabetes* 60(3), pp. 766-774. doi: 10.2337/db10-1148

Huot, G. et al. 2014. CHES1/FOXN3 regulates cell proliferation by repressing PIM2 and protein biosynthesis. *Molecular Biology of the Cell* 25(5), pp. 554-565. doi: 10.1091/mbc.E13-02-0110

Huston, E. et al. 2008. EPAC and PKA allow cAMP dual control over DNA-PK nuclear translocation. *Proceedings of the National Academy of Sciences of the United States of America* 105(35), pp. 12791-12796. doi: 10.1073/pnas.0805167105

Hwang, B. et al. 2018. Single-cell RNA sequencing technologies and bioinformatics pipelines. *Experimental and Molecular Medicine* 50, doi: 10.1038/s12276-018-0071-8

Imada, K. et al. 2009. Birt-Hogg-Dube syndrome with clear-cell and oncocytic renal tumour and trichoblastoma associated with a novel FLCN mutation. *British Journal of Dermatology* 160(6), pp. 1350-1353. doi: 10.1111/j.1365-2133.2009.09134.x

Inoki, K. et al. 2003. TSC2 mediates cellular energy response to control cell growth and survival. *Cell* 115(5), pp. 577-590. doi: 10.1016/s0092-8674(03)00929-2

Iribe, Y. et al. 2015. Immunohistochemical characterization of renal tumors in patients with Birt-Hogg-Dube Syndrome. *Pathology International* 65(3), pp. 126-132. doi: 10.1111/pin.12254

Isono, M. et al. 2017. BRCA1 Directs the Repair Pathway to Homologous Recombination by Promoting 53BP1 Dephosphorylation. *Cell Reports* 18(2), pp. 520-532. doi: 10.1016/j.celrep.2016.12.042

Iwakura, T. et al. 2014. A high ratio of G1 to G0 phase cells and an accumulation of G1 phase cells before S phase progression after injurious stimuli in the proximal tubule. *Physiol Rep* 2(10), doi: 10.14814/phy2.12173

Jackson, R. J. et al. 2010. The mechanism of eukaryotic translation initiation and principles of its regulation. *Nature Reviews Molecular Cell Biology* 11(2), pp. 113-127. doi: 10.1038/nrm2838

Jackson, S. P. and Bartek, J. 2009. The DNA-damage response in human biology and disease. *Nature* 461(7267), pp. 1071-1078. doi: 10.1038/nature08467

Jacob, C. I. and Dover, J. S. 2001. Birt-Hogg-Dube syndrome: Treatment of cutaneous manifestations with laser skin resurfacing. *Archives of Dermatology* 137(1), pp. 98-99.

Janssens, V. and Goris, J. 2001. Protein phosphatase 2A: a highly regulated family of serine/threonine phosphatases implicated in cell growth and signalling. *Biochemical Journal* 353, pp. 417-439. doi: 10.1042/0264-6021:3530417

Jette, N. and Lees-Miller, S. P. 2015. The DNA-dependent protein kinase: A multifunctional protein kinase with roles in DNA double strand break repair and mitosis. *Progress in Biophysics & Molecular Biology* 117(2-3), pp. 194-205. doi: 10.1016/j.pbiomolbio.2014.12.003

Jiao, W. et al. 2006. Nucleocytoplasmic shuttling of the retinoblastoma tumor suppressor protein via Cdk phosphorylation-dependent nuclear export. *Journal of Biological Chemistry* 281(49), pp. 38098-38108. doi: 10.1074/jbc.M605271200

Jimeno, S. et al. 2015. Neddylation inhibits CtIP-mediated resection and regulates DNA double strand break repair pathway choice. *Nucleic Acids Research* 43(2), pp. 987-999. doi: 10.1093/nar/gku1384

Jiricny, J. 2013. Postreplicative Mismatch Repair. *Cold Spring Harbor Perspectives in Biology* 5(4), doi: 10.1101/cshperspect.a012633

Johannesma, P. C. et al. 2014a. The pathogenesis of pneumothorax in Birt-Hogg-Dub, syndrome: A hypothesis. *Respirology* 19(8), pp. 1248-1250. doi: 10.1111/resp.12405

Johannesma, P. C. et al. 2014b. Spontaneous pneumothorax as indicator for Birt-Hogg-Dube syndrome in paediatric patients. *Bmc Pediatrics* 14, doi: 10.1186/1471-2431-14-171

Jones, R. G. et al. 2005. AMP-activated protein kinase induces a p53-dependent metabolic checkpoint. *Molecular Cell* 18(3), pp. 283-293. doi: 10.1016/j.molcel.2005.03.027

Kahle, B. et al. 2001. Multiple mantelomas in Birt-Hogg-Dube syndrome. Successful therapy with the CO2 laser. *Hautarzt* 52(1), pp. 43-46. doi: 10.1007/s001050051260

Kanai, M. et al. 2007. Inhibition of Crm1-p53 interaction and nuclear export of p53 by poly(ADP-ribosyl)ation. *Nature Cell Biology* 9(10), pp. 1175-1183. doi: 10.1038/ncb1638

Kanaya, T. et al. 1998. hTERT is a critical determinant of telomerase activity in renal-cell carcinoma. *International Journal of Cancer* 78(5), pp. 539-543. doi: 10.1002/(sici)1097-0215(19981123)78:5<539::aid-ijc2>3.3.co;2-9

Kann, M. G. 2007. Protein interactions and disease: computational approaches to uncover the etiology of diseases. *Briefings in Bioinformatics* 8(5), pp. 333-346. doi: 10.1093/bib/bbm031

Kar, G. et al. 2009. Human Cancer Protein-Protein Interaction Network: A Structural Perspective. *Plos Computational Biology* 5(12), doi: 10.1371/journal.pcbi.1000601

Karanjawala, Z. E. et al. 1999. The nonhomologous DNA end joining pathway is important for chromosome stability in primary fibroblasts. *Current Biology* 9(24), pp. 1501-1504. doi: 10.1016/s0960-9822(00)80123-2

Karanjawala, Z. E. et al. 2002. Oxygen metabolism causes chromosome breaks and is associated with the neuronal apoptosis observed in DNA double-strand break repair mutants. *Current Biology* 12(5), pp. 397-402. doi: 10.1016/s0960-9822(02)00684-x

Karbowniczek, M. et al. 2008. MTOR is activated in the majority of malignant melanomas. *Journal of Investigative Dermatology* 128(4), pp. 980-987. doi: 10.1038/sj.jid.5701074

Karve, T. M. and Cheema, A. K. 2011. Small changes huge impact: the role of protein posttranslational modifications in cellular homeostasis and disease. *J Amino Acids* 2011, p. 207691. doi: 10.4061/2011/207691

Kasai, S. et al. 2013. beta-Catenin signaling induces CYP1A1 expression by disrupting adherens junctions in Caco-2 human colon carcinoma cells. *Biochimica Et Biophysica Acta-General Subjects* 1830(3), pp. 2509-2516. doi: 10.1016/j.bbagen.2012.11.007

Kase, M. et al. 2011. Impact of PARP-1 and DNA-PK expression on survival in patients with glioblastoma multiforme. *Radiotherapy and Oncology* 101(1), pp. 127-131. doi: 10.1016/j.radonc.2011.06.024

Kass, E. M. and Jasin, M. 2010. Collaboration and competition between DNA double-strand break repair pathways. *Febs Letters* 584(17), pp. 3703-3708. doi: 10.1016/j.febslet.2010.07.057

Katayama, M. et al. 2007. DNA damaging agent-induced autophagy produces a cytoprotective adenosine triphosphate surge in malignant glioma cells. *Cell Death and Differentiation* 14(3), pp. 548-558. doi: 10.1038/sj.cdd.4402030

Kato, I. et al. 2016. Fluorescent and chromogenic in situ hybridization of CEN17q as a potent useful diagnostic marker for Birt-Hogg-Dube syndrome-associated chromophobe renal cell carcinomas. *Human Pathology* 52, pp. 74-82. doi: 10.1016/j.humpath.2016.01.004

Kauffman, E. C. et al. 2014. Molecular genetics and cellular features of TFE3 and TFEB fusion kidney cancers. *Nature Reviews Urology* 11(8), pp. 465-475. doi: 10.1038/nrurol.2014.162

Kauffmann, A. et al. 2008. High expression of DNA repair pathways is associated with metastasis in melanoma patients. *Oncogene* 27(5), pp. 565-573. doi: 10.1038/sj.onc.1210700

Kawai, A. et al. 2013. Folliculin regulates cyclin D1 expression through cis-acting elements in the 3 ' untranslated region of cyclin D1 mRNA. *International Journal of Oncology* 42(5), pp. 1597-1604. doi: 10.3892/ijo.2013.1862

Kennedy, J. C. et al. 2016. Mechanisms of pulmonary cyst pathogenesis in Birt-Hogg-Dube syndrome: The stretch hypothesis. *Seminars in Cell & Developmental Biology* 52, pp. 47-52. doi: 10.1016/j.semcdb.2016.02.014

Kenny, P. A. et al. 2007. Targeting the tumor microenvironment. *Frontiers in Bioscience-Landmark* 12, pp. 3468-3474. doi: 10.2741/2327

Kenyon, E. J. et al. 2016. Expression and knockdown of zebrafish folliculin suggests requirement for embryonic brain morphogenesis. *Bmc Developmental Biology* 16, doi: 10.1186/s12861-016-0119-8

Khabibullin , D. et al. 2014. Folliculin regulates cell–cell adhesion, AMPK, and mTORC1 in a cell-type-specific manner in lung-derived cells. 2 (8).

Khacho, M. et al. 2008. eEF1A Is a Novel Component of the Mammalian Nuclear Protein Export Machinery. *Molecular Biology of the Cell* 19(12), pp. 5296-5308. doi: 10.1091/mbc.E08-06-0562

Khoo, S. K. et al. 2001. Birt-Hogg-Dube syndrome: mapping of a novel hereditary neoplasia gene to chromosome 17p12-q11.2. *Oncogene* 20(37), pp. 5239-5242. doi: 10.1038/sj.onc.1204703

Khoo, S. K. et al. 2002. Clinical and genetic studies of Birt-Hogg-Dube syndrome. *Journal of Medical Genetics* 39(12), pp. 906-912. doi: 10.1136/jmg.39.12.906

Khoo, S. K. et al. 2003. Inactivation of BHD in sporadic renal tumors. *Cancer Research* 63(15), pp. 4583-4587.

Kim, B. H. et al. 2007. On the functions of the h subunit of eukaryotic initiation factor 3 in late stages of translation initiation. *Genome Biology* 8(4), doi: 10.1186/gb-2007-8-4-r60

Kim, J. et al. 2011. AMPK and mTOR regulate autophagy through direct phosphorylation of Ulk1. *Nature Cell Biology* 13(2), pp. 132-U171. doi: 10.1038/ncb2152

Kim, J. K. and Diehl, J. A. 2009. Nuclear Cyclin D1: An Oncogenic Driver in Human Cancer. *Journal of Cellular Physiology* 220(2), pp. 292-296. doi: 10.1002/jcp.21791

Kim, K. H. and Sederstrom, J. M. 2015. Assaying Cell Cycle Status Using Flow Cytometry. *Curr Protoc Mol Biol* 111, pp. 28.26.21-11. doi: 10.1002/0471142727.mb2806s111

Kim, S. and Dynlacht, B. D. 2013. Assembling a primary cilium. *Current Opinion in Cell Biology* 25(4), pp. 506-511. doi: 10.1016/j.ceb.2013.04.011

Kinner, A. et al. 2008. gamma-H2AX in recognition and signaling of DNA double-strand breaks in the context of chromatin. *Nucleic Acids Research* 36(17), pp. 5678-5694. doi: 10.1093/nar/gkn550

Klein, H. L. 2008. The consequences of Rad51 overexpression for normal and tumor cells. *DNA Repair* 7(5), pp. 686-693. doi: 10.1016/j.dnarep.2007.12.008

Klomp, J. A. et al. 2010. Birt-Hogg-Dube renal tumors are genetically distinct from other renal neoplasias and are associated with up-regulation of mitochondrial gene expression. *Bmc Medical Genomics* 3, doi: 10.1186/1755-8794-3-59

Kluger, N. et al. 2010. Birt-Hogg-Dube syndrome: clinical and genetic studies of 10 French families. *British Journal of Dermatology* 162(3), pp. 527-537. doi: 10.1111/j.1365-2133.2009.09517.x

Koboldt, D. C. et al. 2012. Comprehensive molecular portraits of human breast tumours. *Nature* 490(7418), pp. 61-70. doi: 10.1038/nature11412

Kolde, R. 2019. pheatmap: Pretty Heatmaps. R package version 1.0.12. https://CRAN.R-project.org/package=pheatmap.

Komori, K. et al. 2009. A novel protein, MAPO1, that functions in apoptosis triggered by O6-methylguanine mispair in DNA. *Oncogene* 28(8), pp. 1142-1150. doi: 10.1038/onc.2008.462

Kondo, K. et al. 2002. Inhibition of HIF is necessary for tumor suppression by the von Hippel-Lindau protein. *Cancer Cell* 1(3), pp. 237-246. doi: 10.1016/s1535-6108(02)00043-0

Koromilas, A. E. et al. 1992. Messenger-RNAs containing extensive secondary structure in their 5' noncoding region translate efficiently in cells overexpressing initiation factor EIF-4E. *Embo Journal* 11(11), pp. 4153-4158. doi: 10.1002/j.1460-2075.1992.tb05508.x

Kosari, F. et al. 2005. Clear cell renal cell carcinoma: Gene expression analyses identify a potential signature for tumor aggressiveness. *Clinical Cancer Research* 11(14), pp. 5128-5139. doi: 10.1158/1078-0432.ccr-05-0073

Kotsis, F. et al. 2013. The ciliary flow sensor and polycystic kidney disease. *Nephrology Dialysis Transplantation* 28(3), pp. 518-526. doi: 10.1093/ndt/gfs524

Koundrioukoff, S. et al. 2013. Stepwise Activation of the ATR Signaling Pathway upon Increasing Replication Stress Impacts Fragile Site Integrity. *Plos Genetics* 9(7), doi: 10.1371/journal.pgen.1003643

Kozlov, S. V. et al. 2011. Autophosphorylation and ATM Activation additional sites add to the complexity. *Journal of Biological Chemistry* 286(11), pp. 9107-9119. doi: 10.1074/jbc.M110.204065

Krokan, H. E. and Bjoras, M. 2013. Base Excision Repair. *Cold Spring Harbor Perspectives in Biology* 5(4), doi: 10.1101/cshperspect.a012583

Kuan, C. T. et al. 2006. Glycoprotein nonmetastatic melanoma protein B, a potential molecular therapeutic target in patients with glioblastoma multiforme. *Clinical Cancer Research* 12(7), pp. 1970-1982. doi: 10.1158/1078-0432.ccr-05-2797

Kubacka, D. et al. 2013. Investigating the Consequences of eIF4E2 (4EHP) Interaction with 4E-Transporter on Its Cellular Distribution in HeLa Cells. *Plos One* 8(8), doi: 10.1371/journal.pone.0072761

Kubbies, M. and Rabinovitch, P. S. 1983. Flow cytometric analysis of factors which influence the BRDURD-Hoechst quenching effect in cultivated human-fibroblasts and lymphocytes. *Cytometry* 3(4), pp. 276-281. doi: 10.1002/cyto.990030408

Kukurba, K. R. and Montgomery, S. B. 2015. RNA Sequencing and Analysis. *Cold Spring Harb Protoc* 2015(11), pp. 951-969. doi: 10.1101/pdb.top084970

Kumar, R. and Cheok, C. F. 2014. RIF1: A novel regulatory factor for DNA replication and DNA damage response signaling. *DNA Repair* 15, pp. 54-59. doi: 10.1016/j.dnarep.2013.12.004

213

Kumareswaran, R. et al. 2012. Chronic hypoxia compromises repair of DNA double-strand breaks to drive genetic instability. *Journal of Cell Science* 125(1), pp. 189-199. doi: 10.1242/jcs.092262

Kunogi, M. et al. 2010. Clinical and genetic spectrum of Birt-Hogg-Dube syndrome patients in whom pneumothorax and/or multiple lung cysts are the presenting feature. *Journal of Medical Genetics* 47(4), pp. 281-287. doi: 10.1136/jmg.2009.070565

Kuo, L. J. and Yang, L.-X. 2008. gamma-H2AX - A novel biomarker for DNA double-strand breaks. *In Vivo* 22(3), pp. 305-309.

LaBaer, J. et al. 1997. New functional activities for the p21 family of CDK inhibitors. *Genes & Development* 11(7), pp. 847-862. doi: 10.1101/gad.11.7.847

Lancaster, M. A. et al. 2011. Subcellular spatial regulation of canonical Wnt signalling at the primary cilium. *Nature Cell Biology* 13(6), pp. 700-U173. doi: 10.1038/ncb2259

Laphanuwat, P. et al. 2018. Cyclin D1 depletion interferes with oxidative balance and promotes cancer cell senescence. *Journal of Cell Science* 131(12), doi: 10.1242/jcs.214726

Larsen, S. C. et al. 2016. Proteome-wide analysis of arginine monomethylation reveals widespread occurrence in human cells. *Science Signaling* 9(443), doi: 10.1126/scisignal.aaf7329

Latimer, J. J. et al. 2010. Nucleotide excision repair deficiency is intrinsic in sporadic stage I breast cancer. *Proceedings of the National Academy of Sciences of the United States of America* 107(50), pp. 21725-21730. doi: 10.1073/pnas.0914772107

Lavin, M. F. and Gueven, N. 2006. The complexity of p53 stabilization and activation. *Cell Death and Differentiation* 13(6), pp. 941-950. doi: 10.1038/sj.cdd.4401925

Laviolette, L. A. et al. 2017. Negative regulation of EGFR signalling by the human folliculin tumour suppressor protein. *Nature Communications* 8, doi: 10.1038/ncomms15866

Laviolette, L. A. et al. 2013. Human Folliculin Delays Cell Cycle Progression through Late S and G2/M-Phases: Effect of Phosphorylation and Tumor Associated Mutations. *Plos One* 8(7), p. 10. doi: 10.1371/journal.pone.0066775

Le Guyadec, T. et al. 1998. Multiple trichodiscomas associated with intestinal polyposis. *Annales De Dermatologie Et De Venereologie* 125(10), pp. 717-719.

Lee, J. S. et al. 2000. hCds1-mediated phosphorylation of BRCA1 regulates the DNA damage response. *Nature* 404(6774), pp. 201-204. doi: 10.1038/35004614

Lee, J. W. et al. 2010. The Association of AMPK with ULK1 Regulates Autophagy. *Plos One* 5(11), doi: 10.1371/journal.pone.0015394

Leesmiller, S. P. et al. 1992. Human DNA-activated protein-kinase phosphorylates serine-15 and serine-37 in the amino-terminal transactivation domain of human p53. *Molecular and Cellular Biology* 12(11), pp. 5041-5049. doi: 10.1128/mcb.12.11.5041

Leon-Buitimea, A. et al. 2012. Ethanol-induced oxidative stress is associated with EGF receptor phosphorylation in MCF-10A cells overexpressing CYP2E1. *Toxicology Letters* 209(2), pp. 161-165. doi: 10.1016/j.toxlet.2011.12.009

Leter, E. M. et al. 2008. Birt-Hogg-Dube syndrome: Clinical and genetic studies of 20 families. *Journal of Investigative Dermatology* 128(1), pp. 45-49. doi: 10.1038/sj.jid.5700959

Levine, B. and Kroemer, G. 2008. Autophagy in the pathogenesis of disease. *Cell* 132(1), pp. 27-42. doi: 10.1016/j.cell.2007.12.018

Li, H. H. et al. 2007. A specific PP2A regulatory subunit, B56 gamma, mediates DNA damage-induced dephosphorylation of p53 at Thr55. *Embo Journal* 26(2), pp. 402-411. doi: 10.1038/sj.emboj.7601519

Li, H. J. et al. 2018. Identification of metabolism-associated genes and pathways involved in different stages of clear cell renal cell carcinoma. *Oncol Lett* 15(2), pp. 2316-2322. doi: 10.3892/ol.2017.7567

Li, J. et al. 2016. Up-regulated expression of phospholipase C, β1 is associated with tumor cell proliferation and poor prognosis in hepatocellular carcinoma. *Onco Targets Ther* 9, pp. 1697-1706. doi: 10.2147/OTT.S97189

Li, T. T. et al. 2014. RNF168-mediated H2A neddylation antagonizes ubiquitylation of H2A and regulates DNA damage repair. *Journal of Cell Science* 127(10), pp. 2238-2248. doi: 10.1242/jcs.138891

Lim, T. H. et al. 2012. Activation of AMP-activated protein kinase by MAPO1 and FLCN induces apoptosis triggered by alkylated base mismatch in DNA. *DNA Repair* 11(3), pp. 259-266. doi: 10.1016/j.dnarep.2011.11.006

Lin, J. Y. et al. 1996. Analysis of wild-type and mutant p21(WAF-1) gene activities. *Molecular and Cellular Biology* 16(4), pp. 1786-1793.

Lindor, N. M. et al. 2001. Birt-Hogg-Dube Syndrome: an autosomal dominant disorder with predisposition to cancers of the kidney, fibrofolliculomas, and focal cutaneous mucinosis. *International Journal of Dermatology* 40(10), pp. 653-656. doi: 10.1046/j.1365-4362.2001.01287-4.x

Lindor, N. M. et al. 2012. Birt-Hogg-Dube syndrome presenting as multiple oncocytic parotid tumors. *Hereditary Cancer in Clinical Practice* 10, doi: 10.1186/1897-4287-10-13

Linehan, W. M. 2012. Genetic basis of kidney cancer: Role of genomics for the development of disease-based therapeutics. *Genome Research* 22(11), pp. 2089-2100. doi: 10.1101/gr.131110.111

Linehan, W. M. 2013. The genetic basis of kidney cancer: A metabolic disease. *Molecular Cancer Therapeutics* 12(11), doi: 10.1158/1535-7163.targ-13-pl02-02

Liou, G. Y. and Storz, P. 2010. Reactive oxygen species in cancer. *Free Radical Research* 44(5), pp. 479-496. doi: 10.3109/10715761003667554

Lips, J. and Kaina, B. 2001. DNA double-strand breaks trigger apoptosis in p53-deficient fibroblasts. *Carcinogenesis* 22(4), pp. 579-585. doi: 10.1093/carcin/22.4.579

Liu, H. et al. 2013a. Characterization of fibrinogen-like protein 2 (FGL2): Monomeric FGL2 has enhanced immunosuppressive activity in comparison to oligomeric FGL2. *International Journal of Biochemistry & Cell Biology* 45(2), pp. 408-418. doi: 10.1016/j.biocel.2012.10.014

Liu, T. et al. 2014. The age- and shorter telomere-dependent TERT promoter mutation in follicular thyroid cell-derived carcinomas. *Oncogene* 33(42), pp. 4978-4984. doi: 10.1038/onc.2013.446

Liu, V. et al. 2000. Parotid oncocytoma in the Birt-Hogg-Dube syndrome. *Journal of the American Academy of Dermatology* 43(6), pp. 1120-1122. doi: 10.1067/mjd.2000.109288

Liu, W. et al. 2013b. Genetic Characterization of the Drosophila Birt-Hogg-Dube Syndrome Gene. *Plos One* 8(6), doi: 10.1371/journal.pone.0065869

Liu, X. D. et al. 2015. Dysregulation of HIF2 alpha and autophagy in renal cell carcinoma. *Molecular & Cellular Oncology* 2(2), doi: 10.4161/23723548.2014.965643

Liu, Y. et al. 2007. Somatic cell type specific gene transfer reveals a tumor-promoting function for p21(Waf1/Cip1). *Embo Journal* 26(22), pp. 4683-4693. doi: 10.1038/sj.emboj.7601886

Livingston, D. et al. 1997. Association of BRCA1 with RAD51 in meiotic and mitotic cells. *Faseb Journal* 11(9), pp. A1015-A1015.

Ljungberg, B. et al. 2011. The Epidemiology of Renal Cell Carcinoma (vol 60, pg 615, 2011). *European Urology* 60(6), pp. 1317-1317. doi: 10.1016/j.eururo.2011.09.001

Lobrich, M. et al. 2010. gamma H2AX foci analysis for monitoring DNA double-strand break repair Strengths, limitations and optimization. *Cell Cycle* 9(4), pp. 662-669. doi: 10.4161/cc.9.4.10764

Longhese, M. P. 2008. DNA damage response at functional and dysfunctional telomeres. *Genes & Development* 22(2), pp. 125-140. doi: 10.1101/gad.1626908

Lopes, C. T. et al. 2010. Cytoscape Web: an interactive web-based network browser. *Bioinformatics* 26(18), pp. 2347-2348. doi: 10.1093/bioinformatics/btq430

Love, M. I. et al. 2014. Moderated estimation of fold change and dispersion for RNA-seq data with DESeq2. *Genome Biology* 15(12), doi: 10.1186/s13059-014-0550-8

Lovejoy, C. A. and Cortez, D. 2009. Common mechanisms of PIKK regulation. *DNA Repair* 8(9), pp. 1004-1008. doi: 10.1016/j.dnarep.2009.04.006

Lovering, R. C. 2017. How Does the Scientific Community Contribute to Gene Ontology? *Methods Mol Biol* 1446, pp. 85-93. doi: 10.1007/978-1-4939-3743-1_7

Lu, J. C. et al. 2016. EBV-LMP1 suppresses the DNA damage response through DNA-PK/AMPK signaling to promote radioresistance in nasopharyngeal carcinoma. *Cancer Letters* 380(1), pp. 191-200. doi: 10.1016/j.canlet.2016.05.032

Lu, X. H. et al. 2011. Therapeutic Targeting the Loss of the Birt-Hogg-Dube Suppressor Gene. *Molecular Cancer Therapeutics* 10(1), pp. 80-89. doi: 10.1158/1535-7163.mct-10-0628

Lu, Z. M. and Hunter, T. 2010. Ubiquitylation and proteasomal degradation of the p21(Cip1), p27(Kip1) and p57(Kip2) CDK inhibitors. *Cell Cycle* 9(12), pp. 2342-2352. doi: 10.4161/cc.9.12.11988

Lucas, R. E. et al. 2001. Genomic organisation of the similar to 1.5 Mb Smith-Magenis syndrome critical interval: Transcription map, genomic contig, and candidate gene analysis. *European Journal of Human Genetics* 9(12), pp. 892-902. doi: 10.1038/sj.ejhg.5200734

Luijten, M. N. H. et al. 2013. Birt-Hogg-Dube syndrome is a novel ciliopathy. *Human Molecular Genetics* 22(21), pp. 4383-4397. doi: 10.1093/hmg/ddt288

Lukas, C. et al. 2004. Mdc1 couples DNA double-strand break recognition by Nbs1 with its H2AX-dependent chromatin retention. *Embo Journal* 23(13), pp. 2674-2683. doi: 10.1038/sj.emboj.7600269

Luo, Y. et al. 1995. Cell-cycle inhibition by independent CDK and PCNA binding domains in p21(CIP1). *Nature* 375(6527), pp. 159-161. doi: 10.1038/375159a0

Ma, T. et al. 2013. RNF111-Dependent Neddylation Activates DNA Damage-Induced Ubiquitination. *Molecular Cell* 49(5), pp. 897-907. doi: 10.1016/j.molcel.2013.01.006

Macosko, E. Z. et al. 2015. Highly Parallel Genome-wide Expression Profiling of Individual Cells Using Nanoliter Droplets. *Cell* 161(5), pp. 1202-1214. doi: 10.1016/j.cell.2015.05.002

Maffe, A. et al. 2011. Constitutional FLCN mutations in patients with suspected Birt-Hogg-Dube syndrome ascertained for non-cutaneous manifestations. *Clinical Genetics* 79(4), pp. 345-354. doi: 10.1111/j.1399-0004.2010.01480.x

Mahaney, B. L. et al. 2009. Repair of ionizing radiation-induced DNA double-strand breaks by non-homologous end-joining. *Biochemical Journal* 417, pp. 639-650. doi: 10.1042/bj20080413

Mailand, N. et al. 2013. Regulation of PCNA-protein interactions for genome stability. *Nature Reviews Molecular Cell Biology* 14(5), pp. 269-282. doi: 10.1038/nrm3562

Makhnevych, T. and Houry, W. A. 2012. The role of Hsp90 in protein complex assembly. *Biochimica Et Biophysica Acta-Molecular Cell Research* 1823(3), pp. 674-682. doi: 10.1016/j.bbamcr.2011.09.001

Malumbres, M. and Barbacid, M. 2009. Cell cycle, CDKs and cancer: a changing paradigm. *Nature Reviews Cancer* 9(3), pp. 153-166. doi: 10.1038/nrc2602

Mammoto, A. et al. 2004. Role of RhoA, mDia, and ROCK in cell shape-dependent control of the Skp2-p27(kip1) pathway and the G(1)/S transition. *Journal of Biological Chemistry* 279(25), pp. 26323-26330. doi: 10.1074/jbc.M402725200

Manzoli, L. et al. 1997. Essential role for nuclear phospholipase C beta(1) in insulin-like growth factor I-induced mitogenesis. *Cancer Research* 57(11), pp. 2137-2139.

Marat, A. L. et al. 2011. DENN Domain Proteins: Regulators of Rab GTPases. *Journal of Biological Chemistry* 286(16), pp. 13791-13800. doi: 10.1074/jbc.R110.217067

Marechal, A. and Zou, L. 2013. DNA Damage Sensing by the ATM and ATR Kinases. *Cold Spring Harbor Perspectives in Biology* 5(9), doi: 10.1101/cshperspect.a012716

Marin, T. L. et al. 2017. AMPK promotes mitochondrial biogenesis and function by phosphorylating the epigenetic factors DNMT1, RBBP7, and HAT1. *Science Signaling* 10(464), doi: 10.1126/scisignal.aaf7478

Markowski, J. et al. 2009. Gene expression profile analysis in laryngeal cancer by high-density oligonucleotide microarrays. *Journal of Physiology and Pharmacology* 60, pp. 57-63.

Marteijn, J. A. et al. 2014. Understanding nucleotide excision repair and its roles in cancer and ageing. *Nature Reviews Molecular Cell Biology* 15(7), pp. 465-481. doi: 10.1038/nrm3822

Martelli, A. M. et al. 1992. Nuclear-localization and signalling activity of phoshoinsositidase-C-beta in swiss 3T3 cells. *Nature* 358(6383), pp. 242-245. doi: 10.1038/358242a0

Martien, S. and Abbadie, C. 2007. Acquisition of oxidative DNA damage during senescence - The first step toward carcinogenesis? *Molecular Mechanisms and Models of Aging* 1119, pp. 51-63. doi: 10.1196/annals.1404.010

Martina, J. A. et al. 2014. The Nutrient-Responsive Transcription Factor TFE3 Promotes Autophagy, Lysosomal Biogenesis, and Clearance of Cellular Debris. *Science Signaling* 7(309), doi: 10.1126/scisignal.2004754

Martinez-Ruiz, G. et al. 2008. Role of Smac/DIABLO in cancer progression. *Journal of Experimental & Clinical Cancer Research* 27, doi: 10.1186/1756-9966-27-48

Maslon, M. M. and Hupp, T. R. 2010. Drug discovery and mutant p53. *Trends in Cell Biology* 20(9), pp. 542-555. doi: 10.1016/j.tcb.2010.06.005

Mastropasqua, F. et al. 2018. PGC1 alpha: Friend or Foe in Cancer? *Genes* 9(1), doi: 10.3390/genes9010048

Mathieu, J. et al. 2019. Folliculin regulates mTORC1/2 and WNT pathways in early human pluripotency. *Nature Communications* 10, doi: 10.1038/s41467-018-08020-0

Matsuoka, S. et al. 2007. ATM and ATR substrate analysis reveals extensive protein networks responsive to DNA damage. *Science* 316(5828), pp. 1160-1166. doi: 10.1126/science.1140321

McCarthy, D. J. and Smyth, G. K. 2009. Testing significance relative to a fold-change threshold is a TREAT. *Bioinformatics* 25(6), pp. 765-771. doi: 10.1093/bioinformatics/btp053

McGranahan, N. and Swanton, C. 2017. Clonal Heterogeneity and Tumor Evolution: Past, Present, and the Future. *Cell* 168(4), pp. 613-628. doi: 10.1016/j.cell.2017.01.018

Medvetz, D. A. et al. 2012. Folliculin, the Product of the Birt-Hogg-Dube Tumor Suppressor Gene, Interacts with the Adherens Junction Protein p0071 to Regulate Cell-Cell Adhesion. *Plos One* 7(11), doi: 10.1371/journal.pone.0047842

Meek, K. et al. 2008. DNA-PK: The Means to Justify the Ends? *Advances in Immunology, Vol 99* 99, pp. 33-58. doi: 10.1016/s0065-2776(08)00602-0

Meek, K. et al. 2007. trans Autophosphorylation at DNA-dependent protein kinase's two major autophosphorylation site clusters facilitates end processing but not end joining. *Molecular and Cellular Biology* 27(10), pp. 3881-3890. doi: 10.1128/mcb.02366-06

Melanson, G. et al. 2017. The eIF4E2-Directed Hypoxic Cap-Dependent Translation Machinery Reveals Novel Therapeutic Potential for Cancer Treatment. *Oxidative Medicine and Cellular Longevity*, doi: 10.1155/2017/6098107

Meng, A. X. et al. 2005. Hypoxia down-regulates DNA double strand break repair gene expression in prostate cancer cells. *Radiotherapy and Oncology* 76(2), pp. 168-176. doi: 10.1016/j.radonc.2005.06.025

Meng, J. and Ferguson, S. M. 2018. GATOR1-dependent recruitment of FLCN-FNIP to lysosomes coordinates Rag GTPase heterodimer nucleotide status in response to amino acids. *Journal of Cell Biology* 217(8), pp. 2765-2776. doi: 10.1083/jcb.201712177

Menko, F. H. et al. 2009. Birt-Hogg-Dube syndrome: diagnosis and management. *Lancet Oncology* 10(12), pp. 1199-1206. doi: 10.1016/s1470-2045(09)70188-3

Mikhaylova, O. et al. 2012. VHL-Regulated MiR-204 Suppresses Tumor Growth through Inhibition of LC3B-Mediated Autophagy in Renal Clear Cell Carcinoma. *Cancer Cell* 21(4), pp. 532-546. doi: 10.1016/j.ccr.2012.02.019

Milhollen, M. A. et al. 2010. MLN4924, a NEDD8-activating enzyme inhibitor, is active in diffuse large B-cell lymphoma models: rationale for treatment of NF-kappa B-dependent lymphoma. *Blood* 116(9), pp. 1515-1523. doi: 10.1182/blood-2010-03-272567

Mills, K. D. et al. 2003. The role of DNA breaks in genomic instability and tumorigenesis. *Immunological Reviews* 194(1), pp. 77-95. doi: 10.1034/j.1600-065X.2003.00060.x

Miyamoto, L. et al. 2007. Effect of acute activation of 5 '-AMP-activated protein kinase on glycogen regulation in isolated rat skeletal muscle. *Journal of Applied Physiology* 102(3), pp. 1007-1013. doi: 10.1152/japplphysiol.01034.2006

Mizushima, N. et al. 2008. Autophagy fights disease through cellular self-digestion. *Nature* 451(7182), pp. 1069-1075. doi: 10.1038/nature06639

Mizushima, N. et al. 2011. The Role of Atg Proteins in Autophagosome Formation. *Annual Review of Cell and Developmental Biology, Vol 27* 27, pp. 107-132. doi: 10.1146/annurev-cellbio-092910-154005

Moloney, J. N. and Cotter, T. G. 2018. ROS signalling in the biology of cancer. *Seminars in Cell & Developmental Biology* 80, pp. 50-64. doi: 10.1016/j.semcdb.2017.05.023

Moloney, J. N. et al. 2017. Subcellular localization of the FLT3-ITD oncogene plays a significant role in the production of NOX- and p22(phox)-derived reactive oxygen species in acute myeloid leukemia. *Leukemia Research* 52, pp. 34-42. doi: 10.1016/j.leukres.2016.11.006

Montecucco, A. et al. 2015. Molecular mechanisms of etoposide. *Excli Journal* 14, pp. 95-108.

Moonen, L. et al. 2018. Epithelial Cell Cycle Behaviour in the Injured Kidney. *International Journal of Molecular Sciences* 19(7), doi: 10.3390/ijms19072038

Morgan, D. O. 1995. Principles of CDK regulation. *Nature* 374(6518), pp. 131-134. doi: 10.1038/374131a0

Morris, C. and Jalinot, P. 2005. Silencing of human Int-6 impairs mitosis progression and inhibits cyclin B-Cdk1 activation. *Oncogene* 24(7), pp. 1203-1211. doi: 10.1038/sj.onc.1208268

Mortensen, D. S. et al. 2015. Optimization of a Series of Triazole Containing Mammalian Target of Rapamycin (mTOR) Kinase Inhibitors and the Discovery of CC-115. *Journal of Medicinal Chemistry* 58(14), pp. 5599-5608. doi: 10.1021/acs.jmedchem.5b00627

Mortusewicz, O. et al. 2005. Recruitment of DNA methyltransferase I to DNA repair sites. *Proceedings of the National Academy of Sciences of the United States of America* 102(25), pp. 8905-8909. doi: 10.1073/pnas.0501034102

Mota-Burgos, A. et al. 2013. Birt-Hogg-Dube syndrome in a patient with melanoma and a novel mutation in the FCLN gene. *International Journal of Dermatology* 52(3), pp. 323-326. doi: 10.1111/j.1365-4632.2012.05742.x

Moynahan, M. E. and Jasin, M. 2010. Mitotic homologous recombination maintains genomic stability and suppresses tumorigenesis. *Nature Reviews Molecular Cell Biology* 11(3), pp. 196-207. doi: 10.1038/nrm2851

Munoz, C. M. et al. 2001. The effect of hydrogen peroxide on the cyclin D expression in fibroblasts. *Cellular and Molecular Life Sciences* 58(7), pp. 990-996. doi: 10.1007/pl00013204

Munster, P. N. et al. 2016. Phase I trial of a dual TOR kinase and DNA-PK inhibitor (CC-115) in advanced solid and hematologic cancers. *Journal of Clinical Oncology* 34(15), doi: 10.1200/JCO.2016.34.15_suppl.2505

Muqbil, I. et al. 2016. Anti-tumor activity of selective inhibitor of nuclear export (SINE) compounds, is enhanced in non-Hodgkin lymphoma through combination with mTOR inhibitor and dexamethasone. *Cancer Letters* 383(2), pp. 309-317. doi: 10.1016/j.canlet.2016.09.016

Murphy, K. A. et al. 2015. Exploiting natural anti-tumor immunity for metastatic renal cell carcinoma. *Human Vaccines & Immunotherapeutics* 11(7), pp. 1612-1620. doi: 10.1080/21645515.2015.1035849

Mydlo, J. H. et al. 1989. Expression of transforming growth factor-alpha and epidermal growth-factor receptor messenger-RNA in neoplastic and non-neoplastic human-kidney tissue. *Cancer Research* 49(12), pp. 3407-3411.

Nagashima, K. et al. 2017. Nutrient-induced FNIP degradation by SCF beta-TRCP regulates FLCN complex localization and promotes renal cancer progression. *Oncotarget* 8(6), pp. 9947-9960. doi: 10.18632/oncotarget.14221

Nahorski, M. et al. 2010. Investigation of the Birt-Hogg-Dube tumour suppressor gene (FLCN) in familial and sporadic colorectal cancer. *Journal of Medical Genetics* 47, pp. S114-S114.

Nahorski, M. S. et al. 2012. Folliculin interacts with p0071 (plakophilin-4) and deficiency is associated with disordered RhoA signalling, epithelial polarization and cytokinesis. *Human Molecular Genetics* 21(24), pp. 5268-5279. doi: 10.1093/hmg/dds378

Nakanishi, M. et al. 1995. The c-terminal region of p21(SDI1/WAF1/CIP1) is involved in proliferating cell nuclear antigen-binding but does not appear to be required for growth-inhibition. *Journal of Biological Chemistry* 270(29), pp. 17060-17063. doi: 10.1074/jbc.270.29.17060

Nardini, C. et al. 2015. Editorial: Multi-omic data integration. *Front Cell Dev Biol* 3, p. 46. doi: 10.3389/fcell.2015.00046

Navin, N. et al. 2011. Tumour evolution inferred by single-cell sequencing. *Nature* 472(7341), pp. 90-U119. doi: 10.1038/nature09807

Negrini, S. et al. 2010. Genomic instability - an evolving hallmark of cancer. *Nature Reviews Molecular Cell Biology* 11(3), pp. 220-228. doi: 10.1038/nrm2858

Ngoh, A. et al. 2014. Severe infantile epileptic encephalopathy due to mutations in PLCB1: expansion of the genotypic and phenotypic disease spectrum. *Developmental Medicine and Child Neurology* 56(11), pp. 1124-1128. doi: 10.1111/dmcn.12450

Nickerson, M. L. et al. 2002. Mutations in a novel gene lead to kidney tumors, lung wall defects, and benign tumors of the hair follicle in patients with the Birt-Hogg-Dube syndrome. *Cancer Cell* 2(2), pp. 157-164. doi: 10.1016/s1535-6108(02)00104-6

Nikolaidou, C. et al. 2016. Multiple angiomatous nodules: a novel skin tumor in Birt-Hogg-Dube syndrome. *Journal of Cutaneous Pathology* 43(12), pp. 1197-1202. doi: 10.1111/cup.12811

Nishida, C. et al. 2015. Possible familial case of Birt-Hogg-Dube syndrome complicated with lung cancer: A possible link between these two disease entities. *Respiratory Medicine* 109(7), pp. 923-925. doi: 10.1016/j.rmed.2015.05.005

Nishii, T. et al. 2013. Unique mutation, accelerated mTOR signaling and angiogenesis in the pulmonary cysts of Birt-Hogg-Dube syndrome. *Pathology International* 63(1), pp. 45-55. doi: 10.1111/pin.12028

Niu, C. et al. 2012. Downregulation and growth inhibitory role of FHL1 in lung cancer. *International Journal of Cancer* 130(11), pp. 2549-2556. doi: 10.1002/ijc.26259

Nollen, E. A. A. and Morimoto, R. I. 2002. Chaperoning signaling pathways: molecular chaperones as stress-sensing 'heat shock' proteins. *Journal of Cell Science* 115(14), pp. 2809-2816.

Nookala, R. K. et al. 2012. Crystal structure of folliculin reveals a hidDENN function in genetically inherited renal cancer. *Open Biology* 2, doi: 10.1098/rsob.120071

Noon, A. P. et al. 2010. p53 and MDM2 in Renal Cell Carcinoma Biomarkers for Disease Progression and Future Therapeutic Targets? *Cancer* 116(4), pp. 780-790. doi: 10.1002/cncr.24841

Nyberg, K. A. et al. 2002. Toward maintaining the genome: DNA damage and replication checkpoints. *Annual Review of Genetics* 36, pp. 617-656. doi: 10.1146/annurev.genet.36.060402.113540

O'Connor, M. J. 2015. Targeting the DNA Damage Response in Cancer. *Molecular Cell* 60(4), pp. 547-560. doi: 10.1016/j.molcel.2015.10.040

Okada, S. and Ouchi, T. 2003. Cell cycle differences in DNA damage-induced BRCA1 phosphorylation affect its subcellular localization. *Journal of Biological Chemistry* 278(3), pp. 2015-2020. doi: 10.1074/jbc.M208685200

Okumura, F. et al. 2007. ISG15 modification of the eIF4E cognate 4EHP enhances cap structure-binding activity of 4EHP. *Genes & Development* 21(3), pp. 255-260. doi: 10.1101/gad.1521607

Okura, M. K. et al. 2013. Pneumothorax Developing for the First Time in a 73-year-old Woman Diagnosed with Birt-Hogg-Dube Syndrome. *Internal Medicine* 52(21), pp. 2453-2455. doi: 10.2169/internalmedicine.52.0338

Olive, P. L. and Banath, J. P. 2004. Phosphorylation of histone H2AX as a measure of radiosensitivity. *International Journal of Radiation Oncology Biology Physics* 58(2), pp. 331-335. doi: 10.1016/j.ijrobp.2003.09.028

Ormerod, M. G. and Kubbies, M. 1992. Cell-cycle analysis of asynchronous cell-populations by flow-cytometry using bromodeoxyuridine label and hoechst-propidium iodide stain. *Cytometry* 13(7), pp. 678-685. doi: 10.1002/cyto.990130703

Otto, T. and Sicinski, P. 2017. Cell cycle proteins as promising targets in cancer therapy. *Nature Reviews Cancer* 17(2), pp. 93-115. doi: 10.1038/nrc.2016.138

Ouchi, T. 2006. BRCA1 phosphorylation - Biological consequences. *Cancer Biology & Therapy* 5(5), pp. 470-475.

Oya, M. et al. 2005. c-Jun activation in acquired cystic kidney disease and renal cell carcinoma. *Journal of Urology* 174(2), pp. 726-730. doi: 10.1097/01.ju.0000164656.99251.77

Pacek, M. and Walter, J. C. 2004. A requirement for MCM7 and Cdc45 in chromosome unwinding during eukaryotic DNA replication. *Embo Journal* 23(18), pp. 3667-3676. doi: 10.1038/sj.emboj.7600369

Paglin, S. et al. 2001. A novel response of cancer cells to radiation involves autophagy and formation of acidic vesicles. *Cancer Research* 61(2), pp. 439-444.

Panier, S. and Boulton, S. J. 2014. Double-strand break repair: 53BP1 comes into focus. *Nature Reviews Molecular Cell Biology* 15(1), pp. 7-18. doi: 10.1038/nrm3719

Panta, G. R. et al. 2004. ATM and the catalytic subunit of DNA-dependent protein kinase activate NF-kappa B through a common MEK extracellular signal-regulated kinase/p90(rsk) signaling pathway in response to distinct forms of DNA damage. *Molecular and Cellular Biology* 24(5), pp. 1823-1835. doi: 10.1128/mcb.24.5.1823-1835.2004

Papaiahgari, S. et al. 2006. Hyperoxia stimulates an Nrf2-ARE transcriptional response via ROS-EGFR-PI3K-Akt/ERK MAP kinase signaling in pulmonary epithelial cells. *Antioxidants & Redox Signaling* 8(1-2), pp. 43-52. doi: 10.1089/ars.2006.8.43

Park, H. et al. 2012. Disruption of Fnip1 Reveals a Metabolic Checkpoint Controlling B Lymphocyte Development. *Immunity* 36(5), pp. 769-781. doi: 10.1016/j.immuni.2012.02.019

Park, S. and Lee, E. J. 2017. Diagnosis and treatment of cystic lung disease. *Korean Journal of Internal Medicine* 32(2), pp. 229-238. doi: 10.3904/kjim.2016.242

Park, S. J. et al. 2017. DNA-PK Promotes the Mitochondrial, Metabolic, and Physical Decline that Occurs During Aging. *Cell Metabolism* 25(5), pp. 1135-+. doi: 10.1016/j.cmet.2017.04.008

Parker, B. L. et al. 2015. Targeted phosphoproteomics of insulin signaling using data-independent acquisition mass spectrometry. *Science Signaling* 8(380), doi: 10.1126/scisignal.aaa3139

Patel, P. I. et al. 1992. The gene for the peripheral myelin protein-pmp-22 is a candidate for Charcot-Marie-tooth disease type-1a. *Nature Genetics* 1(3), pp. 159-165. doi: 10.1038/ng0692-159

Patra, K. C. and Hay, N. 2014. The pentose phosphate pathway and cancer. *Trends in Biochemical Sciences* 39(8), pp. 347-354. doi: 10.1016/j.tibs.2014.06.005

Paull, T. T. et al. 2000. A critical role for histone H2AX in recruitment of repair factors to nuclear foci after DNA damage. *Current Biology* 10(15), pp. 886-895. doi: 10.1016/s0960-9822(00)00610-2

Pavlovich, C. P. et al. 2005. Evaluation and management of renal tumors in the Birt-Hogg-Dube syndrome. *Journal of Urology* 173(5), pp. 1482-1486. doi: 10.1097/01.ju.0000154629.45832.30

Pavlovich, C. P. et al. 2002. Renal tumors in the Birt-Hogg-Dube syndrome. *American Journal of Surgical Pathology* 26(12), pp. 1542-1552. doi: 10.1097/00000478-200212000-00002

Pelletier, J. et al. 2015. Targeting the eIF4F Translation Initiation Complex: A Critical Nexus for Cancer Development. *Cancer Research* 75(2), pp. 250-263. doi: 10.1158/0008-5472.can-14-2789

Pennisi, R. et al. 2015. Hsp90: A New Player in DNA Repair? *Biomolecules* 5(4), pp. 2589-2618. doi: 10.3390/biom5042589

Petermann, E. and Caldecott, K. W. 2006. Evidence that the ATR/Chk1 pathway maintains normal replication fork progression during unperturbed S phase. *Cell Cycle* 5(19), pp. 2203-2209. doi: 10.4161/cc.5.19.3256

Petit, C. S. et al. 2013. Recruitment of folliculin to lysosomes supports the amino acid-dependent activation of Rag GTPases. *Journal of Cell Biology* 202(7), pp. 1107-1122. doi: 10.1083/jcb.201307084

Petrelli, F. et al. 2019. Comparative efficacy of palbociclib, ribociclib and abemaciclib for ER plus metastatic breast cancer: an adjusted indirect analysis of randomized controlled trials. *Breast Cancer Research and Treatment* 174(3), pp. 597-604. doi: 10.1007/s10549-019-05133-y

Petrides, P. E. et al. 1990. Modulation of pro-epidermal growth-factor, pro-transforming growth factor-alpha and epidermal growth-factor receptor gene-expression in human renal carcinomas. *Cancer Research* 50(13), pp. 3934-3939.

Pezzuto, A. and Carico, E. 2018. Role of HIF-1 in Cancer Progression: Novel Insights. A Review. *Current Molecular Medicine* 18(6), pp. 343-351. doi: 10.2174/1566524018666181109121849

Piao, X. H. et al. 2009. Regulation of folliculin (the BHD gene product) phosphorylation by Tsc2-mTOR pathway. *Biochemical and Biophysical Research Communications* 389(1), pp. 16-21. doi: 10.1016/j.bbrc.2009.08.070

Pimenta, S. P. et al. 2012. Birt-Hogg-Dube syndrome: metalloproteinase activity and response to doxycycline. *Clinics* 67(12), pp. 1501-1504. doi: 10.6061/clinics/2012(12)25

Plentz, R. R. et al. 2007. Telomere shortening and inactivation of cell cycle checkpoints characterize human hepatocarcinogenesis. *Hepatology* 45(4), pp. 968-976. doi: 10.1002/hep.21552

Podust, V. N. et al. 1995. Mechanism of inhibition of proliferating cell nuclear antigen-dependent DNA-synthesis by the cyclin-dependent kinase inhibitor p21. *Biochemistry* 34(27), pp. 8869-8875. doi: 10.1021/bi00027a039

Polo, S. E. and Jackson, S. P. 2011. Dynamics of DNA damage response proteins at DNA breaks: a focus on protein modifications. *Genes & Development* 25(5), pp. 409-433. doi: 10.1101/gad.2021311

Poratti, M. and Marzaro, G. 2019. Third-generation CDK inhibitors: A review on the synthesis and binding modes of Palbociclib, Ribociclib and Abemaciclib. *European Journal of Medicinal Chemistry* 172, pp. 143-153. doi: 10.1016/j.ejmech.2019.03.064

Possik, E. et al. 2014. Folliculin Regulates Ampk-Dependent Autophagy and Metabolic Stress Survival. *Plos Genetics* 10(4), doi: 10.1371/journal.pgen.1004273

Pradella, L. M. et al. 2013. Where Birt-Hogg-Dube meets Cowden Syndrome: mirrored genetic defects in two cases of syndromic oncocytic tumours. *European Journal of Human Genetics* 21(10), pp. 1169-1172. doi: 10.1038/ejhg.2013.8

Predina, J. D. et al. 2011. Recurrent spontaneous pneumothorax in a patient with Birt-Hogg-Dube syndrome. *European Journal of Cardio-Thoracic Surgery* 39(3), pp. 404-406. doi: 10.1016/j.ejcts.2010.06.009

Preston, R. S. et al. 2011. Absence of the Birt-Hogg-Dube gene product is associated with increased hypoxia-inducible factor transcriptional activity and a loss of metabolic flexibility. *Oncogene* 30(10), pp. 1159-1173. doi: 10.1038/onc.2010.497

Price, P. M. et al. 2009. The cell cycle and acute kidney injury. *Kidney International* 76(6), pp. 604-613. doi: 10.1038/ki.2009.224

Puustinen, P. 2018a. DNA-PKcs-mediated phosphorylation of AMPKg1 regulates lysosomal AMPK activation by LKB1. In: Keldsbo, A. ed. bioRxiv.

Puustinen, P. 2018b. DNA-PKcs-mediated phosphorylation of AMPKg1 regulates lysosomal AMPK activation by LKB1. In: Keldsbo, A. ed. bioRxiv.

Puyol, M. et al. 2010. A synthetic lethal interaction between K-Ras oncogenes and Cdk4 unveils a therapeutic strategy for non-small cell lung carcinoma. *Cancer Cell* 18(1), pp. 63-73. doi: 10.1016/j.ccr.2010.05.025

Qin, C. P. et al. 2014. Glycoprotein non- metastatic melanoma protein B as a predictive prognostic factor in clear- cell renal cell carcinoma following radical nephrectomy. *Molecular Medicine Reports* 9(3), pp. 851-856. doi: 10.3892/mmr.2014.1896

Qin, Y. et al. 2011. Anti-proliferative effects of the novel squamosamide derivative (FLZ) on HepG2 human hepatoma cells by regulating the cell cycle-related proteins are associated with decreased Ca2+/ROS levels. *Chemico-Biological Interactions* 193(3), pp. 246-253. doi: 10.1016/j.cbi.2011.07.004

Quanz, M. et al. 2012. Heat Shock Protein 90 alpha (Hsp90 alpha) Is Phosphorylated in Response to DNA Damage and Accumulates in Repair Foci. *Journal of Biological Chemistry* 287(12), pp. 8803-8815. doi: 10.1074/jbc.M111.320887

Rad, E. et al. 2018. Oncogenic Signalling through Mechanistic Target of Rapamycin (mTOR): A Driver of Metabolic Transformation and Cancer Progression. *Cancers* 10(1), doi: 10.3390/cancers10010005

Ralph, S. J. et al. 2010. The causes of cancer revisited: "Mitochondrial malignancy" and ROS-induced oncogenic transformation - Why mitochondria are targets for cancer therapy. *Molecular Aspects of Medicine* 31(2), pp. 145-170. doi: 10.1016/j.mam.2010.02.008

Raman, K. et al. 2014. The organisational structure of protein networks: revisiting the centrality-lethality hypothesis. *Syst Synth Biol* 8(1), pp. 73-81. doi: 10.1007/s11693-013-9123-5

Ramaswamy, S. et al. 2003. A molecular signature of metastasis in primary solid tumors. *Nature Genetics* 33(1), pp. 49-54. doi: 10.1038/ng1060

Raval, R. R. et al. 2005. Contrasting properties of hypoxia-inducible factor 1 (HIF-1) and HIF-2 in von Hippel-Lindau-associated renal cell carcinoma. *Molecular and Cellular Biology* 25(13), pp. 5675-5686. doi: 10.1128/mcb.13.5675-5686.2005

Raymond, V. M. et al. 2014. An oncocytic adrenal tumour in a patient with Birt-Hogg-Dube syndrome. *Clinical Endocrinology* 80(6), pp. 925-927. doi: 10.1111/cen.12292

Reiman, A. et al. 2012. Gene Expression and Protein Array Studies of Folliculin-regulated Pathways. *Anticancer Research* 32(11), pp. 4663-4670.

Rello-Varona, S. et al. 2012. Autophagic removal of micronuclei. *Cell Cycle* 11(1), pp. 170-176. doi: 10.4161/cc.11.1.18564

227

Resnitzky, D. et al. 1994. Acceleration of the G(1)/S phase- transition by expression of cyclin D1 and cyclin E with an inducible system *Molecular and Cellular Biology* 14(3), pp. 1669-1679. doi: 10.1128/mcb.14.3.1669

Reyes, N. L. et al. 2015. Fnip1 regulates skeletal muscle fiber type specification, fatigue resistance, and susceptibility to muscular dystrophy. *Proceedings of the National Academy of Sciences of the United States of America* 112(2), pp. 424-429. doi: 10.1073/pnas.1413021112/-/DCSupplemental

Rich, T. et al. 2000. Defying death after DNA damage. *Nature* 407(6805), pp. 777-783.

Ricketts, C. J. et al. 2018. The Cancer Genome Atlas Comprehensive Molecular Characterization of Renal Cell Carcinoma. *Cell Reports* 23(1), pp. 313-+. doi: 10.1016/j.celrep.2018.03.075

Rieber, M. and Rieber, M. S. 2008. Sensitization to radiation-induced DNA damage accelerates loss of bcl-2 and increases apoptosis and autophagy. *Cancer Biology & Therapy* 7(10), pp. 1561-1566. doi: 10.4161/cbt.7.10.6540

Rizzardi, L. F. and Cook, J. G. 2012. Flipping the switch from g1 to s phase with e3 ubiquitin ligases. *Genes Cancer* 3(11-12), pp. 634-648. doi: 10.1177/1947601912473307

Roberts, S. A. et al. 2010. Ku is a 5 '-dRP/AP lyase that excises nucleotide damage near broken ends. *Nature* 464(7292), pp. 1214-U1139. doi: 10.1038/nature08926

Roncaglia, P. et al. 2013. The Gene Ontology (GO) Cellular Component Ontology: integration with SAO (Subcellular Anatomy Ontology) and other recent developments. *Journal of Biomedical Semantics* 4, doi: 10.1186/2041-1480-4-20

Roninson, I. B. 2002. Oncogenic functions of tumour suppressor p21 (Waf1/Cip1/Sdi1): association with cell senescence and tumour-promoting activities of stromal fibroblasts. *Cancer Letters* 179(1), pp. 1-14. doi: 10.1016/s0304-3835(01)00847-3

Rothaeusler, K. and Baumgarth, N. 2007. Assessment of cell proliferation by 5-bromodeoxyuridine (BrdU) labeling for multicolor flow cytometry. *Curr Protoc Cytom* Chapter 7, p. Unit7.31. doi: 10.1002/0471142956.cy0731s40

Rousseau, D. et al. 1996. Translation initiation of ornithine decarboxylase and nucleocytoplasmic transport of cyclin D1 mRNA are increased in cells overexpressing eukaryotic initiation factor 4E. *Proceedings of the National Academy of Sciences of the United States of America* 93(3), pp. 1065-1070. doi: 10.1073/pnas.93.3.1065

Roy, K. et al. 2015. NADPH oxidases and cancer. *Clinical Science* 128(12), pp. 863-875. doi: 10.1042/cs20140542

Rudresha, A. H. et al. 2017. First-line tyrosine kinase inhibitors in metastatic renal cell carcinoma: A regional cancer center experience. *Indian Journal of Cancer* 54(4), pp. 626-630. doi: 10.4103/ijc.IJC_380_17

Sabharwal, S. S. and Schumacker, P. T. 2014. Mitochondrial ROS in cancer: initiators, amplifiers or an Achilles' heel? *Nat Rev Cancer* 14(11), pp. 709-721. doi: 10.1038/nrc3803

Sacco, F. et al. 2014. Combining affinity proteomics and network context to identify new phosphatase substrates and adapters in growth pathways. *Frontiers in Genetics* 5, doi: 10.3389/fgene.2014.00115

Safari-Alighiarloo, N. et al. 2017. Identification of new key genes for type 1 diabetes through construction and analysis of protein-protein interaction networks based on blood and pancreatic islet transcriptomes. *Journal of Diabetes* 9(8), pp. 764-777. doi: 10.1111/1753-0407.12483

Sak, A. and Stuschke, M. 2010. Use of gamma H2AX and Other Biomarkers of Double-Strand Breaks During Radiotherapy. *Seminars in Radiation Oncology* 20(4), pp. 223-231. doi: 10.1016/j.semradonc.2010.05.004

Sakimoto, I. et al. 2006. alpha-sulfoquinovosylmonoacylglycerol is a novel potent radiosensitizer targeting tumor angiogenesis. *Cancer Research* 66(4), pp. 2287-2295. doi: 10.1158/0008-5472.can-05-2209

Salaun, P. et al. 2008. Cdk1, Plks, auroras, and Neks: The mitotic bodyguards. *Hormonal Carcinogenesis V* 617, pp. 41-56.

Salazar-Roa, M. and Malumbres, M. 2017. Fueling the Cell Division Cycle. *Trends in Cell Biology* 27(1), pp. 69-81. doi: 10.1016/j.tcb.2016.08.009

Saletta, F. et al. 2010. The translational regulator eIF3a: The tricky eIF3 subunit! *Biochimica Et Biophysica Acta-Reviews on Cancer* 1806(2), pp. 275-286. doi: 10.1016/j.bbcan.2010.07.005

Salic, A. and Mitchison, T. J. 2008. A chemical method for fast and sensitive detection of DNA synthesis in vivo. *Proceedings of the National Academy of Sciences of the United States of America* 105(7), pp. 2415-2420. doi: 10.1073/pnas.0712168105

Samuel, S. and Naora, H. 2005. Homeobox gene expression in cancer: Insights from developmental regulation and deregulation. *European Journal of Cancer* 41(16), pp. 2428-2437. doi: 10.1016/j.ejca.2005.08.014

Santoni, M. et al. 2014. Role of natural and adaptive immunity in renal cell carcinoma response to VEGFR-TKIs and mTOR inhibitor. *International Journal of Cancer* 134(12), pp. 2772-2777. doi: 10.1002/ijc.28503

Santos, A. L. and Lindner, A. B. 2017. Protein Posttranslational Modifications: Roles in Aging and Age-Related Disease. *Oxidative Medicine and Cellular Longevity*, doi: 10.1155/2017/5716409

Sanz-Pamplona, R. et al. 2012. Tools for protein-protein interaction network analysis in cancer research. *Clinical & Translational Oncology* 14(1), pp. 3-14. doi: 10.1007/s12094-012-0755-9

Sartori, A. A. et al. 2007. Human CtIP promotes DNA end resection. *Nature* 450(7169), pp. 509-U506. doi: 10.1038/nature06337

Scharer, O. D. 2013. Nucleotide Excision Repair in Eukaryotes. *Cold Spring Harbor Perspectives in Biology* 5(10), doi: 10.1101/cshperspect.a012609

Schiavi, A. et al. 2013. Autophagy induction extends lifespan and reduces lipid content in response to frataxin silencing in C. elegans. *Experimental Gerontology* 48(2), pp. 191-201. doi: 10.1016/j.exger.2012.12.002

Schmidt, L. S. and Linehan, W. M. 2015. Clinical features, genetics and potential therapeutic approaches for Birt-Hogg-Dube syndrome. *Expert Opinion on Orphan Drugs* 3(1), pp. 15-29. doi: 10.1517/21678707.2014.987124

Schmidt, L. S. and Linehan, W. M. 2018. FLCN: The causative gene for Birt-Hogg-Dube syndrome. *Gene* 640, pp. 28-42. doi: 10.1016/j.gene.2017.09.044

Schmidt, L. S. et al. 2005. Germline BHD-mutation spectrum and phenotype analysis of a large cohort of families with Birt-Hogg-Dube syndrome. *American Journal of Human Genetics* 76(6), pp. 1023-1033. doi: 10.1086/430842

Schmidt, L. S. et al. 2001. Birt-Hogg-Dube syndrome, a genodermatosis associated with spontaneous pneumothorax and kidney neoplasia, maps to chromosome 17p11.2. *American Journal of Human Genetics* 69(4), pp. 876-882. doi: 10.1086/323744

Schulz, T. and Hartschuh, W. 1999. Birt-Hogg-Dube-syndrome and Hornstein-Knickenberg-syndrome are the same. Different sectioning technique as the cause of different histology. *Journal of Cutaneous Pathology* 26(1), pp. 55-61. doi: 10.1111/j.1600-0560.1999.tb01792.x

Schwanhausser, B. et al. 2011. Global quantification of mammalian gene expression control. *Nature* 473(7347), pp. 337-342. doi: 10.1038/nature10098

Schwanhausser, B. et al. 2013. Global quantification of mammalian gene expression control (vol 473, pg 337, 2011). *Nature* 495(7439), pp. 126-127. doi: 10.1038/nature11848

Scott, S. P. and Pandita, T. K. 2006. The cellular control of DNA double-strand breaks. *Journal of Cellular Biochemistry* 99(6), pp. 1463-1475. doi: 10.1002/jcb.21067

Scully, R. et al. 1997. Association of the BRCA1 gene product with Rad51 in meiotic and mitotic cells. *European Journal of Cell Biology* 72, pp. 9-9.

Seabra , L. et al. 2010. Abstract 1129: FLCN-putative tumor suppressor. *Proceedings of the 101st Annual Meeting of the American Association for Cancer Research.* Washington, DC. Philadelphia AACR; Cancer Res.

Shackelford, D. B. and Shaw, R. J. 2009. The LKB1-AMPK pathway: metabolism and growth control in tumour suppression. *Nature Reviews Cancer* 9(8), pp. 563-575. doi: 10.1038/nrc2676

Shah, N. and Sukumar, S. 2010. The Hox genes and their roles in oncogenesis. *Nature Reviews Cancer* 10(5), pp. 361-371. doi: 10.1038/nrc2826

Shang, L. B. et al. 2011. Nutrient starvation elicits an acute autophagic response mediated by Ulk1 dephosphorylation and its subsequent dissociation from AMPK. *Proceedings of the National Academy of Sciences of the United States of America* 108(12), pp. 4788-4793. doi: 10.1073/pnas.1100844108

Sharma, K. et al. 2014. Ultradeep Human Phosphoproteome Reveals a Distinct Regulatory Nature of Tyr and Ser/Thr-Based Signaling. *Cell Reports* 8(5), pp. 1583-1594. doi: 10.1016/j.celrep.2014.07.036

Sharma, V. et al. 2016. Oxidative stress at low levels can induce clustered DNA lesions leading to NHEJ mediated mutations. *Oncotarget* 7(18), pp. 25377-25390. doi: 10.18632/oncotarget.8298

Shi, T. et al. 2013. Rif1 and Rif2 Shape Telomere Function and Architecture through Multivalent Rap1 Interactions. *Cell* 153(6), pp. 1340-1353. doi: 10.1016/j.cell.2013.05.007

Shiina, H. et al. 1997. Clinical significance of immunohistochemically detectable p53 protein renal cell carcinoma. *European Urology* 31(1), pp. 73-80.

Shivji, M. K. K. et al. 1998. Resistance of human nucleotide excision repair synthesis in vitro to p21(Cdn1). *Oncogene* 17(22), pp. 2827-2838. doi: 10.1038/sj.onc.1202352

Shortt, J. et al. 2013. Combined inhibition of PI3K-related DNA damage response kinases and mTORC1 induces apoptosis in MYC-driven B-cell lymphomas. *Blood* 121(15), pp. 2964-2974. doi: 10.1182/blood-2012-08-446096

Shrivastav, M. et al. 2008. Regulation of DNA double-strand break repair pathway choice. *Cell Research* 18(1), pp. 134-147. doi: 10.1038/cr.2007.111

Sibanda, B. L. et al. 2017. DNA-PKcs structure suggests an allosteric mechanism modulating DNA double-strand break repair. *Science* 355(6324), pp. 520-+. doi: 10.1126/science.aak9654

Siggs, O. M. et al. 2016. Mutation of Fnip1 is associated with B-cell deficiency, cardiomyopathy, and elevated AMPK activity. *Proceedings of the National Academy of Sciences of the United States of America* 113(26), pp. E3706-E3715. doi: 10.1073/pnas.1607592113

Silverman, J. et al. 2004. Human Rif1, ortholog of a yeast telomeric protein, is regulated by ATM and 53BP1 and functions in the S-phase checkpoint. *Genes & Development* 18(17), pp. 2108-2119. doi: 10.1101/gad.1216004

Simon, M. et al. 2015. TERT promoter mutations: a novel independent prognostic factor in primary glioblastomas. *Neuro-Oncology* 17(1), pp. 45-52. doi: 10.1093/neuonc/nou158

Singh, S. R. et al. 2006. The Drosophila homolog of the human tumor suppressor gene BHD interacts with the JAK-STAT and Dpp signaling pathways in regulating male germline stem cell maintenance. *Oncogene* 25(44), pp. 5933-5941. doi: 10.1038/sj.onc.1209593

Singh, S. S. et al. 2018. Dual role of autophagy in hallmarks of cancer. *Oncogene* 37(9), pp. 1142-1158. doi: 10.1038/s41388-017-0046-6

Slade, L. and Pulinilkunnil, T. 2017. The MiTF/TFE Family of Transcription Factors: Master Regulators of Organelle Signaling, Metabolism, and Stress Adaptation. *Molecular Cancer Research* 15(12), pp. 1637-1643. doi: 10.1158/1541-7786.mcr-17-0320

Smith, G. C. M. and Jackson, S. P. 1999. The DNA-dependent protein kinase. *Genes & Development* 13(8), pp. 916-934. doi: 10.1101/gad.13.8.916

Sodickson, A. et al. 2009. Recurrent CT, Cumulative Radiation Exposure, and Associated Radiation-induced Cancer Risks from CT of Adults. *Radiology* 251(1), pp. 175-184. doi: 10.1148/radiol.2511081296

Sonenberg, N. and Gingras, A. C. 1998. The mRNA 5 ' cap-binding protein eIF4E and control of cell growth. *Current Opinion in Cell Biology* 10(2), pp. 268-275. doi: 10.1016/s0955-0674(98)80150-6

Sonenberg, N. and Hinnebusch, A. G. 2009. Regulation of Translation Initiation in Eukaryotes: Mechanisms and Biological Targets. *Cell* 136(4), pp. 731-745. doi: 10.1016/j.cell.2009.01.042

Soria, G. et al. 2006. P21(Cip1/WAF1) downregulation is required for efficient PCNA ubiquitination after UV irradiation. *Oncogene* 25(20), pp. 2829-2838. doi: 10.1038/sj.onc.1209315

Sreedhar, A. S. et al. 2004. Hsp90 isoforms: functions, expression and clinical importance. *Febs Letters* 562(1-3), pp. 11-15.

St Laurent, G. et al. 2013. On the importance of small changes in RNA expression. *Methods* 63(1), pp. 18-24. doi: 10.1016/j.ymeth.2013.03.027

Stankiewicz, P. and Lupski, J. R. 2002. Genome architecture, rearrangements and genomic disorders. *Trends in Genetics* 18(2), pp. 74-82. doi: 10.1016/s0168-9525(02)02592-1

Starling, G. P. et al. 2016. Folliculin directs the formation of a Rab34-RILP complex to control the nutrient-dependent dynamic distribution of lysosomes. *Embo Reports* 17(6), pp. 823-841. doi: 10.15252/embr.201541382

Starostina, N. G. and Kipreos, E. T. 2012. Multiple degradation pathways regulate versatile CIP/KIP CDK inhibitors. *Trends in Cell Biology* 22(1), pp. 33-41. doi: 10.1016/j.tcb.2011.10.004

Steinlein, O. K. et al. 2018. Birt-Hogg-Dube syndrome: an underdiagnosed genetic tumor syndrome. *Journal Der Deutschen Dermatologischen Gesellschaft* 16(3), pp. 278-284. doi: 10.1111/ddg.13457

Stintzing, S. and Lenz, H. J. 2014. Molecular Pathways: Turning Proteasomal Protein Degradation into a Unique Treatment Approach. *Clinical Cancer Research* 20(12), pp. 3064-3070. doi: 10.1158/1078-0432.ccr-13-3175

Stockl, P. et al. 2006. Sustained inhibition of oxidative phosphorylation impairs cell proliferation and induces premature senescence in human fibroblasts. *Experimental Gerontology* 41(7), pp. 674-682. doi: 10.1016/j.exger.2006.04.009

Stott, F. J. et al. 1998. The alternative product from the human CDKN2A locus, p14(ARF), participates in a regulatory feedback loop with p53 and MDM2. *Embo Journal* 17(17), pp. 5001-5014. doi: 10.1093/emboj/17.17.5001

Strogatz, S. H. 2001. Exploring complex networks. *Nature* 410(6825), pp. 268-276. doi: 10.1038/35065725

Strzalka, W. and Ziemienowicz, A. 2011. Proliferating cell nuclear antigen (PCNA): a key factor in DNA replication and cell cycle regulation. *Annals of Botany* 107(7), pp. 1127-1140. doi: 10.1093/aob/mcq243

Subramanian, A. et al. 2005. Gene set enrichment analysis: A knowledge-based approach for interpreting genome-wide expression profiles. *Proceedings of the National Academy of Sciences of the United States of America* 102(43), pp. 15545-15550. doi: 10.1073/pnas.0506580102

233

Svitkin, Y. V. et al. 2001. The requirement for eukaryotic initiation factor 4A (eIF4A) in translation is in direct proportion to the degree of mRNA 5 ' secondary structure. *Rna* 7(3), pp. 382-394. doi: 10.1017/s135583820100108x

Szabo, E. et al. 1996. Altered cJUN expression: An early event in human lung carcinogenesis. *Cancer Research* 56(2), pp. 305-315.

Szklarczyk, D. et al. 2017. The STRING database in 2017: quality-controlled protein-protein association networks, made broadly accessible. *Nucleic Acids Research* 45(D1), pp. D362-D368. doi: 10.1093/nar/gkw937

Szumiel, I. 2006. Epidermal growth factor receptor and DNA double strand break repair: The cell's self-defence. *Cellular Signalling* 18(10), pp. 1537-1548. doi: 10.1016/j.cellsig.2006.03.010

Taipale, M. et al. 2010. HSP90 at the hub of protein homeostasis: emerging mechanistic insights. *Nature Reviews Molecular Cell Biology* 11(7), pp. 515-528. doi: 10.1038/nrm2918

Takagi, Y. et al. 2008. Interaction of folliculin (Birt-Hogg-Dube gene product) with a novel Fnip1-like (FnipL/Fnip2) protein. *Oncogene* 27(40), pp. 5339-5347. doi: 10.1038/onc.2008.261

Tan, J. et al. 2015. Genetic variants in the inositol phosphate metabolism pathway and risk of different types of cancer. *Scientific Reports* 5, doi: 10.1038/srep08473

Tan, W. Q. et al. 2011. Role of Inflammatory Related Gene Expression in Clear Cell Renal Cell Carcinoma Development and Clinical Outcomes. *Journal of Urology* 186(5), pp. 2071-2077. doi: 10.1016/j.juro.2011.06.049

Tang, F. C. et al. 2009. mRNA-Seq whole-transcriptome analysis of a single cell. *Nature Methods* 6(5), pp. 377-U386. doi: 10.1038/nmeth.1315

Taron, M. et al. 2004. BRCA1 mRNA expression levels as an indicator of chemoresistance in lung cancer. *Human Molecular Genetics* 13(20), pp. 2443-2449. doi: 10.1093/hmg/ddh260

Taugbol, A. et al. 2014. Small Changes in Gene Expression of Targeted Osmoregulatory Genes When Exposing Marine and Freshwater Threespine Stickleback (Gasterosteus aculeatus) to Abrupt Salinity Transfers. *Plos One* 9(9), doi: 10.1371/journal.pone.0106894

Taya, M. and Hammes, S. R. 2018. Glycoprotein Non-Metastatic Melanoma Protein B (GPNMB) and Cancer: A Novel Potential Therapeutic Target. *Steroids* 133, pp. 102-107. doi: 10.1016/j.steroids.2017.10.013

Tee, A. R. et al. 2003. Tuberous sclerosis complex gene products, tuberin and hamartin, control mTOR signaling by acting as a GTPase-activating protein complex toward Rheb. *Current Biology* 13(15), pp. 1259-1268. doi: 10.1016/s0960-9822(03)00506-2

Tee, A. R. and Pause, A. 2013. Birt-Hogg-Dube: tumour suppressor function and signalling dynamics central to folliculin. *Familial Cancer* 12(3), pp. 367-372. doi: 10.1007/s10689-012-9576-9

Tobino, K. et al. 2012. Differentiation between Birt-Hogg-Dube syndrome and lymphangioleiomyomatosis: Quantitative analysis of pulmonary cysts on computed tomography of the chest in 66 females. *European Journal of Radiology* 81(6), pp. 1340-1346. doi: 10.1016/j.ejrad.2011.03.039

Tom, S. et al. 2001. Regulatory roles of p21 and apurinic/apyrimidinic endonuclease 1 in base excision repair. *Journal of Biological Chemistry* 276(52), pp. 48781-48789. doi: 10.1074/jbc.M109626200

Tomasetti, C. and Vogelstein, B. 2015. Variation in cancer risk among tissues can be explained by the number of stem cell divisions. *Science* 347(6217), pp. 78-81. doi: 10.1126/science.1260825

Tong, Y. et al. 2018. Birt-Hogg-Dube Syndrome: A Review of Dermatological Manifestations and Other Symptoms. *American Journal of Clinical Dermatology* 19(1), pp. 87-101. doi: 10.1007/s40257-017-0307-8

Toogun, O. A. et al. 2008. The Hsp90 molecular chaperone modulates multiple telomerase activities. *Molecular and Cellular Biology* 28(1), pp. 457-467. doi: 10.1128/mcb.01417-07

Topisirovic, I. et al. 2003. The proline-rich homeodomain protein, PRH, is a tissue-specific inhibitor of eIF4E-dependent cyclin D1 mRNA transport and growth. *Embo Journal* 22(3), pp. 689-703. doi: 10.1093/emboj/cdg069

Topisirovic, I. et al. 2011. Cap and cap-binding proteins in the control of gene expression. *Wiley Interdisciplinary Reviews-Rna* 2(2), pp. 277-298. doi: 10.1002/wrna.52

Toro, J. R. et al. 1999. Birt-Hogg-Dube syndrome - A novel marker of kidney neoplasia. *Archives of Dermatology* 135(10), pp. 1195-1202. doi: 10.1001/archderm.135.10.1195

Toro, J. R. et al. 2007. Lung cysts, spontaneous pneumothorax, and genetic associations in 89 families with Birt-Hogg-Dube syndrome. *American Journal of Respiratory and Critical Care Medicine* 175(10), pp. 1044-1053. doi: 10.1164/rccm.200610-1483OC

Toro, J. R. et al. 2004. Birt-Hogg-Dube syndrome: Identification of a novel gene and its clinical manifestations. *Journal of the American Academy of Dermatology* 50(3), pp. P89-P89. doi: 10.1016/j.jaad.2003.10.283

235

Toro, J. R. et al. 2008. BHD mutations, clinical and molecular genetic investigations of Birt-Hogg-Dube syndrome: a new series of 50 families and a review of published reports. *Journal of Medical Genetics* 45(6), pp. 321-331. doi: 10.1136/jmg.2007.054304

Toschi, A. et al. 2008. Differential Dependence of Hypoxia-inducible Factors 1 alpha and 2 alpha on mTORC1 and mTORC2. *Journal of Biological Chemistry* 283(50), pp. 34495-34499. doi: 10.1074/jbc.C800170200

Trail, P. A. et al. 2018. Antibody drug conjugates for treatment of breast cancer: Novel targets and diverse approaches in ADC design. *Pharmacology & Therapeutics* 181, pp. 126-142. doi: 10.1016/j.pharmthera.2017.07.013

Trimarchi, J. M. and Lees, J. A. 2002. Sibling rivalry in the E2F family. *Nature Reviews Molecular Cell Biology* 3(1), pp. 11-20. doi: 10.1038/nrm714

Truong, H. T. et al. 2010. Frameshift mutation hotspot identified in Smith-Magenis syndrome: case report and review of literature. *Bmc Medical Genetics* 11, doi: 10.1186/1471-2350-11-142

Tsuji, T. et al. 2017. CC-115, a dual inhibitor of mTOR kinase and DNA-PK, blocks DNA damage repair pathways and selectively inhibits ATM-deficient cell growth in vitro. *Oncotarget* 8(43), pp. 74688-74702. doi: 10.18632/oncotarget.20342

Tsun, Z. Y. et al. 2013. The Folliculin Tumor Suppressor Is a GAP for the RagC/D GTPases That Signal Amino Acid Levels to mTORC1. *Molecular Cell* 52(4), pp. 495-505. doi: 10.1016/j.molcel.2013.09.016

Turgeon, M. O. et al. 2018. DNA Damage, Repair, and Cancer Metabolism. *Frontiers in Oncology* 8, doi: 10.3389/fonc.2018.00015

Turner, J. G. et al. 2012. Nuclear export of proteins and drug resistance in cancer. *Biochemical Pharmacology* 83(8), pp. 1021-1032. doi: 10.1016/j.bcp.2011.12.016

Turner, J. G. and Sullivan, D. M. 2008. CRM1-Mediated Nuclear Export of Proteins and Drug Resistance in Cancer. *Current Medicinal Chemistry* 15(26), pp. 2648-2655. doi: 10.2174/092986708786242859

Udeshi, N. D. et al. 2013. Refined Preparation and Use of Anti-diglycine Remnant (K-epsilon-GG) Antibody Enables Routine Quantification of 10,000s of Ubiquitination Sites in Single Proteomics Experiments. *Molecular & Cellular Proteomics* 12(3), pp. 825-831. doi: 10.1074/mcp.O112.027094

Um, J. H. et al. 2004. Association of DNA-dependent protein kinase with hypoxia inducible factor-1 and its implication in resistance to anticancer drugs in hypoxic tumor cells. *Experimental and Molecular Medicine* 36(3), pp. 233-242. doi: 10.1038/emm.2004.32

Umar, A. et al. 1996. Requirement for PCNA in DNA mismatch repair at a step preceding DNA resynthesis. *Cell* 87(1), pp. 65-73. doi: 10.1016/s0092-8674(00)81323-9

van Slegtenhorst, M. et al. 2007. The Birt-Hogg-Dube and tuberous sclerosis complex homologs have opposing roles in amino acid homeostasis in Schizosaccharomyces pombe. *Journal of Biological Chemistry* 282(34), pp. 24583-24590. doi: 10.1074/jbc.M700857200

Verbon, E. H. et al. 2012. The influence of reactive oxygen species on cell cycle progression in mammalian cells. *Gene* 511(1), pp. 1-6. doi: 10.1016/j.gene.2012.08.038

Verhagen, A. M. et al. 2002. HtrA2 promotes cell death through its serine protease activity and its ability to antagonize inhibitor of apoptosis proteins. *Journal of Biological Chemistry* 277(1), pp. 445-454. doi: 10.1074/jbc.M109891200

Verlinden, L. et al. 2007. The E2F-regulated gene Chk1 is highly expressed in triple-negative estrogen receptor-/progesterone receptor-/HER-2- Breast carcinomas. *Cancer Research* 67(14), pp. 6574-6581. doi: 10.1158/0008-5472.can-06-3545

Vernooij, M. et al. 2013. Birt-Hogg-Dube syndrome and the skin. *Familial Cancer* 12(3), pp. 381-385. doi: 10.1007/s10689-013-9600-8

Vinuela, A. et al. 2018. Age-dependent changes in mean and variance of gene expression across tissues in a twin cohort. *Human Molecular Genetics* 27(4), pp. 732-741. doi: 10.1093/hmg/ddx424

Vocke, C. D. et al. 2005. High frequency of somatic frameshift BHD gene mutations in Birt-Hogg-Dube-associated renal tumors. *Journal of the National Cancer Institute* 97(12), pp. 931-935. doi: 10.1093/jnci/dji154

Vogetseder, A. et al. 2008. Proliferation capacity of the renal proximal tubule involves the bulk of differentiated epithelial cells. *American Journal of Physiology-Cell Physiology* 294(1), pp. C22-C28. doi: 10.1152/ajpcell.00227.2007

Wada, S. et al. 2016. The tumor suppressor FLCN mediates an alternate mTOR pathway to regulate browning of adipose tissue. *Genes & Development* 30(22), pp. 2551-2564. doi: 10.1101/gad.287953.116

Wagner, A. et al. 2016. Revealing the vectors of cellular identity with single-cell genomics. *Nature Biotechnology* 34(11), pp. 1145-1160. doi: 10.1038/nbt.3711

Wagner, S. A. et al. 2011. A Proteome-wide, Quantitative Survey of In Vivo Ubiquitylation Sites Reveals Widespread Regulatory Roles. *Molecular & Cellular Proteomics* 10(10), doi: 10.1074/mcp.M111.013284

237

Walker, C. et al. 1991. Altered expression of transforming growth factor-alpha in hereditary rat renal-cell carcinoma. *Cancer Research* 51(11), pp. 2973-2978.

Walsh, C. P. and Xu, G. L. 2006. Cytosine methylation and DNA repair. *DNA Methylation: Basic Mechanisms* 301, pp. 283-315.

Wang, C. and Lees-Miller, S. P. 2013. Detection and Repair of Ionizing Radiation-Induced DNA Double Strand Breaks: New Developments in Nonhomologous End Joining. *International Journal of Radiation Oncology Biology Physics* 86(3), pp. 440-449. doi: 10.1016/j.ijrobp.2013.01.011

Wang, J. L. et al. 2019. RNA sequencing (RNA-Seq) and its application in ovarian cancer. *Gynecologic Oncology* 152(1), pp. 194-201. doi: 10.1016/j.ygyno.2018.10.002

Wang, K. et al. 2014. TERT promoter mutations in renal cell carcinomas and upper tract urothelial carcinomas. *Oncotarget* 5(7), pp. 1829-1836. doi: 10.18632/oncotarget.1829

Wang, L. et al. 2010. Serine 62 is a phosphorylation site in folliculin, the Birt-Hogg-Dube gene product. *Febs Letters* 584(1), pp. 39-43. doi: 10.1016/j.febslet.2009.11.033

Wang, Y. H. et al. 2013. Phosphorylation and Recruitment of BAF60c in Chromatin Remodeling for Lipogenesis in Response to Insulin. *Molecular Cell* 49(2), pp. 283-297. doi: 10.1016/j.molcel.2012.10.028

Wang, Y. N. et al. 2016. Autophagy Regulates Chromatin Ubiquitination in DNA Damage Response through Elimination of SQSTM1/p62. *Molecular Cell* 63(1), pp. 34-48. doi: 10.1016/j.molcel.2016.05.027

Wang, Z. et al. 2009. RNA-Seq: a revolutionary tool for transcriptomics. *Nature Reviews Genetics* 10(1), pp. 57-63. doi: 10.1038/nrg2484

Warren, M. B. et al. 2004. Expression of Birt-Hogg-Dube gene mRNA in normal and neoplastic human tissues. *Modern Pathology* 17(8), pp. 998-1011. doi: 10.1038/modpathol.3800152

Watts, K. L. et al. 2006. RhoA signaling modulates cyclin D1 expression in human lung fibroblasts; implications for idiopathic pulmonary fibrosis. *Respiratory Research* 7, doi: 10.1186/1465-9921-7-88

Wei, C. et al. 2018. Efficacy of targeted therapy for advanced renal cell carcinoma: A systematic review and meta-analysis of randomized controlled trials. *International Braz J Urol* 44(2), pp. 219-237. doi: 10.1590/s1677-5538.ibju.2017.0315

Wenger, R. H. et al. 2005. Integration of oxygen signaling at the consensus HRE. *Sci STKE* 2005(306), p. re12. doi: 10.1126/stke.3062005re12

238

Wettersten, H. I. et al. 2015. Grade-Dependent Metabolic Reprogramming in Kidney Cancer Revealed by Combined Proteomics and Metabolomics Analysis. *Cancer Research* 75(12), pp. 2541-2552. doi: 10.1158/0008-5472.can-14-1703

White, E. 2012. Deconvoluting the context-dependent role for autophagy in cancer. *Nature Reviews Cancer* 12(6), pp. 401-410. doi: 10.1038/nrc3262

Winnepenninckx, V. R. et al. 2006. Gene expression profiling of primary cutaneous melanoma and clinical outcome. *Journal of the National Cancer Institute* 98(7), pp. 472-482. doi: 10.1093/jnci/djj103

Witzgall, R. et al. 1994. Localization of proliferating cell nuclear anitgen, vimentin, c-fos, and clusterin in the postischemic kidney - evidence for a heterogeneous genetic response among nephron segments, and a large pool of mitotically active and dedifferentiated cells. *Journal of Clinical Investigation* 93(5), pp. 2175-2188. doi: 10.1172/jci117214

Wojtaszewski, J. F. P. et al. 2002. Glycogen-dependent effects of 5-aminoimidazole-4-carboxamide (AICA)-riboside on AMP-activated protein kinase and glycogen synthase activities in rat skeletal muscle. *Diabetes* 51(2), pp. 284-292. doi: 10.2337/diabetes.51.2.284

Wong, A. K. C. et al. 1998. Characterization of a carboxy-terminal BRCA1 interacting protein. *Oncogene* 17(18), pp. 2279-2285. doi: 10.1038/sj.onc.1202150

Wong, M. C. S. et al. 2017. Incidence and mortality of kidney cancer: temporal patterns and global trends in 39 countries. *Scientific Reports* 7, doi: 10.1038/s41598-017-15922-4

Wong, R. H. F. et al. 2009. A Role of DNA-PK for the Metabolic Gene Regulation in Response to Insulin. *Cell* 136(6), pp. 1056-1072. doi: 10.1016/j.cell.2008.12.040

Wong, S. P. and Harbottle, R. P. 2013. Genetic modification of dividing cells using episomally maintained S/MAR DNA vectors. *Molecular Therapy-Nucleic Acids* 2, doi: 10.1038/mtna.2013.40

Woodbine, L. et al. 2011. Endogenously induced DNA double strand breaks arise in heterochromatic DNA regions and require ataxia telangiectasia mutated and Artemis for their repair. *Nucleic Acids Research* 39(16), pp. 6986-6997. doi: 10.1093/nar/gkr331

Woodford, M. R. et al. 2016. The FNIP co-chaperones decelerate the Hsp90 chaperone cycle and enhance drug binding. *Nature Communications* 7, doi: 10.1038/ncomms12037

Wrann, S. et al. 2013. HIF mediated and DNA damage independent histone H2AX phosphorylation in chronic hypoxia. *Biological Chemistry* 394(4), pp. 519-528. doi: 10.1515/hsz-2012-0311

239

Wu, H. J. and Humphreys, B. D. 2017. The promise of single-cell RNA sequencing for kidney disease investigation. *Kidney International* 92(6), pp. 1334-1342. doi: 10.1016/j.kint.2017.06.033

Wu, M. S. et al. 2015. Flcn-deficient renal cells are tumorigenic and sensitive to mTOR suppression. *Oncotarget* 6(32), pp. 32761-32773. doi: 10.18632/oncotarget.5018

Xia, Q. et al. 2016. Folliculin, a tumor suppressor associated with Birt-Hogg-Dube (BHD) syndrome, is a novel modifier of TDP-43 cytoplasmic translocation and aggregation. *Human Molecular Genetics* 25(1), pp. 83-96. doi: 10.1093/hmg/ddv450

Xie, P. et al. 2014. The covalent modifier Nedd8 is critical for the activation of Smurf1 ubiquitin ligase in tumorigenesis. *Nature Communications* 5, doi: 10.1038/ncomms4733

Xu, B. et al. 2001. Involvement of Brca1 in S-phase and G(2)-phase checkpoints after ionizing irradiation. *Molecular and Cellular Biology* 21(10), pp. 3445-3450. doi: 10.1128/mcb.21.10.3445-3450.2001

Xu, B. et al. 2002a. Two molecularly distinct G(2)/M checkpoints are induced by ionizing irradiation. *Molecular and Cellular Biology* 22(4), pp. 1049-1059. doi: 10.1128/mcb.22.4.1049-1059.2002

Xu, B. et al. 2002b. Phosphorylation of serine 1387 in brca1 is specifically required for the Atm-mediated S-phase checkpoint after ionizing irradiation. *Cancer Research* 62(16), pp. 4588-4591.

Xu, D. R. et al. 2012. NESdb: a database of NES-containing CRM1 cargoes. *Molecular Biology of the Cell* 23(18), pp. 3673-3676. doi: 10.1091/mbc.E12-01-0045

Xu, L. F. and Blackburn, E. H. 2004. Human Rif1 protein binds aberrant telomeres and aligns along anaphase midzone microtubules. *Journal of Cell Biology* 167(5), pp. 819-830. doi: 10.1083/jcb.200408181

Yamada, Y. et al. 2015. Case of bilateral and multifocal renal cell carcinoma associated with Birt-Hogg-Dube syndrome. *International Journal of Urology* 22(2), pp. 230-231. doi: 10.1111/iju.12649

Yamashita, T. et al. 2006. Suppression of invasive characteristics by antisense introduction of overexpressed HOX genes in ovarian cancer cells. *International Journal of Oncology* 28(4), pp. 931-938.

Yamaura, M. et al. 2009. NADPH Oxidase 4 Contributes to Transformation Phenotype of Melanoma Cells by Regulating G(2)-MCell Cycle Progression. *Cancer Research* 69(6), pp. 2647-2654. doi: 10.1158/0008-5472.can-08-3745

Yan, M. et al. 2016a. Chronic AMPK activation via loss of FLCN induces functional beige adipose tissue through PGC-1 alpha/ERR alpha. *Genes & Development* 30(9), pp. 1034-1046. doi: 10.1101/gad.281410.116

Yan, M. et al. 2014. The tumor suppressor folliculin regulates AMPK-dependent metabolic transformation. *Journal of Clinical Investigation* 124(6), pp. 2640-2650. doi: 10.1172/jci71749

Yan, M. J. et al. 2016b. DNA damage response in nephrotoxic and ischemic kidney injury. *Toxicology and Applied Pharmacology* 313, pp. 104-108. doi: 10.1016/j.taap.2016.10.022

Yang, Q. et al. 2006. Identification of Sin1 as an essential TORC2 component required for complex formation and kinase activity. *Genes & Development* 20(20), pp. 2820-2832. doi: 10.1101/gad.1461206

Yang, W. et al. 2014. Identification of genes and pathways involved in kidney renal clear cell carcinoma. *Bmc Bioinformatics* 15, doi: 10.1186/1471-2105-15-s17-s2

Yang, X. et al. 2017. The hypoxia-inducible factors HIF1 and HIF2 are dispensable for embryonic muscle development but essential for postnatal muscle regeneration. *Journal of Biological Chemistry* 292(14), pp. 5981-5991. doi: 10.1074/jbc.M116.756312

Yano, K. I. et al. 2008. Ku recruits XLF to DNA double-strand breaks. *Embo Reports* 9(1), pp. 91-96. doi: 10.1038/sj.embor.7401137

Yao, K. C. et al. 2003. Molecular response of human glioblastoma multiforme cells to ionizing radiation: cell cycle arrest, modulation of the expression of cyclin-dependent kinase inhibitors, and autophagy. *Journal of Neurosurgery* 98(2), pp. 378-384. doi: 10.3171/jns.2003.98.2.0378

Yarden, R. I. et al. 2002. BRCA1 regulates the G2/M checkpoint by activating Chk1 kinase upon DNA damage. *Nature Genetics* 30(3), pp. 285-289. doi: 10.1038/ng837

Yoo, H. Y. et al. 2006. Site-specific phosphorylation of a checkpoint mediator protein controls its responses to different DNA structures. *Genes & Development* 20(7), pp. 772-783. doi: 10.1101/gad.1398806

Yoon, J. et al. 2006. An algorithm for modularity analysis of directed and weighted biological networks based on edge-betweenness centrality. *Bioinformatics* 22(24), pp. 3106-3108. doi: 10.1093/bioinformatics/btl533

Yu, Y. H. et al. 2011. Phosphoproteomic Analysis Identifies Grb10 as an mTORC1 Substrate That Negatively Regulates Insulin Signaling. *Science* 332(6035), pp. 1322-1326. doi: 10.1126/science.1199484

Zannini, L. et al. 2014. CHK2 kinase in the DNA damage response and beyond. *Journal of Molecular Cell Biology* 6(6), pp. 442-457. doi: 10.1093/jmcb/mju045

Zbar, B. et al. 2002. Risk of renal and colonic neoplasms and spontaneous pneumothorax in the Birt-Hogg-Dube syndrome. *Cancer Epidemiology Biomarkers & Prevention* 11(4), pp. 393-400.

Zeisel, A. et al. 2015. Cell types in the mouse cortex and hippocampus revealed by single-cell RNA-seq. *Science* 347(6226), pp. 1138-1142. doi: 10.1126/science.aaa1934

Zeman, M. K. and Cimprich, K. A. 2014. Causes and consequences of replication stress. *Nature Cell Biology* 16(1), pp. 2-9. doi: 10.1038/ncb2897

Zhang, C. S. et al. 2017. Fructose-1,6-bisphosphate and aldolase mediate glucose sensing by AMPK. *Nature* 548(7665), pp. 112-+. doi: 10.1038/nature23275

Zhang, C. S. et al. 2014a. The Lysosomal v-ATPase-Ragulator Complex Is a Common Activator for AMPK and mTORC1, Acting as a Switch between Catabolism and Anabolism. *Cell Metabolism* 20(3), pp. 526-540. doi: 10.1016/j.cmet.2014.06.014

Zhang, G. M. et al. 2014b. Metabolic syndrome and renal cell carcinoma. *World Journal of Surgical Oncology* 12, doi: 10.1186/1477-7819-12-236

Zhang, Q. et al. 2013. Suppression of autophagy enhances preferential toxicity of paclitaxel to folliculin-deficient renal cancer cells. *Journal of Experimental & Clinical Cancer Research* 32, doi: 10.1186/1756-9966-32-99

Zhang, T. F. et al. 2019. Distinct Prognostic Values of Phospholipase C Beta Family Members for Non-Small Cell Lung Carcinoma. *Biomed Research International*, doi: 10.1155/2019/4256524

Zhang, X. X. et al. 2016. A rapid NGS strategy for comprehensive molecular diagnosis of Birt-Hogg-Dube syndrome in patients with primary spontaneous pneumothorax. *Respiratory Research* 17, doi: 10.1186/s12931-016-0377-9

Zhang, Y. et al. 2002. Overexpression of copper zinc superoxide dismutase suppresses human glioma cell growth. *Cancer Research* 62(4), pp. 1205-1212.

Zhao, H. and Piwnica-Worms, H. 2001. ATR-mediated checkpoint pathways regulate phosphorylation and activation of human Chk1. *Molecular and Cellular Biology* 21(13), pp. 4129-4139. doi: 10.1128/mcb.21.13.4129-4139.2001

Zhao, H. et al. 2002. Disruption of the checkpoint kinase 1/cell division cycle 25A pathway abrogates ionizing radiation-induced S and G(2) checkpoints. *Proceedings of the National Academy of Sciences of the United States of America* 99(23), pp. 14795-14800. doi: 10.1073/pnas.18557299

Zhao, Y. et al. 2006. Preclinical evaluation of a potent novel DNA-dependent protein kinase inhibitor NU7441. *Cancer Research* 66(10), pp. 5354-5362. doi: 10.1158/0008-5472.can-05-4275

Zheng, B. et al. 2016. Over-expression of DNA-PKcs in renal cell carcinoma regulates mTORC2 activation, HIF-2α expression and cell proliferation. *Sci Rep* 6, p. 29415. doi: 10.1038/srep29415

Zhong, M. M. et al. 2016. Tumor Suppressor Folliculin Regulates mTORC1 through Primary Cilia. *Journal of Biological Chemistry* 291(22), pp. 11689-11697. doi: 10.1074/jbc.M116.719997

Zhong, Q. et al. 1999. Association of BRCA1 with the hRad50-hMre11-p95 complex and the DNA damage response. *Science* 285(5428), pp. 747-750. doi: 10.1126/science.285.5428.747

Zhou, B. B. S. and Elledge, S. J. 2000. The DNA damage response: putting checkpoints in perspective. *Nature* 408(6811), pp. 433-439. doi: 10.1038/35044005

Zhou, C. S. et al. 2005. PCI proteins eIF3e and eIF3m define distinct translation initiation factor 3 complexes. *Bmc Biology* 3, doi: 10.1186/1741-7007-3-14

Zhou, L. S. et al. 2018. Protein neddylation and its alterations in human cancers for targeted therapy. *Cellular Signalling* 44, pp. 92-102. doi: 10.1016/j.cellsig.2018.01.009

Zhou, Q. W. et al. 2019. RNA Sequencing Analysis of Molecular Basis of Sodium Butyrate-Induced Growth Inhibition on Colorectal Cancer Cell Lines. *Biomed Research International*, doi: 10.1155/2019/1427871

Zhuang, W. Z. et al. 2011. Knockdown of the DNA-dependent protein kinase catalytic subunit radiosensitizes glioma-initiating cells by inducing autophagy. *Brain Research* 1371, pp. 7-15. doi: 10.1016/j.brainres.2010.11.044

Zigeuner, R. et al. 2004. Value of p53 as a prognostic marker in histologic subtypes of renal cell carcinoma: A systematic analysis of primary and metastatic tumor tissue. *Urology* 63(4), pp. 651-655. doi: 10.1016/j.urology.2003.11.011

Zois, C. E. et al. 2014. Glycogen metabolism in cancer. *Biochemical Pharmacology* 92(1), pp. 3-11. doi: 10.1016/j.bcp.2014.09.001

Zou, L. and Elledge, S. J. 2003. Sensing DNA damage through ATRIP recognition of RPA-ssDNA complexes. *Science* 300(5625), pp. 1542-1548. doi: 10.1126/science.1083430